Pharmaceutical analysis and in-vitro aerodynamic characterisation of inhaled theophylline formulations containing drug particles prepared by supercritical fluid processing

Chromatographic, spectroscopic, and thermal analysis of micron-sized theophylline particles prepared by supercritical fluid technology and in-vitro evaluation of their performance as inhaled dry powder formulations

Noha Nahedj Atia MOHAMED

Submitted for the degree of Doctor of Philosophy

Institute of Pharmaceutical Innovation

School of Pharmacy

University of Bradford

2009

Pharmaceutical analysis and in-vitro aerodynamic characterisation of inhaled theophylline formulations containing drug particles prepared by supercritical fluid processing

Noha Nahedj Atia Mohamed

Keywords: Methylxanthines, theophylline, HPLC, monolith column, SEDS, characterisation, particle size, aerodynamic performance

Abstract:
The aim of this work is to study the *in-vitro* aerodynamic performance of a new inhaled theophylline formulation prepared by supercritical fluids technique.

For the analysis of the output from the *in-vitro* tests (and further *in-vivo* tests) a new, fast, sensitive high performance liquid chromatographic (HPLC) method was developed and validated for the determination of theophylline and other related derivatives in aqueous and urine samples using new packing materials (monolithic columns). These columns achieve efficient separation under lower backpressure and shorter time comparing to other traditionally or newly introduced C18 columns.

Solution enhanced dispersion by supercritical fluid (SEDS) process has been applied for the production of anhydrous theophylline as pure crystals in the range 2-5 μm to be used as new inhaled dry powder formulation for asthma. Fifteen theophylline samples have been prepared under different experimental conditions.

The drug produced by this method has been subject to a number of solid-phase analytical procedures designed to establish the crystal structure [X-ray powder diffraction (XRPD)], the structure and conformation [(FTIR), Fourier-transform Raman spectroscopy (FT-Raman)], and the morphology and particle size [scanning electron microscope (SEM)]. While, thermal gravimetric analysis (TGA), and differential scanning calorimetry (DSC) have been used to monitor any phase transition or polymorphic changes after processing. All these analytical techniques gave a satisfactory indication of the solid-state chemistry of the processed particles and assess the development of new inhalation product.

The performance of inhaled SEDS theophylline with or without a carrier was evaluated using the developed HPLC method. Three samples having different particle sizes were selected out of the prepared powders by SEDS technique to be tested. The dose sampling unit and the Anderson Cascade Impactor were used to determine the *in-vitro* emitted dose and the deposition profiles of SEDS samples, respectively. The effect of different inhalation flows was studied using two different flows 28.3, and 60 L min^{-1} with 4 L inhalation volume. Different DPI devices were investigated in this study; Easyhaler® and Spinhaler®. The particle size has an important effect on the aerodynamic behaviour and deposition profile of inhaled drug, the smaller the particles the greater the total lung deposition. The presence of a carrier improves the respirable fraction for all the tested formulations.

Publications

- Noha N. Atia, Peter York, Brian J. Clark, (2009);"Development and validation of a rapid and efficient method for simultaneous determination of methylxanthines and their metabolites in urine using monolithic HPLC columns" Journal of Separation Science 2009, 32, 931 – 938.

- Noha N. Atia, Peter York, Brian J. Clark, (2009) "Comparison between monolithic and particle-packed platinum C18 columns in HPLC determination of acidic and basic test mixtures". Accepted and in press in Journal of Separation Science (DOI 10.1002/jss.200900254).

Conference Contributions

- Noha N. Atia, Brian J. Clark, Peter York (2009) "Dose Emission and *in-vitro* evaluation of the aerodynamic behaviour of xanthine derivative prepared by supercritical fluid (SEDS) technique as inhaled dry powder formulation". Open day of School of Life Science, University of Bradford, UK.

- Noha N. Atia, Peter York, Brian J. Clark, (2008) "Optimization of analytical procedures for examination of a new inhaled drug formulation for respiratory diseases". Emerging Scientists Symposium, Loughborough, UK.

- Noha N. Atia, Peter York, Brian J. Clark, (2008) "Development of pharmaceutical analysis procedures to assess the suitability of a new xanthine drug formulation for inhaled therapy". Analytical Research Forum (RSC), Hull, UK.

Acknowledgment

This thesis is dedicated to my Parents whose support, love and encouragement have always been a constant source of strength in my life.

Words fail me to express my appreciation to my husband Hamdy, whose help and support has taken the load off my shoulder. I owe him the finishing of this work and without him I would never have been able to complete this thesis.

I wish to thank my supervisor Prof. Brian J. Clark whose help, stimulating suggestions and encouragement helped me in all the research and writing times of this thesis. He has been supportive since the first day I began working on the project of research

I would like to express my sincere and special thanks to my supervisors Prof. Peter York, and Prof. Henry Chrystyn for their enthusiasm, inspiration and great efforts throughout this project.

At Bradford, I must express my gratitude to Dr. Dinesh Nadarassan and Dr Lyn Daintree for their valuable support in developing the project.

Finally, I must appreciate the help of all my friends in IPI, University of Bradford for their encouragement and help.

List of Contents

List of Contents

List of Contents

List of Figures

List of Tables

List of Abbreviations and Symbols

1MX	1-methylxanthine
3MX	3-methylxanthine
1,3-DMU	1,3-Dimethyluric acid
1,7-DMU	1,7-Dimethyluric acid
1,3,7-TMU	1,3,7-Trimethyluric acid
ACI	Andersen Cascade Impactor
ASES	Aerosol solvent extraction system
BP	British Pharmacopoeia
CA	Caffeine (1,3,7-Trimethylxanthine)
CE	Capillary electrophoresis
CFC	Chlorofluorocarbons
COPD	Chronic abstractive disease
DCM	Dichloromethane
DPIs	Dry powder inhalers
DSC	Differential scanning calorimetry
ECD	Effective cut-off diameter
EP	European Pharmacopoeia
EtOH	Ethanol
FPD	Fine particle dose
FPF	Fine particle fraction
FT-IR	Fourier transform infra-red
FT-Raman	Fourier transform Raman
g	Gram
GAS	Gas antisolvent recrystallisation
GC	Gas chromatography
GSD	Geometric standard deviation
IS	Internal standard
HPLC	High performance liquid chromatography
Kpa	Kilo pascal
L	Litre
L min^{-1}	Litre per minute
LOD	Limit of detection
LOQ	Limit of quantitation
mg	Milligarm
mg ml^{-1}	Milligarm per minute
ml	Milliliter
mM	Millimolar
MMAD	Mass median aerodynamic diameter

MS	Mass spectroscopy
NGI	Next Generation Imactor
nm	Nanometer
Pc	Critical pressure
PA	Paraxanthine (1,7-Dimethylxanthine)
PCA	Precipitation with compressed fluid antisolvent
PGSS	Precipitation from gas-saturated solution
pKa	Dissociation constant
pMDIs	Pressurised metered dose inhaler
PS	Preseparator
PSD	Particle size distribution
R^2	Correlation coefficient
RSD	Relative standard deviation
SAS	Supercritical antisolvent precipitation
SC-CO_2	Supercritical carbon dioxide
SCF	Supercritical fluid
SD	Standard deviation
SEDS	Solution enhanced dispersion by supercritical fluid
SEM	Scanning electron microscope
SPE	Solid phase extraction
Tc	Critical temperature
TB	Theobromine (3,7-Dimethylxanthine)
TGA	Thermal gravimetric analysis
TLC	Thin layer chromatography
TP	Theophylline (1,3-Dimethylxanthine)
USP	United States Pharmacopoeia
UV	Ultraviolet
v/v	Volume per volume
v/w	Volume per weight
w/w	Weight per weight
XRPD	X-ray powder diffraction
λ	Wavelength
°C	Degree Centigrade (Celsius)
μg	Microgram
μl	Microliter
μm	Micrometer

Chapter 1

General introduction

1.1. Introduction

Asthma is a chronic inflammatory pulmonary disorder that is characterized by reversible obstruction of the airways. Since the 1980s, there has been a worldwide increase in the prevalence of asthma in both children and adults [1]. This led to significant increases in morbidity and mortality because of the disease. Theophylline is one of the medications used for treatment of asthma; it belongs to a group of medicines known as *xanthine-derivatives bronchodilators*. Bronchodilators work by opening up the air passages in the lungs so that air can freely flow into the lungs. In doing so, they help to relieve symptoms such as coughing, wheezing and shortness of breath. Theophylline is a naturally occurring alkaloid found in many plant species and food products as tea, coffee.

Current British Thoracic Society (BTS) guidelines [2] recommend the use of theophylline at step 3/4 in asthma management. However, treatment with theophylline has undergone a number of cycles of passion and disapproval over the past 50 years. The high incidence of side effects within the therapeutic range and the narrow therapeutic index as well as the availability of more potent and less toxic alternatives, accompanied with the broadcasting of clinical practice guidelines that list theophylline as a "not preferred" drug, all have resulted in recent less frequent prescribing of theophylline [3]. However, the request for this work originated from senior medics in hospital, who are still prescribing theophylline as a low cost efficient therapeutic option. Furthermore, theophylline has antiinflammatory, immunomodulatory, as well as bronchoprotective effects that potentially contribute to its efficacy as a prophylactic anti-asthma drug. [1, 3-6].

Theophylline is currently available as sustained release tablet or capsule, intravenous injections and suppositories (Aminophylline). But modern asthma therapy has promoted the benefits of aerosol drug delivery to the lung. This inhaled route allows drug delivery

directly to its required site of action, and as a result only a small quantity is required for sufficient therapeutic response. Therefore, there is a low incidence of systemic side effects compared with the oral or intravenous administration. In addition, the onset of action for the inhaled drugs is generally faster than the oral administration. Thus administration of theophylline by inhalation may alleviate some of drawbacks of its available dosage forms. As such the purpose of this research program was to explore further a new formulation of theophylline, to particularly examine the possibility of an inhaled product, which could be tested at a later stage clinically.

Pulmonary delivery using dry powder inhalers (DPIs) by virtue of their propellant free nature, high patient compliance and high dose carrying capacity have encouraged their rapid development. Traditionally DPIs are produced by drug crystallization followed by milling to micronize the drug particles (2-5 μm) for respiratory delivery [7, 8]. However, these methods have various limitations such as poor control over the powder crystallinity, shape, size and size distribution [7-9]. Over the recent years methods utilising supercritical fluid (SCF) have been designed to produce respirable particles in a single step operation. Solution Enhanced Dispersion by Supercritical fluid (SEDS) process has been used in various pharmaceutical operations including crystallization and size reduction [10, 11]. The advantages of this technique include the production of particles with controllable physical and chemical properties with narrow size distribution. Although, it was reported that theophylline has been prepared by other SCF techniques [12-14] no studies were performed on the *in-vitro* lung deposition profiles of SEDS produced particles. This program is the first stages of development of SEDS theophylline particles and *in-vitro* evaluation of their performance as inhaled dry powder formulation.

One of the challenging and time consuming tasks in the *in-vitro* determination of the aerodynamic behaviour as well as the quality assurance of an inhaled drug is the

requirement of analysis of a large number of samples. Therefore an HPLC method with reduced total analysis time was needed. In recent years, to improve the method development speed, a number of new column packings have been introduced. The HPLC monolithic packing is one of these approaches. It has a different structure when compared with conventional silica based columns. They consist of a single piece of either an organic polymer or silica that possesses an interconnected skeleton and flow path through this skeleton. The column has a total porosity of over 80 % v/v, with fast mass transfer and low-pressure resistance, which enables rapid separation [15, 16]. Therefore in this thesis the performance of monolithic columns for separation of theophylline and other related compounds in comparison with different packed C_{18} columns has been investigated.

1. 2. Thesis Hypothesis

Our hypothesis has been that an inhalable theophylline formulation with good aerodynamic performance may give a new approach to alleviate the side effects associated mainly with oral or parentral dosage forms. These new inhalable formulations will permit an efficient local delivery of theophylline to its site of action deeply in the human airways to relieve the bronchoconstriction in asthmatic patients. For effective drug deposition in the lung, a number of factors associated with theophylline particle size, shape and crystallinity as well as the inhaler type have to be investigated.

1. 3. Aims and Objectives

The aim of work is to produce different SEDS theophylline samples within the range of 2-5 μm. Then take the produced samples through quality assurance assessments using different analytical tools. This will be followed by in-vitro evaluation of the aerodynamic behaviour of these SEDS samples. Since there will be a large number of

samples collected after in-vitro dose emission or in-vitro inhalation of the theophylline development of a fast and efficient HPLC method is required for quantification of theophylline and its related compounds and for further in-vivo work.

The objectives of this work are:

1- Investigation of the performances of different stationary phases (focussing on recently introduced columns) regarding the total analysis time.

2- Development of fast and efficient HPLC method for the determination of theophylline and related compounds in aqueous solutions and urine samples.

3- Evaluation of the performance of monolithic C_{18} column in comparison with other traditionally or newly introduced particle- packed C_{18} columns.

4- Crystallisation of theophylline using Solution enhanced dispersion with super critical fluids (SEDS) technique.

5- Develop knowledge and understanding on how the SEDS process parameters influence and control the produced particle properties.

6- Studying the solid-state chemistry of the SEDS samples using a number of analytical techniques.

7- Evaluate the SEDS theophylline aerodynamic performances for potential benefit in inhaled formulated products using conditions that mimic the patient use.

1. 4. Thesis structure

This thesis consists of six chapters:

Chapter 1 a general introduction with the aim and objectives of the work.

Chapter 2 the literature review of the issues related to this research including:

- Asthma and its management using various types of bronchodilators and corticosteroids.

- Theophylline; its structure, mechanism of action, pharmacological effects and

pharmacokinetics.

- Analytical review containing some of the reported methods for theophylline analysis

- HPLC stationary phases used in this study, including monolith and platinum columns.

- SEDS technique; its principle and application

- Different analytical techniques used for characterisation of SEDS products

- Respiratory physiology-structure and function of respiratory system

- Inhalation therapies, mechanism of particle deposition from dry powder inhaler, and drug delivery systems to lungs.

Chapter 3 describes development and validation of a HPLC method for determination of theophylline in urine samples (with other related compounds) and in aqueous solution using different types of stationary phases.

Chapter 4 includes crystallisation of theophylline by SEDS technique and the effect of different crystallisation parameters on the product properties.

Characterisation of SEDS samples using different analytical techniques such as scanning electron microscopy (SEM), differential scanning calorimetry (DSC), thermal gravimetric analysis (TGA), x-ray powder diffraction, infrared spectroscopy (FT-IR), and Raman spectroscopy (FT-Raman).

Chapter 5 focuses on *in-vitro* evaluation of the aerodynamic behaviour of SEDS theophylline either alone or blended with lactose. This chapter includes determination of the total emitted dose and the in-vtiro aerodynamic particle size distribution of SEDS theophylline at different inhalation flows using two dry powder inhaler devices; Easyhaler[®] and Spinhaler[®].

Chapter 6   includes general conclusion for this study.

Chapter 2

Literature review

2.1. Asthma

Asthma-like symptoms were first mentioned from 3500 years ago in an Egyptian manuscript called the Ebres Papyrus. Five hundred years later, the word "asthma" was first used by Hippocrates, to describe these symptoms; the word means" laboured breathing" in Greek [4]. Although the occurrence of asthma continues to increase in most countries, finding a universally harmonized and suitable definition for this condition remains problematic [6].

Early definitions of asthma include the airways obstruction that could be relieved with treatment and the bronchial hyper-responsiveness (BHR) as the essential symptoms, which characterise asthma from other similar conditions, such as chronic bronchitis, and chronic obstructive pulmonary diseases (COPD). More recently, the definition of asthma has been improved by the recognition that the airway submucosa of asthmatic patients are chronically inflamed with a typical inflammatory infiltrate, and these inflammatory processes are important causes of the main asthma symptoms. Furthermore, the loss of reversibility of the airway obstruction is recognized as a long-term effect of the chronic inflammation [5].

2.1.1. Epidemiology of Asthma [1].

- Asthma is most commonly found in children (10-15 %), with about half of all cases developing before the age of 10. However, up to 70 % of children with asthma go into remission by the age of 20.

- Asthma affects approximately 5 – 10 % of adults.

- There are about 150 million of people who suffer from asthma all over the world.

- Asthma predominance is greater in industrialized countries.

- Hospital admissions with asthma are increasing, especially in children.

- Prescribed therapy for asthma is increasing (especially inhaled β2- agonists).

  However until now, the real reasons for the worldwide increases in asthma morbidity

  and mortality are unknown.

2.1.2. Pathophysiology and mechanism of asthma.

Immunological mechanisms play an essential role in the asthmatic reaction and both immediate and delayed responses are involved. Inhalation of an appropriate antigen by asthmatic patients causes a rapid decline in the patient lung function associated with an immediate bronchoconstriction response (early-phase response). After this initial phase, the lung function returns toward the baseline within the first hour either spontaneously or by treatment [4]. However, a further apparently unprovoked reaction may occur hours later (late-phase response). This late response may be less severe than during first response but is more prolonged and lasting several hours [4, 6].

Many inflammatory cells are involved in the pathogenesis of asthma including the mast cells, T-lymphocytes, eosinophils, and macrophages [6].

The mast cells are responsible for the immediate reaction following exposure to an allergen. Cross linkage of IgE antibodies by allergens on the surface of the mast cells leads to cells degranulation and rapid release of the inflammatory mediators such as histamine, leukotrienes, prostaglandins, platelet activation factor (PAF) and a number of intracellular messengers called cytokines [17]. Also following the allergen stimulation T-lymphocytes become activated producing a number of interleukins [4]. Eosinophils play an important role in the asthmatic inflammation reaction as they are capable of causing severe damage to the bronchial epithelium [17]. The macrophages are considered as scavengers in the air ways and also release some mediators such as PAF and leukotrienes [4].

9

The release of these inflammatory mediators results in bronchoconstriction, mucus secretion, exudation of plasma and BHR. On the other hand, cytokines play an important role in coordination and persistence of the inflammatory process in chronic cases (Figure 2.1) [4]. Structural changes may occur with sub-epithelial fibrosis (basement membrane thickening), airway smooth muscle hyperplasia and new vessel formation if the inflammation and bronchoconstriction are left untreated causing irreversible airflow obstruction (Figure 2.2.) [1, 6].

There are different risk factors that increase the possibility of the development of asthma such as family history, sex, exercise and certain drugs. These factors play an important role in causing asthma or triggering the asthma symptoms [4, 6]. Figure 2.3 shows a simplified diagram for the mechanism of the development of asthmatic symptoms.
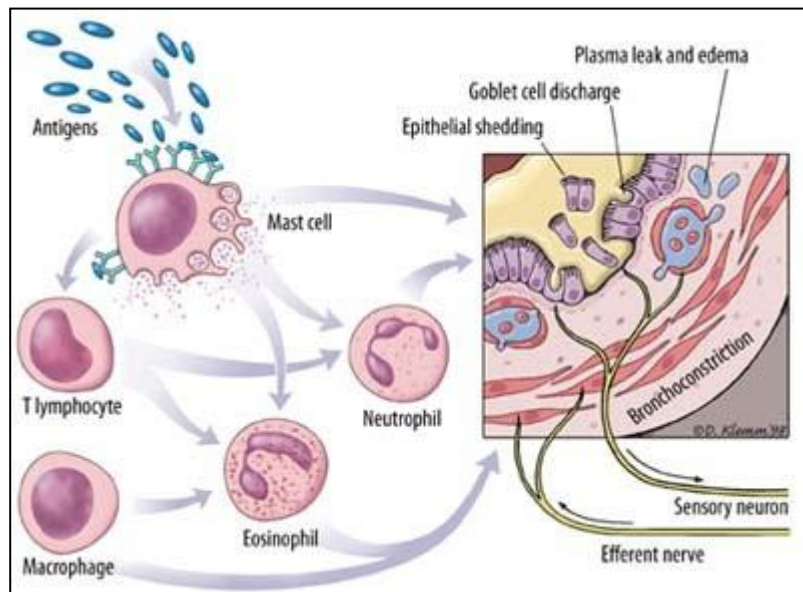
Figure 2. 1. *Diagrammatic representation of the mechanism of asthma (copied from www8.georgetown.edu/dml/facs/graphics/gallery.htm)*
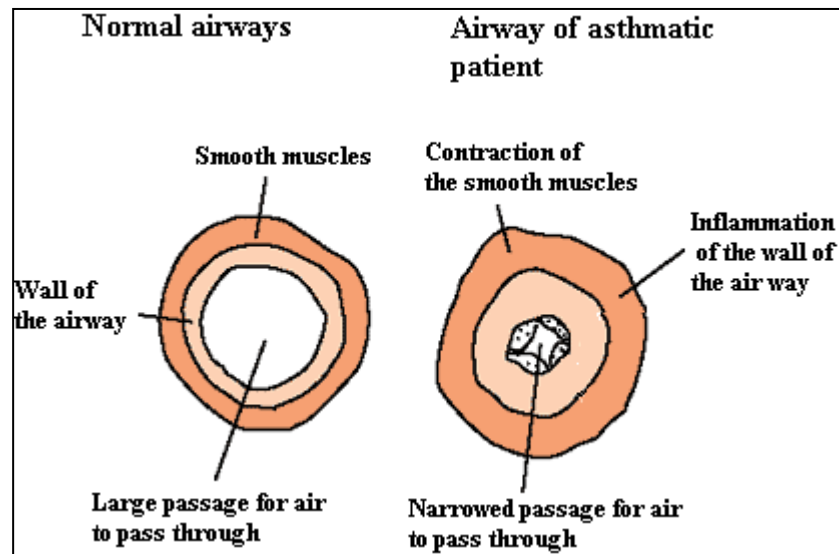
Figure 2. 2. *What happen in asthma; (adapted from http://www.lunguk.org)*
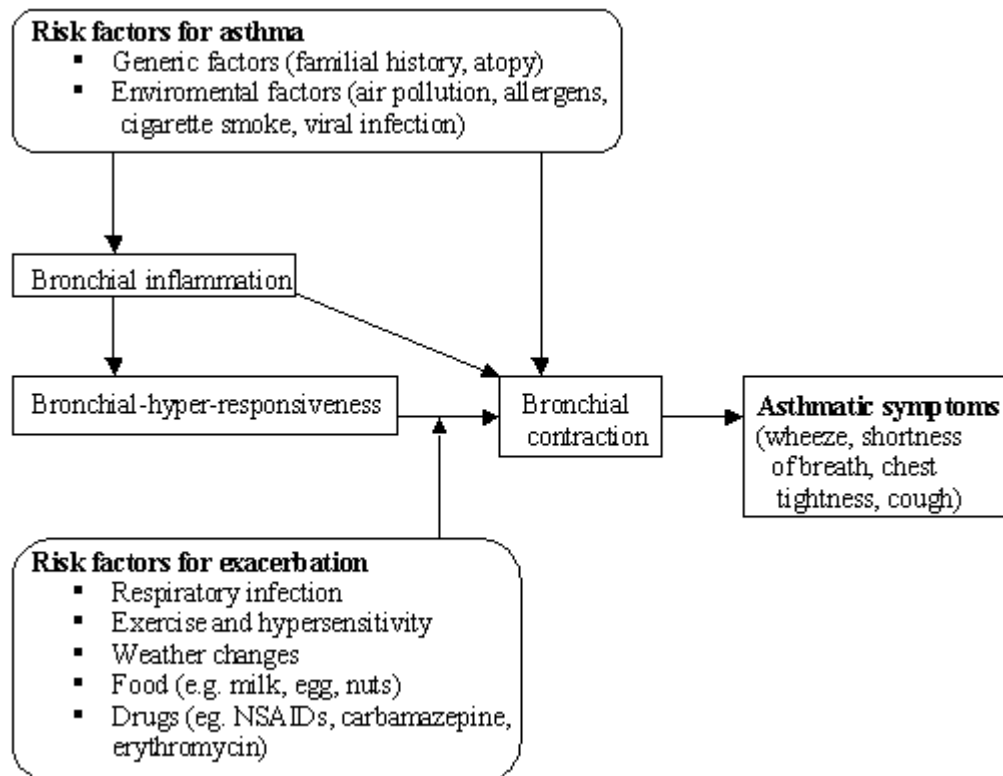
Figure 2. 3. *Development of asthmatic symptoms* [6].

2.1.3. Types of asthma

1- *Extrinsic asthma*

This type of asthma is initiated by known external allergens. Patients with this type tends to be atopic, where they readily develop immunoglobulin E (IgE) antibodies against common materials present in the environment [18].

2- *Intrinsic asthma*

It is also known as cryptogenic or late-onset asthma where the agents responsible for the attacks are unknown or sometimes poorly defined. Patients are not atopic and the condition is usually found in adulthood [18]. The distinction between the two types of asthma is however largely academic, because in clinical practice, many patients do not belong to either category but instead fall into a mixed group with features of each [4].

3- *Occupational asthma*

This type of asthma is triggered only by factors inside the work place and it can occur in workers with or without previous history of asthma [6].

2.1.4. Clinical Features

Asthma symptoms may vary in intensity and symptoms but the frequent symptoms seen in asthmatic patients are [1].

1- Wheezing; it is only heard during exercise or forced expiration.

2- Cough; usually non-productive, but can be accompanied by the expectoration of mucoid sputum especially in children.

3- Chest tightness

4- Unpredicted symptoms may be observed before an attack; itching under the chin, and discomfort between shoulder blades.

2.1.5. Drug therapy of asthma.

2.1.5.1. β_2-agonists

They are sympathomimetic bronchodilators produce their actions by direct stimulation of β_2-adrenoceptors in airway smooth muscles. Short acting β_2-agonists (Sulbutamol, Terbutaline) relax bronchial smooth muscle and cause a rapid increase in the airflow (within 3-5 min.). The long acting β_2-agonists (Salmeterol, Formoterol) cause bronchodilation for at least 12 hours following a single-dose administration. β_2-agonists are contraindicated in patients with hypertropic cardiomyopathy as well as diabetic patients because of their positive inotropic and hyperglycemic effects, respectively [4].

2.1.5.2. Corticosteroids

Corticosteroids provide an efficient anti-inflammatory effect in asthma. They have a highly complex mechanism of action. They inhibit the increase in the airways BHR, reverse β-receptor down-regulation, inhibit cytokines production, and reduce the mucus secretion as well as the airway oedema. In acute attacks of asthma the early use of systemic corticosteroids often terminates the evolution, which decreases the need for hospitalization, prevents relapse, and speeds recovery and they can be administered by oral, intravenous, and inhalation routes. Inhaled corticosteroids are now recommended as first-line therapy for patients with mild to severe asthma. The most widely used inhaled corticosteroids are Beclomethasone dipropionate, Budesonide, and Fluticasone propionate. Their local side effects include dysphonia and oral candidiasis, while the systemic effects which are dose related, include inhibition of the adrenal-pituitary axis, osteoporosis, cataracts, and skin atrophy [4].

2.1.5.3. Methylxanthines

Methylxanthines belong to the group of purine alkaloids. They are basic compounds present in many plant species and food products as tea, coffee grains, guarana fruit, cocoa, and cola nuts. Caffeine and theophylline are used to alleviate neonatal apnoea, to relieve bronchial spasm and in the therapy of asthma. In addition, they are components of the over-the-counter drug mixtures for pain, cold, and cough [19].

As long ago as 1786 Withering recommended strong coffee as a therapy for asthma symptoms, and during the last century Salter, also stated that strong coffee on an empty stomach was the best treatment available for asthma [20]. Theophylline was first identified in extracts from tealeaves by Kossel in Berlin in 1888 and was first synthesized in 1900 by the Boehringer Ltd [21]. Macht and Ting [22] first demonstrated the bronchodilator action of theophylline on pig airways in 1921. In the following year Hirsh reported the beneficial effects of rectally administered theophylline in four asthmatic patients [21]. It was not until the 1930's that theophylline was widely used in the treatment of asthma. There was also a great interest in theophylline in 1980s when slow-release preparations were developed and assays for measuring plasma concentrations became available [4, 5].

2.1.5.4. Anticholinergics

These drugs relax the bronchial smooth muscles through competitive inhibition of the muscarinic acetylcholine receptors. By blocking of these receptors, they inhibit the cholinergic reflex bronchoconstriction, reduce the vagal cholinergic tone leading to bronchodilation and decrease the mucus secretion. Inhaled anticholinergics have no value in the management of stable asthma however they may be useful in acute asthma if the patient not respond to short acting β_2-agonists. Atropine, a naturally occurring compound, was the first anticholinergic drug to be used for treatment of asthma.

However, its side effects were too troublesome, and further development led to the introduction of less soluble quaternary compounds such as Ipratropium bromide. Tiotropium bromide is a newer long acting anticholinergic drug licensed for the treatment of COPD but not for asthma [1, 4].

2.1.5.5. Mast cells stabilizers

These compounds inhibit histamine release from mast cells, reduce airway hyperresponsiveness, and block the early and late responses to allergens. They are ineffective once symptoms have occurred. They are the safest of all antiasthmatic drugs but the least effective [1, 4-6].

2.1.5.6. Leukotriene receptor antagonists

Leukotrienes are inflammatory mediators released by inflammatory cells such as mast cells, and neutrophils. Their mediated effects include airways oedema, smooth muscle contraction, and mucus secretion. Leukotriene receptor antagonists prevent leukotrienes from binding to cys-LT1 receptors found in human airways, and so hinder their physiological action. Both Montelukast and Zafirlukast are orally active leukotrienes receptor antagonists that bind with high affinity to the cys-LT1 receptors [4, 5].

2.1.5.7. New therapies and future developments in asthma management [1, 4-6].

(1) Immunomodulators

Improved recognition of asthma has led to the development of several new approaches of treatments. One of these approaches is Omalizumab (licensed in 2005), which is an anti-immunoglobulin E (IgE) used for the organization of atopic asthma. It is a monoclonal antibody that binds to circulating IgE, which is released upon exposure to an allergen, so prevents receptor binding on the effector cells and stops the release of inflammatory mediators including histamine, and leukotriene.

(2) Selective phosphodiesterase (PDE) inhibitors

The cAMP is metabolised and inactivated by PDE enzymes. Therefore, selective inhibitors for PDE3 and PDE4, which are the major PDEs within the bronchial smooth muscles, increase cAMP levels leading to brochodilation.

(3) Mediator antagonists

Antagonism of the inflammatory mediators which are involved in pathogenesis of asthma is a new logical approach for treatments. They include antagonists/inhibitors of histamine, thromboxane, bradykinin, and tachykinins. However several of the mediator antagonists have been found to be ineffective in asthma.

(4) Anti-tumour necrosis factor-alpha (TNF-α)

They are used to antagonize the inflammatory effect of the tumour necrosis factor, which is released in allergic responses from mast cells, and macrophages [23, 24]. TNF-α antagonists such as Infliximab and Entanercept present a new approach in asthma therapy especially for patients with severe disease.

(5) Anti-adhesion therapies

Infiltration of blood-brone inflammatory cells into tissues is dependant on their adhesion to certain receptors located in the airway membranes before migration to the inflammatory sites. Agents (such as a monoclonal antibody ICAM-1) that block these adhesion receptors are able to be effective anti-inflammatory drugs [25].

2.2. Theophylline

The use of theophylline to treat asthma has undergone a number of cycles of passion and disapproval over the last 50 years. The broadcasting of clinical practice guidelines that list theophylline as a "not preferred" alternative, the availability of newer agents, and concerns regarding the risk-benefit ratio of the drug have resulted in infrequent prescribing of theophylline [3].

However, theophylline was selected as the object of these studies due to several advantages including its low cost compared with other long-term maintenance medications as well as its ability to control chronic asthma as a result of its modest degree of bronchodilator activity. Furthermore, theophylline has antiinflammatory, immunomodulatory, and bronchoprotective effects that potentially contribute to its efficacy as a prophylactic anti-asthma drug [1, 3-6].
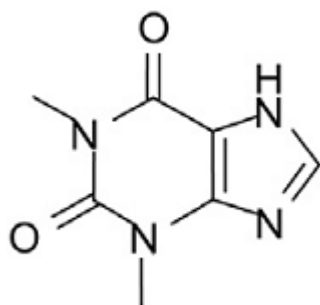
Figure 2. 4 *Chemical structure of theophylline*

Theophylline is a methylxanthine derivative, similar in structure to the common dietary xanthines; caffeine and theobromine (Figure 2.4.). Several substituted derivatives have been synthesized but none has any advantage over theophylline except the 3-propyl derivative, enprofylline, which is more potent and has less toxic effects [26, 27]. Many salts of theophylline have also been marketed, the most common being aminophylline. To increase solubility at neutral pH the ethylenediamine salt is used, so that the

intravenous administration is possible. Other salts, have been used such as choline theophylline, but they do not have any particular advantages while, others, such as aceifylline, are virtually inactive [21, 26].

2.2.1. Mechanism of action [4, 5]

Although theophylline has been in clinical use for many years its full mechanism of action is still uncertain .There are several modes of action have been proposed including:

• *Inhibition of phosphodiesterase (PDE)*

Theophylline is thought to cause bronchodilation by interfering with the chemical mechanism by which the smooth muscle contracts. This occurs by inhibiting the action of PDE, which breaks down cyclic nucleotides in the cell producing an increase in the intracellular levels of cyclic adenosine monophosphate (cAMP) and cyclic guanosine monophosphate (cGMP). This leads to dilatation of the air ways smooth muscles. (Figure 2.5.) [4, 28].
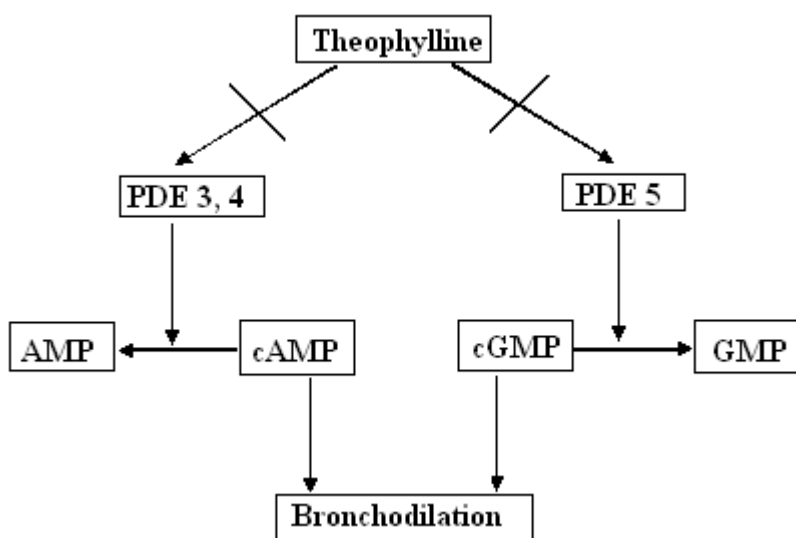
Figure 2. 5. *Inhibition of phosphopdiesterases (PDEs) by theophylline* [1]

- *Adenosine receptor antagonist*

Theophylline at the therapeutic concentrations prevents adenosine (a natural bronchoconstrictor) from binding to the smooth muscle cells by blocking adenosine receptors, which may account for its bronchodilator effect. Blocking of adenosine receptors could also responsible for some of side effects of theophylline, such as central nervous system stimulation, cardiac arrhythmias, and diuresis [29, 30].

- *Stimulation of catecholamine release*

Although, theophylline increases the secretion of adrenaline from the adrenal medulla, the increase in plasma concentration is small to account for any significant bronchodilator effect [31].

- *Mediator inhibition*

Some *in-vitro* tests show that theophylline antagonizes the effect of some prostaglandins on vascular smooth muscle. It also inhibits the secretion and hinders the action of tumour necrosis factor that may be involved in asthmatic inflammation [22, 32].

- *Inhibition of intracellular calcium release*

There is also some evidence that theophylline may interfere with calcium mobilization in airway smooth muscles. As the elevation of the intracellular Ca^{2+} level plays an important role in the development and maintenance of the force in the airway smooth muscles [22]. It has been also reported that the increase in the influx of Ca^{2+}, increases the contractile response to histamine in asthmatic patients [33].

2.2.2. Clinical effects of theophylline

All the molecular mechanisms of action of theophylline produce the following clinical responses [1, 4-6] (Figure 2.6.);

- Bronchodilation.

- Improvement in diaphragmatic and respiratory muscles strength

- Anti-inflammatory effects, and increased mucociliary clearance
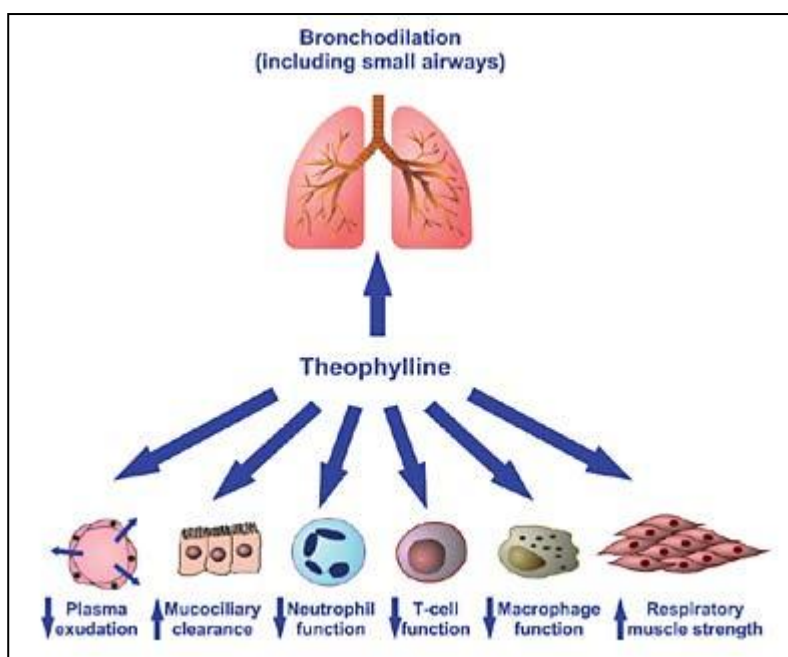
Figure 2.6. *Cellular and clinical effects of theophylline*
(adapted from http://journals.prous.com.)

2.2.3. Pharmacokinetics

2.2.3.1. Theophylline serum level

Theophylline has a narrow therapeutic index and its serum level must be monitored carefully in order to avoid the development of serious side effects. In adults low therapeutic effect is seen below 10 mg/l, while above 25 mg/l increasingly more serious side effects are likely and therefore the serum level of theophylline need to be maintained in the therapeutic range 10-20 mg/l [26, 34].

2.2.3.2. Metabolism of theophylline and other related methylxanthines

Both theophylline (TP) and caffeine (CA) are extensively metabolised in the liver by cytochrome P450 enzymes, in particular CYP1A2. Therefore, less than 10 % of TP and less than 2 % of CA are excreted unchanged in the urine. CA in healthy human subjects is metabolised producing paraxanthine (80 %), theobromine (12 %), and TP (7 %). The main metabolic pathway for TP is hydroxylation at position 8 to generate 1,3-dimethyuric acid, which accounts for 45-55 % of its clearance. Other important steps in the metabolism of TP are N-demethylation to form 1-methylxanthine (20-25 %), and 3-methylxanthine (13-16 %) [35, 36]. Figure 2.7 shows schematic diagram for the metabolism of methylxanthines in humans.

There are various environmental factors, inter-individual variations, and concurrent administered drugs which may affect theophylline hepatic metabolism [37].

- *Factors that increase the metabolism* (reduced plasma level; dose increase is required)

  - Enzyme induction (rifampicin, phenobarbital, anticonvulsant)

  - Smoking (tobacco, marijuana), chronic alcoholism, and childhood

  - Barbecued meat, high protein, and low-carbohydrate diet

- *Factors that decrease metabolism* (increased plasma level; dose reduction is required)

  - Bacterial infection (e.g. pneumonia), viral hepatitis, cirrhosis/liver disease, congestive heart failure, respiratory acidosis, and old age.

  - Enzyme inhibition (e.g. cimetidine, ciprofloxacine, contraceptives, allopurinol).
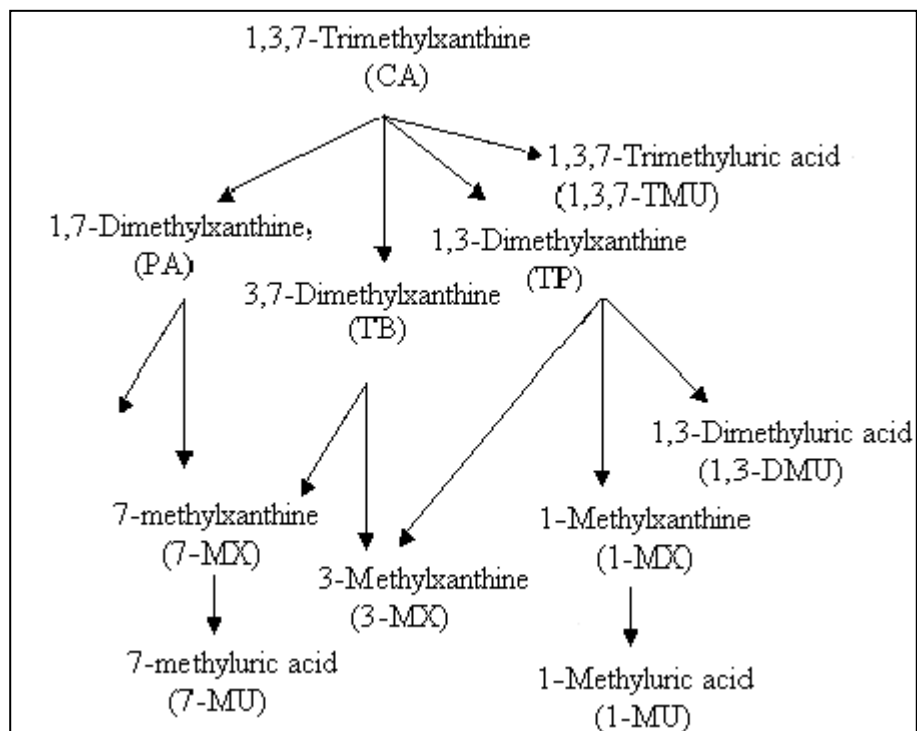
Figure 2.7. *Schematic diagram of the metabolism of methylxanthines in humans*

2. 2. 4. Routes of administration [1, 4-6].

Oral: Plain theophylline tablets are available but they are rapidly absorbed producing wide fluctuations in plasma levels and therefore are not recommended. However, several effective sustained release formulations are more convenient, that are absorbed at a relatively constant rate and provide steady plasma concentrations over 12-24h.

Intravenous: Aminophylline is a mixture of theophylline with ethylenediamine, which is 20 times more soluble than theophylline alone, and is administered intravenously to patients with acute and severe asthma.

Other routes: Aminophylline may be given as suppository, although rectal absorption is considered unreliable and proctitis may occur. On the other hand, intramuscular injections are also used for theophylline

2.3. Analytical review

2.3.1 Chromatographic methods

Several analytical methods have been reported for the analysis of theophylline, caffeine, and their metabolites in different biological samples, dietary supplements, and pharmaceutical dosage forms.

 High Performance Liquid Chromatography (HPLC) seems to be the most popular method for the determination of these compounds (Table 2.1). Ultraviolet detection (UV) is widely used at 247-280 nm. Diode array and mass spectrometry have been also used for detection. In respect of HPLC columns, C_{18} silica gel reversed-phase columns with isocratic elution are commonly used in a number of reported methods. Gradient elution has been also used to resolve many interferences but it is more time consuming than isocratic methods.

On the other hand, ***Gas chromatography (GC) and GC/MS*** have been used for the determination of TP, CA and other methylxanthines in biological fluids and pharmaceutical dosage forms [38 - 44].

Because a large number of samples can be run, in addition to the use of small quantities of solvents, ***thin layer chromatography (TLC) and HPTLC*** have been used for the assay of methylxanthines in plasma [45,46], and saliva [47] using UV-Vis spectrophotometer or a UV- densitometer for detection.

Several methods have been reported for the assay of TP and related substances in pharmaceutical formulations and different body fluids using ***capillary electrophoresis (CE)*** coupled with UV or MS for detection [48-54].

Table 2. 1. *Published HPLC procedures for the determination of theophylline, different methylxanthines, and their metabolic products.*

Sample	Detection	Column	Mobile phase	Ref.
TP, CA, and other drugs, in different dosage forms	UV at 273 nm	Hypersil ODS	Methanol: phosphate buffer (pH 6)	[55]
TP, CA, & metabolites in plasma and saliva	UV at 274 nm	ODS 5μm	0.01M sodium acetate, Methanol (pH 4.75) (87.5:12.5 % v/v)	[56]
CA metabolites in plasma	UV at 280 nm	Normal phase	Dichloromethane containing 2.5% formate buffer in 1.2-2 % methanol	[57]
CA, and TP in urine	UV at 280 nm	Hypersil ODS	0-12.75% acetonitrile in 1% THF (pH 4.8)	[58]
TP and its metabolites in urine	UV at 276 nm	Hypersil ODS	(A) 1.28 g/L CH_3COONa cont. 0.4% v/v conc. acetic acid (pH 4) (B) 20 % w/v acetonitrile and 0.5 v/v glacial acetic acid	[59]
TP in plasma and urine	UV at 267nm	Sepralyte C_{18}	0.05 M phosphate buffer : methanol (1:4 % v/v)	[60]
TP, CA in plasma	UV at 273 nm	C18 (Water)	Acetonitrile: THF: conc. acetic acid: water (50:30:5:915 % v/v)	[61]
TP and CA in plasma	DAD	ODS 3μm	(A) 25% acetonitrile and 2% THF in 10 mM acetate buffer (B) 0.01% THF in 10 mM acetate buffer	[62]
Methylxanthines in human breast milk	UV at 272 nm	ODS 5μm	0-16% methanol in 10 mM sodium acetate and 5 mM TBA	[63]
TP, CA and their metabolites in serum and saliva	UV at 247 nm	ODS 3μm	Acetonitrile/methanol/buffer (pH 4.7) 0.05 M (4:7:89 % v/v)	[64]
TP, TB, and PA in rat brain	UV at 273 nm	μBondapak	THF / 10mM Na_2HPO_4 (pH 6.5) (3:97 % v/v)	[65]

Cont. **Table 2.1.**

Sample	Detection	Column	Mobile phase	Ref.
CA, TP, TB, and PA	UV at 274 nm	ODS 5μm	Methanol: 0.1 M phosphat buffer (30:70 v/v% v/v)	[66]
TP in blood.	DAD -UV	ODS 2 μm	Acetonitrile in phosphate buffer (pH 3.1) (10- 60 v/v %)	[67]
CA and TP in serum	UV at 280 nm	Spheri-5μm	Acetonitrile/ water (5:95 % v/v)	[68]
TP metabolites in urine.	UV at 280 nm	ODS 5μm	10 mM Sodium acetate, acetonitrile, THF, and TBA 5mM	[69]
TP in plasma and saliva	UV at 268 nm	μBondapak	0.08 M Phosphate buffer (pH 2.5): methanol (75:35 % v/v)	[70]
TP and its metabolites in urine and plasma	UV at 273 nm	ODS 5μm	Methanol: 0.01 M acetate buffer (pH 4) (7:93 %v/v) for urine and (9:91 % v/v) for plasma	[71]
CA and TP in plasma	UV at 273 nm	ODS 5μm	Acetonitrile: THF: conc. acetic acid: water (20:20:5:955 % v/v)	[72]
Urinary CA metabolities	UV at 280 nm	Spherisorb S5	Acetic acid: THF: acetonitrile: water (1:2.5:44:925.5 % v/v)	[73]
TP and CA in urine and plasma	UV 254 nm	Silicalite slurry	20 mM phosphate buffer pH 6.9: acetonitrile from 80:20 % v/v	[74]
TP and CA in blood serum	UV at 273 nm	ODS	0.2 mM sodium hydrogenphosphate solution (pH 4.7)	[75]
(1-methyl-C^{14}) CA and its metabolites in rat urine	UV at 280 nm	Lichrosphere RP-18	(A) 10 mM sodium acetate buffer (pH 5.5): methanol: DMF (99:0.5:0.5 % v/v) (B) Methanol: A (50:50 % v/v)	[76]
TP in plasma	UV at 280m	LiChrospher	Acetonitrile: acidified distilled water (pH 4) (10/90 % v/v)	[77]
TP metabolites in plasma.	UV at 275 nm	ODS 5μm	20mM sodium acetate buffer (pH 4.8): acetonitrile: methanol	[78]

Cont. **Table 2. 1.**

Sample	Detection	Column	Mobile phase	Ref.
CA metabolites in biological samples	UV at 275 nm	Kromasil C_4	Acetate buffer (pH 3): methanol (97:3 % v/v) changing to (80:20 % v/v)	[79]
Urinary CA metabolites	UV -DAD at 270 nm	Eclipse C_{18}	(A) Water: acetic acid: THF (pH 3) (996.5: 1:2.5 % v/v) (B) Acetonitrile	[80]
Urinary CA metabolites	Tandem MS	ODS 5μm	(A) Acetic acid (B) Methanol: 2-propanol (C) Methanol	[81]
TP and other drugs in plasma	Tandem MS	Monolith	Acetonitrile/water/formic (90:10:1 %v/v)	[82]
Methylxanthines in urine	DAD -UV	Supelcosil	Methanol: 5mM citric acid (pH 5) (20:80 %v/v)	[83]
Methylxanthines in urine	DAD -UV	Lichrosorb RP-18	Gradient elution using 0.05% TFA and acetonitrile	[19]
TP, CA, & TB in plasma	UV at 275 nm	5μm TSK gel ODS	Methanol:0.01 M phosphate buffer (pH 3.5) (30: 70 % v/v)	[84]
TP& its metabolites in plasma	MS	YMC C_{18}	Methanol: aq. 0.5 ml/L acetic acid	[85]
Methylxanthines and turine in dietary supplements	MS	Luna-C_{18}	Water/methanol/acetic acid (75:20:5 % v/v)	[86]
Urinary CA metabolites	Tandem MS	YMC-Pack C_{30}	(A) 0.5% acetic acid (B) 100% Acetonitrile	[87]
CA and TP in serum	UV at 272 nm	Kromasil C_{18}	50 mM SDS/propanol/10mM phosphate buffer (pH 7)	[88]
TP, CA, in green tea	UV at 271 nm	Imprinted monolith	Dichloromethane /Methanol and acetic acid (20:1 %v/v)	[89]
TP and etofylline in plasma	UV at 272	Intersil C_{18}	10 mM acetate buffer: methanol: acetonitrile (86:7:7 %v/v)	[90]
TB, TP and CA in coca	UV-DAD	Novapack C_{18}	20 % methanol in water	[91]

2.3.2. Spectrophotometric techniques

Different spectrophotometric methods were used for the determination of theophylline in combined pharmaceutical tablets forms with ephedrine [92, 93]. A novel-coupling reagent (3-methyl 2-benzo thiazolinone hydrazone hydrochloride) and diazotized p-nitroaniline have been to assay of TP and CA in pure form or in pharmaceutical formulations [94, 95]. Derivative UV-spectrophotometric techniques were used for determination of TP, TB, and CA in various food products. [96, 97]. Double wavelength and multi-wavelength spectrophotometric methods have been used for the determination of theophylline in serum and in pharmaceutical dosage forms without interference from TB, CA or phenobarbital (a common co-drug component in oral theophylline preparations) [98-102].

2.3.3. Electrochemical methods

Theophylline and different methylxanthines were determined by voltammetric [103] and amperometric techniques, using different types of electrodes [104, 105].

2.3.4. Immunoassay

Different methods were reported for measuring TP level in biological fluids using fluorescence polarization immunoassay (FPIA) [106, 107], immunoaffinity solid-phase microextraction (SPME) [108], or liposome-based flow injection immunoassay (FIIA) system [109]. In addition, a fluoroimmunosensor was developed for the assay of TP in human serum using immobilised antibody [110]

2.4. Production of inhaled particles

The inhaled route has a number of well-recognized advantages over other routes for administration of drugs. As the drug is delivered directly to its required site of action, only a small quantity is required for a sufficient therapeutic response. Accordingly, there is a low incidence of systemic side effects compared with oral or intravenous administration. In addition, the onset of action of inhaled drugs is generally faster than that achieved by oral administration. There are expanding markets for different drugs used for asthma and chronic obstructive pulmonary diseases (COPD), and promising new drugs (e.g. for diabetes, osteoporosis, pain) with new targets and absorption mechanisms requiring new delivery approaches. Inhalation technology gives new opportunities to recognize the full potential of many existing drug substances [7]. The technology has primarily focused on two principals; engineering of efficient inhaler devices, and improvement of the drug formulation technology. Therefore, the goal was to prepare theophylline of physical and chemical characteristics suitable to be used as inhalable drug, that may alleviate some of its drawbacks when administered by different routes [7, 8].

Different reported studies [111, 112] highlighted the influences of the particle size on the distribution and site of deposition of the inhaled drug within the airways. Randomised, double placebo-controlled study was carried out by Usami et al [113] in twelve subjects with asthma. The subjects inhaled technetium-99m-labeled monodisperse Albuterol aerosols of 1.5, 3, and 6 μm mass median aerodynamic diameter. The results showed that the smaller particles achieved greater total lung deposition while a greater oropharyngeal deposition for lager particles with less bronchodilation effect. On other hand, the micrometer-sized particles can exhibit really different physicochemical properties depending on the manufacturing conditions,

the quality and the uniformity of the powder produced [8]. Therefore, the production of ultra fine particles (micrometer or sub micrometer) with narrow particle size distribution (PSD) and desired propertied for efficient respiratory delivery, still represents a significant challenge to the pharmaceutical industry [7].

Many conventional processes for particle production have a number of limitations in producing a desirable end product. Milling often results in 10-50 μm particles with large PSD, and the process can generate a high local temperature that is likely to modify or even damage the product. In contrast, spray drying yields particles of suitable size, but exposes the product to locally high temperature [8].

Lyophilization produces particles with very broad PSD. A final method is precipitation from solution by adding an organic antisolvent but this does not allow precise control of the particle size and result in a high content of residual organic solvent, which needs to be removed later. These techniques therefore, fail to yield particles of suitable size or size distribution. In addition, some of these methods subject liable molecules to high thermal stress. Thus, the need to find alternative approaches to produce small and consistent particles was an important driving force in the development of SCF technology [8, 9].

As an alternative, particle formation using the SCF technique can efficiently produce particles reproducibly over a broad range of physicochemical characteristics that may alleviate issues and associated effects of conventional crystallisation and micronisation used to form inhalable particles [7-9].

2.4.1. Supercritical fluids (SCFs)

This technique is based on gases and liquids at temperatures and pressures above their critical points (Tc- critical temperature; Pc critical pressure) [114]. As shown in Figure 2.8 the critical point is located at the upper end of the liquid: gas-vapour pressure curve and the phase area in excess of this point is the SCF region.
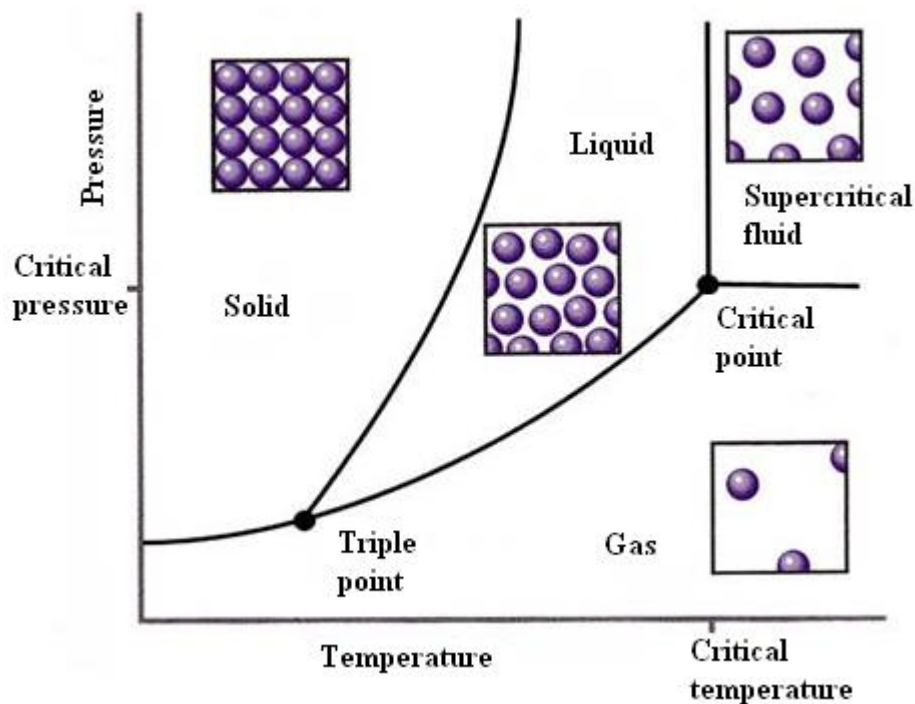
Figure 2.8. *Phase diagram of a pure substance*
(adapted from www.le.ac.uk/supercritical_fluids.html)

2.4.1.1. History

SCFs were discovered as early as 1822, when Cagniard de la Tour first reported that the critical point of substances can be observed when a liquid in a sealed glass vessel was heated till the meniscus between the liquid and vapour disappeared and the substances became a fluid [115]. Later, Hanny and Hogarth [116] reported an experiment in which the dissolved solute precipitated as a snow in the SCF by reducing the pressure. This was the first reported use of supercritical fluid to form particles. However, commercial interest in SCFs techniques has taken place only over the past 30 years. This was

initiated in the 1970s by increased concern over energy costs as the SCF techniques might provide cost saving alternatives to liquid extraction and distillation. More recently, SCF techniques have been used in different commercial applications include extraction processes [115] particularly the decaffeination of coffee and tea as well as extraction of essential oils and flavours from natural products. In 1980s other SCF industrial applications were studied as purification of surfactants and pharmaceuticals, fractionation of polymeric materials, and polymerization. In the same period, interest in using SCFs for precipitation and crystallisation processes was developed for pharmaceutical materials. This has steadily increased in recent years with the aim to prepare powdered pharmaceuticals with discrete and targeted properties such as particle size distribution [7-9].

2.4.1.2. Choice of SCF

All gases can form SCFs above specific sets of critical conditions although extremely high temperatures and/or pressure may be required. Several SCFs with corresponding T_c and P_c values have been used for particle formation in several industrial sectors. Critical temperatures and pressures for a number of pure substances used as SCF are shown in Table 2.2. For pharmaceutical applications the most widely used SCF is carbon dioxide (CO_2) ($T_{c;}$ 31.1°C, P_c 73.8 bar) because it has many advantages over other SCFs. These include [115];

- Low critical temperature (31.1 °C), so it is suitable for heat sensitive materials.

- Non-flammable

- Non-toxic, so it is selective and acceptable in the food and pharmaceutical industries

- Non-oxidizing, so chemical degradation of the compounds is less likely.

- Inexpensive.

Table 2. 2. *Critical temperature (T_c), and pressure (P_c), of some selected SCFs* [115].

Solvent	T_c (°C)	P_c (bar)
Carbon dioxide	31.1	73.8
Ethane	32.2	48.8
Ethylene	9.3	50.4
Propane	96.7	42.5
Propylene	31.9	46.2
Cyclohexane	280.3	40.7
Isopropanol	235.2	47.6
Trichlorofluoromethane	198.1	44.1
Ammonia	132.5	112.8
Water	374.2	220.5

2.4.1.3. Properties of supercritical fluids

SCFs have interesting physical characteristics that can be directed between liquid-like and gas-like properties. SCFs have density values that permit considerable solvation power, whilst the viscosity of solutes in SCFs is lower than in liquids and so the solute diffusivity is higher, which facilitates high mass transfer [8]. SCFs are highly compressible particularly near the critical point which allows their density and thus the solvation power to be carefully controlled by small changes in temperature and/or pressure [9]. They also exhibit very low surface tensions allow better penetration into microporous solids, which conventional liquids may not be able to penetrate. Table 2.3 shows a comparison of the density, viscosity, compressibility, and diffusivity of gases, liquids and SCFs [117].

Table 2. 3. *Comparisons of some physical properties of gases, liquids and SCFs* [117]

State	Density (kg cm^{-3})	Mass Diffusivity (m^2. s)	Viscosity (Pa.s)	Compressibility (Mpa^{-1})
Gas	$(0.5\text{-}2.0) \times 10^{-3}$	$(1.0\text{-}3.0) \times 10^{-5}$	$(1\text{-}4) \times 10^{-5}$	1.0-10
Liquid	0.6 -1.6	$(0.2\text{-}2.0) \times 10^{-9}$	$(0.2\text{-}3.0) \times 10^{-3}$	$(1.0\text{-}5.0) \times 10^{-3}$
SCF	0.2 - 1.0	$(1.0\text{-}7.0) \times 10^{-8}$	$(1.0\text{-}9.0) \times 10^{-5}$	$0.1 \rightarrow \infty$

2.4.1.4. Mechanisms of particle formation using SCF methods

Several reviews have considered with SCF particle formation processes [118-120], which can be divided into three broad groups;

(1) Precipitation from supercritical solutions composed of SCF and the solute

Rapid expansion of supercritical solutions (RESS) exemplifies this first group. The principle of this method is described in Figure 2.9. The solid is packed into the extraction vessel at a controlled temperature and pressure. Then the SCF extracts the solid and the resultant solution is then sprayed through a nozzle into a precipitating column held at ambient or reduced temperature, which causes rapid expansion, leading to a high supersaturation level, and precipitation of the product. A wide range of materials and pharmaceutical products has been processed by RESS and it is also used for encapsulation processes [7-9]. RESS is thus a simple process usable with molecules having good or fair SCF-solubility. However, for compounds with limited solubility in SCF a low output will result making the process economically unfavourable. Other challenges includes the high consumption of SCFs and high pressure required at large scale [8].
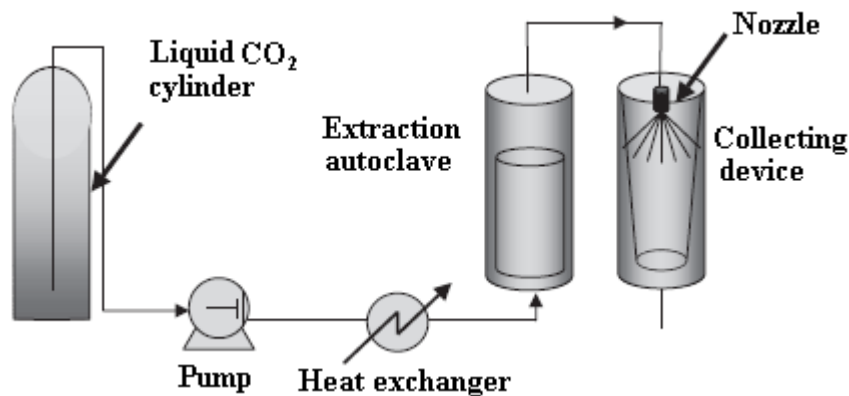
Figure 2. 9. *Schematic diagram of RESS process* [121]

(2) Precipitation from gas saturated solutions (PGSS)

This process involves dissolving a SCF in molten solute, then the resulting solution is fed via an orifice leading to a rapid expansion under ambient conditions [122]. PGSS has the same principle as RESS, but it has the benefits of using significantly less SCF and lower pressure during the process (Figure 2.10.). Although polymers, different kinds of lipids and two pharmaceuticals (nifedipine and felodipine) have been successfully micronized with the PGSS process, the high temperatures and high stability of solute in molten form limit this application for most pharmaceuticals, biologicals and any thermal liable materials [7-9].
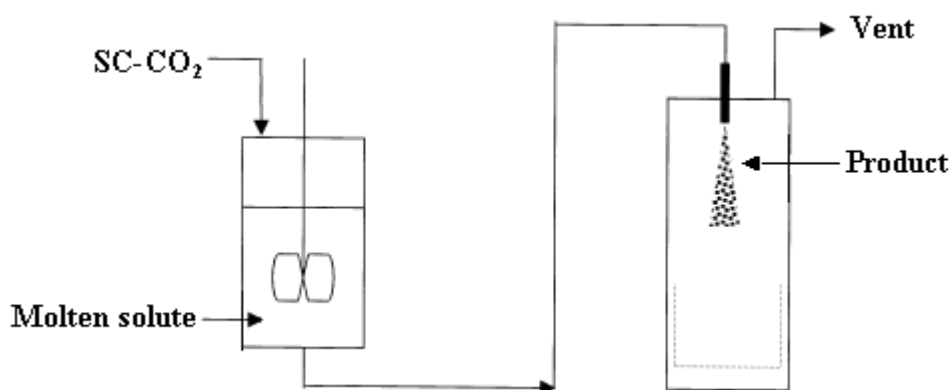
Figure 2. 10. *Schematic diagram of PGSS process* [122]

(3) Precipitation from saturated solutions using SCF as antisolvent

Solids that are insoluble in SCFs or compressed gas can be prepared as fine particles by mean of this method. This technique utilizes the same basic principle to the use of antisolvent-based crystallization processes. With high solubilities of SCFs in organic solvents a volume expansion occurs when the two fluids make contact which leads to a reduction in solvent density and a fall in the solvent capacity. Such reductions cause increased levels of supersaturation, solute nucleation, and particle formation. Precipitation with compressed fluid antisolvent (PCA), gas antisolvent (GAS), supercritical antisolvent (SAS), aerosol solvent extraction system (ASES), and solution-enhanced dispersion by supersaturation (SEDS) are the designations proposed for techniques relevant to this group [121, 122].

3.a. Gas antisolvent process (GAS)

Gallager *et al.* [123] first proposed the GAS technique to overcome the limitations of RESS. This technique was first tested to prepare particles of explosives [121, 122]. The GAS process is a batch technique, which includes the gradual introduction of a compressed gas into a liquid solution of the solute of interest in an organic solvent. Due to the dissolution of the compressed gas, there is a rapid increase in the volume followed by a drop in the solvent strength, and then solid precipitation (Figure 2.11.).
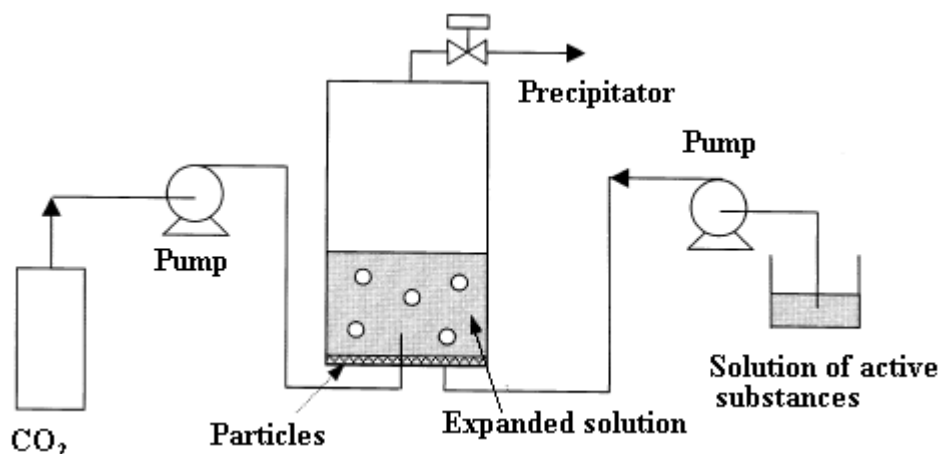
Figure 2. 11. *Schematic diagram of GAS process* [122].

3.b. Precipitation with compressed gas fluid anti-solvent (PCA), supercritical anti-solvent (SAS), and aerosol solvent extraction system (ASES) processes

Many pharmaceuticals have been processed by means of these three precipitation processes such as antibiotics, proteins, and drug substances such as sulbutamol [7-9]. These processes are modified from the GAS method in that the organic solvent drug solution is sprayed through a capillary or a nozzle into a continuous flowing stream of SCF as antisolvent (Figure 2.12.). This is to maximize the exposure of small amounts of solution to large quantities of SCF antisolvent, to accelerate the solubilization of the organic solvent in the SCF leading to precipitation of dry particles, therefore avoiding the drying stage in the GAS process.
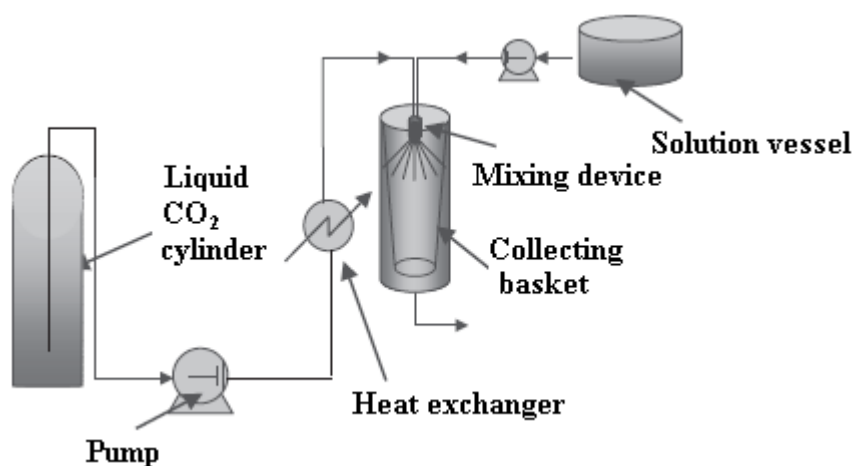
Figure 2. 12. *Schematic diagram of PCA, SAS, and ASES processes* [121]

3.c Solution enhanced dispersion by supercritical fluids (SEDS) process

The SEDS process was first developed and patented by Bradford Particle Design [10, 11]. The general principle is the same as that for SAS process; supercritical CO_2 and the organic solution are introduced concurrently in mixing chamber, followed by precipitation of the solid is due to anti-solvent effect. The essential difference is related to the way of introducing the different phases; in SEDS, a coaxial nozzle design with a mixing chamber is used. This arrangement provides a means whereby the drug in the organic solvent solution interacts and mixes with the SCF in the mixing chamber of the

nozzle before prior to dispersion, and then flows into a particle-formation vessel through a restricted orifice. Thus high mass transfer rates are achieved with a high ratio of SCF to solvent, and the high velocities of the SCF accelerate the break up of solution feed [9]. Over recent years this process has been used for several drugs and drug formulation application, with evidence of successful scale-up. This process has been further developed to process water-soluble materials, including carbohydrates and biological samples using three component-axial nozzle [124].

2.4.1.5. Summary of the advantages of SCF techniques over conventional crystallisation and particle size reduction methods.

• Minimal or no residual solvents in the material without further drying have been demonstrated with SCF.

• Sensitive compounds and heat liable compounds can be processed such as explosives.

• Reduced static in materials compared to fluid energy milling such as micronization.

• Small particles with narrow size distribution have been reported in many papers.

• Control over crystallinity and the ability to condition less crystalline material.

•SCF yield requires no further processing and can be used directly in pharmaceutical applications.

• Reproducibility and repeatability have been demonstrated at several process scales.

• Fewer processing steps that led to higher overall process yield within lower cost compared to other techniques.

2.4.2. Product Characterization

A range of analytical methods can be used to establish the quality and properties of the

drug particles produced by SCF techniques.

2.4.2.1. Scanning electron microscope (SEM)

SEM is an instrument that produces largely magnified images by using electrons instead

of light to form an image. A beam of electrons is produced at the top of the microscope

by an electron gun. The electron beam follows a vertical path through the microscope,

which is held within a vacuum. Once the beam hits the sample, electrons and X-rays are

ejected from the sample. Detectors collect these X-rays, backscattered electrons, and

secondary electrons and convert them into a signal that is sent to a screen similar to a

television screen producing the final image (Figure 2.13). It allows direct measurements

of the particle size and provides full details about the particle shape and texture [7].
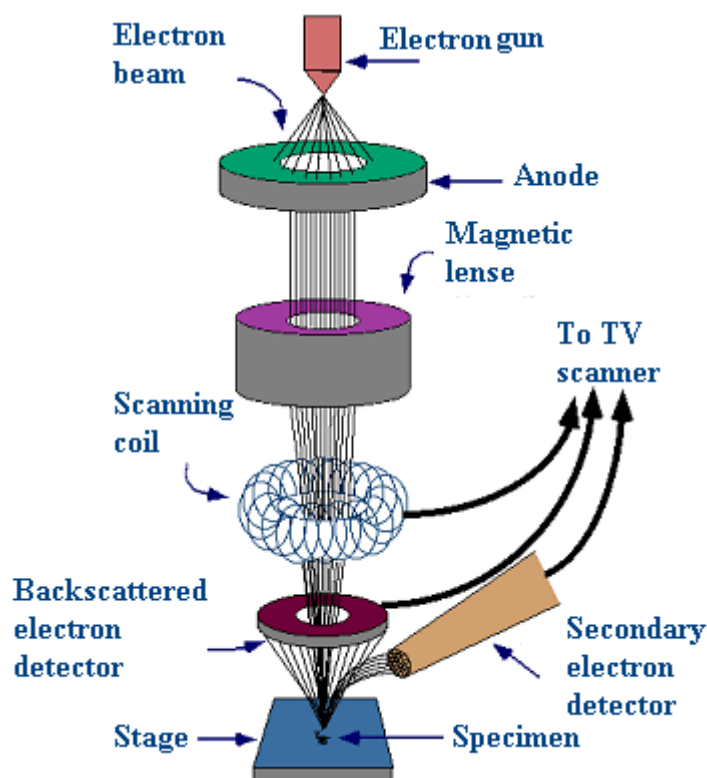
Figure 2.13. *Schematic diagram of SEM*

(adapted from www.purdue.edu/REM/rs/sem.htm)

2.4.2.2. Thermal Methods of analysis

Thermal analysis generally refers to any method involving heating of the sample and measuring the changes in some physical properties. The most important thermal methods for the study of solid-state chemistry are thermogravimetric analysis (TGA) and differential scanning calorimetry (DSC). TGA involves the measurement of the change in mass with temperature and is often used to study the loss of solvent of crystallisation or other solid /gas reactions. TGA is commonly used in research to determine the degradation temperatures, the absorbed moisture content of materials, the level of inorganic and organic components in materials, the decomposition points and the solvent residues. DSC is a technique for measuring the energy necessary to establish a nearly zero temperature difference between a tested substance and an inert reference material, as the two specimens are subjected to identical temperature regimes in an environment heated or cooled at a controlled temperature. DSC used to monitor any phase transition and changes in polymorphic form after processing or storage of the samples [128].

2.4.2.3. X-ray powder diffraction (XRPD)

XRPD is a powerful tool for the investigation of crystalline solids. Experimental results can lead to a complete determination of the solid structure and the packing relationship between individual molecules. This knowledge is often helpful in understanding the solid-state chemistry of the drug. XRPD gives a clear image about any changes in the crystallinity or the polymorphic forms of the tested substance [128].

2.4.2.4. Fourier Transform Infrared spectroscopy (FT-IR)

IR spectroscopy is a useful method for the analysis of solids. IR spectroscopy is extremely sensitive to the structure and conformation of the compound of interest. This

technique is used to assess the polymorphic changes by detecting any change in the molecular vibration in samples. The relative position of the molecules alter in different polymorphs and these changes affect the molecular vibrations which are shown by corresponding shifts in IR banding of the spectra [129].

2.4.2.5. Fourier Transform Raman Spectroscopy (FT-Raman)

This technique is a complementary vibrational spectroscopic method to IR. The Raman effect is not an absorption effect as in infrared spectroscopy, but is depending on the polarizability of a vibrating group and on its ability to interact and couple with exciting radiation. The advantages of Raman includes its increased sensitivity, the ease of sample preparation and the fact that water, frequently present at low concentrations in many materials, has very low absorbance (at 3654 cm^{-1}) and so gives minimal interference, unlike FTIR [130].

2.4.2.6. High Performance Liquid Chromatography (HPLC)

HPLC is a dominant separation tool in all of the analytical areas such as for pharmaceuticals, chemicals, food industries, and environmental laboratories. The stationary phase is the heart of the HPLC system, and silica based packing materials are the most widely applied reversed-phase in the pharmaceutical industry. The hydrophobic surfaces of these packings are made by covalent bonding of monofunctional alkyldimethylchlorosilanes (RMe_2SiCl) on to a silica surface. Octadecylsilane (C_{18}) was the first commercially available silica-based bonded phase. Also alkyl-type ligands of different number of carbon atoms (C_8, C_4) as well as phases with phenyl or cyano- function groups have been used [131]. These phases are familiar to most chromatographers, with a large number of published applications [131-133].

Polar-endcapped, and polar embedded phases have been recently introduced providing an opportunity for potential modification of the chromatographic selectivity. A number

of these stationary phases have enhanced the retention of polar analytes [132].

Although the silica based phases are the most widely applied reversed phases there are still some limitations for which selectivity, reproducibility, or repeatability is not obtained easily. These limitations include [131-133];

- At low pH the silica-based phases are subject to chemical attack, also the basic instability of bonded silica causes retention drift, short column life, and frequent replacement of the column and re-qualification of HPLC system. This is expensive in both terms of actual expenditure, and low productivity in the pharmaceutical process.

- Many silica-based bonding chemistries are not stable at high temperatures (> 40 ° C). On the other hand hydrolysis of the siloxane bond may occur at lower temperatures leading to stationary phase bleed resulting in retention time irreproducibility and high background noise for many applications as LC/MS.

- Additionally, these stationary phases exhibit decreased and poorly reproducible retention under high portion of aqueous conditions. Unusual chromatographic behaviour and unfavourable results may be generated when these phases are used under such conditions [133].

- In bonded phase silica, the partition mechanism responsible for retention in RP-HPLC often does not provide adequate chemical selectivity for chiral or structurally similar compounds.

Nowadays the trend in the liquid chromatography is toward the development of new sorbents, which are able to separate efficiently complicated substances. Such sorbents should be able to work in a wide pH range and enable rapid analysis while sufficient separation; method sensitivity and selectivity remain unaffected. One of these novel types of sorbents is a monolithic column [131].

2.4.2.6.1. Monolithic packing material

Researchers working in the pharmaceutical field are looking for improved methods and tools which can attain a high resolution and separation in short experimental periods.

When using HPLC columns packed with particulate materials, high pressures (sometimes up to 250 bar) have to be used to produce an acceptable flow rate and separations with more than 30 minutes for each run. Also, the high pressure used creates high backpressure on the instrumentation, which reduces the life of the pumps and seals. Moreover, in between runs these columns require a lengthy flushing or equilibration period before the next sample injection can take place. All these limitations of the particulate silica columns, have led to the development of novel and innovative new forms of HPLC stationary phases such as the monolithic columns which can provide practical solutions for all these difficulties [16, 134].

Monolith packing is one of the new developments used to achieve a high-speed separation without loss of column efficiency. The monolithic phase is an example of the fourth generation support for HPLC. As Guiochon claimed " The invention and development of monolith columns is a major technological change in column technology, indeed the first original breakthrough to have occurred in this area since Tswett invented chromatography a century ago" [135]. A large number of experiments have been done so far using these columns [136-138]. The commercial availability of various monolithic columns provides great potential for these new continuous separation media.

The first continuous separation media was produced from open-pore polyurethane foams and highly swollen polymer gels developed during the late 1960s and early 1970s [139, 140]. However, these attempts were less successful because the materials lacked sufficient permeability or solvent stability and could only be applied under low operational pressure. However, Hjerten et al. [141] developed another swollen,

compressed soft gel called a continuous 'polymer bed' in 1989 but these beds were unable to work under higher backpressures, and therefore, limited the application for fast analyses. In 1992, Svec and Freschet [142] created a rigid, polymer monolith for capillary electro-chromatography (CEC) to overcome the drawbacks mentioned above. Because the porous inorganic materials are popular supports, Nakanishi, and Soga developed a technique to produce a porous silica monolith [143-146]. However, it was not until 2000, that silica-based monolithic HPLC columns were commercially available from Merck KgaA in Germany [15].

 Monolithic columns are characterized by having a different structure when compared with conventional packed columns. The column packings consist of one piece of either an organic polymer or silica with a continuous homogenous phase instead of a packed bed with individual particles. This column is usually made by sol-gel technology, with two types of pores (macropores and mesopores) in its structure (Figure 2.14) [147]. The column has a total porosity of over 80 % v/v, providing fast mass transfer and low-pressure resistance, which allow rapid separation. The large pores (typically 2 μm) are responsible for a low flow resistance and therefore permit the application of high eluent flow rates, while the small pores (about 13 nm) verify sufficient surface area for separation efficiency. Due to these facts, relatively higher flow rates (up to 9.9 ml min^{-1}) can be used as the resolution of the silica rod column is less affected in comparison to particulate materials from increasing the flow rate and the column backpressure is still generally low. This makes the monolithic columns attractive for high throughput applications [15, 16, 134, 147].
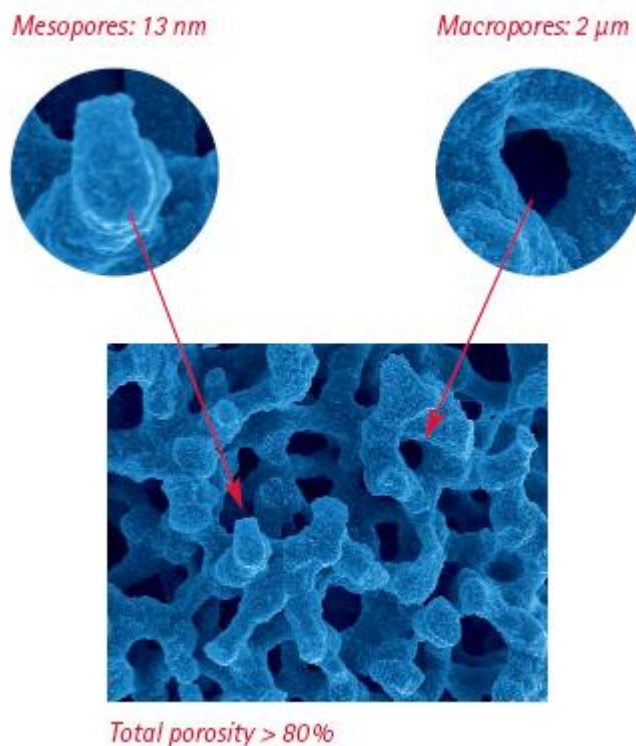
Figure 2.14. *SEM picture of a cross section from a silica monolith (adapted from http://www.vwrsp.com)*

In addition, as the mass transport properties of these phases seem to be determined by convection rather than by diffusion, higher molecular weight molecules such as proteins, and peptides can be separated more efficiently with a monolith than with packed capillary phases [148, 149]. Another practical advantage is a short time needed for column equilibration when a mobile phase gradient is used. It is also possible to apply a gradient flow rate as well. However, it is interesting to note that the practical use of monolithic columns has not been as wide as one should expect, in spite of all their advantages. Whilst, there are a number of papers concerning monolithic columns, most of them consider mainly the preparation and testing of monolithic columns. A relatively small numbers of articles have been published which demonstrate their applications in a variety of chromatographic modes and these include GC, HPLC, and CEC [15, 150-156]. The less common functions of monolithic materials include supports for solid-phase and combinatorial synthesis , scavenger carriers for immobilization of enzymes,

immuno-adsorption using monolithic discs as well as solid-phase extractors and pre-concentrators [156]. The comparison between a silica monolith and conventional columns packed with 3- to 5-µm particles has shown that they have equivalent efficiency and sample capacity [157-160]. However, the monolith offers three- to five-times lower flow resistance and better permeability to allow higher flow rates and higher productivity.

Although the monolithic columns are relative new formats of stationary phases for HPLC and much remains to be investigated, their unique properties, in particular the ease of preparation, tolerance to high flow rate, and rapid speed that can be achieved at acceptable back pressures, make these packings equal or superior to the more conventional packed columns. It is just a matter of time until the range covered by monolithic technology will be extended and it will successfully compete with all of other well-established separation technique.

2.4.2.6.2. Platinum ^{TM} columns

Polar drugs have always been problematic in HPLC and during its continual development much research has been applied to assessing in, particularly for basic drugs. The major problems have been associated with the interaction between the polar drugs and C_{18} phases. One suggested solution has been to use shorter alkyl based phases but very short chain materials ($<C_4$) suffer stability problems at low (< 2) and high (> 8) pHs. Polar embedded phases (such as carbamate and amide) have been also introduced to provide improved polar retention and are reported to give high stability in 100% aqueous mobile phases [161].

Recently, a novel approach was taken by Grace Davison Discovery Sciences® with the introduction of their Platinum™ columns. In these columns instead of thoroughly covering the silica with bonded phase (as traditional C_{18} columns), the exposure of the

silica is controlled to provide a dual-mode separation with both polar and non-polar sites [161, 162]. Therefore, platinum phases have enhanced polar selectivity in addition to reversed phase retention. In operation, it is proposed that the hydrophobic compounds are retained by the bonded phase (alkyl C_{18}) while the polar compounds are retained by the inert silanol groups. Because of the claimed highly pure nature of the surface and the uniform covering of inert vicinal silanol groups, peak shape is generally considered to be very good. The columns are available in two types, which offer different levels of silica exposure. The standard column has a moderate silica exposure and is best used for neutral and moderately polar compounds. The other column platinum EPS (Extended Polar Selectivity) has a high level of silica exposure and can be used for highly polar analytes [161].

2.5. The basic factors affecting deposition of inhaled particles

Over the past decades inhalation therapy has established itself as a valuable tool in the local therapy of pulmonary diseases, such as asthma or chronic obstructive pulmonary diseases (COPD). When an aerosolized drug product is orally inhaled, there are many factors that may influence the effectiveness of the drug deposition in the lung including respiratory tract anatomy, particle size and the type of the inhaler. [7]. To investigate the performance of theophylline as inhaled drug all these factors will be discussed.

2.5.1. Anatomy of the respiratory tract

The anatomy of the respiratory tract and the individual differences have an important effect on the particle deposition within lungs [163]. The respiratory tract represents a unique organ system in the body; its structure allows air to come into close contact with the blood. This fact makes the respiratory tract a useful route of administration of the drugs in the inhaled or aerosol form. The respiratory tract consists of branching airways

that progressively decrease in diameter but increase in number and in total surface area (Figure 2.15). Because, their overall shape looks like a tree, the airways are often described as the pulmonary tree. The tree trunk is related to the trachea of the airways that divided into the two main bronchi. These are subdivided to form smaller bronchi that enter the left and right lobes of the lung. The bronchi undergo additional division to form the bronchioles. This process continues through the terminal bronchioles, the respiratory bronchioles, alveolar ducts and ends with the alveolar sacs [164].
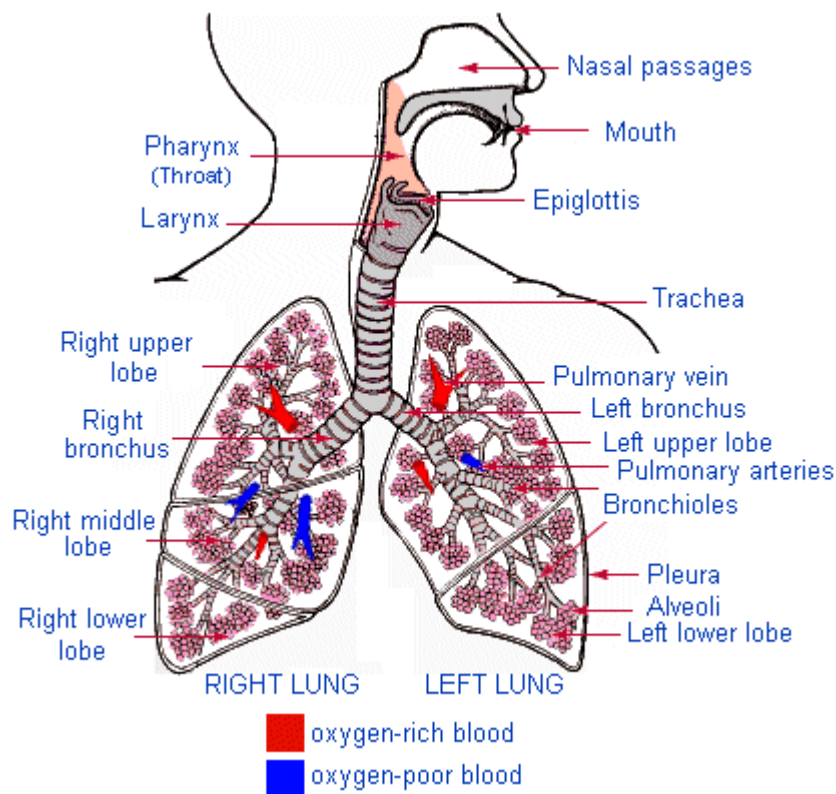
Figure 2. 15. *Anatomy of the respiratory tract (adapted from*
          http://webschoolsolutions.com/patts/systems/lungs.htm)

The most widely used morphological model for the description of the airways structures, was primarily introduced by Weibl [165]. The model proposed the existence of 24 airway generations in total, with the trachea being generation 0 and the alveolar sacs being generation 23 (Table 2.4). The summed cross sectional area from the mouth to the alveolar sacs rapidly increases and results in trumpet shaped lung model, with a total absorptive surface area of up to 100 m^2 [164].

The first region in the respiratory tract includes nose, mouth, and the pharynx. The main function of this region is heating and moistening air as well as acting as a filter. The various levels of the airways may be categorized functionally as being either conducting or respiratory airways. Those airways, which are not involved in gas exchange, constitute the conducting zone of the airway and extend from the trachea to the terminal bronchioles, while, the respiratory zone includes airways involved in gas exchange and consists of respiratory bronchioles, alveolar ducts, and alveolar sacs.

The luminal surface of the airways is lined with a continuous sheet of the epithelial cells. This surface is exposed to the inhaled substances such as gases, particulates or aerosols. It has an important function of limiting access of inhaled substances to the internal environment of the body (subepithelial structure). The epithelial cells are separated from smooth muscle cells by lamina propria, a region of connective tissues containing nerves and blood vessels. The cilia on the surface of epithelia out side the alveolar region and the presence of mucus influence the efficient drug delivery via the lung. Contraction or relaxation of the smooth muscles has a direct effect on the airway branches and also on the airflow in the respiratory tract. Therefore, for efficient deposition and absorption of the inhaled drugs, it is essential to consider firstly the anatomy and air velocities within the respiratory tract [7, 164].

Table 2. 4. *A schematic model of the airways branching according to Weibel* [165]

zone	generation		diameter (cm)	length (cm)	number	total cross sectional area (cm²)	Powder deposition by particle diameter
conducting zone	trachea	0	1.80	12.0	1	2.54	7 - 10 µm
	bronchi	1	1.22	4.8	2	2.33	2 - 10 µm
		2	0.83	1.9	4	2.13	
		3	0.56	0.8	8	2.00	
	bronchioles	4	0.45	1.3	16	2.48	
		5 ↓	0.35 ↓	1.07 ↓	32 ↓	3.11 ↓	
	terminal bronchioles	16	0.06	0.17	$6 \cdot 10^4$	180.0	
transitional and respiratory zones	respiratory bronchioles	17 18 19	↓ 0.05	↓ 0.10	↓ $5 \cdot 10^5$	↓ 10^3	0.5 - 2 µm and < 0.25 µm
	alveolar ducts	20 21 22	↓	↓	↓	↓	
	alveolar sacs	23	0.04	0.05	$8 \cdot 10^6$	10^4	

2.5.2. Particle size

The most important physicochemical determinant for the deposition of aerosols in the lung is the particle size, which is generally characterized by aerodynamic diameter. The aerodynamic diameter is the most relevant to the lung delivery and ultimately to the therapeutic effect [112]. Since it relates to the particle dynamic behaviour and describes the main mechanisms of aerosol deposition (inertial impaction and sedimentation). The aerodynamic diameter is defined as the diameter of a unit density sphere having the same settling velocity (generally in air) as the particle regardless of the shape and density [7]. This is then generally referred to as the mass median aerodynamic diameter (MMAD). The MMAD is the particle diameter that has 50 % of the aerosol mass residing above and 50 % below it. While, the geometric standard deviation (GSD) is a measure of the variation of the particles diameters within the aerosol [7, 166].

To reach the peripheral airways where the drug is most efficiently absorbed particles

need to be in the 2-5 μm aerodynamic range. Larger particles deposit in the oral cavity or pharynx producing no therapeutic effects. Particles smaller than 2 μm are thought to be exhaled or deposited in alveolar region [111]. The amount of an aerosol contained in particles having an aerodynamic diameter approximately within 2-5 μm, is generally referred to the fine particle dose (FPD) [7]. This parameter is expressed with respect to the emitted or nominal dose and is defined as fine particle fraction (FPF).

2.5.3. Mechanisms of deposition of aerosol particles

After inhalation, particles have the potential to be deposited at different regions in the respiratory tract depending on their size and velocity. Different physical mechanisms drive the inhaled particles and move them in the airflow to the respiratory tract walls [167, 168]. These mechanisms are; inertial impaction, sedimentation, diffusion, interception, and electrostatic (Figure 2.16).
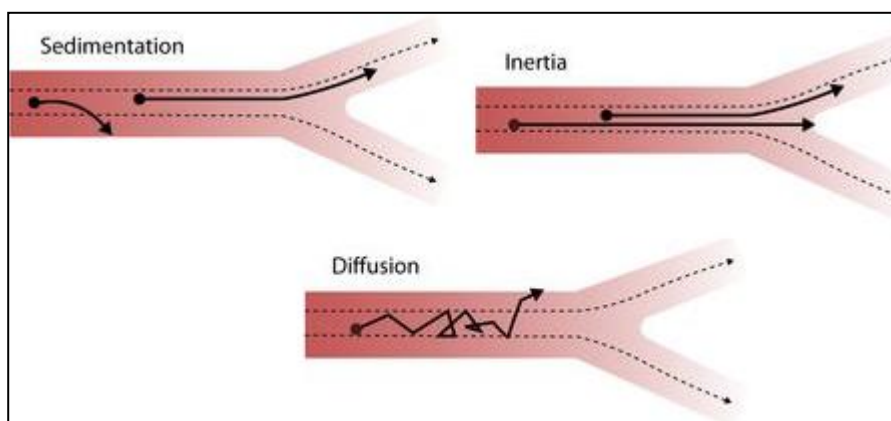
Figure 2. 16. *Schematic diagrams of the three main mechanisms of aerosol particle deposition (adapted from http://ocw.jhsph.edu/imageLibrary/index)*

2.5.3.1. Inertial impaction

Inertial impaction is an important mechanism of deposition of fast travelling large particles [169]. Inertial impaction is caused by the affinity of the particles and droplets to move in a straight direction instead of following the gas streamlines. Impaction may thus take place against the airways walls and is usually occurring within the first generation of the lung where the air velocity is high. The air flow velocity in the main bronchi is estimated to be 100 fold higher than in the terminal bronchioles, and 1000 fold higher than in the alveolar region. Inertial impaction is dependent on the mass, and velocity of the inhaled particles, therefore the greater the particle mass and velocity, and the higher the chances of hitting the airways walls. Particles above 5 μm are deposited in the oropharynx by this mechanism. After impaction in the oropharengeal region large particles are subsequently swallowed and may produce some systematic effects, while, particles less than 5 μm will be carried by the air streams into deeper airways [168-170].

2.5.3.2. Sedimentation

Sedimentation is the main method of deposition of smaller particles (2- 5 μm). It tends to occur in the small airways and alveoli, where air velocity is negligible [169]. At this point the particles traveling in the air streams tend to settle out under the force of gravity. To enhance this settling it is important that there is a breath-hold during each inhalation. Therefore, the rate of settling is not only proportional to the density and size of the inhaled particles but on the time spend in the airways [7, 169].

2.5.3.3. Diffusion

When the particles become sufficiently small, deposition by diffusion becomes a significant mechanism. It results from the constant random collision of gas molecules with the particles, thus pushing them in an irregular fashion called Brownian motion

leading to deposition of the submicron molecules in the airways walls. In contrast to impaction and sedimentation, diffusional deposition increases with decreasing the size of particles regardless the particle density. It is similar to sedimentation in that it occurs in the smaller airways and is enhanced by breath holding after inhalation [170].

2.5.3.4. Interception

Unlike inertial impaction, interception occurs when particles impact on the airway surface because of their size rather than their inertia. The deposition occurs when the centre of gravity of the particle is within the streamlines of the gas phase but a distal end of the particle is already touching a solid or liquid surface. It is an important mechanism for deposition of elongated particles in lower airways [168].

2.5.3.5. Electrostatic precipitation

In the initial stages of generation of the aerosols significant electrostatic charges may be produced on the particles. The charged particles can induce an opposite charge on the walls of the airways leading to electrostatic attraction between them and so deposition occurs. There is no strong evidence that such a mechanism can led to major increases in the deposition of aerosols in human respiratory tract [170, 171].

2.5.4. Methods used for assessing the drug deposition

Both *in-vitro* and *in-vivo* methods have been used to study the deposition of inhaled drugs within the lung. *In-vivo* studies reflect the real situation and are subjected to more intra- and inter-subject variations than *in-vitro* studies but they are more expensive and time consuming compared with *in-vitro* methods.

2.5.4.1. *In-vitro* methods

A variety of analytical techniques have been used for *in-vitro* evaluation of the performance of inhaled formulations. They can test the dose uniformity, the emitted dose, and the particle size distribution. The *in-vitro* methods give an estimation of the *in-vivo* deposition. One of the most widely used techniques is the inertial impaction method. Different apparatus can be used all of them mimic the anatomy of the respiratory tract to give predictions of lung deposition. On the other hand, microscopic and laser diffraction techniques have been also used [7].

2.5.4.1.1. Inertial Impaction

Inertial impaction methods have been widely used for determination of the aerodynamic characteristics of the emitted dose from aerosols [172-174] many years ago. The original devices were designed to test the atmospheric air for pollutants, followed by their use in pharmaceutical applications [175, 176]. The applications of these methods for the assessment of the medical aerosols have been widely reviewed, showing different types of the impactors and their abilities or drawbacks in the determination of the performance of different inhaler devices [177]. The inertial impactors used mimic the dimensions of the airways and are based on the aerodynamic behaviour of the aerosol particles (Figure 2.17). The cascade impactor consists of several stages each with collecting plates. The air stream directs the inhaled particles towards the surface of the collection plates for that particulate stage. At each stage the airflow turns rapidly to run parallel to the collection plates. Particles in the air stream with high inertial mass will not be retained in the airflow and will be deposited on the plates, while the smaller particles with inadequate inertia will be held in the air-stream to the next stage where the process is repeated. The stages of the impactor are fixed in a stack, in order of decreasing particle size. As the air stream becomes smaller the air velocity increases and

finer particles are collected. Any remaining particles in the air stream after the final

collector plate will be collected on a filter [178]. Finally, the amount of the deposited

particles on each plate is determined by different analytical methods, mainly HPLC,

after recovering of the drug particles using a suitable solvent. Then all the aerodynamic

features of the aerosol including FPD, FPF, MMAD, and GSD can be calculated.
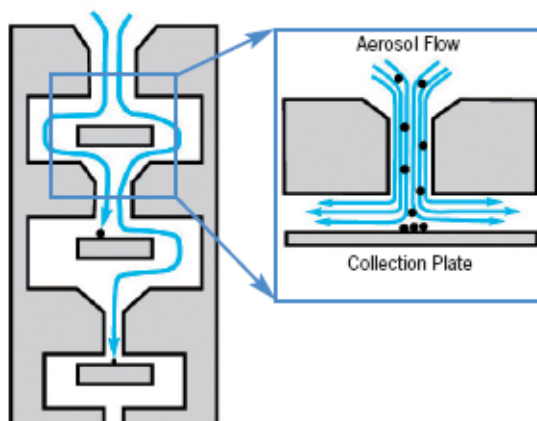
Figure 2. 17. *Schematic representation of the principle of operation of cascade*
impactors [178].

The United States (USP) and European (EP) Pharmacopoeia, list no less than five

different cascade impactors/ impingers suitable for the aerodynamic assessment of fine

particles. Selection of a certain impactor will mainly depend on the product to be tested,

the data that is required, the geographical location where the product is to be marketed.

The EP [173] specifies four impactors for the aerodynamic assessment of fine particles

in both dry powder inhalers (DPI) and metered dose inhalers (MDIs) which are; single-

stage glass impinger (SSGI), multi-stage liquid impinger (MSLI), Andersen cascade

impactor (ACI), and next generation impactor (NGI).

The USP [174] specifies six impactors suitable for aerodynamic size distribution; ACI

(with and without preseparator), Marple Miller impactor (MMI), MSLI and NGI (with

or without separator). Nowadays, a discussion has taken place to harmonize the

different systems with DPI's and MDI's and only three impactors appear in the Ph.Eur., and USP which are; MSLI, ACI, and NGI.

(1) Glass impinger

The glass impinger (GI) comprises of a jet or nozzle plate containing one or more circular or slot-shaped orifices placed a fixed distances from a flat collection surface that is usually horizontal (Figure 2.18). Its usage is restricted to the assessment of MDIs and DPIs at airflow of 60 ± 5 L min^{-1}. It is based on the principle of liquid impingement to divide the emitted dose from the inhaler into respirable dose and non-respirable portion. At the beginning the impinger chambers are filled with specified amounts of solvent, and then at the end of the test, the drug collected in the lower chamber can be assayed and expressed as a respirable fraction (or percentage) of the delivered dose. As the GI uses only two stages, it is not possible to determine the MMAD of particles under testing. At a flow rate of 60 L min^{-1}, the mean aerodynamic particle cut-off size of the lower stage is 6.4 μm [173, 178].

Figure 2. 18. *Single stage impinger* [178].

(2) Multistage Liquid Impinger

The Multi-Stage Liquid Impinger (MSLI) consists of a metal throat, five impaction stages, and final filter. It is suitable for use within the airflow range 30 - 100 L min^{-1}. Its collection stages are kept moist, which helps to reduce the problem of re-entrainment of powder. At a flow rate of 60 L min^{-1}, the cut-off diameters of stages 1, 2, 3 and 4 are 13, 6.8, 3.1 and 1.7 μm respectively [173, 174, 178], while stage 5 is a filter, for collection of the smaller particles (Figure 2.19).

Figure 2.19. *Multistage Liquid impinger* [178]

(3) Andersen Cascade Impactor (ACI)

It consists of a stack of eight plates, each containing a series of precision drilled holes, and a final filter stage [173, 174]. The diameter of the holes decreases progressively for each succeeding stage; therefore the jet velocity increases as the particles travel through the impactor. When sampling particles larger than 10 μm, a preseparator is used to prevent the particle bouncing and re-entrainment errors. The eight stages correspond approximately to the various parts of the human respiratory system (Figure 2.20).
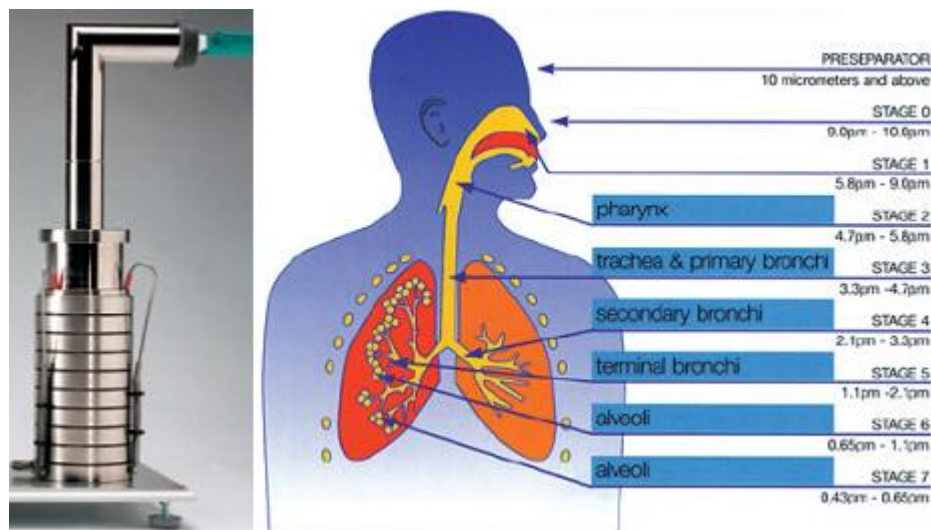
Figure 2.20. *Diagram shows the ACI stages corresponding to the human respiratory system* [178].

The standard ACI is designed for use at 28.3 L min^{-1}. However, it is important to consider the change in effective cut-diameter (ECD) that will occur for each stage upon changing the airflow over the range of 28.3 - 100 L min^{-1} using Van Oort equation [179];

$$ECD^* = ECD^{\bullet}(28.3/Q)^{0.5}$$

where; ECD* is the stage ECD at sampling flow rate Q (L min^{-1})

ECD$^{\bullet}$ is the stage ECD at sampling flow rate 28.3 L min^{-1}

When operated at 60 L/min stages 0 and 7 are removed and replaced with two additional stages, -0 and -1. Similarly, at 90 L min^{-1}, stages 0, 6 and 7 are removed and replaced with three additional stages, -0, -1 and –2 [178].

By determination of the amount of the drug deposited on the collection plates, it is possible to calculate FPD, FPF and all other aerodynamic features of the studied aerosol. Many studies have been carried out to evaluate cascade impactors [180, 181]. It was found that FPD recovery was lower when using a glass and metal impinger as compared

to values from the MSLI or ACI. It has also been reported that large differences in results between different ACIs, could result in variability in size distribution measurements. Therefore the same impactor should be used throughout a study [182].

(5) Next Generation Impactor (NGI)

The NGI is a high performance, precision, particle classifying, cascade impactor with friendly design for the ease testing of MDIs, DPIs and similar devices. The NGI has seven stages plus a Micro-Orifice Collector (MOC) that eliminates the need for a final paper filter (Figure 2.21). At an airflow of 60 L min^{-1}, the cut-off points for stages range from 8.06-0.34 μm. The airflow passes through the impactor in a saw-tooth pattern. Particle separation and sizing is achieved by successively increasing the velocity of the air stream as it passes through each stage by directing it through a series of nozzles containing reducing jet sizes [173, 174, 178]. The NGI has several features to enhance its utility for inhaler testing including [178];

- Particles deposited on collection cups, which are held in a tray from the impactor as a single unit, facilitating quick turn around times if multiple trays are used.

- The user can add up to 40 ml of any appropriate solvent directly to the cups for more efficient drug recovery.

- MOC can capture very fine particles normally collected on the final filter.
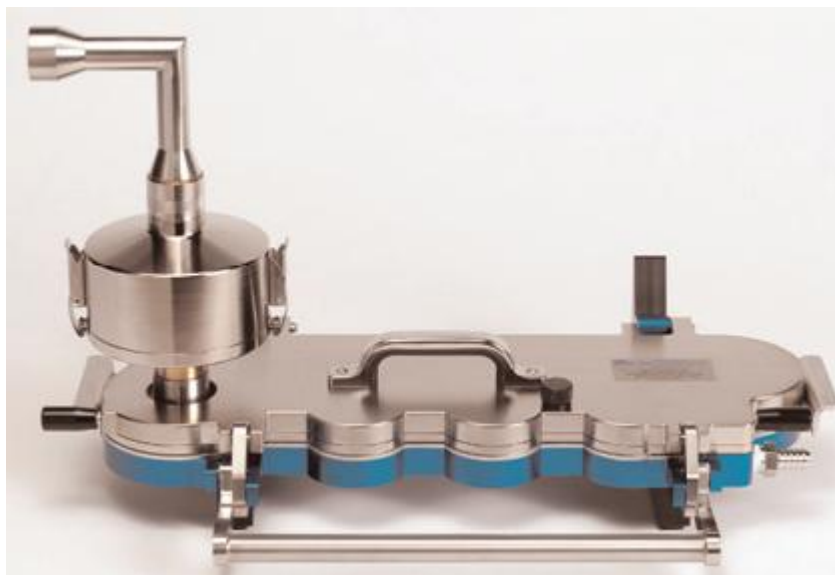
Figure 2.21. *Next Generation Impactor* [178].

There are however, in general number problems associated with the impaction techniques. These include;

1- Loss of the sample via impaction to the walls of the stages but this problem is reduced with modern impactors [183].

2- Re-entrainment errors can occur when the plates are overloaded with the sample upon using large doses.

3- Particle bouncing, although this can be alleviated by using glass filters instead of the metal plates, spraying the collecting plates with a small amount of silicone oil, or dipping the plates in oil that has been diluted with a solvent [184].

4- Data from impaction techniques do not give an actual prediction for the *in-vivo* deposition. This may be attributed to the highly complex anatomy of the respiratory tract along with the effects of temperature, humidity, and pathological changes.

2.5.4.1.2. Microscopy techniques

(1) Optical microscope

Microscopy is an important tool for particle sizing using manual, semi-manual technique or automatic techniques. It is versatile, user-friendly, and relatively inexpensive. The microscope usually consists of an eyepiece, objective, stage, condenser and a telescoping drawtube for adjusting of the distance of the eyepiece to the objective and provides a direct examination of the particles usually by means of a linear scale or globe-and circle graticules. The inability to provide a sharp image of two objects located at different distances and the appearance of point objects as fuzzy discs surrounded by diffraction rings at high magnifications are considered as the main limitations of the optical microscope [185, 186].

(2) Scanning electron microscope (SEM)

This was discussed in detail in section 2.4.2.1.

(3) Image analysis

This technique includes taking digital images of particle samples, converting them to binary data, designating the key dimension, and deriving particle-size data. Image analysis has the potential to account for the particles shape, though the images are only 2-dimensional representations of three dimension particles. Another limitation of this approach is low capacity, since individual particles are imaged so a long time may be required. The image analysis technique is illustrated schematically in Figure 2.22 [185, 186].
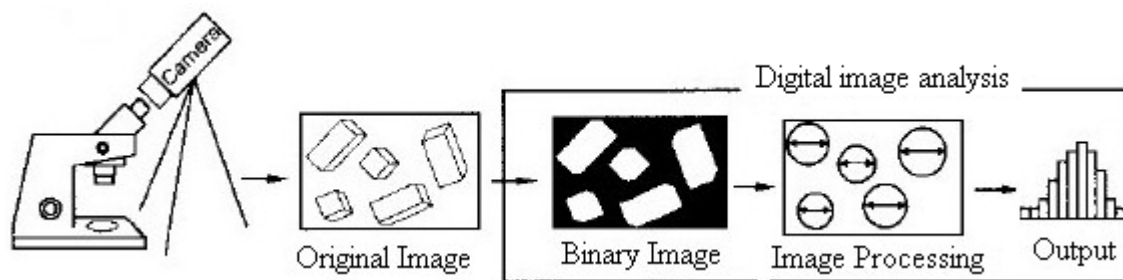
Figure 2.22. *Schematic diagram represents the digital image analysis* [185].

2.5.4.1.3. Laser diffraction technique

This method is considered as one of the most important, and reproducible, techniques used for the particle size determination [185]. The technique is based on the fact that the particles passing through a laser beam will scatter light at an angle that is directly related to their size (Figure 2.23). As particle size decreases, the observed scattering angle increases logarithmically. In laser diffraction, particle size distributions are calculated by comparing a sample's scattering pattern with a suitable optical model, which assumes that the particles being measured are spherical [185]. However, laser diffraction has some practical limitations such as measurements with non-spherical particles which tend to be oversized and have exaggerated size distribution due to deviation from the spherical models used in the data processing. In addition, a poor particle size distribution may be observed for dry powders with agglomerated particles [185, 186].
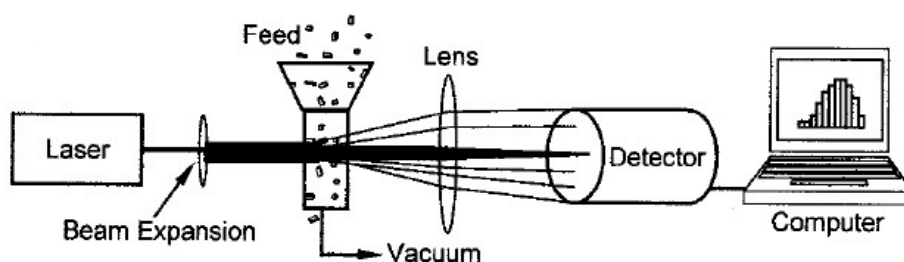
Figure 2.23. *Schematic diagram represents particle sizing via laser diffraction* [185].

2.5.4.2. In-vivo methods

2.5.4.2.1. Pharmacokinetic methods

Many pharmacokinetic methods have been developed to identify the amount of the drug delivered to the lungs following an inhalation. The pharmacokinetic evaluation can be done by a variety of direct approaches, including the determination of drug levels in the lung itself. Such studies have been performed in lung cancer patients who inhaled the drug before resectomy of sections of the lung. Determination of drug levels in a variety of patients at different time points enables the assessment of pulmonary kinetics. Such studies, however, show high variability and can be affected by pathological changes in the lungs of the cancer patients [187]. Other approaches determined the pulmonary fate of drugs by analyzing drug concentrations in the bronchopulmonary lavage fluid, however this methodology has not been frequently used as it is tedious, and difficult to standardize. Alternative methods such as the use of microdialysis offers a complementary procedure to these methods [186].

The more established way of assessing the fate of a drug after inhalation has been achieved by standard pharmacokinetic approaches using plasma–concentration time profiles. It was reported [188, 189] that following inhalation up to 20 % of the dose is delivered to the lungs whilst the majority is swallowed. The proportion of the dose delivered to the lungs, will be cleared either by the mucociliary clearance or by absorption through the airway wall into the systemic circulation (Figure 2.24). The plasma concentration–time profiles obtained after drug inhalation might therefore include contributions from both pulmonary and gastrointestinal absorption and thus provide valuable data which predict the extra-pulmonary side effects [188]. To identify the effective lung dose, methods which differentiate between drug delivered to the systemic circulation via the oral and inhaled routes, are needed particularly for the drugs with high oral bioavailability.

The oral charcoal block technique or sampling during the lag time of the absorption phase has been used for this purpose [188, 189]. These approaches are not necessary for the drugs with poor oral absorption (e.g. sodium cromoglycate) or when the first pass effect is substantial (e.g. fluticasone) because the drugs can only enter the circulation via the lungs [186, 189]. The total systemic delivery can also be assessed using urinary excretion, especially if the molecules are polar and basic. Both physicochemical properties prevent the passive tubular reabsorption within the kidney so the urine pH does not have to be controlled [188].
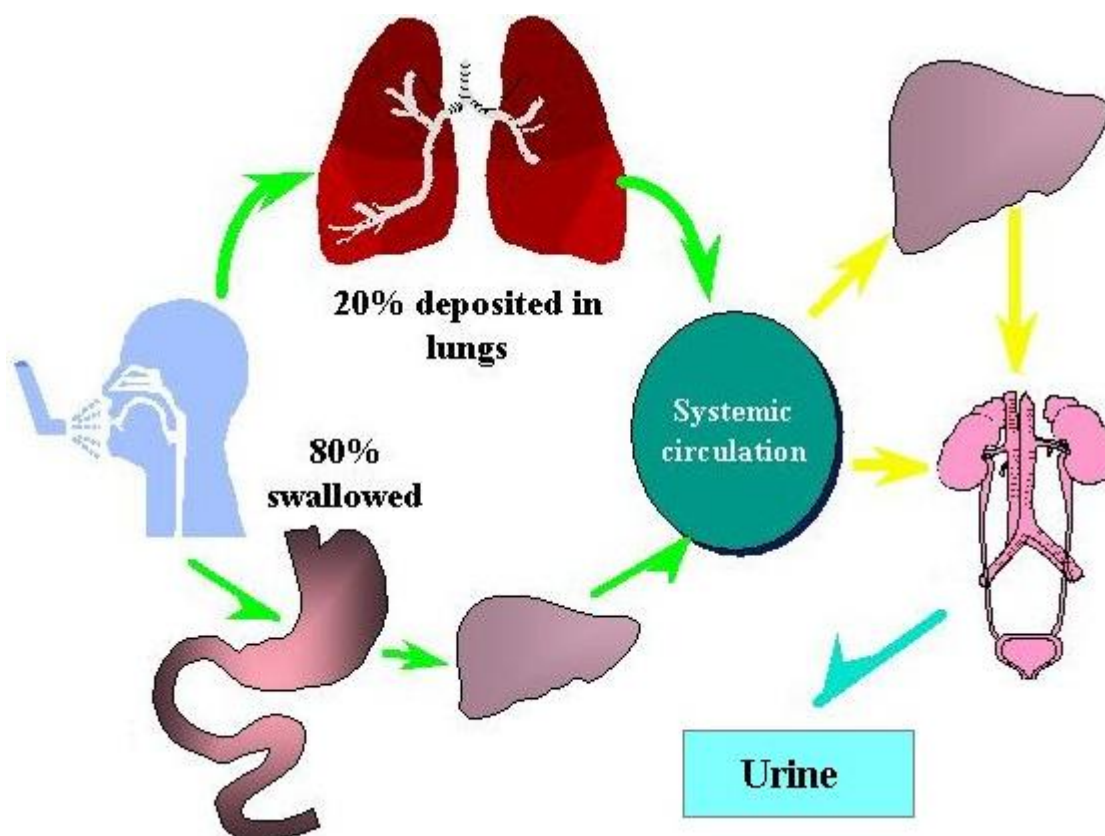
Figure 2. 24. *Diagram represents the pharmacokinetic fate of a drug following inhalation* [189].

(1) The charcoal block technique

In order to recognize the lung deposition of an inhaled drug accurately, the gastrointestinal absorption of the orally swallowed fraction of the inhaled product can be blocked by giving the patient concomitant doses of charcoal to adsorb this drug fraction. In this technique, the mouth is thoroughly rinsed with charcoal slurry, which is swallowed immediately before drug inhalation. Charcoal administration is repeated 5 min, 1h and 2h after drug inhalation [190]. Great care must be taken to ensure that for a given drug under the specific conditions of the clinical trial, a complete block of the oral absorption is actually observed. This approach has been used for determination of different drugs such as budesonide [190] and other glucocorticoids. Urinary excretion of drug following the oral administration of charcoal has also been reported to identify the total effective lung dose [191].

(B) Utilizing the absorption lag times

It is an important method that can be also used to determine the pulmonary absorption of inhaled drugs [192, 193]. For example, after oral administration of salbutamol, the maximum urinary excretion rate is reached after 2 h; by contrast, for a lung-deposited drug, the maximum rate is reached after 30 min. Therefore, urine sampling up to 30 min after inhalation of salbutamol gives an indication of the fraction of the dose deposited in lung and can therefore be used to assess the pulmonary absorption of the drug. However, these methods are less reliable because variability in absorption rates will significantly affect the results [194]. The oral charcoal block technique or sampling during the lag time of the absorption phase are considered as a guide for determination of the relative amount of the inhaled dose, which has the potential to produce a clinical effect within the airways. Therefore, these approaches are useful to investigate the concordance between two inhaled products or differences between inhalation techniques.

2.5.4.2.2. Imaging techniques to assess pulmonary drug deposition

(1) Gamma scintigraphy

This method is a helpful technique in determining drug pulmonary deposition. It was first used during diagnostic testing and then extended to pharmaceuticals in the 1970s. Originally, radio-labeled Teflon particles [195] were used. Recently, versions of this techniques have been developed to attach the gamma emitting radionuclide ^{99m}Tc (99 m technetium) to either a component of the formulation or the drug molecule [196]. Immediately following inhalation of the radiolabeled aerosol, images of the lung are recorded by a gamma camera. These images provide an immediate idea of where the drug is deposited, depending on the fact that the radioactive label follows the drug with high reliability. However conventional planar gamma cameras can only produce a two-dimensional pictures and it cannot differentiate between the conducting airways and alveolated parts of the lung or between certain overlying structures. Three-dimensional imaging methods (SPECT and PET) have recently been introduced which overcome all these problems [195, 196].

(2) Single photon-emission computed tomography (SPECT) and positron-emission tomography (PET)

SPECT and PET have been used to examine the fate of inhaled drugs [197-199]. An advantage of these methods is that they can be used to construct three-dimensional images. Compared with planar gamma scintigraphy, these techniques allow the determination of the pulmonary deposition with a higher degree of resolution and differentiate between the central and peripheral lung deposition as well as the pulmonary and gastrointestinal deposition. On the other hand, PET permits the drug to be labeled itself without changing its chemical structure and in that way it can overcome some of the drawbacks of scintigraphy. The positron emitters used in PET include ^{11}C,

[13]N, [15]O and [19]F. This technique has recently been used to study the deposition of fluticasone [200]. The main disadvantages of this method are that the positron emitters used so far have short half-lives and the method is very expensive.

2.6. Inhaler devices

Since 1930 various types of inhaler devices have been used to deliver the medical aerosol particles in the required size range for lung deposition. Three basic types of commercial drug delivery systems are available. These are nebulizers, pressurized metered dose inhalers (p-MDIs), and dry powder inhalers (DPI). p-MDIs are the most frequently used as they have demonstrated value in therapy. In Europe, especially Scandinavian countries DPIs, are frequently prescribed [7].

2.6.1. Nebulizers

Nebulizers have been used in inhalation therapy since early 20th century [201]. Nebulizers are used for both drug solutions and suspensions. They are commonly used for the treatment of hospitalized or disabled patients as well as for children and infants [202]. In a few cases, nebulizers may be used for local drug delivery to the trachea [202]. There are two general types of nebulizers available.

(1) Ultrasonic nebulizer

Ultrasound waves are produced in an ultrasonic nebulizer chamber by a ceramic piezoelectronic crystal that vibrates when electrically excited. These set up high-energy waves in the solution within the device chamber of precise frequency leading to creation of an aerosol cloud at the solution surface [7].

(2) Air-jet nebulizer

In this nebulizer the compressed air is forced through an orifice, and an area of low pressure is formed where the air-jet exits. A liquid is withdrawn from the perpendicular nozzle (the Berboulli effect) to mix with the air-jet to form droplets (Figure 2.25). Only the smallest droplets in the desired range are able to follow the streamlines of air and pass the baffle, which facilitates the formation of the aerosol cloud. Larger droplets impact on the baffle and return to the liquid reservoir [7, 202].

The main disadvantages of nebulizers are their poor lung deposition, the long inhalation time, the high residual amount of the drug, and the need of a power supply. However recent generations of the nebulizers have improved technology and examples include the AeronebGO, e-flow, and Micro Air [7].
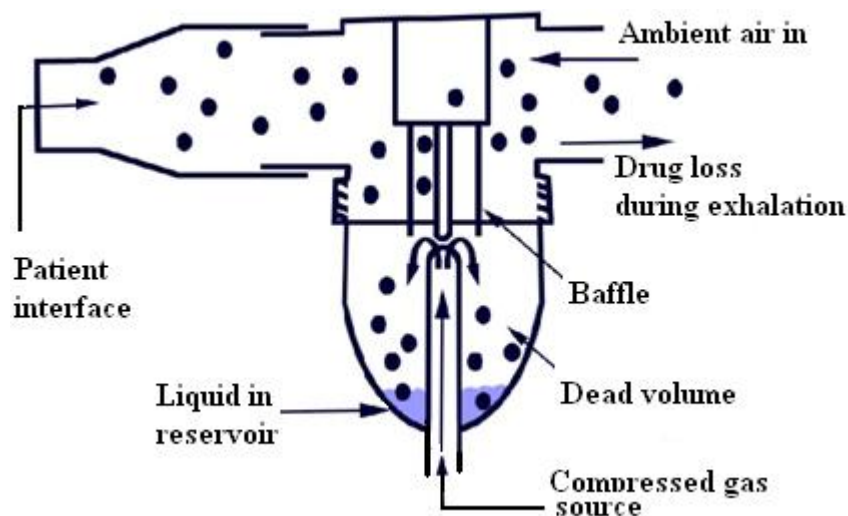
Figure 2. 25. *Schematic diagram of air jet nebulizer*
(adapted from www. img.medscape.com)

2.6.2. Pressurized metered dose inhalers

Pressurized metered dose inhalers (p-MDIs) are based on a spray-can principle, such as used for hair sprays [7]. The p-MDI consists of four basic parts; container, metering valve, actuator, and mouthpiece (Figure 2.26). There are two types of p-MDI formulation; suspension and solution. The propellant used in p-MDI formulation has a dual function. Firstly, it works as a dispersion medium for the drug and the excipients. Secondly, it serves as an energy source to eject the formulation from the valve as droplets [7] which evaporates as soon as it leaves the device. One of the main disadvantages of the p-MDI is the required co-ordination of the dose release with the breath inspiration. This has been shown to be difficult with large numbers of asthmatic patients including children and elderly people [203] but the development of spacers makes the p-MDI easier to use [204], as they increase the amount of the drug available to the lung by decreasing the impaction of the drug with the oropharynx. There are still inherent problems in the basic design of a p-MDI involving propellant, surfactants, and lubricants used in the formulation. Some lubricants and surfactants can produce an irritant effect. Chlorofluorocarbons (CFC's) were the most commonly used propellant in p-MDI but their harmful effect became clear when the ozone hole was discovered over Antarctica. As a result CFC consumption was reduced and different p-MDIs have been redeveloped using alternative propellants based on hydrofluoroalkanes [205].
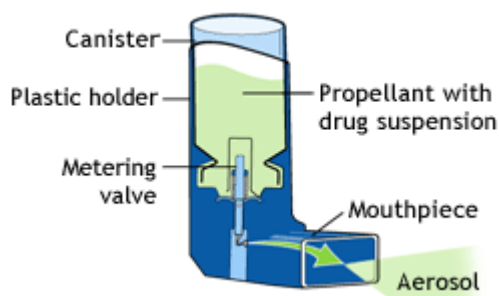
Figure 2. 26. *Pressurized metered dose inhaler (adapted from*
http://www.asthma.ca/adults/treatment/meteredDoseInhaler)

2.6.3. Dry powder inhalers

The main alternative to the p-MDI is the breath-actuated dry powder inhaler (DPI). DPIs are typically designed to produce a metered quantity of powder in a stream of air drawn through a device by the patient own inspiration. The DPI was first introduced in 1939, in a US patent by Stuart [206], who gave a description of what is called the first DPI. The patent describes a device, which had been designed to aid the inhalation of aluminum dust for the chelation of inhaled silica. However, the device was never commercialized. In 1949 a patent by Fields, described the first DPI for the administration of pharmaceuticals, the so-called Aerohaler. It was the first commercially available DPI for the delivery of isoprenaline sulphate [206]. There was then considerable interest in these devices especially when the harmful effects of CFC, as propellant in p-MDI on the environment were observed. However, although these devices do overcome the need for coordination of actuation and inspiration because they are breath actuated, this operation is also considered one of their disadvantages. They are classified into two types; single dose devices (e.g Spinhaler, Rotahaler) and multidose DPI. Multidose DPI are divided into two different types of designs; the reservoir systems (Turbohaler[®], Ultrahaler[®], Clickhaler[®], Easyhaler[®]) and the multiple unit-dose inhalers (Diskhaler[®], Diskus[®]) (Table 2.5) [207, 208].

Table 2. 5. *Dry powder inhalers currently available in the market*

Device	Company (Country)
Single dose factory-metered	
Spinhaler®	Fisons (UK)
Rotahaler®	GlaxoWellcome (UK)
Cyclohaler	Pharmachemie (NDL)
Aerolizer	Novartis (Switzerland)
Aerohaler	Boehringer-Ingelheim (Germany)
Multidose factory-metered	
Diskhaler®	GlaxoWellcome (UK)
Diskus®	GlaxoWellcome, (UK)
Multidose patient/device-metered	
Turbohaler	AstraZeneca (Sweden)
Ultrahaler®	Rhone-Poulenc Rorer (France)
Clickhaler®	ML Laboratries (UK)
Easyhaler®	Orion Pharma (Finland)
Pulvinal	Chiesi (Italy)

2.6.3.1. Single dose inhalers

The concept of the first single-dose DPI, the Spinhaler® (Fisons, Loughborough, UK) was described in early 1970s by Bell et al [209]. This device was developed for the administration of powdered sodium cromoglycate, which is used as a topical, non-steroid preventer for allergic asthma. A mixture of the drug and a bulk carrier is pre-filled into a hard gelatine capsule and then loaded into the device. Following activation, where the capsule is pierced, the patient inhales the dose by the inspired air (Figure 2.27).
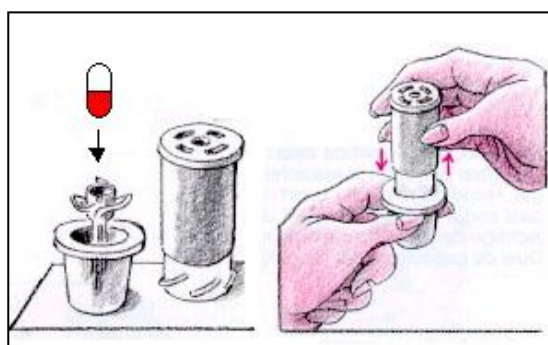
Figure 2. 27. *Diagram represents Spinhaler® (Fisons, Loughborough, UK)*

This device was suitable in the treatment of children and elderly patients, as it avoided the problems of coordination by utilizing the patient's inspiratory flow for the energy required to dispense the particles from a pierced capsule [207, 208]

The preference of using single dose DPI was expanded with the introduction of devices that were easier to manipulate such as the Rotahaler[®] (GlaxoWellcome, Ware, UK) [210]. The Rotahaler[®] has been developed for the delivery of salbutamol, and beclomethasone dipropionate powders. Here, the drug mixture is again filled into a hard gelatin capsule and the capsule is inserted into the device where it is broken open and the powder inhaled through a screened tube [211]. Over the last few years several new single-dose DPIs have been developed having similar designs such as; Foradil Aerolizer (Novartis/Schering-Plough) and Spiriva HandiHaler (Boehringer Ingelheim/Pfizer).The main disadvantage of single dose DPIs is the difficulty of loading the capsule, especially for elderly patients and those undergoing an asthma attack who require immediate delivery of the drug this led to the innovation of multidose DPIs [212].

2.6.3.2. Multidose inhalers

The development of multidose DPIs has been pioneered by Darco in 1988 who produced the Turbuhaler[®] (Astrazeneca, Lund, Sweden) [213] which was really the first true metered-dose drug powder delivery system. This inhaler includes up to 200 doses in the drug powder reservoir, which can be dispensed in the dosing chamber by a simple back-and- forth twisting on the base unit. The Turbuhaler[®] has been used to deliver carrier free particles of the β- agonist, terbutaline sulphate as well as the steroid budesonide [214]. The main drawbacks for the Turbuhaler[®], is its variable delivery at different flow rates and its high internal resistance. The optimum aerosol dispersion threshold for the Turbohaler[®] occurs at a peak inhalation flow rate of at least 60 L min^{-1} [211]. Studies have shown that young children and patients with COPD [215, 216] have

problems in achieving the minimum required inhalation rate through a Turbohaler[®]. It has been reported that newer multiple dose reservoir devices such as the Easyhaler[®] (Orion Pharma, Kuopio, Finland) demonstrate a more consistent and flow rate-independent delivery system than the Turbohaler[®] when tested in-vitro [217, 218].

Easyhaler[®] (Orion Pharma, Kuopio, Finland) is a multiple dose reservoir DPI. It was designed to deliver at least 200 preloaded doses of sulbutamol or beclomethasone dipropionate. Shaking aids a dose (drug and carrier) being deposited from the powder reservoir to the dosing cup. The device actuation rotates the filled dosing cup into the inhalation channels where turbulent airflow breaks the drug mixture up into a fine particle dose, which is then deposited into the patient's lung during the inhalation (Figure 2.28). A dose counting mechanism is provided by the dose counter which allows patients to see if they have loaded a dose and prevent double dosing or the use of empty device [215].
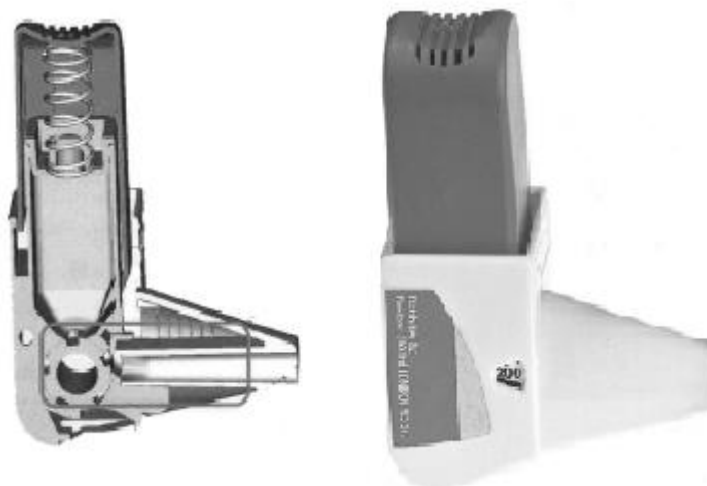
Figure 2. 28. *Easyhaler[®] (Orion Pharma, Kuopio, Finland)* [215]

The Easyhaler® more closely demonstrates the characteristics of an ideal inhaler than its competitors [215] whilst being available at a price comparable to that of a p-MDI. Consistency in the fine particle dose of the Easyhaler® is the main clinical advantage compared with its competitors. Studies have shown superior consistency both versus other inhalers and within a random sample of the Easyhaler® [217, 218]. This device also performs consistently irrespective of inspiration rate, which is in contrast to flow rate-dependent inhalers [215]. Therefore, patients can receive the same dose every time they used their Easyhaler®, providing the ability to prescribe salbutamol, beclometasone and, more recently, budesonide in a DPI to children and COPD patients with low inspiration rates. A study of 120 children using the Easyhaler® measured the peak inspiratory flow. Only four achieved > 28 L min^{-1}, but even in patients with these low flow rates, use of the Easyhaler® provided the required clinical response [219]. Equivalent therapeutic responses have been shown in various studies following the use of the Easyhaler® versus p-MDI, or other DPIs in the market [220, 221]. Pharmacological equivalence to the Turbuhaler® shows the possibility for changing to the Easyhaler® [215, 222]. Furthermore, a meta-analysis of the opinions of asthmatic patients about different inhaler devices showed the Easyhaler® to be the preferred device when compared with pMDI or other DPIs [215].

On the other hand the multiple unit-dose inhaler was first developed by GlaxoWellcome which introduced Diskhaler® [207, 208]. It has been used for the delivery of both the short acting β-agonist sulbutamol, as well as the long acting salmeterol. In addition, the steroids, beclomethasone dipropionate and fluticasone propionate are also available in disks. This device has a circular disk that contains a number of powder charges (four or eight) depending on a typical dosing schedule. The doses are stored in separate aluminium blister reservoirs, thus ensuring the integrity of the powder blend to be protected from moisture attack. On priming the device, the

aluminium blister is pierced and the powder charge is dropped into the dosing chamber. One of the advantages of the Diskhaler® is the ability to see the remaining doses through a window on the surface. However, this device has a limited commercial success [207, 208] mainly because it held only a few doses per disk and also the loading difficulty. Further improvements in patient convenience and the ease of use were included into the next generation of a factory-metered doses inhaler, called the Diskus® (GlaxoWellcome, UK) in the mid-1990s. It represents a further development of the Diskhaler® approach, with pre-metered doses sealed in blisters on a foil strip. The use of coiled strip rather than a disk, allows 60 doses of medication to be contained within the device [207, 208]. Metered dose inhalers produce high quality, and consistent dosing performance as well as efficient protection for the drug powder from moisture, but they are more expensive to the manufacturer [212, 213]. Generally multidoses reservoir devices are becoming more common because they have simple design, which are also cheaper to produce than multiple unit-dose inhalers. However some of them may show dose variability because of inconsistent powder dispensing or reduced moisture protection of the drug powder [223]. Therefore, accurate dose metering for this type of inhaler requires careful manipulation of the device by the patient [207].

DPIs are generally described as breath actuated devices use the inspiratory flow as the energy source for dispersion and delivery of the particles into the airflow. The DPIs currently available have different airflow resistances that govern the flow rates, which might be generated from them for a given level of inspiratory effort from a patient. This process follows an inverse relationship; the higher the resistance, the lower the flow rate, the higher the level of inspiratory efforts from the patient required to deliver the dose out of the device. This is considered the major disadvantage of DPIs especially for the treatment of patients with low inhalation flow rate [207, 223, 224]. The main advantages and disadvantages of DPIs are summarized in Table 2.6.

Table 2. 6. *Advantages and disadvantages of DPIs versus p-MDIs* [207].

Advantages of dry powder inhalers	*Disadvantages of dry powder inhalers*
Environmental sustainability propellant free design	Efficient drug delivery dependent on the patient's inspiratory flow rate and the device resistance
Little or no need for synchronising the dose release with the patient inspiration	Potential for problems in dose consistency
Less potential for formulation problems	Development and manufacture processes are more complex and expensive
Less problems associated with the drug stability	The drug is not highly protected from the environmental effects such as moisture

2.6.3.3. Carrier material

DPIs are often composed of fine drug particles and inert coarse carrier particles. The carrier particles are often used to aid the mixing of the drug particles, enable filling of every small doses in capsules or blisters, improve powder flow and to facilitate drug dispersion during inhalation [225-227].

The adhesion between carrier and drug must be sufficient for the blend drug/carrier to be stable, and the adhesive forces between drug and carrier particle have to be weak enough to enable the release of drug from carrier during patient inhalation [227]. Then, the drug particles will be able to reach the lungs. Interactions between particles are mainly dependent on their physicochemical characteristics such as particle size, shape, surface morphology, contact area, and the hygroscopicity [228, 229].

Therefore, any factor that affects drug-carrier interaction will have an impact effect on the delivery and deposition of the drug. For example, increasing the surface smoothness of the lactose carrier particles was shown to improve the potentially respirable fraction of salbutamol sulphate from the Rotahaler® [225-227] and this was attributed to lowered

adhesion forces between the drug and carrier particles with a smooth surface.

The shape of the carrier particles as well as the carrier surface smoothness have an important effect in determining the dispersion and deaggregation of the drug [227]. The effect of particle size of the carrier on drug deposition is also reported in different articles [230]. Fine particles of ternary components, such as magnesium stearate and L-leucine, were found to improve drug delivery from DPIs by reducing inter-particulate forces between the drug and carrier particles. More recently, the addition of fine particles of carrier to dry powder formulation was also shown to enhance the dispersion and deposition of drug particles [227]. The finer particles tend to occupy the high energy binding sites on the coarse carrier material, leaving lower energy sites available for the drug. Therefore the best dry powder performance will be achieved when the formulation contain both coarse and fine carrier particles at optimal proportions [225-227].

At present glucose and mainly lactose are the only carriers used in DPIs. The advantages of monohydrate lactose are its low toxicity, wide availability and its relatively low price. However its reducing sugar function; which prevents its use with certain drugs may be considered as its main disadvantage. Several studies on technological properties of dry powder inhalers provide alternatives to lactose such as mannitol [229].

Chapter 3

Development and validation of HPLC method for the determination of theophylline and other related methylxanthines and methyluric acids in urine samples and aqueous solution

3.1. Introduction

Methylxanthines such as theophylline (TP) and caffeine (CA) are commonly taken by patients as over-the-counter drug mixtures for pain, cold and cough. In addition, they are found in many plant species and food products including coffee, tea, chocolate, cola drinks and many other beverages. As a drug TP is a bronchodilator used in the treatment of acute and chronic asthma with a narrow therapeutic range (10-20 μg ml^{-1}). Similarly CA is also used to alleviate neonatal apnoea to relieve bronchial spasm, and in the therapy of asthma. The analysis of these compounds in body fluids is therefore important for monitoring of asthma, or neonatal apnoea, in the non-invasive assessment of various isoforms of cytochrome P-450 (CYP) activity [80] and also to detect the drug abuse in athletics [231].

HPLC is the most popular technique used for the determination of these compounds in biological samples (Table 2.1). However, many of the HPLC methods for CA or TP and their metabolites show interference from caffeine metabolites and especially paraxanthine [78]. Therefore, the number of HPLC methods, which report the simultaneous determination of TP, and CA and their metabolites in one run is somewhat limited. Thus, in this study the goal was to develop a simple and fast method for efficient separation of theophylline and its related compounds, which allow straightforward quantitative analysis of these compounds in either urine matrix or aqueous solutions. Two methods, which are increasingly being explored to achieve separation and high resolution of drugs in a short experimental period; ultra-performance liquid chromatography (UPLC^{TM}) and HPLC using monolithic columns [51]. UPLC uses particle-packed columns with sub-2.0 μm packing materials and pressures up to approximately 1400 bar. However, in this process special high quality equipment is obligatory to meet these requirements [16]. Monolithic packed columns, on the other hand allow for flow rates up to 9.9 ml min^{-1} with backpressures lower than

400 bar. Therefore, monolithic columns can be used with conventional HPLC equipment [134] and can achieve a high-speed separation without loss of column efficiency [232]. The monolithic column consists of one piece of either an organic polymer or silica with a continuous homogenous phase instead of a packed bed with individual particles. The column has a total porosity of over 80 % v/v, fast mass transfer and low-pressure resistance which enables rapid separation [147]. Packed and monolithic silica columns have been compared in different applications, and the results indicated that the porous rod provides equivalent efficiency when compared to microparticulate columns but the monolith generally produces faster separation [157, 160].

3.2. Materials and Methods

3.2.1. Instruments

3.2.1.1. High performance liquid chromatography

(1) Pump and auto sampler

Chromatographic analyses were performed by using Hewlett Packard (HP) 1050 system; with a multiple solvent delivery system containing an autosampler with a variable injection loop.

(2) Detectors

Variable wavelength UV-visible detector HP 1050 series has been used in the study. All connections from the autosampler to column and from the column to detector were made from stainless steel with 0.005 i.d. All connection tubes were made as short as possible to minimize extra-column band broadening. All end fittings used were carefully chosen to give a zero dead volume.

(3) Integrator

Prime Multichannel Data Station (version 4.2.0) (HPLC Technonlgies, Herts, UK)

(4) HPLC columns and Guard columns

• Two Monolithic columns RP-18e 100 × 4.6 mm (Merck, Darmstadt, Germany) from two different batches (Batch 1. OB452773, Batch 2. HX754226) were used. Columns specifications as supplied from the manufacturer were as follow;

Macropore size $2 \ \mu m$

Mesopore size   13 nm (130 Å)

Pore volume   1 ml/g

Surface area $300 \ m^2/g$

Surface modification C_{18} endcapped

• Six traditionally available particulate columns were used for the comparison with the monolithic column. The columns details; manufacturer, dimensions, the particle size and the pore sizes, are listed in Table 3.1.

Table 3. 1. *Details of the HPLC columns used in the study*

Columns	Company	Dimensions (mm)	Particle size (μm)	Pore size (Å)
Symmetry-C_{18}	Waters, Milford, USA	150 × 4.6	3.5	100
Hypersil BDS-C_{18}	Shandon Scientific, Cheshire, UK	150 × 4.6	5	100
ACE- C_{18}	ACT, Aberdeen, UK	150 × 4.6	5	100
Nucleosil-C_{18}	Hichrom Ltd, Berkshire, UK	150 × 4.6	3	150
Nucleosil-C_{18}	Hichrom Ltd, Berkshire, UK	150 × 4.6	5	100
Hichrom RPB-C_{18}	Hichrom Ltd, Berkshire, UK	150 × 4.6	5	150
Zorbax Eclipse XDB-C_8	Agilent Technologies, CA, USA	150 × 4.6	5	80

•The performance of a novel stationary phase platinum ^{TM} C_{18} 3 μm column 100×4.6 mm (Grace® Davison Discovery Sciences, Lokeren, Belgium) was tested and compared with the monolithic column. Two different columns were tested in this study; their serial numbers were; 608121210, and 608121211, respectively.

• For the protection of the analytical columns during working with urine samples Phenomenex C_{18} (4×3 mm i.d.) security guard cartridge system (Phenomenex, Torrance, USA) was used.

3.2.1.2. Solid phase extraction (SPE)

(1) SPE Cartridges

SPE octadecyl (C_{18}) disposable extraction columns, 1 ml/100mg, (J.T. Baker Inc., Phillipsburg, USA).

(2) SPE vacuum manifolds

Vacmaster international sorbent technology, Ltd.

Vac-Elut analytichem international (Harbour city, CA, USA)

3.2.1.3. General Laboratory Instruments
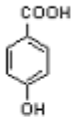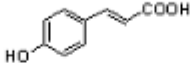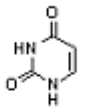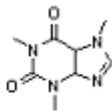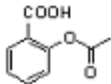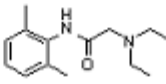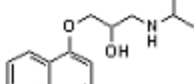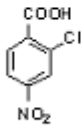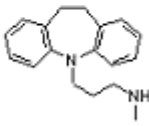
• Utrasonic bath (Decon laboratories, Hove, UK)

• Syringe filters 0.2 μm pore size (Scientific Resources Inc., NJ, USA) for filtration of the samples after solid phase extraction before injection in HPLC instruments

• Nylaflo® nylon membrane filter, 47 mm, 0.45 μm pore size (Pall Gelaman Sciences, Michigan, USA) for filtration of the mobile phase.

• Metler Toledo (AL) analytical balance (Leicester, UK)

• pH meter Accumet AB10 Basic (Fisher Scientific, Leicester, UK)

• Nitrogen-drier (Fisher Scientific, Leicester, UK)

• ELGA ultra-pure water dispensing system (High Wycombe, UK)

3.2.2. Materials

3.2.2.1. Analytes

• Basic and acidic test compounds were used for the initial studies of the performance of monolithic column in comparison with different traditional packed columns. Analytical grades of all the studied drugs were purchased from Sigma-Aldrich Inc. (St. Louis, MO, USA). Structures and pKa values of each solute are listed in Figure 3.1.
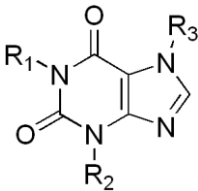
Figure 3. 1 *Structures and (pKa) of the studied acidic and basic drugs.*

• Methylxanthines, methyluric acids, and the internal standard; 8-chlorotheophylline used in this study were obtained from Sigma-Aldrich Inc. (St. Louis, MO, USA).

Figure 3.2 shows the chemical structure and abbreviations of all the tested methylxanthines and their metabolites.

Figure 3. 2. *Chemical structures and abbreviations of the studied methylxanthines and methyluric acids.*

Methylxanthines			
R₁	**R₂**	**R₃**	
CH_3	H	H	1-Methylxanthine (1-MX)
H	CH_3	H	3-Methylxanthine (3-MX)
CH_3	CH_3	H	1,3-Dimethylxanthine (Theophylline;TP)
CH_3	H	CH_3	1,7-Dimethylxanthine (Paraxanthine; PA)
H	CH_3	CH_3	3,7-Dimethylxanthine (Theobromine;TB)
CH_3	CH_3	CH_3	1,3,7-Trimethylxanthine (Caffeine; CA)

Methyluric acids

R₁	**R₂**	**R₃**	
CH_3	CH_3	H	1,3-Dimethyluric acid (1,3-DMU)
CH_3	H	CH_3	1,7-Dimethyluric acid (1,7-DMU)
CH_3	CH_3	CH_3	1,3,7-Trimethyluric acid (1,3,7-TMU)

3.2.2.2. Pharmaceutical formulations

• **Nulein® SA tablets** (3M Health Care Limited, Loughborough, England) labelled to contain 175 mg of theophylline BP / tablet.

• **Uniphyllin® prolonged release** harmaceuticals Ltd, Cambridge, UK) labelled to contain 200 mg of theo
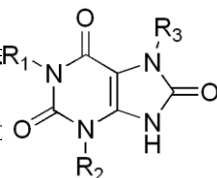
• **Slo-Phyllin**® **capsules** (Merck Sante s.a.s., Lyon, France) labelled to contain 60 mg of theophylline anhydrous / capsule.

3.2.2.3. HPLC mobile phase

• HPLC-grade acetonitrile, and methanol (Fisher Scientific, Loughborough, UK).

• Spectrophotometric grade trifluroacetic acid (TFA) (Alderich Chemical Co. Inc., Steinheim, Germany).

• Potassium dihydrogen phosphate ASC reagent ≥ 99% (Sigma-Aldrich, Inc.)

• Ortho-phosphoric acid and sodium hydroxide (BDH, Poole, UK)

• Analar grade sodium acetate anhydrous (BDH)

3.2.3. Methods

3.2.3.1 Preparation of buffer solutions

An accurately weighed amount of the desired buffer salt was transferred into a volumetric flask, and then dissolved in about 60 % v/v of double distilled water before being made up to the exact volume. The pH of the buffer was then adjusted using appropriate acid or alkali. The buffer solution was then filtered through a 0.45μm membrane filter. The pH meter was calibrated using commercially available buffers.

3.2.3.2 Preparation of mobile phase

In order to minimize the volume error that may occurs upon the addition of the organic solvents to aqueous solutions, they were measured separately and then mixed together. The mobile phase was then filtered through a 0.45μm membrane filter and degassed using ultrasonic bath under vacuum for 10 min.

3.2.3.3. Preparation of the aqueous standard solution of acidic and basic drugs

The standard stock solution of each test compound was dissolved in a methanol: water mixture (70: 30 v/v) at concentration 1.0 mg ml^{-1}. A mixture solution contain 100 μg ml^{-1} of each drug was prepared from the stock solution with further dilutions by the mobile phase.

3.2.3.4. HPLC analysis of the acidic and basic mixtures

The HPLC methods for the separation of acidic and basic test mixtures used in the initial study were based on those published by Wang *et al* [147, 233]. However, the mobile phase compositions were modified to adapt the studied tested compounds. The following are the optimized HPLC conditions used for separation of the acidic and basic compounds.

(1) Optimized HPLC conditions for separation of acidic compounds

Stationary Phase:	Monolithic and all packed columns mentioned in Table 3.1. as well as the platinum column were tested
Mobile phase:	Acetonitrile: 0.1% Trifluroacetic acid (TFA) (35: 65 % v/v)
Flow rate:	1 ml min^{-1}
Temperature:	Room temperature
Injection volume:	20 μl
UV- Detection:	220 nm

(2) Optimized HPLC conditions for separation of basic compounds

Stationary Phase: Monolithic and all packed columns mentioned in Table 3.1. as

well as the platinum column were tested

Mobile phase: Methanol: 25mM potassium dihydrogen phosphate buffer (pH 6)

(80: 20 % v/v)

Flow rate: 1 ml min^{-1}

Temperature: Room temperature

Injection volume: 20 μl

UV- Detection: 220 nm

3.2.3.5. Preparation of the stock solution of the internal standard

The stock solution of the internal standard (IS); 8-chlorotheophylline was prepared at

concentration of 1mg ml^{-1}. Working standard solutions were prepared by further

dilutions with the mobile phase or urine matrix.

3.2.3.6. Collection of urine samples

Blank urine samples were obtained from 5 healthy volunteers after 5-days on

methylxanthines-free diets. All samples were pooled, frozen and stored at -20°C until

analysis. Standard freeze/thaw procedures were carried out.

3.2.3.7. Preparation of standard solutions of methylxanthines and methyluric acids

An accurately weighed amount of each drug was dissolved in appropriate volume of

methanol: water (30:70 % v/v) mixture, to provide a stock solution containing 1.0 mg

ml^{-1}. Few drops of sodium hydroxide (1M) were added to some solutions for complete

solubilization. From this stock solution, working standards were prepared by serial

dilutions using either the mobile phase or urine matrix. Aqueous stock and working solutions were stored in the fridge at temperature below 4°C in well-closed containers. While the spiked urine samples were stored below –20 ºC in well-closed, light resistant containers prior to analysis.

3.2.3.8. Preparation of sample solutions of theophylline formulations

For Nulein®, or Uniphyllin®, twenty tablets were accurately weighed, finely powdered and mixed thoroughly. While, for Slo-Phyllin® the contents of twenty capsules of were carefully evacuated, collected, mixed, and then accurately weighed. An accurately weighed quantity of the powder equivalent to the weight of one tablet or one capsule was dissolved in 100 ml of methanol/water (30:70 % v/v) mixture, shaken well for 5 min, sonicated for 5 min and finally filtered using qualitative filter papers (Whatman International Ltd). The obtained filtrate was then used as a stock sample solution and further dilutions were made using the mobile phase.

3.2.3.9. Solid phase extraction

(1) Pre-treatment of the spiked urine samples

Before treatment, spiked urine samples were filtered through 0.45 μm nylon filters (Millipore-Whatman Ltd, Kent UK). The filtered urine samples (2 ml) were then acidified to pH 4 by the addition of 0.5 ml of 10 mM sodium acetate buffer.

(2) Conditioning of the SPE cartridge

Octadecyl (C_{18}) disposable SPE cartridges with 1.0 ml reservoir (J.T. Baker) were conditioned with methanol (2 x 1 ml), and then water (2 x 1 ml).

(3) Separation of a mixture of methylxanthines and their metabolites from the

   urine matrix

The urine samples (2.5 ml) containing a fixed concentration of the I.S. (30 μg ml^{-1}), and

varying concentrations of the methylxanthines and methyluric acids were loaded onto a

RP-C$_{18}$ SPE cartridge. The samples were then extracted at a flow rate of approximately

1-1.2 ml min^{-1}. The interferences of the urine matrix were removed by washing the

cartridge with water (2 x 1 ml) after applying the sample. The SPE cartridge was then

dried at full vacuum pressure for 5 min to remove any residual amount of water. The

compounds of interest were then eluted by; chloroform: methanol mixture (80:20 % v/v)

(5 x 0.5 ml). The eluate was collected and dried under a stream of nitrogen at 40°C for 7

min, and then the residue reconstituted with the mobile phase (2.5 ml).

3.2.3.10. Optimized HPLC conditions used for the analysis of methylxanthines and

methyluric acids mixture in urine matrix and for theophylline in aqueous solutions

Stationary Phase	Monolithic column RP-18e 100 × 4.6 mm
Mobile phase	Methanol: 10 mM KH$_2$PO$_4$ (pH 4) (12.5: 87.5 % v/v)
Flow rate	1 ml min^{-1}
Temperature	Room temperature
Injection volume	20 μl
UV- Detection	274 nm

3.2.3.11. Validation of the developed HPLC method for the determination of methylxanthines and their metabolites in urine samples

(1) Linearity, detection, and quantitation limits

Six calibration standard solutions were prepared covering the desired concentration range (0.03-40 µg ml^{-1}) for 3-MX, 1-MX, TB, TP &CA, and (0.05- 40 µg ml^{-1}) for 1,3-DMU, 1,7-DMU, PA and 1,3,7-TMU. The standards were prepared using pooled urine samples. All working standard solutions contained 30 µg ml^{-1}of 8-chlorotheophylline as internal standard. The samples were then extracted and analysed by the developed HPLC method.

Calibration curves were constructed as peak area ratios (compound/internal standard) versus the standard concentrations and the linear relationship was determined.

The regression analysis of the results was calculated according to the following linear regression equation [234];   **y = bc + a**

Where, y: peak area ratios, a: intercept, b: slope, and c: drug concentration in µg ml^{-1}.

The limit of detection LOD and quantitation LOQ were calculated for all of the cited drugs using the following equations [234];   **LOD = (3.3σ)/S   LOQ = (10σ)/S**

where σ = S.D. of y-intercept   S = the slope of the calibration curves

(2) Recovery

The recovery of the studied methylxanthines and their metabolites was investigated using urine samples spiked with three known concentrations of each drug corresponding to low (5 µg ml^{-1}), medium (15 µg ml^{-1}) and high (30 µg ml^{-1}) levels in the calibration curve. The analytical recovery was assessed (n= 6) by comparing the peak areas of the studied compounds after extraction from urine and those obtained from direct injections of equivalent quantities of pure standards.

(3) Precision and accuracy

Method validation regarding intra-day precision was achieved by replicate analysis (n= 6) of extracted urine samples spiked with standard solutions at low (5 μg ml^{-1}), medium (15 μg ml^{-1}) and high (30 μg ml^{-1}) levels in the calibration curve. The inter-day precision was conducted during routine operation of the system, over a period of five consecutive working days. The overall precision of the method was expressed as relative standard deviations (RSD). The accuracy was determined by comparing the calculated concentration of the extracted compounds with their true (actual) concentrations.

(4) Batch-to-Batch reproducibility on monolithic column packing

The reproducibility of the developed method was investigated by comparing the chromatographic data acquired upon working with two-monolith columns from two different batches (Batch 1: No. OB452773, Batch 2: No. HX754226).

In addition, as a comparison; our newly developed and validated method was examined alongside other C18 packings for the separation time and efficiency required for resolving the compounds of interest.

3.2.3.12. Validation of the developed HPLC for the quantitation of theophylline in aqueous solutions

The developed HPLC method was also validated for the analysis of theophylline in aqueous solutions; to allow the analysis of its formulations and the in-vitro determination of the aerodynamic behaviour of inhaled theophylline (Chapter 5).

(1) Linearity, detection, and quantitation limits

Six consecutive concentrations of the standard solution 20, 50, 80, 100, 150, and 200 μg ml^{-1} of theophylline were prepared, by further dilutions of suitable aliquots from the stock solution (1 mg ml^{-1}) with the mobile phase. All working standard solutions contained 30 μg ml^{-1} of 8-chlorotheophylline as internal standard. Calibration curves were constructed as peak area ratios (compound/internal standard) versus the theophylline concentrations and the linear relationship was determined. The limit of detection LOD and quantitation LOQ were calculated.

(2) Recovery

Recovery of theophylline from its formulations (tablets or capsules) were assessed (n= 6) at three concentration levels (50, 100, 150 μg ml^{-1}) by comparing the peak area after extraction from the pharmaceutical formulations (as described in 3.2.3.8.) and that obtained from direct injection of equivalent quantities of pure standard.

(3) Precision and accuracy

Intra-day precision was determined by replicate analysis (n= 6) of standard solutions at low, medium, and high concentration levels (50, 100, 150 μg ml^{-1}). The inter-day precision was conducted by repeating the analysis over a period of five consecutive working days. The overall precision of the method was expressed as relative standard deviations (RSD) and the accuracy was expressed as percent to the true value.

3.3. Results and Discussions

3.3.1. Optimization of HPLC method for the analysis of the mixture of methylxanthines and their metabolites

For method development, optimization of the different key factors governing the separation to obtain the highest quality data is required. The main analytical parameters that required to be optimized are the stationary phase, mobile phase composition (organic modifier, buffer, and pH). As a starting point the procedures reported by Rasmussen and Brosen [71] was investigated. The chromatographic conditions in this article was; ODS column, 5 μm, 250 × 4.66 mm, mobile phase consisted of methanol: 10mM acetate buffer (pH 4) (7:93 % v/v), flow rate; 1 ml min^{-1} and UV detection at 274 nm. These conditions were used with the monolithic column, but unresolved peaks with poor shape were obtained. Therefore further trials were done for optimisation of the chromatographic conditions required for efficient separation of the studied compounds.

3.3.1.1. Stationary phase

3.3.1.1.1. Performance comparison between monolithic and traditional C$_{18}$ columns for the separation of acidic and basic test mixtures

In the initial study it was considered important to study and understand the performance of the monolithic column in comparison with conventional packed columns using acidic and basic test mixtures. The HPLC procedures was based on those reported by Wang *et al* [147, 233] as a starting point and then the mobile phase composition was modified to adapt the selected mixtures. The final optimised HPLC procedure for separation of the acidic mixture containing 100 μg ml^{-1} of each drug was; acetonitrile: 0.1 % TFA (35: 65 % v/v), flow rate; 1 ml min^{-1}, injection volume; 20 μl, and UV detection at 220nm. Figure 3.3 represents the separation of the acidic mixture on monolithic and other tested packed columns.
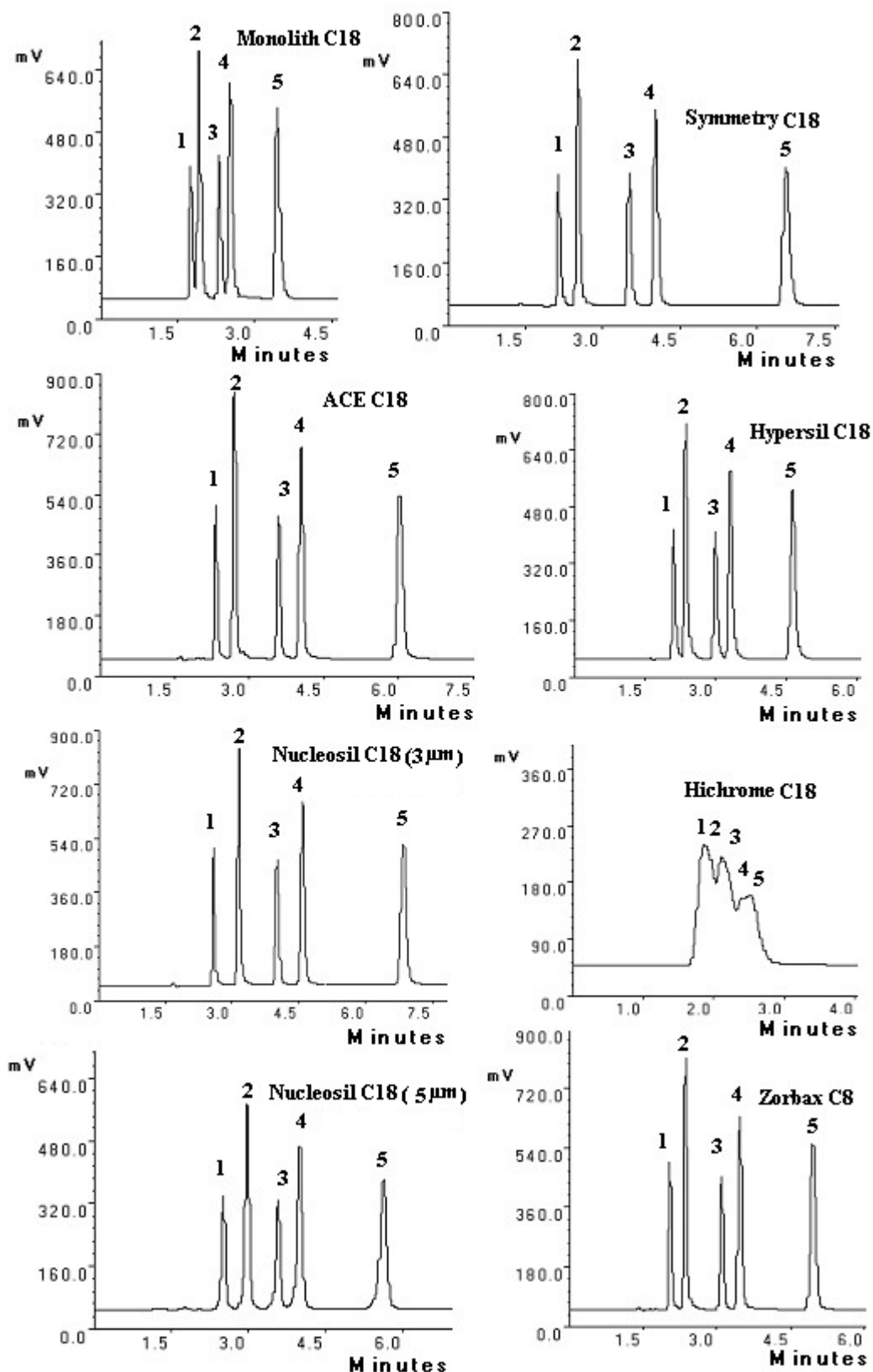
Figure 3.3. *Chromatograms of the acidic compounds on monolithic (Batch1) and traditionally packed columns with optimal conditions: acetonitrile: 0.1 % TFA (35: 65 % v/v), flow rate; 1 ml min^{-1}, Injection volume; 20 μl, and UV detection at 220nm. (1) 4-Hydroxybenzoic acid, (2) Coumaric acid, (3) Acetylsalicylic acid, (4) Benzoic acid, (5) 2-chloro-4-nitrobenzoic acid.*

While the final optimised procedures for determination of basic mixture containing 100

μg ml^{-1} of each drug was; methanol: 25mM KH$_2$PO$_4$ (pH 6) (80:20 %v/v), flow rate; 1

ml min^{-1}, injection volume; 20 μl, and UV detection at 220 nm. Figure 3.4 shows the

separation of the basic compounds on the tested columns under the optimised conditions.
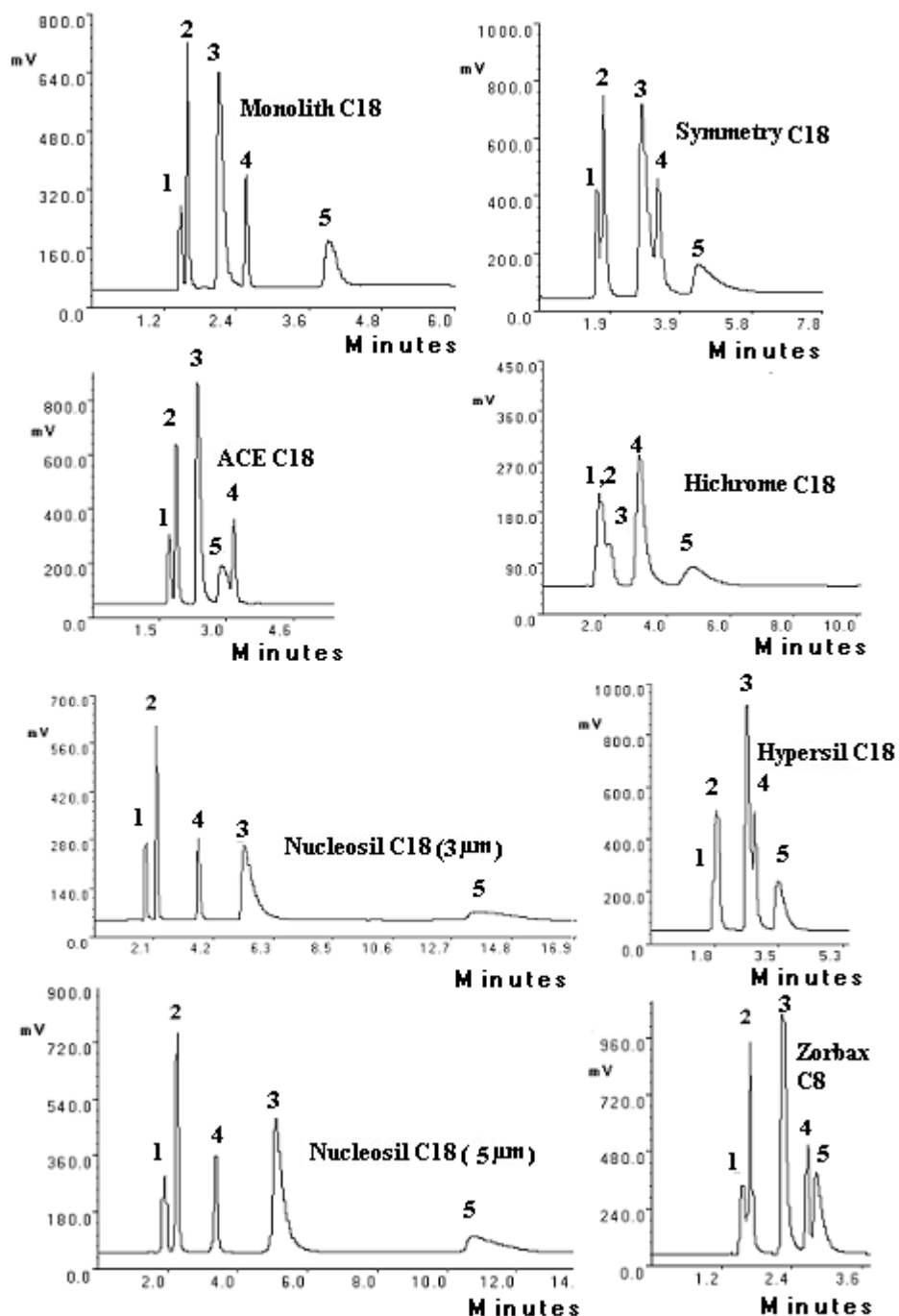
Figure 3.4. *Chromatograms of the basic compounds on monolithic (Batch1) and traditionally packed columns with optimal conditions: Methanol: 25mM KH$_2$PO$_4$ (pH 6) (80:20 % v/v), flow rate; 1 ml min^{-1}, Injection volume; 20 μl, and UV detection at 220nm. (1) Uracil, (2) Caffeine, (3) Propranolol, (4) Lidocaine, (5) Desipramine.*

The performance of the test columns for acidic and basic mixtures was also evaluated and compared using different chromatographic parameters (Tables 3.2 and 3.3). These chromatographic parameters include [157, 235];

- The capacity factor (K′) which gives a measure of the retention time independent on the flow rate and column dimension. $K' = (t_R - t_M)/t_M$

    t_M = unretained peak's retention time t_R = retention time of the peak of interest

- Number of theoretical plates (N) is a measure of the efficiency or resolving power of a column. $N = 5.54 \, (t_R/w_{0.5})^2$

    t_R = retention time of the peak of interest $w_{0.5}$ = the peak width at half peak height

- Peak resolution (Rs), is a measure of the separation between two peaks as well as the column efficiency. It is expressed as the distance between two maxima to the mean of the peaks width at base. $R_S = 2[(t_R)_B - (t_R)_A] / [w_A + w_B]$

- Tailing factor (T $_{0.05}$) is a measure of the peak symmetry.

$$T_{0.05} = w_{0.05}/2f$$

$w_{0.05}$ = width at 5% of the peak height   f = distance between maximum and the

leading edge of the peak

Table 3. 2. *Performances of monolithic and traditional packed columns for separation of the acidic mixture*

Analytes	Monolith				Symmetry				Hypersil				ACE			
	K'	$N \times 10^3$	Rs	$T_{0.05}$	K'	$N \times 10^3$	Rs	$T_{0.05}$	K'	$N \times 10^{-3}$	Rs	$T_{0.05}$	K'	$N \times 10^3$	Rs	$T_{0.05}$
4-hydroxy benzoic acid	1.33	5.45	-	1.44	1.85	5.36	-	1.58	1.81	5.56	-	1.59	2.10	8.66	-	1.37
Coumaric acid	1.54	6.98	1.80	1.50	2.35	7.72	3.24	1.47	2.15	7.14	2.26	1.50	2.59	10.02	3.57	1.19
Acetylsalicylic acid	2.07	6.76	3.88	1.51	3.69	13.16	8.43	1.28	2.99	9.10	5.30	1.52	3.79	10.67	7.26	1.17
Benzoic acid	2.37	7.39	1.92	1.35	4.38	13.06	3.92	1.30	3.42	8.63	2.39	1.40	4.39	13.02	3.23	1.10
2-chloro-4-nitrobenzoic acid	3.58	7.96	6.72	1.38	7.76	13.86	13.9	1.27	5.18	10.43	8.17	1.31	7.04	14.51	11.6	1.10

Analytes	Nucleosil-3µm				Nucleosil -5µm				Hichrome				Zorbax C$_8$			
	K'	$N \times 10^3$	Rs	$T_{0.05}$	K'	$N \times 10^3$	Rs	$T_{0.05}$	K'	$N \times 10^{-3}$	Rs	$T_{0.05}$	K'	$N \times 10^3$	Rs	$T_{0.05}$
4-hydroxy benzoic acid	2.44	10.52	-	1.34	2.35	7.09	-	1.00	1.45	0.46	-	-	1.73	8.57	-	1.28
Coumaric acid	3.20	14.65	5.58	1.41	2.97	9.44	3.82	0.97	-	-	0.92	-	2.15	7.32	3.18	1.31
Acetylsalysylic acid	4.36	17.10	7.64	1.20	3.77	9.19	4.45	0.88	2.13	0.97		-	3.13	10.93	6.74	1.19
Benzoic acid	5.12	15.34	4.21	1.18	4.34	9.34	2.69	0.85	-	-		-	3.63	10.39	2.91	1.14
2-chloro-4-nitrobenzoic acid	8.15	13.97	11.9	1.11	6.51	9.58	8.23	0.83	2.53	-		-	5.61	11.58	9.28	1.07

K'; capacity factor,   N; number of theoretical plates   Rs; peak resolution $T_{0.05}$; tailing factor at 5% of the peak height
N.B. absence of data (-) indicates that insufficient resolution was observed

Table 3. 3. *Performances of monolithic and traditional packed columns for separation of the basic mixture*

Analytes	Monolith				Symmetry				Hypersil				ACE			
	K′	N ×10³	Rs	T$_{0.05}$	K′	N ×10³	Rs	T$_{0.05}$	K′	N ×10³	Rs	T$_{0.05}$	K′	N ×10³	Rs	T$_{0.05}$
Uracil	1.01	1.47	-	1.44	1.08	4.62	-	-	1.38	-	-	-	1.31	3.50	-	-
Caffeine	1.15	4.73	1.42	1.34	1.33	3.36	1.09	0.92	1.57	-	-	-	1.53	5.90	1.51	1.18
Propranolol	2.09	1.45	5.23	2.18	2.69	1.40	3.93	-	1.92	-	-	-	2.17	2.75	3.42	2.23
Lidocaine	2.46	11.12	3.41	1.24	3.66	3.88	1.35	-	3.13	0.69	-	1.76	3.28	7.53	1.29	0.64
Desipramine	4.32	8.39	1.89	2.14	4.54	0.55	3.31	4.87	5.38	0.27	2.07	1.74	2.88	1.34	2.15	-

Analytes	Nucleosil-3µm				Nucleosil -5µm				Hichrome				Zorbax C$_8$			
	K′	N ×10³	Rs	T$_{0.05}$	K′	N ×10³	Rs	T$_{0.05}$	K′	N ×10³	Rs	T$_{0.05}$	K′	N ×10³	Rs	T$_{0.05}$
Uracil	1.43	2.18	-	1.52	1.56	1.40	-	0.98	1.45	0.45	-	-	1.07	1.71	-	-
Caffeine	1.94	6.89	2.29	1.51	2.03	5.36	2.16	1.05	-	-	0.92	-	1.26	6.39	1.17	1.02
Propranolol	6.09	1.01	3.93	3.78	5.78	1.77	5.26	2.33	2.13	0.97		-	1.99	2.58	4.21	2.25
Lidocaine	3.93	8.69	11.2	1.50	3.51	6.84	7.73	1.01	-	-		-	2.56	8.73	2.95	-
Desipramine	17.1	4.59	5.16	-	13.3	0.66	5.26	2.94	2.53	-		-	2.75	3.57	0.94	-

K′; capacity factor,   N; number of theoretical plates   Rs; peak resolution   T$_{0.05}$; tailing factor at 5% of the peak height
N.B. absence of data (-) indicates that insufficient resolution was observed

From the abovementioned results the following points could be concluded:

- All the tested columns (except Hichrome) were able to resolve the acidic and basic mixtures with variable resolution, peak symmetry, total analysis time and column back- pressure.

- The total run times of the acidic mixture on Symmetry, Hypersil, ACE, Nucleosil 3 μm, Nucleosil 5 μm, Hichrome, and Zorbax C_8 were 6.57, 4.64, 6.03, 6.86, 5.63, 2.54, and 4.96 min respectively. For the monolithic column the total analytical runs took only 3.44 min, which is shorter than all the test columns except Hichrome, which did not resolve the mixture under the same conditions.

- For the basic mixture; the total run times on Symmetry, Hypersil, ACE, Nucleosil 3 μm, Nucleosil 5 μm, Hichrome, and Zorbax C_8 were 4.16, 3.50, 3.21, 13.60, 10.74, 4.79, and 2.81 min respectively. The monolithic column took 3.99 min to separate the mixture, which is shorter than the investigated columns with the exception of the ACE and Zorbax C_8 columns, which show poor resolution between uracil / caffeine, and lidocaine / desipramine peaks.

- Thus we can conclude that the main advantage of the monolithic column is the reduction of the run time while the separation efficiency is less affected compared to the particulate columns.

- Furthermore, the monolithic column enables the performance of the analytical run under back-pressure of only about 60 bar, which was much lower than that produced by conventional columns (150-180 bar). This is attributed to that the fact that the monolithic support has a total porosity of over 80 %, which permits fast mass transfer and low-pressure resistance. Decreasing the backpressure extends the lifetime of the analytical column and also the HPLC instrument.

3.3.1.1. 2. Performance comparison between platinum and monolithic columns for the separation of acidic and basic test mixtures

To complete the overview on the monolithic columns, its performance was compared with platinum column, which was considered as a novel stationary phase. This phase has hydrophobic and polar selectivity providing a dual mode separation medium with both polar and non-polar sites. The acidic and basic test mixtures mentioned in section 3.2.2.1 were used. The optimal chromatographic conditions for separation of these mixtures were mentioned in section 3.2.3.4.

(1) Columns selectivity

Figures 3.5 shows the acidic and basic test compounds separated on monolith and platinum columns at the optimised conditions using flow rate of 1 ml min^{-1}.
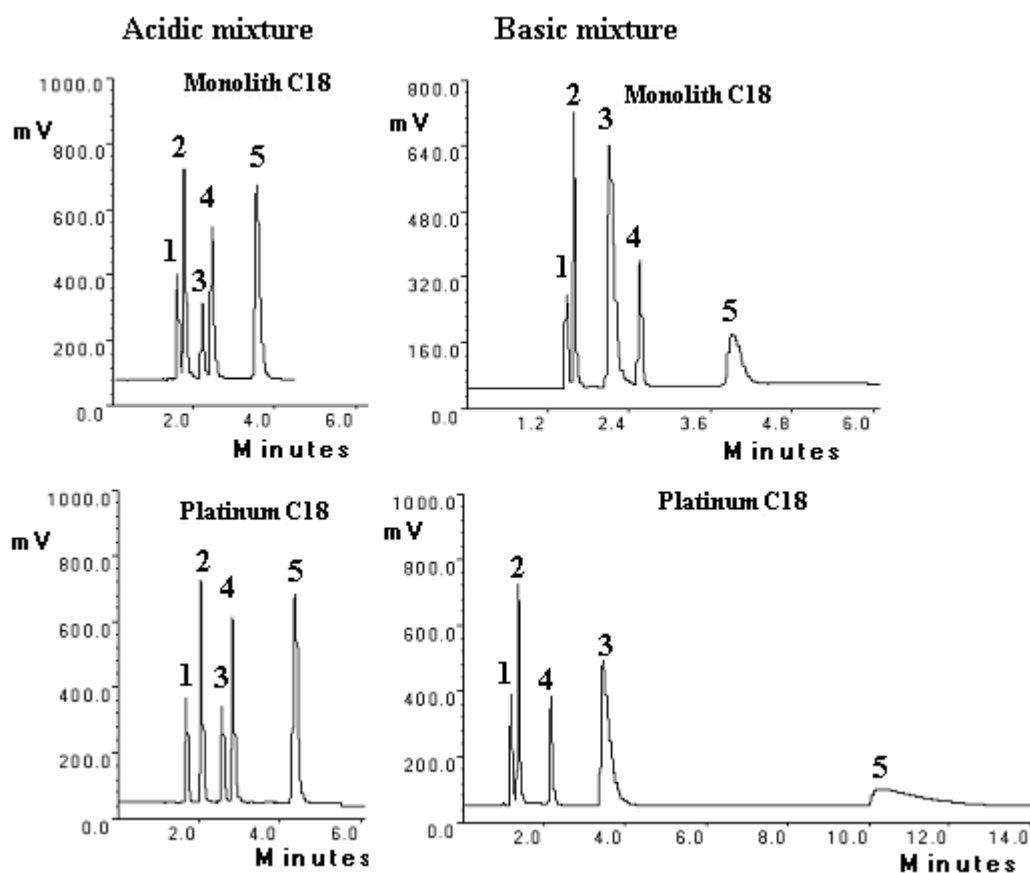
Figure 3. 5. *Chromatograms represent separation of the acidic and basic compounds on monolithic and platinum columns. The acidic compounds are; (1) 4-Hydroxybenzoic acid, (2) Coumaric acid, (3) Acetylsalicylic acid, (4) Benzoic acid, (5) 2-chloro-4-nitrobenzoic acid. The basic compounds are; (1) Uracil, (2) Caffeine, (3) Propranolol, (4) Lidocaine, (5) Desipramine.*

From this chromatogram it can be noted that both columns were able to separate all compounds in both mixtures with sufficient resolution under the same chromatographic conditions. However, the total run times for the acidic and basic mixture using the monolith were 3.44, and 4.16 min., respectively, and for the platinum were 4.51, and 10.76 min., respectively. The equivalent selectivity allows for easy transfer of existing methods from platinum to monolith in order to reduce the analysis time.

(2) Comparison between the different chromatographic data obtained from the monolithic and platinum columns

The following operating parameters for the monolithic column were compared to those of the platinum column for both test mixtures (Table 3.4) [157, 235];

The capacity factor (K′), which gives an indication of how long each component, is retained on the column, number of theoretical plates (N) that measures the sharpness of the peak and therefore the efficiency of the column. The plate height (H) another parameter can be used to determine the column efficiency $H = L/N$

  L= Length of the column   N= number of theoretical plates

They also include peak resolution (Rs), that a measure of the separation between two peaks in addition to the efficiency of the column, and the tailing factor ($T_{0.05}$) which a measure of the peak symmetry.

Table 3. 4. *Performances of monolithic and platinum columns for separation of acidic and basic test mixtures*

Acidic mixture	Monolith				Platinum C_{18}			
	K′	N ×10³	Rs	T$_{0.05}$	K′	N ×10³	Rs	T$_{0.05}$
4-hydroxy benzoic acid	1.33	5.45	-	1.44	1.35	5.09	-	1.28
Coumaric acid	1.54	6.98	1.80	1.50	1.74	5.35	3.31	1.18
Acetyl-salicylic acid	2.07	6.76	3.88	1.51	2.43	6.67	3.86	1.11
Benzoic acid	2.37	7.39	1.92	1.35	2.78	7.08	2.13	1.06
2-chloro-4-nitrobenzoic acid	3.58	7.96	6.72	1.38	4.83	7.83	8.49	1.08
Basic mixture	**K′**	**N ×10³**	**Rs**	**T$_{0.05}$**	**K′**	**N ×10³**	**Rs**	**T$_{0.05}$**
Uracil	1.01	1.47	-	1.44	0.61	1.39	-	1.55
Caffeine	1.15	4.73	1.42	1.34	0.84	3.94	1.76	1.54
Propranolol	2.09	1.45	5.23	2.18	3.78	1.39	5.23	3.57
Lidocaine	2.46	11.1	3.41	1.24	1.89	5.41	7.89	1.46
Desipramine	4.32	0.84	1.89	2.14	13.2	0.69	5.43	4.94

From the results presented in Table 3.4, it was observed that the total run time for the monolith column is shorter than that of the platinum column. The efficiency of the monolith with respect to the number of theoretical plates is higher than the platinum column for the entire acidic and basic compounds. On the other hand, the peak symmetry for the acidic compounds when using platinum column is better than monolith, which is the reverse of the results from the basic compounds separation.

(3) The effect of the flow rate on the column efficiency

The influence of the mobile phase flow rate on the performance of the monolith and platinum columns for the separation of acidic and basic compounds was investigated. The flow rate for both columns was varied in the range 0.5-2 ml min^{-1}. The Van Deemter plots (H versus flow rate) of the tested columns for the acidic and basic mixtures are shown in are shown in Figures 3.6 and 3.7, respectively. These plots show the effect of the flow rate on the columns efficiency for separation of both mixtures.
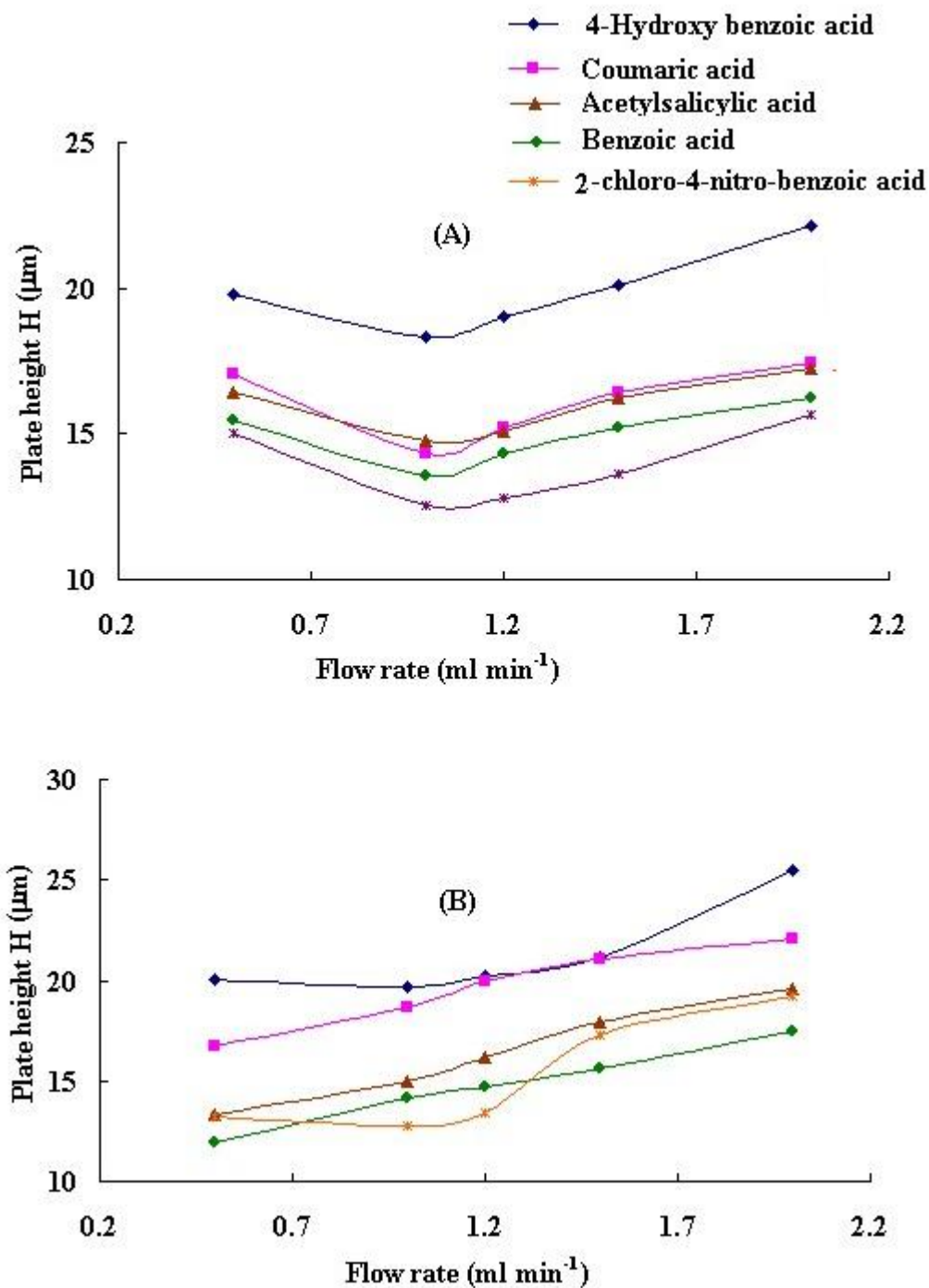
Figure 3. 6. *Van Deemter plot of the height equivalent to a theoretical plate versus flow rate for monolithic (A) and platinum (B) columns for separation of acidic mixture. Chromatographic conditions: mobile phase was; acetonitrile: 0.1 % TFA (35: 65 % v/v), flow rate; 1 ml min^{-1}, Injection volume; 20 μl, and UV detection at 220nm.*
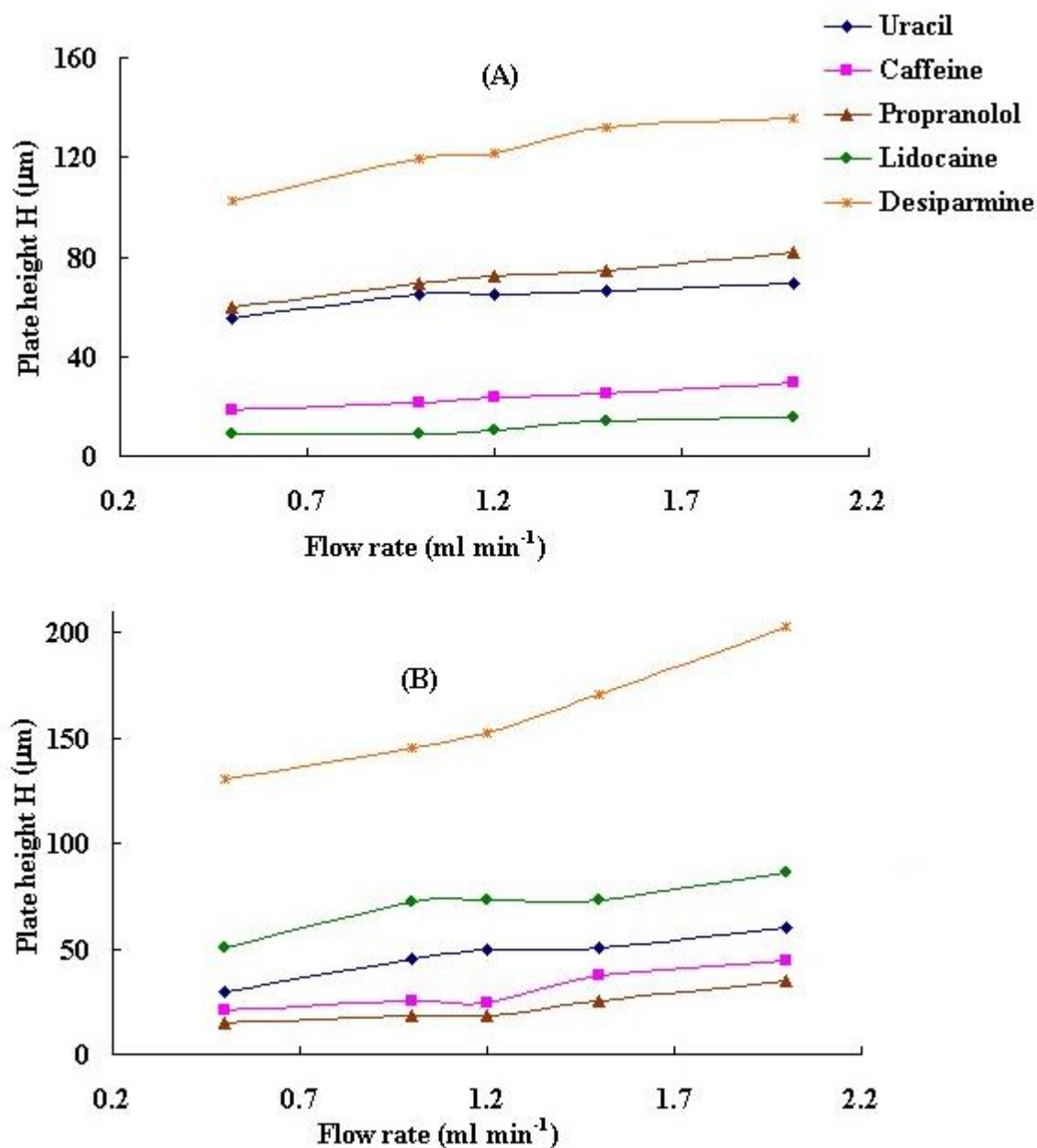
Figure 3. 7. *Van Deemter plot of the height equivalent to a theoretical plate versus flow rate for monolithic (A) and platinum (B) columns for separation of basic mixture. Chromatographic conditions: mobile phase; methanol: 25mM KH$_2$PO$_4$ (pH 6) (80:20 % v/v), flow rate; 1 ml min^{-1}, Injection volume; 20 μl, and UV detection at 220nm. (1) Uracil, (2) Caffeine, (3) Propranolol, (4) Lidocaine, (5) Desipramine.*

As can be seen, at higher flow rates there was slow loss in the resolution efficiency for the acidic mixture. But for the basic mixture the separation efficiency of both of them does not significantly decrease when the flow rate is increased. Although the efficiency

of the platinum column is not significantly affected by increasing the flow rate, the backpressure increases significantly. Therefore, the monolithic column is more convenient as it allows performing an analytical run under lower backpressure with a shorter analysis time. This is mainly due to the high porosity of the monolithic compared to particulate columns. Figure 3.8 illustrates the backpressure required to achieve a flow rate in the range 0.5-2 ml min^{-1} through monolith against particulate backed platinum column. It was observed that at a flow rate of 2 ml min^{-1} the backpressure on the monolith was of only 65-74 bar while, on the platinum column packed with 3μm particles reached 175-220 bar. On the other hand, at a flow rate 1 ml min^{-1}, which is the commonly used flow in the HPLC methods, the backpressure is about 3-folds smaller on the monolithic than on the platinum column.
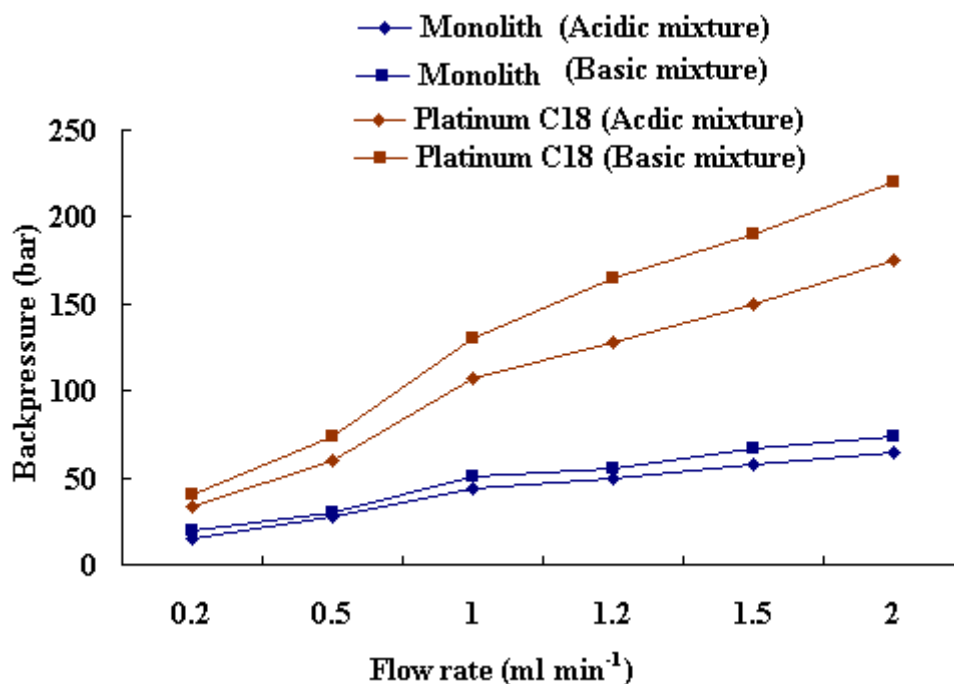
Figure 3. 8. *Column backpressure as a function of the flow rate on monolithic and platinum columns.*

(4) Precision and reproducibility of chromatographic data obtained from monolithic and platinum columns

The intra-day and inter-day precision for the chromatographic data acquired from two different batches of monolith and platinum columns were determined by repeating six consecutive runs of the test mixture on each column within one and five working days, respectively. The RSDs of the retention time, resolution factor and the tailing factor obtained with the monolithic column varies between 0.04 - 2.47 % for both the acidic and basic compounds (Table 3.5). On the other hand, the precision values obtained from the platinum column, which ranged from 0.16 to 4.83 % for both mixtures (Table 3.6). This demonstrates the good precision of the chromatographic data obtained from the monolith which is possibly due to the better peak shape and reduced baseline noise that can lead to more precise integration [16]. Batch-to-Batch reproducibility is presented by the RSD of six injections on the two batches. The RSDs for all compounds in both monolithic batches were < 2.50 %, while with platinum column they ranged from 0.97 to 4.47 %. A high level of batch to batch reproducibility achieved on the monolith is in agreement with earlier reports [236], while poor reproducibility was observed with the platinum columns.

As a conclusion, on comparison with both traditional packed and newly introduced C_{18} columns, the monolith provides two important features required for method development; short analysis time with low backpressure. Therefore, the monolithic column was selected for analysis of the methylxanthines and their metabolites in urine samples as well as the determination of theophylline in aqueous solutions.

Table 3. 5. *Precision and reproducibility of the chromatographic data obtained from separation of acidic and basic mixture on two different batches of monolithic column.*

Analytes	RSD of the chromatographic data (n=6)														
	Intra-day precision						Inter-day precision						Batch-to- Batch reproducibility		
	Batch 1 (OB452773)			Batch 2 (HX754226)			Batch 1 (OB452773)			Batch 2 (HX754226)					
	t_R	$T_{0.05}$	R_S	t_R	$T_{0.05}$	R_S	t_R	$T_{0.05}$	R_S	t_R	$T_{0.05}$	R_S	t_R	$T_{0.05}$	R_S
Acidic mixture															
4-hydroxy- benzoic acid	0.04	1.90	-	0.18	1.34	-	0.05	1.21	-	0.26	0.35	-	0.06	2.01	-
Coumaric acid	0.17	1.79	1.61	0.22	1.47	1.32	0.32	1.54	1.23	1.29	2.04	2.15	0.15	1.58	1.33
Acetyl-salicylic acid	0.12	2.18	2.14	0.23	2.31	2.05	0.11	2.01	1.33	1.69	0.66	0.75	0.54	1.64	2.31
Benzoic acid	0.11	2.31	2.40	0.19	2.17	1.18	0.65	1.71	2.13	2.10	1.82	0.57	0.36	1.87	2.14
2-chloro-4-nitrobenzoic acid	0.09	2.33	1.72	0.23	1.54	1.47	0.05	1.39	1.87	2.35	1.78	2.08	1.02	2.36	2.47
Basic mixture Uracil	0.17	1.91	-	0.35	1.25	-	0.06	1.58	-	0.54	1.47	-	0.16	1.57	2.14
Caffeine	0.65	2.33	1.24	0.05	1.47	2.25	0.08	1.54	2.47	0.37	1.23	2.47	0.03	1.87	2.36
Propranolol	1.81	2.14	1.58	0.08	1.88	2.36	0.54	1.29	2.36	0.14	1.54	2.14	0.05	1.65	2.25
Lidocaine	0.53	2.01	2.36	0.14	1.54	2.34	0.25	1.36	2.14	0.06	2.18	2.01	1.28	2.14	2.17
Desipramine	0.69	1.58	2.41	0.87	2.25	2.01	0.36	2.36	2.25	0.14	2.04	1.98	0.87	2.43	1.65

Table 3. 6. *Precision and reproducibility of the chromatographic data obtained from separation of acidic and basic mixture on two different batches of platinum column.*

Analytes	RSD of the chromatographic data (n=6)														
	Intra-day precision						Inter-day precision						Batch-to- Batch reproducibility		
	Batch 1 (608121210)			Batch 2 (608121211)			Batch 1 (608121210)			Batch 2 (608121211)					
	t_R	$T_{0.05}$	R_S	t_R	$T_{0.05}$	R_S	t_R	$T_{0.05}$	R_S	t_R	$T_{0.05}$	R_S	t_R	$T_{0.05}$	R_S
Acidic mixture 4-hydroxy- benzoic acid	0.35	4.91	-	0.98	4.83	-	2.03	1.89	-	2.03	1.54	-	0.97	4.23	-
Coumaric acid	0.30	3.77	3.38	0.83	4.03	4.98	2.19	0.96	2.42	1.91	1.66	1.69	1.12	3.36	4.11
Acetyl-salicylic acid	0.19	3.22	2.42	0.75	2.98	4.04	1.53	1.82	1.33	0.43	1.76	1.58	1.78	4.24	4.65
Benzoic acid	0.16	4.29	3.33	0.68	2.64	4.14	1.60	1.48	1.62	0.46	2.39	1.98	1.68	4.11	3.95
2-chloro-4-nitrobenzoic acid	0.24	2.21	1.73	0.62	0.96	1.17	1.43	1.45	0.31	1.37	1.37	0.22	2.46	4.11	4.25
Basic mixture Uracil	0.61	4.73	-	1.54	1.60	-	0.33	4.03	-	2.22	1.97	-	1.30	3.99	-
Caffeine	0.64	3.24	3.39	1.97	4.49	4.20	0.73	4.04	3.61	3.43	2.57	3.27	1.60	4.27	4.51
Propranolol	0.58	4.74	4.75	1.28	3.62	3.22	2.26	2.82	4.83	1.78	1.68	0.78	2.81	3.15	4.47
Lidocaine	0.95	2.31	2.33	0.49	2.41	1.31	2.07	3.51	4.14	1.29	4.36	3.98	2.70	3.20	1.95
Desipramine	0.75	3.79	2.77	2.03	4.28	5.53	1.50	0.30	4.06	1.16	4.88	1.92	4.43	4.14	3.96

3.3.1.2. Mobile phase composition

A number of variables relating to the mobile phase composition were studied such as buffer (type and concentration, pH) organic modifier (type and proportion).

(1) Buffer (type, concentration)

Acetate and phosphate buffers are commonly used in different reported articles for the determination of methylxanthines and methyluric acids. Therefore the effect of each of them as a constituent of the mobile phase on the elution of the studied compounds was investigated. Using 10 mM of acetate buffer (pH 4) as reported in Rasmussen and Brosen [71] was not ideal for efficient separation of the tested compounds on the monolithic column. It was observed that TB could not be separated from 1,3-DMU, and also the eluted peaks of PA, TP and 1,3,7TMU were not completely base line separated (Figure 3.9). While, using of 10mM of phosphate buffer (pH 4) was found to show good separation between all the studied compounds. Therefore potassium dihydrogen phosphate (KH_2PO_4) buffer was chosen for method optimisation.
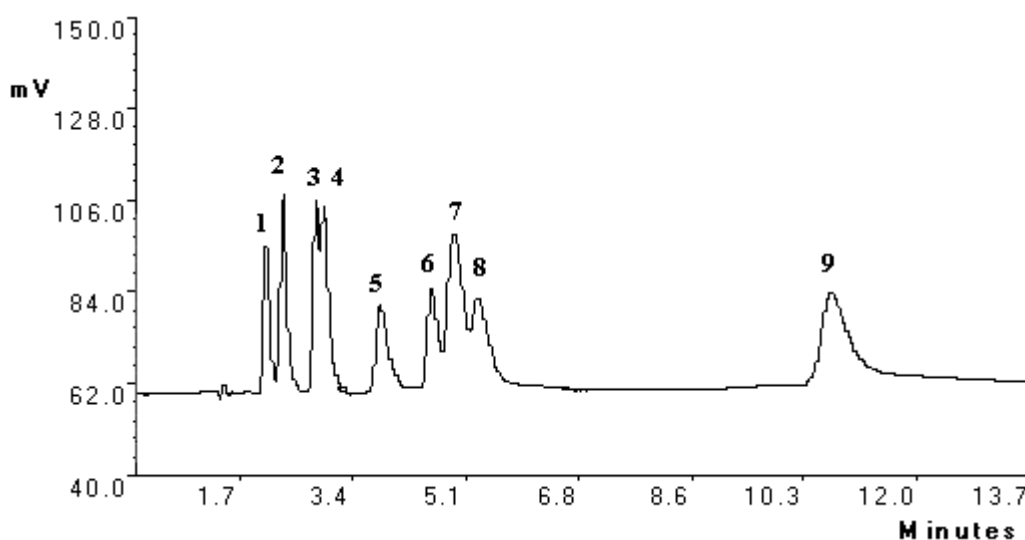
Figure 3.9. *The effect of using acetate buffer in the mobile phase on the chromatographic behaviour of the studied methylxanthines and methyluric acids (20 μg ml^{-1}). (1) 3-MX, (2) 1-MX, (3) 1,3-DMU, (4) TB, (5) 1,7-DMU, (6) PA, (7) TP, (8) 1,3,7-TMU, (9) CA. Chromatographic conditions was; monolithic column (Batch1), methanol: 10 mM acetate buffer (pH 4) (12.5:87.5 % v/v), flow rate 1ml min^{-1}, injection volume 20 μl, and UV detection at 274 nm.*

The effect of buffer concentration was studied by preparing phosphate buffer solutions on different molar concentrations; 10, 20, 50, 100 mM. It was observed that changing the buffer concentration from 10-100 mM provides little effect on both the retention times and the peak resolution of the tested drug (Figure 3.10). Phosphate buffer with the concentration of 10 mM was chosen for further development, because this concentration is low enough to avoid problems associated with precipitation, when significant amounts of organic modifiers are used in the mobile phase. In the case of phosphate buffers particularly, the use of lower concentrations was advisable to minimize the abrasive effect on pump seals.
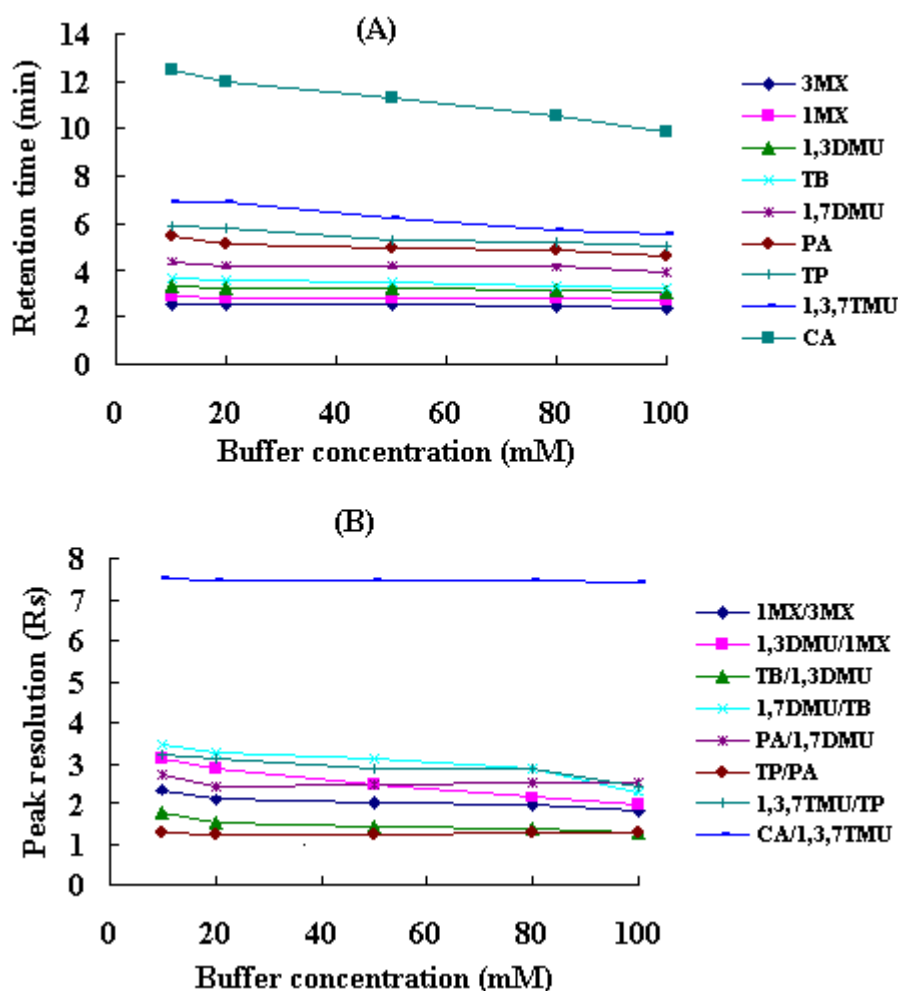
Figure 3. 10. *The effect of different buffer concentrations on the retention times (A) and peak resolution (B) of the studied methylxanthines and methyluric acids. Chromatographic conditions was; monolithic column (Batch1), methanol: KH_2PO_4 (pH 4) (12.5:87.5 % v/v), flow rate 1ml min^{-1}, injection volume 20 μl, and UV detection at 274 nm.*

(2) Effect of buffer pH

The effect of pH of the selected phosphate buffer was studied, because the pH could alter the retention time, resolution or the shape of the eluted peaks. At pH values lower than 2.0 or higher than 7.5, dissolution of silica could occur and hence shorten the lifetime of the stationary phase. Therefore pH from 2.5-7 was tested using a phosphate buffer. Five separate buffered solutions were prepared and their pHs were adjusted to 2.5, 4, 5, 6, and 7. The retention times of all the studied compounds were unaffected by pH changes from 4 to 6 but optimum peak resolution and shape were obtained at pH 4. At pH 2.5, 3-MX and 1-MX were not well resolved and this was the case with PA and TP, this was accompanied with increase in retention times as well as poor peak shape for all the compounds. While at pH 7, PA and TP are completely overlapped and a decrease in the retention times of all the compounds was also observed (Figures 3.11 and 3.12). This may be attributed to that the drugs are considered as weak acids (except caffeine is weak base) and so their degree of ionization is increased at high pHs leading to decrease in the retention times [55, 237]. However, caffeine is less affected by changes in pH than other drugs studied that is in agreement with that reported in the literatures [238, 239]. Hence pH 4 was chosen as the optimal pH.
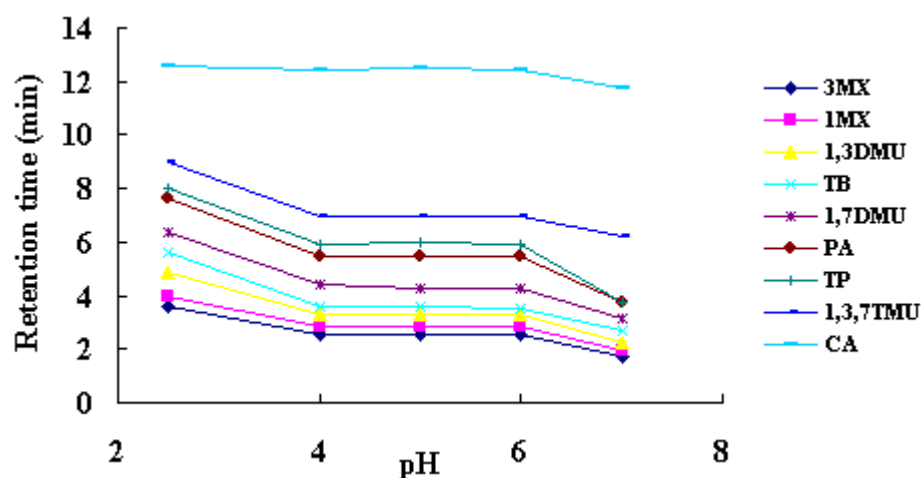
Figure 3.11. *The effect of mobile phase pH on the retention time of the studied methylxanthines and methyluric acids. Chromatographic conditions was; monolithic column (Batch1), methanol: 10 mM KH$_2$PO$_4$, flow rate 1ml min^{-1}, injection volume 20 μl, and UV detection at 274 nm.*
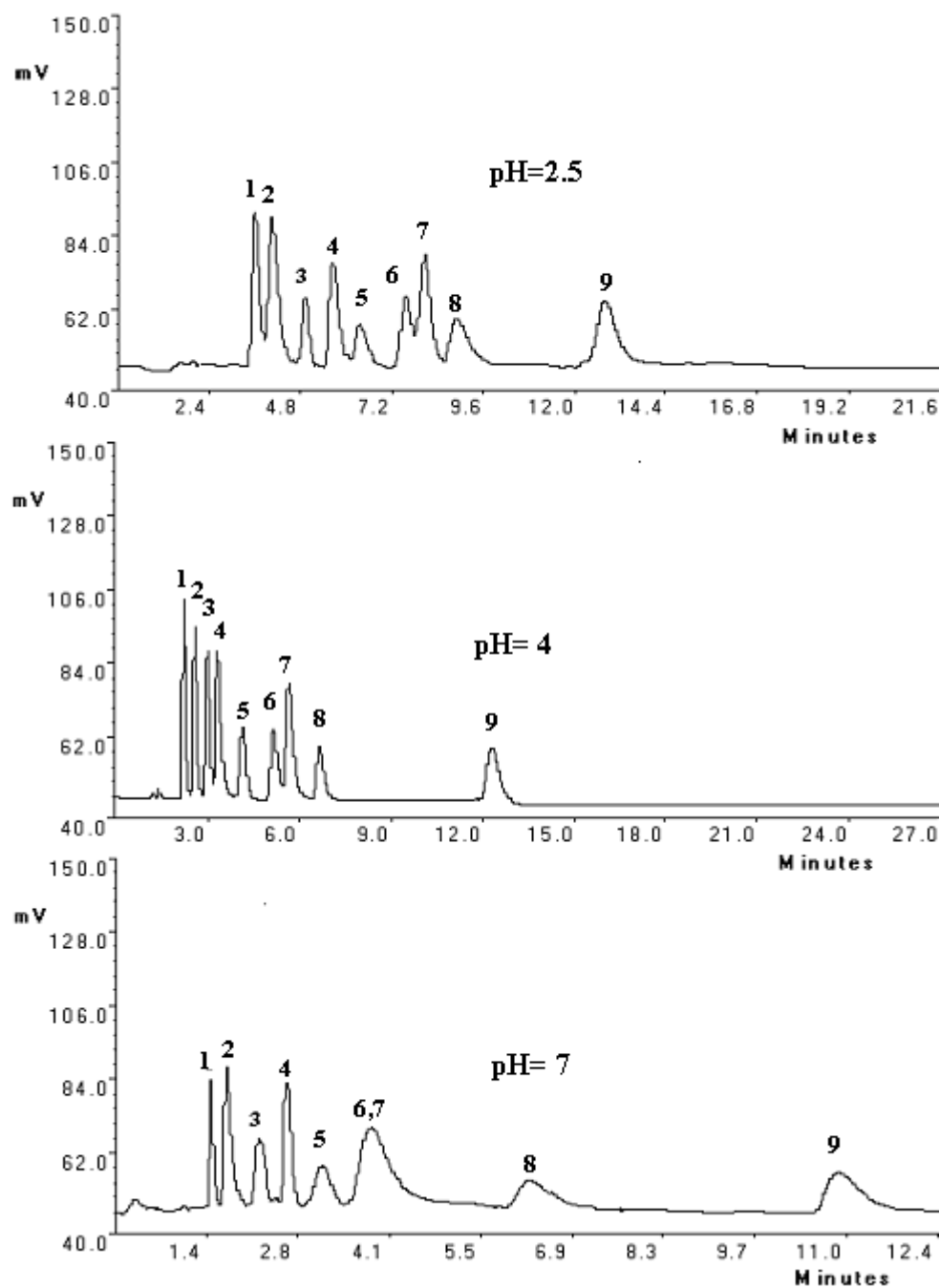
Figure 3. 12. *Chromatograms represent the effect of the pH of the mobile phase on the chromatographic behaviour of the studied methylxanthines and methyluric acids (20 μg ml^{-1}). (1) 3-MX, (2) 1-MX, (3) 1,3-DMU, (4) TB, (5) 1,7-DMU, (6) PA, (7) TP, (8) 1,3,7-TMU, (9) CA. Chromatographic conditions was; monolithic column (Batch1), methanol: 10 mM KH$_2$PO$_4$ (12.5:87.5 % v/v), flow rate 1ml min^{-1}, injection volume 20 μl, and UV detection at 274 nm.*

(3) Organic modifier (type and proportion)

The retention time and peak resolution of the studied compounds were extensively affected by the type of organic modifier used. The effect of using acetonitrile, methanol or both of them as organic modifiers was investigated. As shown in Figure 3.13 acetonitrile has an accelerating effect on early eluted peaks and only four peaks could be recorded these are; PA, TP, 1,3,7-TMU, and CA. The same effect was also observed upon using acetonitrile /methanol mixture in different proportions. Therefore, methanol was selected as the ideal organic modifier in the studies.
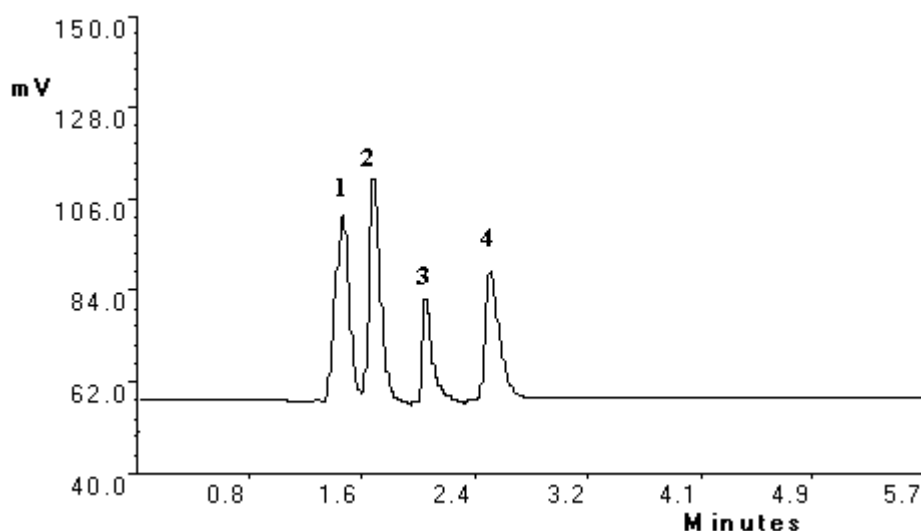
Figure 3. 13. *The effect of acetoniltrile as an organic modifier, on the chromatographic behaviour of the studied methylxanthines and methyluric acids (1) PA, (2) TP, (3) 1,3,7-TMU, (4) CA. Chromatographic conditions; monolithic column (Batch1), acetonitrile: 10 mM KH_2PO_4 (pH 4) (12.5:87.5 % v/v), flow rate 1ml min^{-1}, injection volume 20 μl, and UV detection at 274 nm.*

The effect of different proportions of methanol on the chromatographic behaviour of the eluted peaks was studied. Four different proportions of methanol in the mobile phase were tested; 10, 12.5, 15, 20 %v/v. It was observed that with reduced amounts of methanol in the mobile phase, the retention time of methylxanthines and their metabolites were extended. On the other hand, peak resolution was decreased for each

of the drugs studied except for PA and TP (Figure 3.14). No sharp effect on peak resolution was observed when changing the methanol percentage in the mobile phase for PA and TP compared to other compounds. Since a reasonably long retention time is important to avoid the interference from urine matrix peaks, the proportion of 12.5 % v/v of methanol was selected. It provides both long retention time and sufficient resolution for the eluted peaks. As an alternative the proportion of 10 % v/v of methanol provides longer retention times than 12.5% v/v, but it was not selected because of the obtained poor peaks shape.
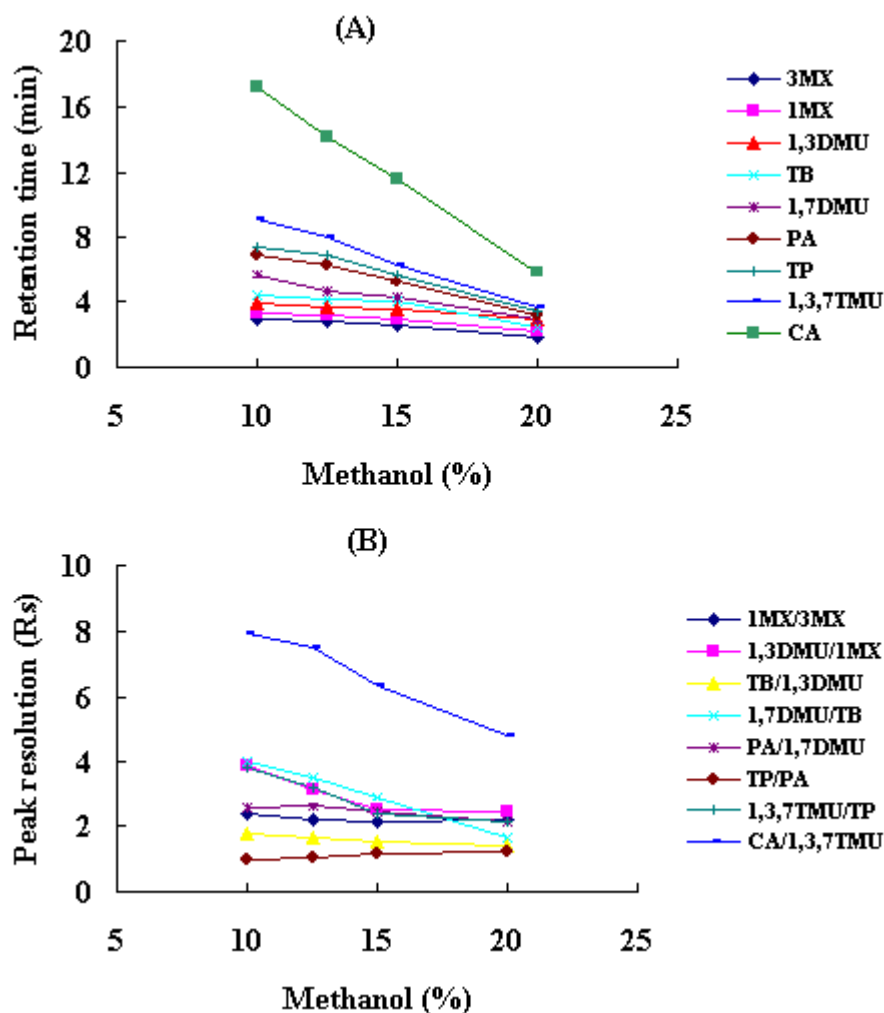
Figure 3. 14. *The effect of different proportions of methanol on the retention times (A) and peak resolution (B) of the studied methylxanthines and methyluric acids Chromatographic conditions; monolithic column (Batch1), methanol: 10 mM KH_2PO_4 (pH 4), flow rate 1ml min^{-1}, injection volume 20 μl, and UV detection at 274 nm.*

3.3.2. The optimized chromatographic conditions

Stationary Phase	Monolithic column RP-18e 100×4.6 mm
Mobile phase	Methanol: 10 mM potassium dihydrogen phosphate (pH 4) (12.5: 87.5 % v/v)
Flow rate	1 ml min^{-1}
Temperature	Room temperature
Injection volume	20 μl
UV- Detection	274 nm

The next objective was to use the developed method to separate and quantitate the methylxanthines and methyluric acids from urine matrix.

3.3.3. The choice of the internal standard

8-chlorotheophylline was a suitable internal standard in the present study. Since it was structurally close to theophylline and had the same UV absorption at 274 nm. Secondly, it had relatively longer retention time (14.06 min) when compared with other studied compounds, therefore it show no interference with their peaks. Furthermore, its polarity is quite similar to the tested drugs and thus was suitable as an internal standard in the SPE of spiked urine samples, and the detection conditions used.

3.3.4. Optimisation of solid phase extraction procedure

Before the quantitative analysis of methylxanthines and their metabolites in urine samples, they were extracted from the matrix and then pre-concentrated. The most common extraction techniques used for the elimination of the matrix interferences are liquid-liquid extraction, or solid phase extraction (SPE). SPE is now the most commonly used technique for sample extraction (especially of biological origins),

concentration, and clean up [240, 241] and it also it offers a wide sorbent selection. SPE prevents, many of the problems associated with liquid/liquid extraction, such as incomplete phase separations, low quantitative recoveries, use of expensive breakable specialty glassware, and disposal of large quantities of organic solvents. Extraction of methylxanthines and their metabolites from urine samples using SPE has been proposed previously [19, 80, 242, 243] but these methods did not give satisfactory recoveries for the compounds of interest. Therefore in this work the influence of various parameters to include; the cartridge type, pH adjustment of the urine samples, and different elution solvents, on the extraction efficiencies were examined.

As the first stage pre-treatment of the spiked urine samples was important where the extraction required isolation of the hydrophilic analytes in the presence of relatively high levels of endogenous hydrophilic compounds typically found in the urine. To delay the elution of the tested compounds and so can be well separated from matrix interferences, the samples have to be in acidic medium thus the analytes will be in non-ionized forms, which are strongly retained on C_{18} cartridge. The effect of adjustment of the spiked urine samples over the pH range of 2-6 by using either 10 mM sodium acetate buffer or 1 M HCl was investigated [71, 80, 244]. It was found that acidification of the urine sample to pH 4 with 0.5 ml of 10 mM sodium acetate buffer is the optimum for good recoveries for all the studied.

(1) SPE cartridge

As recommended in most the reported SPE procedures for the tested drugs, octadecyl C_{18} cartridge (1ml/100mg) was used in the study as it gave good reproducible recoveries for all compounds. RP-C_{18} cartridge was conditioned with methanol (2 x 1 ml), and then water (2 x 1 ml). Methanol wets the surface of the sorbent and penetrates bonded alkyl phases, allowing water to wet the silica surface efficiently.

(2) Elution mixture

As an initial step the elution mixture reported by Zydron [19], which is chloroform: 2-propanol (80:20 % v/v) was examined. This elution solvent gave low recoveries for all the studied compounds in the range of 33-71 % w/w. Methanol has been used with chloroform instead of propan-2-ol in the same ratio and good recoveries were obtained (> 80 % w/w) for all the studied compounds (Figure 3.15).
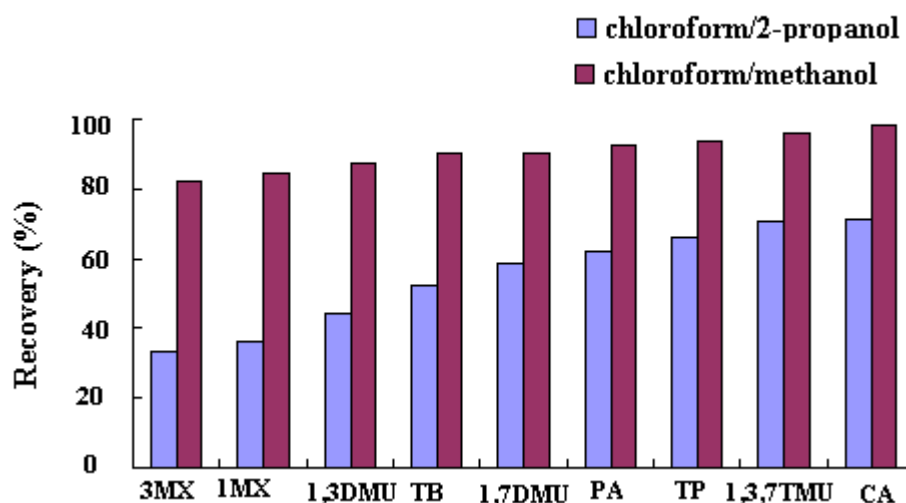
Figure 3. 15. *The effect of using different elution mixtures on the extraction efficiencies of the studied methylxanthines and methyluric acids.*

Different ratios of the chloroform: methanol mixtures have been also tested. The recoveries of the tested drugs decreased upon decreasing the amount of methanol in the elution mixture (5, 10 % v/v) as it became insufficient for the elution of the compounds from the C18 cartridge. Higher proportions of methanol (30, 40 % v/v) gave good recoveries but elution of some retained urine impurities was observed. Therefore, it was clear that 20 % v/v of methanol as the optimum amount. The Chromatograms of the blank urine and the extracted urine sample spiked with 40 μg ml^{-1}of studied compounds according to the optimized SPE method are shown in Figure 3.16. No interference from

any endogenous compounds in the sample matrix was observed. Peak resolution factors (Rs) ranged from 1.27 to 7.64 which indicating satisfactory separation of the resolved analytes.
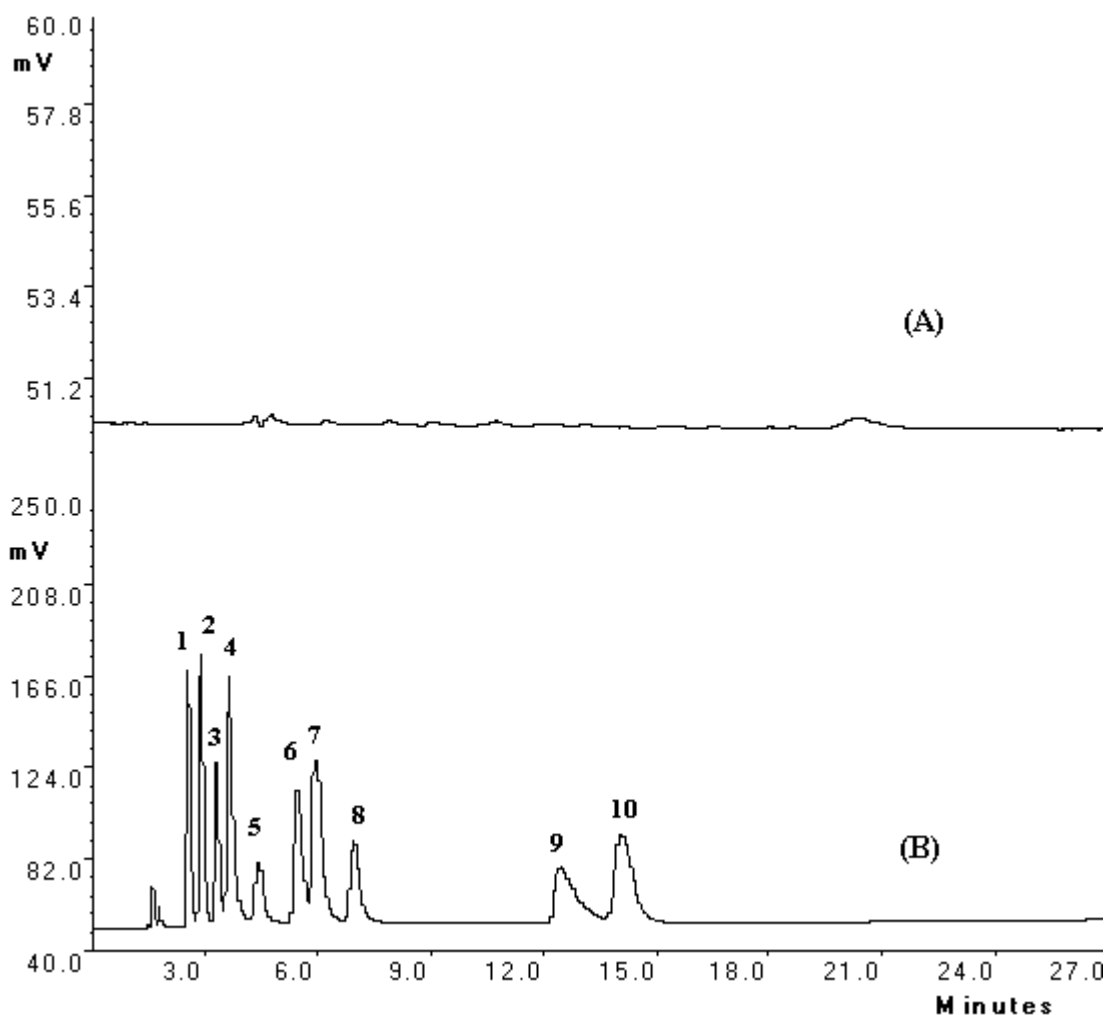
Figure 3. 16. *Chromatograms of blank urine sample (A), and extracted urine sample (B) spiked with standard solutions of the tested methylxanthines and methyluric acids at 40 μg ml^{-1}; with the optimal conditions; monolithic column (Batch1), methanol: 10 mM KH_2PO_4 (pH 4)(12.5:87.5 % v/v), flow rate 1ml min^{-1}, injection volume 20 μl, and UV detection at 274 nm. (1) 3-MX, (2) 1-MX, (3) 1,3-DMU, (4) TB, (5) 1,7-DMU, (6) PA, (7) TP, (8) 1,3,7-TMU, (9) CA, and (10) IS (30 μg ml^{-1}).*

The retention times of the studied compounds under the developed chromatographic conditions in both aqueous solution and in the extracted urine samples are presented in Table 3.7. It can be seen from the data that the retention times of the compounds of interest in urine sample is slightly increased from that in aqueous solution. This is

attributed to the use of a guard column connected to the monolithic column during the

work with biological samples leading to the increase of the actual length.

Table 3. 7. *Retention times of methylxanthines and methyluric acids in*

aqueous standard solutions and urine samples (n= 6)

Analytes	Retention times in aqueous solutions (min) ± SD	Retention times in urine samples (min) ± SD
3-MX	2.39 ± 0.01	2.55 ± 0.05
1-MX	2.68 ± 0.01	2.88 ± 0.05
1,3-DMU	3.04 ± 0.02	3.31 ± 0.03
TB	3.35 ± 0.02	3.63 ± 0.04
1,7-DMU	4.14 ± 0.03	4.43 ± 0.02
PA	5.22 ± 0.02	5.43 ± 0.04
TP	5.63 ± 0.03	5.94 ± 0.03
1,3,7-TMU	6.59 ± 0.09	6.95 ± 0.05
CA	12.02 ± 0.11	12.45 ± 0.05

3.3.5. Validation of the developed HPLC method for the determination of methylxanthines and methyluric acids mixture in urine samples

(1) Linearity

As stated in the ICH guideline [234] the linearity of an analytical procedure is its ability

to produce test results, which are proportional to the concentration of the analytes

within a certain concentration range. This also suggests that if there is a linear

relationship, the test results should be evaluated by appropriate statistical methods as

calculation of the regression line using least square equation; **y = bc + a**

Where, y: peak area ratios, a: intercept, b: slope, and c: drug concentration in $\mu g\ ml^{-1}$.

Under the developed procedure, the relationship between the peak area ratios versus the

standard concentrations was linear over the desired concentration range for all the tested

compounds. The intercepts (a), slopes (b), correlation coefficients (R^2), limits of

detection (LOD), and limits of quantitation (LOQ), for all studied compounds are

summarized in Table 3.8. From these results it was seen that the values of correlation

coefficients (R^2) of the calibration curves were > 0.9991 (n = 6). This proves that the

response of the detector showed a good linearity for quantification of the

methylxanthines and their metabolites over the studied concentration range. LODs and

LOQs were ranged from 0.004 - 0.014 µg ml^{-1}, and 0.014 - 0.041 µg ml^{-1}, respectively,

which indicates the good sensitivity of the analytical method.

Table 3. 8. *Data from the regression equations for determination of the studied methylxanthines and their metabolites after SPE from urine samples*

Analytes	Linear range (µg ml^{-1})	Slope*	Intercept*	R^2*	LOD (µg ml^{-1})	LOQ (µg ml^{-1})
3-MX	0.03- 40	0.062 ± 0.46	0.001 ± 0.08	0.9995 ± 0.07	0.005	0.014
1-MX	0.03- 40	0.057 ± 0.61	0.003 ± 0.09	0.9996 ± 0.38	0.005	0.016
1,3- DMU	0.05- 40	0.041 ± 0.07	0.001 ± 0.13	0.9995 ± 0.21	0.011	0.032
TB	0.03- 40	0.057 ± 0.39	0.002 ± 0.01	0.9994 ± 0.04	0.006	0.018
1,7- DMU	0.05- 40	0.044 ± 0.55	0.001 ± 0.13	0.9998 ± 0.12	0.009	0.029
PA	0.05- 40	0.043 ± 0.27	0.001 ± 0.13	0.9996 ±0.34	0.010	0.030
TP	0.03- 40	0.051 ± 0.13	0.001 ± 0.11	0.9993 ± 0.05	0.007	0.021
1,3,7- TMU	0.05- 40	0.027 ± 0.09	0.003 ± 0.11	0.9995 ± 0.21	0.014	0.041
CA	0.03- 40	0.049 ± 0.16	0.001 ± 0.11	0.9991 ± 0.05	0.007	0.022

* Average of six determinations ± S.D. x 10^{-3}.

(2) Recovery

The mean recoveries of all methylxanthines and their metabolites from the urine matrix for low and high spiked concentrations ranged from 82.28 to 98.73 % w/w.

The recoveries of these compounds were found to be consistent, precise and reproducible as their RSDs were < 2.5 % (Table 3.9).

Table 3. 9. *Recovery of the methylxanthines and their metabolites from urine samples after SPE (n = 6).*

Analytes	*Nominal conc. (µg/ml)	**Recovered conc. (µg/ml) ± SD	RSD (%)	Recovery (%)
3-MX	5.36	4.41 ± 0.08	1.81	82.28
	15.16	12.65 ± 0.24	1.89	83.44
	29.65	24.57 ± 0.45	1.83	82.87
1-MX	4.29	3.76 ± 0.02	0.53	87.65
	15.06	12.99 ± 0.23	1.77	86.25
	29.88	25.51 ± 0.05	0.20	85.37
1,3- DMU	5.40	4.78 ± 0.01	0.29	88.52
	14.86	13.15 ± 0.11	0.84	88.49
	30.24	26.86 ± 0.24	0.89	88.82
TB	5.06	4.52 ± 0.10	2.21	89.33
	15.22	13.73 ± 0.15	1.09	90.21
	30.11	26.94 ± 0.34	1.26	89.47
1,7- DMU	5.71	5.26 ± 0.06	1.14	92.12
	15.13	13.72 ± 0.22	1.60	90.68
	30.24	27.46 ± 0.59	2.15	90.81
PA	5.34	4.90 ± 0.10	2.04	91.76
	15.66	14.29 ± 0.24	1.68	91.25
	29.78	27.36 ± 0.06	0.22	91.87
TP	5.01	4.64 ± 0.02	0.43	92.61
	15.24	13.93 ± 0.33	2.37	91.40
	30.33	28.16 ± 0.06	0.21	92.85
1,3,7- TMU	5.11	4.78 ± 0.11	2.30	93.54
	14.81	14.03 ± 0.24	1.71	94.73
	30.02	28.41 ± 0.55	1.94	94.64
CA	5.01	4.93 ± 0.10	2.03	98.40
	15.21	14.99 ± 0.36	2.40	98.55
	29.88	29.50 ± 0.11	0.37	98.73

[*]Mean concentration of six injections of aqueous standard solutions.

[**] Mean concentration of six injections of extracted spiked urine samples.

(3) Precision and accuracy

Precision of an analytical method describes the closeness of a series of measurements obtained from multiple analysis of the same homogenous sample using certain analytical conditions [234]. The intra-day and inter-day precision of the developed method were checked by replicate analysis of six separate spiked urine samples of each of the three concentration levels within the same day or in different days respectively. The RSD's were less than 2.6 % in all cases, indicating good precision of the proposed method (Table 3.10). While the accuracy is described as the closeness between the true value and the measured values by the proposed analytical procedures [234]. The accuracy of the developed method was determined by comparing the actual concentrations with the measured concentrations after their extraction from urine samples. The accuracy percentages of all compounds ranged from 82.60-98.08 %w/w.

(4) Precision and reproducibility of the chromatographic data recovered from two different batches of monolithic columns [245].

The intra-day precision and inter-day precision of the chromatographic data acquired from two different batches of monolith columns were determined by repeating six consecutive runs of the test mixture on each column within one day and five working days respectively. The RSD measurements for all methylxanthines and their metabolites < 2.00 % and this indicates that the developed method using monolithic columns is precise (Table 3.11). Batch-to-Batch reproducibility is presented by the RSD of six injections on the two batches. The RSD for all compounds in both columns was< 2.50 % except for 3-MX (RSD = 4.59%), TB (RSD = 3.23 %) and 1,3-DMU (RSD = 2.94 %). From these results it is possible to suggest that there is no difference between the two monolith batches in terms of the retention time (t_R) or peak resolution (R_s) or in terms of peaks symmetry, which is expressed as the tailing factor (T $_{0.05}$) (Table 3.11).

Table 3. 10. *Precision and accuracy for the developed HPLC method for the determination of the methylxanthines and methyluric acids mixture in urine matrix*

	Actual conc. (µg/ml)	Intra-day precision (n= 6)		Accuracy (%)	Inter-day precision (n= 6)		Accuracy (%)
		Measured conc.(µg/ml)	RSD (%)		Measured conc. (µg/ml)	RSD (%)	
3-MX	5	4.16 ± 0.03	0.79	83.28	4.18 ± 0.06	1.51	84.90
	15	12.63 ± 0.22	1.72	84.22	12.40 ± 0.29	2.32	82.60
	30	25.27 ± 0.31	1.23	84.22	25.59 ± 0.31	1.22	85.29
1-MX	5	4.27 ± 0.06	1.35	85.44	4.28 ± 0.03	0.72	85.62
	15	12.80 ± 0.22	1.74	85.32	12.81 ± 0.33	2.55	85.39
	30	25.82 ± 0.36	1.41	86.06	25.73 ± 0.35	1.36	85.58
1,3-DMU	5	4.48 ± 0.05	1.04	89.56	4.48 ± 0.07	1.65	89.68
	15	13.29 ± 0.15	1.13	88.57	13.34 ± 0.18	1.37	88.91
	30	26.62 ± 0.14	0.53	88.72	26.64 ± 0.27	1.00	88.78
TB	5	4.45 ± 0.07	1.59	89.08	4.37 ± 0.04	0.92	87.33
	15	13.49 ± 0.25	1.86	89.93	13.45 ± 0.18	1.37	89.65
	30	26.71 ± 0.23	0.85	89.04	26.74 ± 0.12	0.45	89.12
1,7-DMU	5	4.51 ± 0.01	0.31	90.28	4.51 ± 0.02	0.34	90.10
	15	13.63 ± 0.17	1.22	90.83	13.63 ± 0.03	0.23	90.83
	30	27.02 ± 0.14	0.53	90.06	27.06 ± 0.06	0.23	90.20
PA	5	4.53 ± 0.07	1.52	90.56	4.54 ± 0.04	0.82	90.84
	15	13.64 ± 0.06	0.40	90.94	13.62 ± 0.14	1.04	90.83
	30	26.75 ± 0.11	0.42	89.18	27.17 ± 0.25	0.93	90.56
TP	5	4.70 ± 0.02	0.51	93.94	4.69 ± 0.04	0.81	93.80
	15	13.87 ± 0.04	0.25	92.46	13.81 ± 0.06	0.44	92.05
	30	27.65 ± 0.18	0.65	92.17	27.62 ± 0.31	1.14	92.08
1,3,7-TMU	5	4.77 ± 0.01	0.21	95.72	4.78 ± 0.01	0.23	95.52
	15	14.87 ± 0.11	0.74	95.01	14.24 ± 0.12	0.86	94.91
	30	28.41 ± 0.31	1.06	94.69	28.43 ± 0.31	1.10	94.75
CA	5	4.92 ± 0.02	0.37	98.44	4.90 ± 0.03	0.63	98.08
	15	14.66 ± 0.21	1.45	97.71	14.60 ± 0.08	0.56	97.33
	30	29.19 ± 0.07	0.25	97.30	29.34 ± 0.19	1.25	97.79

Table 3. 11. *Precision and reproducibility of the chromatographic data obtained from separation of methylxanthines and their metabolites on two different batches of monolithic columns (Batch 1. OB452773, Batch 2. HX754226)*

Analytes	RSD (%) of the chromatographic data (n=6)														
	Intra-day precision						Inter-day precision						Batch-to- Batch reproducibility		
	Batch 1			Batch 2			Batch 1			Batch 2					
	t_R *	$T_{0.05}$ •	R_S ••	t_R *	$T_{0.05}$ •	R_S ••	t_R *	$T_{0.05}$ •	R_S ••	t_R *	$T_{0.05}$ •	R_S ••	t_R *	$T_{0.05}$ •	R_S ••
3-MX	1.23	0.89	-	1.24	1.02	-	1.55	0.52	-	1.63	0.33	1.63	1.59	4.59	-
1-MX	1.02	0.70	0.88	1.23	1.36	1.35	0.90	0.66	1.82	1.28	0.84	0.47	1.57	0.42	2.27
1,3-DMU	0.65	0.76	1.12	0.86	0.69	1.87	0.32	1.09	1.18	0.95	2.34	0.92	1.76	2.94	2.10
TB	0.88	1.52	1.28	0.93	1.25	1.33	0.63	1.05	1.27	0.68	1.36	1.13	1.69	1.55	0.71
1,7-DMU	1.41	1.20	1.57	1.15	1.87	0.98	0.48	1.46	1.62	0.76	2.12	1.88	1.17	1.28	1.39
PA	1.19	1.36	1.44	1.66	0.56	0.81	0.46	1.72	1.53	1.26	1.32	1.65	1.04	1.75	2.00
TP	0.96	1.55	1.30	2.03	0.87	1.02	0.98	1.63	1.30	1.06	1.69	1.35	0.98	0.42	0.46
1,3,7- TMU	1.05	1.00	1.50	1.69	1.13	0.63	0.94	1.23	1.47	1.13	1.47	0.56	1.34	0.11	0.93
CA	1.71	1.53	0.58	1.39	1.52	0.56	1.80	0.41	1.64	1.87	0.68	0.43	0.51	2.14	0.62

* t_R: Retention time   • $T_{0.05}$; tailing factor at 5% of the peak height   •• R_S: Resolution factor

3.3.6. Performance comparison between the monolithic and traditional C$_{18}$ columns for separation of methylxanthines and methyluric acids mixture

Figures 3.17 and 3.18 show the chromatograms for all the studied methylxanthines and methyluric acids on the monolith and seven conventional HPLC columns. The tested columns were compared using relevant chromatographic parameters including; capacity factor (K′), peak resolution (Rs), and tailing factor (T$_{0.05}$) which express the peak symmetry (Table 3.12). Most of the tested columns were able to separate the mixture albeit with variable resolution peak symmetry, and total run time. From these results, it was observed the separation efficiency of monolith might be less than the symmetry or Hypersil columns even after extensive trials in optimization step. However, for all the tested columns at least 28 min is required for complete separation of the compounds of interest, while monolith needs only 14.06 min. The total run times for the Symmetry, Hypersil, ACE, Nucleosil 3 μm, Nucleosil 5 μm, Hichrome, and Zorbax C$_8$ were 30.18, 34.41, 49.34, 55.42, 44.13, 7.19, 28.01 min, respectively. Furthermore, lower backpressure (60 bar) was obtained upon working with monolith compared to other particulate packed columns (150-180 bar). Thus it can be concluded that the high permeability combined with high efficiency makes monolithic columns more convenient for high-speed separations especially when there is a complex mixture like the methylxanthines and their metabolites.
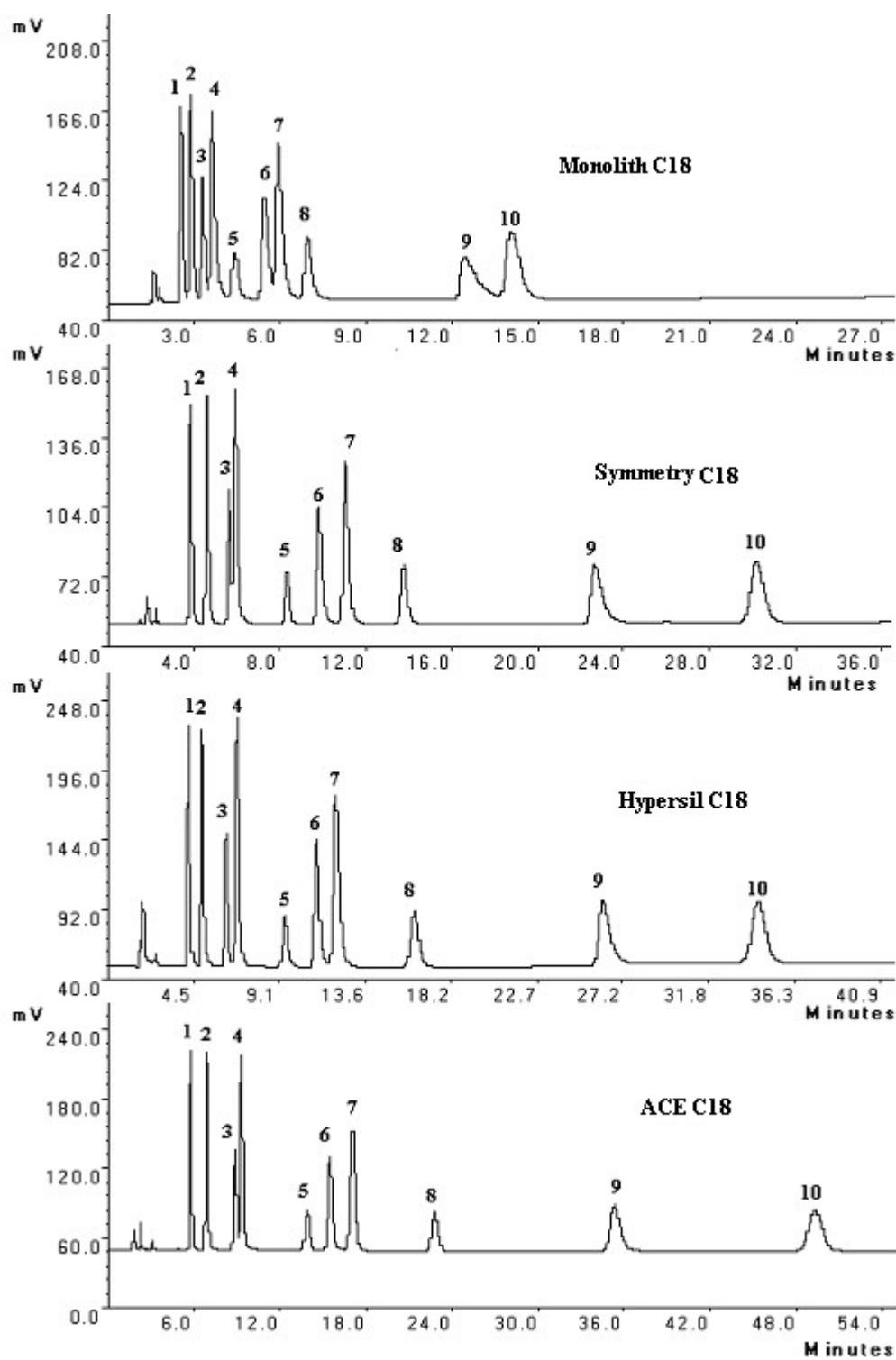
Figure 3. 17. *The chromatograms represent the separation of extracted urine samples spiked with 40 µg ml^{-1} of methylxanthines and their metabolites on monolithic (Batch1), Symmetry, Hypersil, and ACE columns with the optimal conditions; methanol: 10mM KH$_2$PO$_4$ (pH 4)(12.5:87.5 % v/v), flow rate 1ml min^{-1}, injection volume 20 µl, and UV detection at 274 nm. (1) 3-MX, (2) 1-MX, (3) 1,3-DMU, (4) TB, (5) 1,7-DMU, (6) PA, (7) TP, (8) 1,3,7-TMU, (9) CA, and (10) IS (30 µg ml^{-1}).*
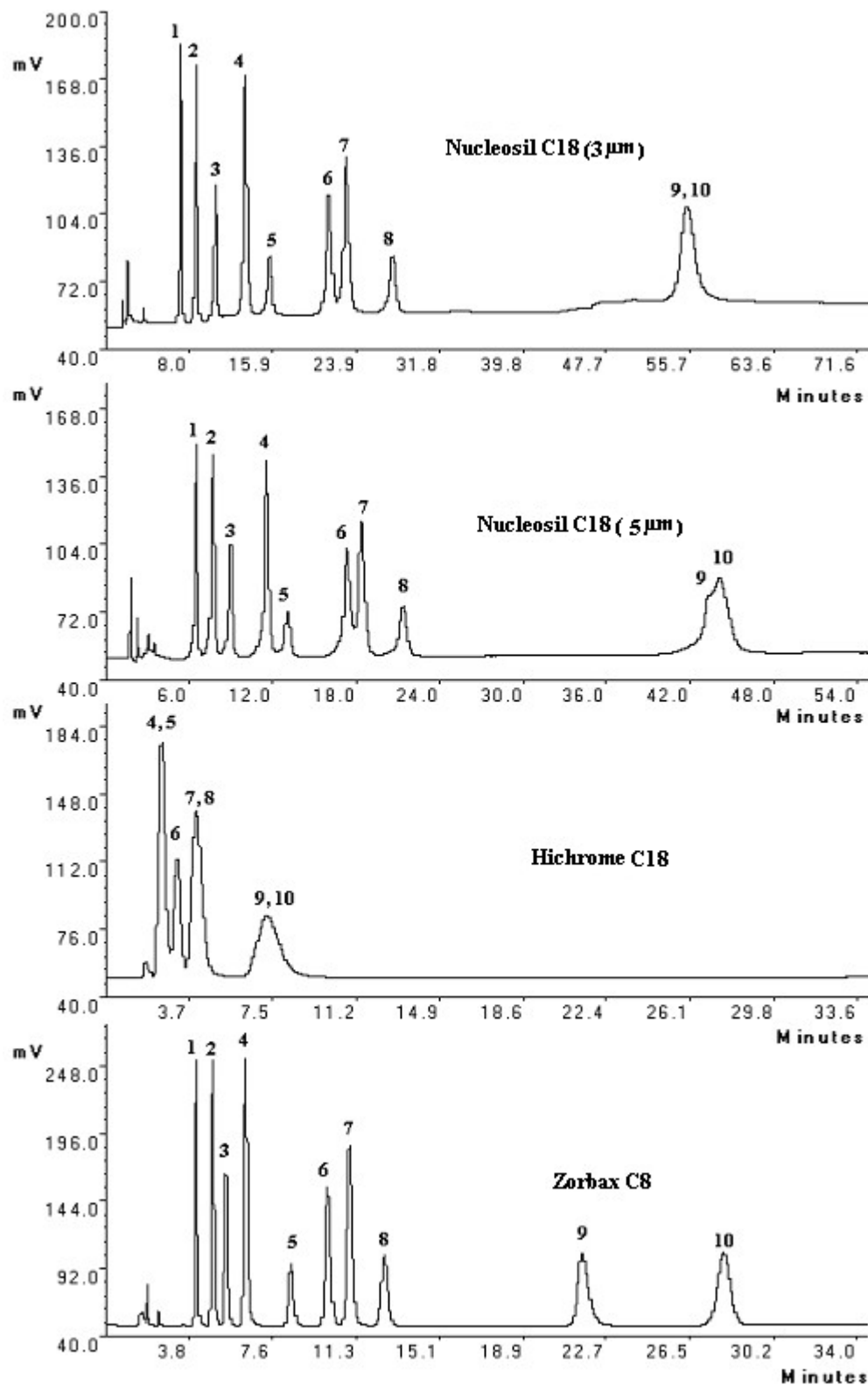
Figure 3. 18. *The chromatograms represent the separation of the extracted urine samples spiked with 40 μg ml^{-1} of methylxanthines and their metabolites on Nucleosil 3μm, Nucleosil 5μm, Hichrome, and Zorbax columns with the optimal conditions; methanol: 10mM KH_2PO_4 (pH 4)(12.5:87.5 % v/v), flow rate 1ml min^{-1}, injection volume 20 μl, and UV detection at 274 nm. (1) 3-MX, (2) 1-MX, (3) 1,3-DMU, (4) TB, (5) 1,7-DMU, (6) PA, (7) TP, (8) 1,3,7-TMU, (9) CA, and (10) IS (30 μg ml^{-1}).*

Table 3. 12. *Performances o f monolithic and traditional C_{18} columns for separation of the methylxanthines and methyluric acids mixture.*

Analytes	Monolith				Symmetry				Hypersil				ACE			
	K′	N ×10³	Rs	T$_{0.05}$	K	N ×10³	Rs	T$_{0.05}$	K′	N ×10³	Rs	T$_{0.05}$	K′	N ×10³	Rs	T$_{0.05}$
3-MX	2.40	3.73	-	1.60	4.12	5.90	-	1.33	4.69	7.19	-	1.38	6.69	11.11	-	1.14
1-MX	2.84	3.22	1.80	1.62	5.14	7.15	3.67	1.34	5.65	6.72	3.24	1.41	8.19	11.79	4.76	1.12
1,3-DMU	3.41	3.33	1.97	-	6.53	7.30	4.32	-	7.33	7.67	4.77	1.30	10.82	16.61	7.47	1.05
TB	3.84	2.60	1.27	-	6.90	6.13	0.97	-	8.09	7.62	1.91	1.40	11.41	10.99	1.40	0.73
1,7-DMU	4.89	1.86	2.27	1.69	10.13	6.68	6.81	1.22	11.50	6.87	6.68	1.22	17.53	10.19	10.1	1.10
PA	6.26	2.94	2.53	-	12.09	8.25	3.51	1.49	13.72	8.56	3.58	1.39	19.65	12.08	2.86	1.20
TP	6.92	3.79	1.26	-	13.74	10.57	2.87	1.40	15.08	7.21	1.95	1.41	21.73	11.88	2.63	1.15
1,3,7-TMU	8.28	4.16	2.49	1.50	17.37	10.20	5.58	1.30	20.63	7.76	6.38	1.22	29.37	12.17	7.89	1.12
CA	15.60	2.33	7.51	-	29.21	9.33	11.9	2.16	33.89	10.08	11.1	1.99	46.09	12.24	11.9	1.42
Analytes	**Nucleosil 3 μm**				**Nucleosil 5 μm**				**Hichrome**				**Zorbax C₈**			
	K′	N ×10³	Rs	T$_{0.05}$	K′	N ×10³	Rs	T$_{0.05}$	K′	N ×10³	Rs	T$_{0.05}$	K′	N ×10³	Rs	T$_{0.05}$
3-MX	8.56	10.87	-	0.86	7.68	7.61	-	0.80	-	-	-	-	4.47	8.18	-	1.22
1-MX	10.54	9.50	4.72	0.90	9.56	6.87	3.52	0.84	-	-	-	-	5.46	8.52	3.79	1.19
1,3-DMU	12.94	9.41	4.57	0.88	10.96	7.54	3.25	0.81	-	-	-	-	6.27	8.61	2.75	1.12
TB	16.72	10.19	5.92	1.05	14.38	7.87	5.10	0.86	2.32	0.32	-	-	7.44	9.49	3.55	1.29
1,7-DMU	19.86	8.48	3.91	0.83	16.44	7.49	2.74	-	-	-	-	-	10.18	7.58	6.37	1.18
PA	27.34	10.22	7.39	-	22.07	9.44	6.41	-	3.28	0.42	1.22	-	12.41	9.05	4.14	1.19
TP	29.49	10.88	1.87	-	23.47	8.77	1.41	0.68	4.42	0.34	1.14	-	13.72	9.94	2.27	1.14
1,3,7-TMU	35.48	10.73	4.65	0.85	27.49	8.43	3.51	0.82	-	-	-	-	15.83	9.41	3.29	1.07
CA	72.89	8.06	15.9	1.25	56.67	-	-	-	8.59	0.23	2.27	1.34	27.78	10.18	13.0	1.41

K′; capacity factor,   N; number of theoretical plates   Rs; peak resolution   T$_{0.05}$; tailing factor at 5% of the peak height

N.B. absence of data (-) indicates that insufficient resolution was observed

3.3.7. Performance comparison between monolithic and platinum columns for separation of methylxanthines and methyluric acids mixture.

The performances of both platinum and monolithic columns for separation of theophylline and its related compounds were compared using the developed HPLC method mentioned in section 3.2.3.10. Figure 3.19 shows the methylxanthines and methyluric acids mixture, which was separated on both columns. Table 3.13 shows different chromatographic parameters obtained from both columns
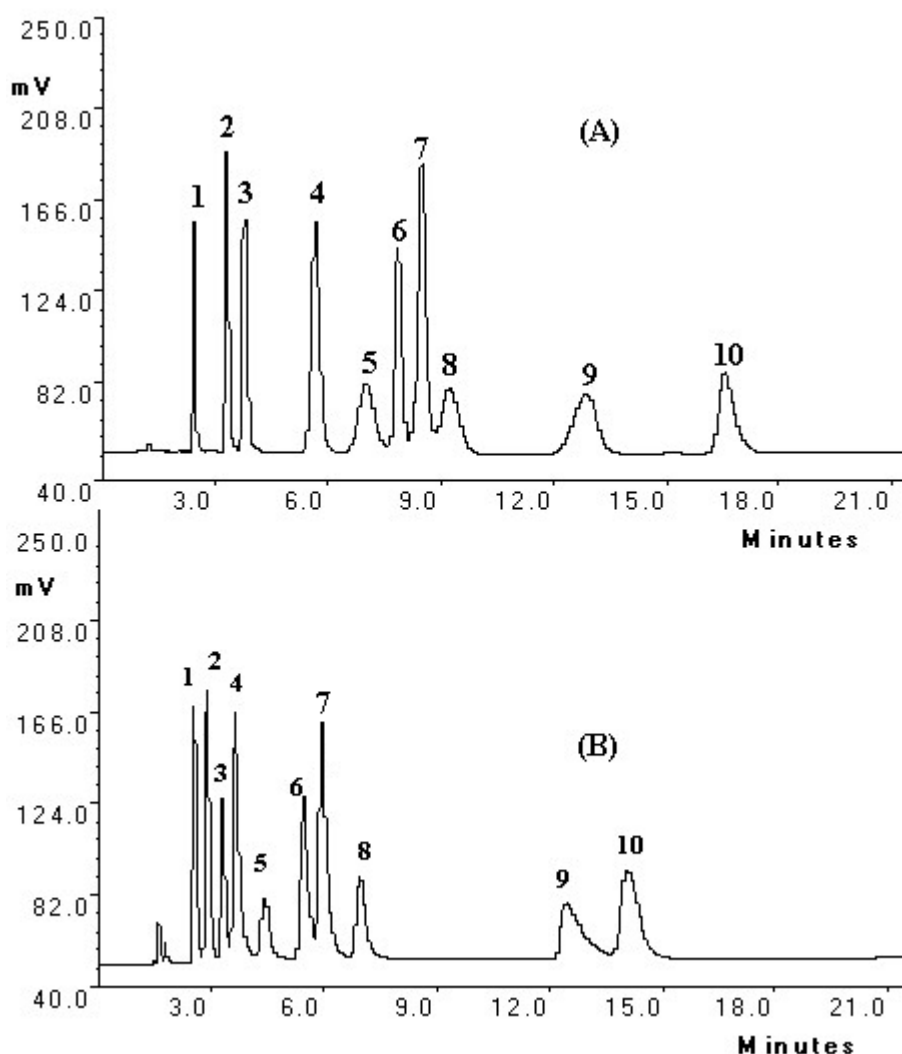
Figure 3. 19. *The chromatograms represent the separation of extracted urine samples spiked with 40 μg ml^{-1} of methylxanthines and their metabolites on platinum (Batch1) (A) and monolithic (Batch1)(B) columns with the optimal conditions; methanol: 10mM KH$_2$PO$_4$ (pH 4)(12.5:87.5 % v/v), flow rate 1ml min^{-1}, injection volume 20 μl, and UV detection at 274 nm. (1) 3-MX, (2) 1-MX, (3) 1,3-DMU, (4) TB, (5) 1,7-DMU, (6) PA, (7) TP, (8) 1,3,7-TMU, (9) CA, and (10) IS (30 μg ml^{-1}).*

Table 3. 13. *Performances of monolithic and platinum C_{18} columns for separation of the methylxanthines and methyluric acids mixture.*

Analytes	Monolith				Platinum C_{18}			
	K′	**N ×10³**	**Rs**	**T$_{0.05}$**	**K**	**N ×10³**	**Rs**	**T$_{0.05}$**
3-MX	2.40	3.73	-	1.60	2.61	10.28	-	1.39
1-MX	2.84	3.22	1.80	1.62	3.42	7.89	2.06	1.11
1,3-DMU	3.41	3.33	1.97	-	4.07	7.53	2.97	1.07
TB	3.84	2.60	1.27	-	6.26	8.52	7.99	1.17
1,7-DMU	4.89	1.86	2.27	1.69	7.02	1.28	3.08	1.62
PA	6.26	2.94	2.53	-	7.81	9.32	1.44	-
TP	6.92	3.79	1.26	-	8.35	9.43	1.60	-
1,3,7-TMU	8.28	4.16	2.49	1.50	9.04	4.41	1.23	-
CA	15.60	2.33	7.51	-	13.03	1.90	6.07	0.97

Platinum and monolith was able to separate the studied mixture efficiently with no sharp difference (2 min.) in the total analysis time with monolith 16.72, 14.03 min., respectively. If a choice was to be made, the peak resolution and symmetry values obtained from the platinum were slightly better however; the lower backpressure of the monolithic column was preferred. The backpressure achieved using monolith was 56 bar while with platinum was about 170 bar.

As a conclusion the monolithic column is a useful tool of achieving efficient separation under lower backpressure and shorter run time which are the most important aspects in method development [246]. This is also important when repeated analyses are required during manufacturing process at quality control laboratories. It also provides rapid washing and equilibrium times. Although some of the tested packed columns have an equivalent selectivity to the monolithic column, but they take more time to re-equilibrate (30 min.) or to wash the stationary phase [16, 247]. These advantages should aid in the reduction of the total time to develop a method using a monolith compared with a packed column.

The high permeability and total porosity in the monolithic column allows the use of high flow rate without a significant increase in backpressure or substantial loss in the resolution power [248]. This will provide a time saving analysis with only minimal resolution loss. On the other hand with all the tested packed columns, the backpressure increases significantly by increasing the flow rate. This considered as the main disadvantage since working at high pressure limits the speed of analysis and reduces the lifetime of the HPLC instrument and the injector seals.

Packed columns are filled with 3-5 μm particles which can be easily block and cause high backpressure, especially with biological samples and thereby reduce the column lifetime. On the other hand, with the monolithic columns, there is a reduced need for tedious sample preparation, as they are very resistant to blocking (even with biological samples).

3.3.8. Validation of the developed HPLC method for the determination of theophylline in aqueous solution

Figure 3.20 represents the typical chromatogram of theophylline and the internal standard in aqueous solution using the optimized HPLC method (section 3.2.3.10).
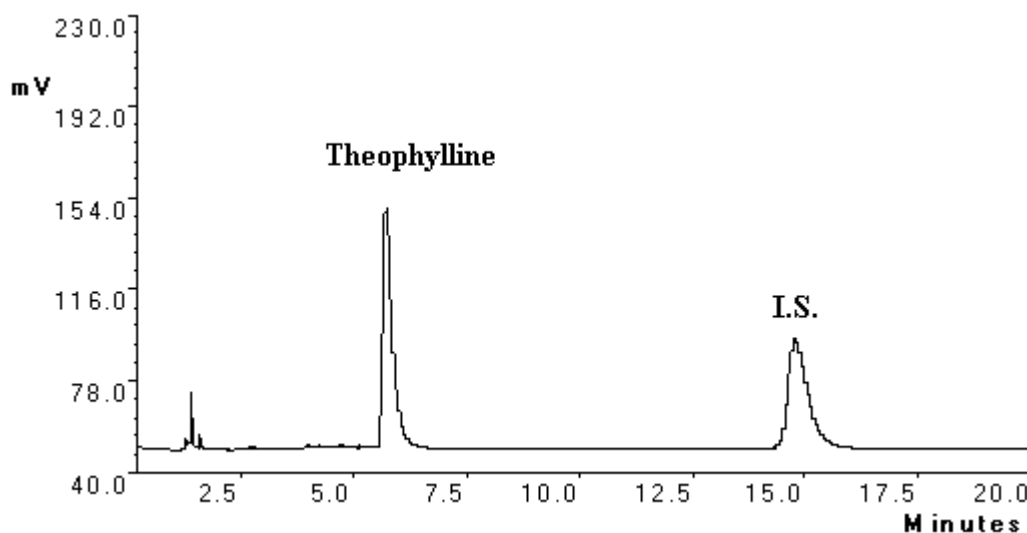
Figure 3. 20. *The typical chromatogram of theophylline (50 μg ml^{-1}) and 8-chlorotheophylline (I.S. 30 μg ml^{-1}) in aqueous solution with the optimal conditions; monolithic column (Batch1), methanol: 10 mM KH$_2$PO$_4$ (pH) 4 (12.5:87.5 % v/v), flow rate 1ml min^{-1}, injection volume 20 μl, and UV detection at 274 nm.*

(1) Linearity

Under the optimized chromatographic conditions, the relationship between peak area ratios (compound/internal standard) and theophylline concentrations was linear in the range 20-200 μg ml^{-1} (Figure 3.21). The mean of slopes and intercepts for five calibration curves (n= 6) were 0.06 ± 0.002 and 0.19 ± 0.001, respectively and correlation coefficient R^2 = 0.9993 ± 0.004. The limits of detection (LOD), and limits of quantitation (LOQ), of theophylline in aqueous solutions were 0.08 and 0.23 μg ml^{-1}, respectively. This enabled the determination of theophylline in different pharmaceutical formulations and in the assessment of the aerodynamic behaviour of theophylline (chapter 5).
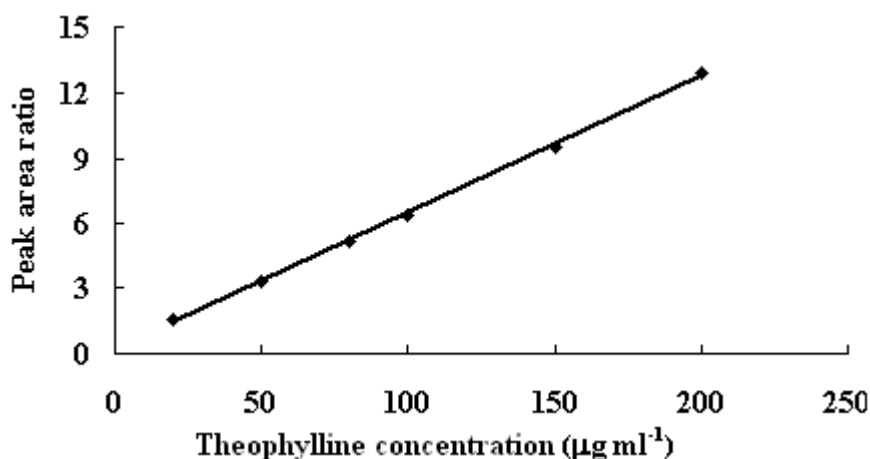
Figure 3. 21. *The calibration curve of theophylline aqueous standard solutions (I.S. concentration 30 μg ml^{-1}) with the optimal conditions; monolithic column (Batch1), methanol: 10 mM potassium dihydrogen phosphate pH 4 (12.5:87.5 % v/v), flow rate 1ml min^{-1}, injection volume 20 μl, and UV detection at 274 nm.*

(2) Recovery from different pharmaceutical formulation

The developed HPLC procedure was applied for the analysis of the commercially available dosage forms of theophylline. Results presented in Table 3.14 indicate good recovery (95.24-98.62 % w/w) of theophylline from the studied formulations and confirm the absence of interference due to common excipients. This is also confirmed by the RSD values at three concentration levels, which are not exceeding 2.00 %.

Table 3. 14. *Recovery of theophylline from its pharmaceutical dosage forms*

Pharmaceutical formulations	*Nominal conc. (μg/ml) ± SD	**Recovered conc. (μg/ml) ± SD	RSD (%)	Recovery (%)
Nulein[®] SA	50.32	49.12 ± 0.25	0.51	97.61
	99.36	95.40 ± 0.69	0.72	96.01
	149.28	143.16 ± 0.83	0.58	95.90
Uniphuylline[®]	50.11	49.34 ± 0.14	0.28	98.47
	100.03	98.65 ± 0.92	0.93	98.62
	151.55	149.46 ± 0.35	0.23	98.62
Slo-phylline[®]	49.23	47.19 ± 0.33	0.69	95.86
	98.01	94.77 ± 0.84	0.89	96.69
	150.26	143.11 ± 0.73	0.51	95.24

*Mean concentration of six injections of aqueous standard solutions.

** Mean concentration of six injections of extracted samples.

(3) Precision and Accuracy

Intra-day precision of the proposed method was tested by replicate analysis of six separate aqueous solutions of the working standard of theophylline, at three different concentration levels. This study was repeated for five days to determine the inter-day precision. RSD % values for theophylline in all cases were ranged from 0.47-1.14 indicating good repeatability and precision (Table 3.15). Accuracy was determined by comparing measured concentrations of theophylline with the actual values and expressed as percentage. The accuracy of the method ranged from 99.02 - 99.78 % w/w.

Table 3. 15. *Precision and accuracy of the developed HPLC method for the determination of theophylline in aqueous standard solutions*

Actual conc. (μg)	Intra-day precision and accuracy (n= 6)			Inter-days precision and accuracy (n= 6)		
	Measured conc. (μg/ml) $\pm$ S.D.	RSD (%)	Accuracy (%)	Measured conc. (μg/ml) $\pm$ S.D.	RSD (%)	Accuracy (%)
50	49.51 ± 0.55	1.11	99.02	49.83 ± 0.31	0.63	99.66
100	99.24 ± 0.47	0.47	99.24	99.78 ± 0.48	0.48	99.78
150	149.65 ± 1.70	1.14	99.76	148.53 ± 0.85	0.57	99.02

In conclusion, the results show that the new developed method gives improved separation and quantitation of the methylxanthines and their metabolites in <15 min, with high precision, and accuracy. Moreover the solid phase extraction procedure described here provides an easier and solvent saving sample preparation technique comparing to traditional liquid-liquid extraction with high recoveries (> 80%). However, many reported of the HPLC methods for CA or TP and their metabolites show interference from caffeine metabolites and especially paraxanthine [78]. In addition some of these methods require complexed pre-treatment steps and long retention times to complete the separation of all the methylxanthines [81-83]. The developed method provides a mean for assessing of theophylline concentration in urine samples for asthmatic patients consuming methylxanthines containing food.

Chapter 4

Crystallisation of theophylline using Solution Enhanced Dispersion by SCFs (SEDS) process and solid-state analysis of the products

4.1. Introduction

The particle size, morphology, and configuration of the crystalline lattice can all play an important role in the therapeutic behaviour of substances especially for respiratory drug delivery. Therefore, the production of micro- and nano- particles with controlled characteristics is a critical step in pharmaceutical industry. Of the many procedures used, crystallisation using supercritical fluids (SCF) was mainly developed to overcome the drawbacks of the conventional techniques used for production of micro- or nano-particles such as spray drying, milling and re-crystallisation using liquid antisolvent [13]. It can provide an improved control of the particle size, a lower concentration of residual solvent in the product as well as the environmental advantage of reducing the solvent wastes [14]. Carbon dioxide (CO_2) is commonly used as an SCF especially for pharmaceutical compounds [9] due to its mild critical conditions of temperature (31.1°C), and pressure (73.8 bar) and its non-reactive characteristics.

There have been different SCF techniques proposed as the Rapid expansion of supercritical solutions (RESS), and Precipitation from gas saturated solutions (PGSS) processes. However, crystallisations using supercritical CO_2 (SC-CO_2) as antisolvent as in the Aerosol solvent extraction system (ASES), and Solution enhanced dispersion by SCFs (SEDS) processes have been commonly used in different pharmaceutical applications. Their main advantages include a totally enclosed single step process, which require reduced amounts of organic solvent compared to traditional crystallisation [9].

Particle formation in these techniques is determined by the mass-transfer of the SCF into the atomised drug solution. In order to obtain small particle and minimize the particle agglomeration frequently observed, increased mass-transfer rates and a reduction in the drying time are required [127]. These have been efficiently achieved in SEDS process by the use of coaxial nozzle design with mixing chamber (Figure 4.1.).
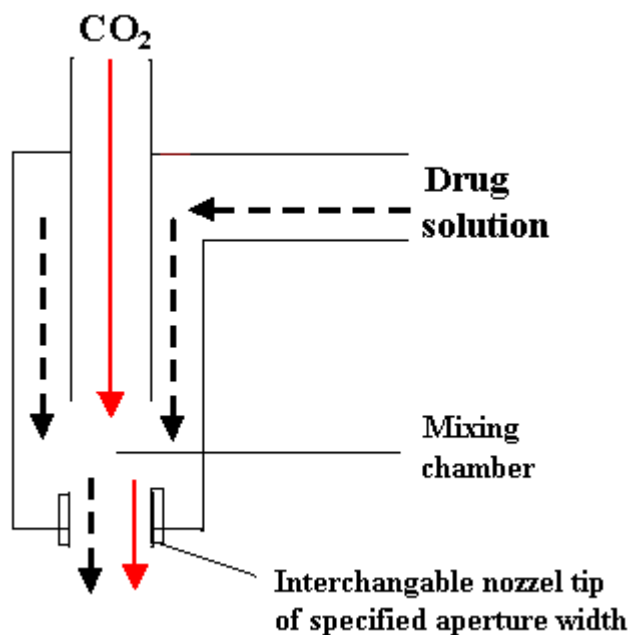
Figure 4. 1. *Schematic diagram of a SEDS two coaxial nozzle.*

This arrangement provides a means by which the drug solution interacts and mixes with the SCF in the mixing chamber before dispersion and then flows to the particle formation vessel via a restricted orifice. Thus high mass transfer rates are achieved with a high ratio of SCF to the solvent and the high velocity of the SCF facilities the jet break-up into small droplets [9].

Theophylline (TP) a methylxanthines derivative has a bronchodilator effect but its low solubility in water restricts its clinical applications. The drug also has a low therapeutic index with a small difference between its therapeutic benefits and toxic effects. Therefore controlling the particle size, morphology and the crystal structure of TP during its production process is important to assist characteristics like bioavailability, functionality and stability [12].

Several important operating parameters have been identified previously as influencing the re-crystallisation and product formation by SEDS process. These are temperature, pressure, and solution flow rate. The working temperature and pressure determine the

density of SC-CO_2, which in turn affects the extraction rate of the solvent into the SC-CO_2 and the supersaturation state of the test compounds [249].

The effect of these parameters on TP produced by SEDS technique was investigated in this study, which focused on the particle size and other important characteristics of the powdered products. The precipitated samples were characterized by scanning electron microscope (SEM), X-ray powder diffraction (XRPD), Fourier transform infrared spectroscopy (FT-IR), Fourier transform Raman (FT-Raman), thermogravimetric analysis (TGA), and differential scanning calorimetry (DSC).

4.2 Material and methods

4.2.1. Material

- Theophylline anhydrous, minimum 99% (Sigma-Aldrich Inc, St. Louis, MO, USA).

- HPLC grade absolute ethanol (EtOH) and dichloromethane (DCM) (Fischer Scientific, Loughborough, UK)

4.2.2. Methods

4.2.2.1. Preparation of the theophylline solution

Solution of unprocessed theophylline with concentration of 1g % w/v (10 mg ml^{-1}) was prepared in ethanol: dichloromethane mixture (50:50 % v/v) assisted by sonication for 15 min.

4.2.2.2. Precipitation of theophylline particles by SEDS process

Figure 4.2 shows a schematic diagram of the SEDS equipment and Table 4.1 lists the components of the laboratory scale equipment
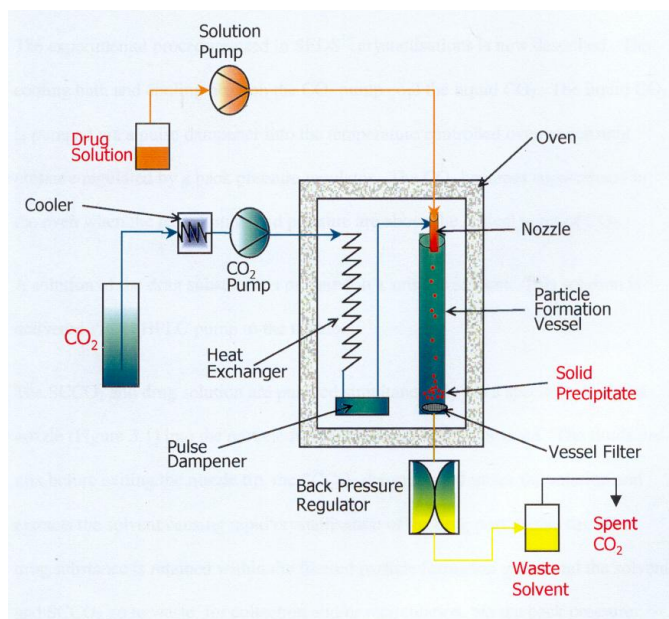
Figure 4. 2. *Schematic diagram represents SEDS process* [250]

Table 4.1. *SEDS equipment components list*

Component	Manufacturer
Cooler Bath. Model: LTD6G	Grant Ltd, Hertfordshire, UK
HPLC Pumps. Models Pu 980, PU 1580	Jasco CO. Tokyo, Japan
Column oven. Model: PU860-CO	Jasco CO. Tokyo, Japan
Back Pressure Regulator and controller. (Model: PU880-81)	Jasco CO. Tokyo, Japan
Pressure vessel 50 ml	Keystone Inc, USA
Nozzle 2 component	Bradford Particle Design PLC, UK

4.2.2.2.1. The experimental procedure used in SEDS crystallisation

The liquid CO_2 temperature is lowered via the cooling bath and the cooling head. The liquid CO_2 is pumped via a pulse dampener into the temperature controlled oven at constant pressure regulated by a backpressure regulator (BPR). The CO_2 becomes supercritical in the oven where the temperature and pressure conditions are above the critical point of CO_2.

The prepared theophylline solution (1g % w/v) and $SCCO_2$ are pumped simultaneously via a specially designed coaxial nozzle into the particle formation vessel within the oven. The fluids premix before exiting the nozzle tip where the $SC-CO_2$ disperses and mixes with the drug solution and extracts the solvent. This results in a high degree of supersaturation causing rapid crystallisation of the drug precipitation post the nozzle tip. The drug substance is retained by the filter in the particle formation vessel, while the solvent and $SC-CO_2$ go to waste for collection or recirculation via the BPR.

Finally, after completion of the precipitation process, the whole system is flushed with $SC-CO_2$ to ensure that the retained drug substance is dry and solvent free. The system is then slowly depressurized, and the drug collected, labelled, stored at ambient temperature and protected from light and moisture prior to analysis. The ratio of the amount of the collected powder to that delivered in the drug solution is defined as the process yield.

Different temperatures, pressures and drug solution flow rate have been used in this study to determine the effect of these parameters on the properties of the theophylline particles produced. Three runs were done for different samples prepared at different conditions.

4.2.2.3. Methods of particle analysis

4.2.2.3.1. Particle size analysis

Particle size analysis of the processed samples was made by using Photon Correlation Spectroscopy (PCS), using a Zetasizer[®] Nano-S (Malvern Instruments Ltd, Worcestershire, UK) (0.6 nm to 6 μm). Analyses provided the mean particle diameter (n=6) of SEDS theophylline samples. PCS relies on measuring the fluctuations in the intensity of the scattered light from large and small particles that occurs because they are undergoing Brownian motion. By determining the diffusion rate of the tested particles, their sizes can be obtained [251]. Suspensions of all the processed samples were firstly prepared in absolute ethanol at a concentration of 500 μg ml^{-1}. About 2.00 ml from each shaken suspensions were transferred into disposable polystyrene cuvettes and then loaded in the instrument for measurement. During all experiments, the viscosity of the suspensions (continuous phase) was taken as the viscosity of ethanol (1.200 cP at 25 °C).

4.2.2.3.2. Scanning electron microscope

The morphology and size of unprocessed and SEDS particles were investigated using a Quanta 400 SEM (FEI Europe Ltd, Cambridge, UK) equipped with a low vacuum facility. The sample was dusted onto a graphite disk that was affixed to the sample holder, then viewed and photographed under varying magnifications. Higher resolution and depth of focusing can be achieved compared with optical microscopy.

4.2.2.3.3. Differential scanning calorimetry (DSC)

DSC measures the differential heat flow required to maintain a pair of sample pans (one containing the sample and the other is an empty reference pan) at the same temperature throughout a thermally dependent process. A baseline was obtained using empty pan holders prior to the analyses. Any deviation from this base line determined in subsequent analyses relates to a thermal event. For the apparatus used in the project, positive deviation from the base line represents an endothermic process such as melting, while the negative deviations represent exothermic processes such as re-crystallisation. DSC is used to monitor any phase transitions after processing and storage of the theophylline samples, which could be related to a change in the crystal structure of the processed samples. DSC analysis was performed using a TA Instrument 2920 Modulated DSC (TA instruments LTD, Sussex, UK). Samples (1-3 mg) were placed in the instrument in pierced crimped pans and scanned from 25-300°C at a heating rate 10°C min^{-1}. The calorimeter was calibrated using pure indium (melting point 156.6°C) and zinc (melting point 419.5°C) standards. Each SEDS sample was analysed three times and the melting point and latent heat of fusion (ΔH_f) were recorded.

4.2.2.3.4. Thermal Gravimetrical analysis (TGA)

This instrument measures thermally induced weight loss of produced materials as a function of applied temperature. Dynamic TGA measures the change in weight of sample over a temperature range at a pre-determined heating rate. TGA analysis was performed using TA Instrument 2920 Modulated TGA (TA instruments LTD, Sussex, UK). Samples were placed in an open pans attached to the microbalance and then heated at a uniform rate of 10°C min^{-1}over a range 25-400°C. The instrument was calibrated with a ferromagnetic standard. Each SEDS sample was analysed three times and the transition temperature was recorded.

4.2.2.3.5. X-ray Powder Diffraction (XRPD)

XRPD analysis of bulk-powdered samples has been used to assess any change in the crystalline structure of SEDS samples under different experimental conditions comparing to the unprocessed sample. Powder X-ray diffraction was recorded with a Bruker D8 diffractometer (Bruker AXS Limited, Coventry, UK). A small quantity of the SEDS sample was packed into the sample holder and then placed in the equipment. The samples were then scanned from 5-50° (2θ) with a 0.01° step width and a 1 second time count using Cu source (x-ray λ = 0.154 nm), voltage 40 kv, and the filament emission 30 mA. The receiving slit on the instrument was 1° and the scatter slit 0.2°. The system was calibrated using the diffraction peaks of crystalline silicone with an accuracy of 10^{-4}° (2θ).

4.2.2.3.6. Fourier Transform Infra-Red (FT-IR)

FT-IR has been used to monitor any structural or polymorphic changes by detecting any changes in molecular vibration for samples. FT-IR was performed using Perkin Elmer 1725-x spectrophotometer (Perkin Elmer Ltd, Bucks, UK). The sample (0.005 g) was mixed well with dried KBr (0.35g) and then the mixture was used to form a compact disc and placed in the instrument. The sample disc was then scanned over wave number 500 to 4000 cm^{-1} at 4 cm^{-1} spectral resolution and 264 spectral scans. Visual inspection of the spectra was used to identify any major differences between the obtained FT-IR spectra of the processed theophylline samples and the reference spectra for unprocessed theophylline [252, 253].

 The instrument resolution is calibrated by recording the spectrum of a polystyrene film approximately 35 μm in thickness. The difference between the absorbances at the absorption minimum at 2870 cm^{-1} and the absorption maximum at 2849.5 cm^{-1} is greater than 0.33. The difference between the absorbances at the absorption minimum at

1589 cm^{-1} and the absorption maximum at 1583 cm^{-1} is greater than 0.08. Calibration of wavenumber is checked by reference to a polystyrene film at 14 specified wavenumbers; the reference values range from 3027.1 $\pm$ 0.3 to 698.9 $\pm$ 0.5 cm^{-1}.

4.2.2.3.7. Fourier Transform Raman Spectroscopy (FT- Raman)

FT-Raman spectra were recorded using a Bruker IFS 66 instrument with an FRA 106 Raman module attached (Bruker Optics Inc., Ettlingen, Germany), with Nd3+/YAG solid state laser operating at 1064 nm and liquid nitrogen cooled InGaAs detector. Spectra were recorded at 4 cm^{-1} spectral resolution, and 200 spectral scans were accumulated to improve signal-to-noise ratios. Laser power was maintained at 26 mW at the sample. The spectral wave number range was typically 4000-80 cm^{-1}. For calibration sulphur was used produced 25,000 counts at 37 mW. The spectra obtained for SEDS samples were compared with that of the unprocessed theophylline sample to detect any differences.

4.3. Results and discussion

4.3.1. Re-crystallisation process

Pure theophylline was re-crystallised from an EtOH-DCM mixture (50: 50 % v/v) by the SEDS process using SC-CO$_2$ as the antisolvent. This solvent mixture is based on number of reported studies for the theophylline solubility in different solvents [12, 254]. Where, it was reported that the addition of solvents like DCM to ethanol enhances the TP solubilization by a factor of 5.8 mg ml^{-1} at 36.15 °C. A 50:50 % v/v of EtOH-DCM mixture was found to produce dispersions of relatively low viscosity. This enabled processing of the solutions by SEDS without the occurrence of nozzle blocking [255].

The concentration of theophylline solution was limited by its viscosity, as highly concentrated solutions causing difficulties in pumping the solutions. Thus the drug solution with concentration of 10 mg ml^{-1} (1g % w/v) provided a balance between a solution suitable to be pumped at moderate backpressure values while still of sufficiently high concentration to allow an acceptable processing rate. On the other hand solutions at lower concentrations were too diluted to produce a precipitation of theophylline [255].

4.3.2. The effect of changing the variable crystallisation parameters on the mean particle size of theophylline

It was reported [256] that changing the crystallisation conditions can alter the produced mean particle size. Therefore, the effect of changing temperature, pressure, and solution flow rate on the mean particle size was investigated to ascertain the significance of varying theses crystallisation parameters in this study. The aim is to provide a general prediction for the mean particle size of theophylline at a given set of crystallisation parameters. Typically, inhalations products require sub 5 μm particles; therefore a predictive method for approximate mean particle size could reduce the number of experiments before the identification of the optimised parameters.

The effects of temperature and pressure in the ranges of 40-60 °C and 80-125 bar, respectively were investigated. These selected ranges allow the operation with CO_2 as antisolvent in supercritical state. The drug solution flow rate ranged from 0.1-0.3 ml min^{-1}, while the SC-CO_2 was pumped at 20 ml min^{-1}. In this study nozzle tips with 0.5 mm internal diameter were used while others with lower diameters were found to be more susceptible to blockage. Table 4.2 shows the operating conditions, yield, and the mean particle size of the theophylline SEDS samples.

Table 4. 2.*The experimental conditions, yield and the mean particle size of theophylline samples re-crystallised from EtOH-DCM mixture using the SEDS technique.*

Sample	Solution flow rate (ml min^{-1})	CO$_2$ flow rate (ml min^{-1})	T (°C)	P (bar)	Nozzle tip i.d. (mm)	Yield (%)	Mean particle size (μm) (n=6) (SD)
1	0.2	20	50	80	0.5	92	2.44 (0.29)
2	0.2	20	50	95	0.5	75	2.69 (0.45)
3	0.2	20	50	125	0.5	45	2.87 (0.13)
4	0.2	20	60	80	0.5	50	1.82 (0.46)
5	0.2	20	60	95	0.5	47.5	1.89 (0.56)
6	0.2	20	60	125	0.5	83	2.44 (0.36)
7	0.2	20	40	80	0.5	33	2.55 (0.47)
8	0.2	20	40	95	0.5	50	2.89 (0.60)
9	0.2	20	40	125	0.5	37.5	3.12 (0.04)
10	0.3	20	50	95	0.5	90	3.11 (0.56)
11	0.3	20	60	125	0.5	70	2.71 (0.91)
12	0.1	20	60	125	0.5	60	2.20 (0.25)
13	0.1	20	50	95	0.5	60	1.82 (0.31)
14	0.3	20	60	80	0.5	60	2.46 (0.22)
15	0.3	20	40	125	0.5	70	3.54 (0.62)

From the results in Table 4.2 it can be observed that the mean particle size obtained from Zetasizer® Nano-S and confirmed by SEM images for all the processed samples were in the range of 2-5 μm. There is a dramatic reduction in the particle size of the processed samples when compared to the unprocessed theophylline sample (30-100 μm). Figure 4.3 illustrates the SEM images of unprocessed theophylline and SEDS sample 1 as a representative example showing the difference in particle size as well as particle shape. It can also be noted from the results in Table 4.2 that the change of temperature, pressure and the solution flow rate over the precipitation process affect the particle size of the precipitated theophylline samples.
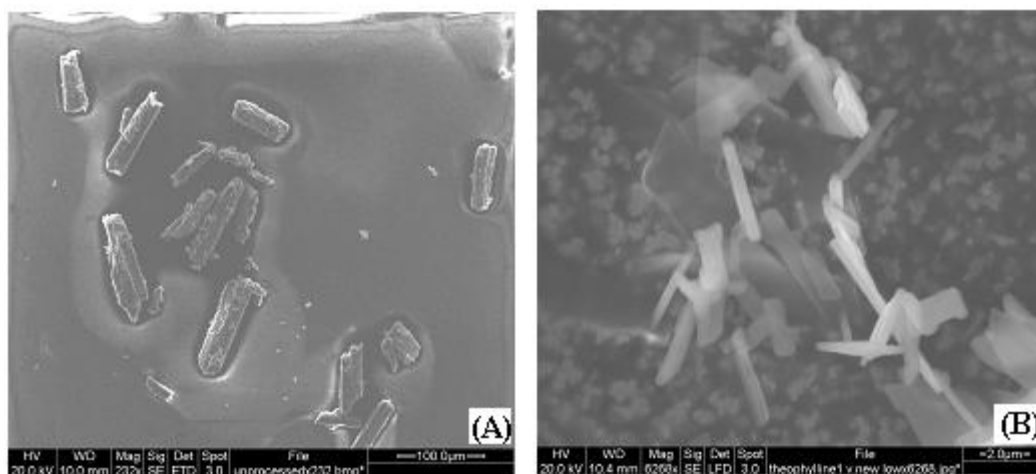
Figure 4. 3. *SEM images of unprocessed theophylline sample (A) and SEDS sample 1.*

The reproducibility of the mean particle size produced by SEDS technique was ascertained by duplicate crystallisation runs of three samples (1, 5, and 9) as representative examples, on different days using freshly prepared solutions each day. The overall reproducibility of the process was expressed as relative standard deviation (RSD). Table 4.3 displays the mean particle size, SD and RSD of the selected samples.

Table 4. 3. *Reproducibility of the mean particle size produced by SEDS technique*

Sample	Mean particle size (μm)	SD	RSD (%)
1	2.44	0.06	2.46
5	1.85	0.03	1.62
9	3.15	0.10	3.17

As shown in Table 4.3 the RSD values for the mean particle size of theophylline < 4 % indicating that SEDS technique can repeatably reproduce material with consistent particle size. This in turn allows confident interpretations to be made based on single crystallisation.

4.3.2.1. Effect of temperature

Increasing the temperature during the precipitation process led to a decrease in the particle size of the processed samples (Figure 4.4.). The effect of temperature can be also observed in the SEM images for SEDS samples 5 and 8, these samples were prepared at the lowest and highest temperatures investigated (Figure 4.5.). At high temperature the SC solution density is the lowest and therefore has expanded from the initial volume pumped at the pump head results in a net increase in the fluid flow velocity through the nozzle exit. This leads to increase in both the supersaturation and the nucleation rate and the formation of smaller particles [257]. Similar observations were reported by Subra *et al* [12] and by Franceschi *et al* [13]. They also suggested that at 60 °C, CO_2 is a SCF and as such its surface tension is insignificant compared to the more liquid like state at 40°C and this might be contributing to produce the smaller particles.
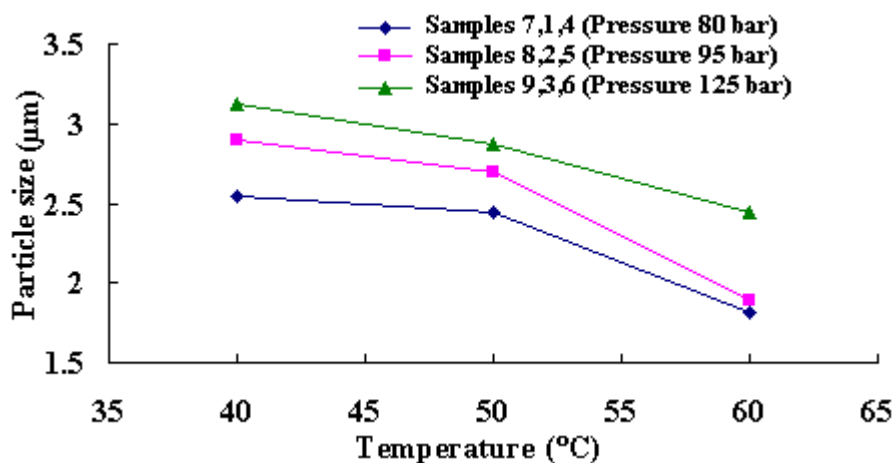
Figure 4. 4. *The effect of temperature on the particle size of the processed theophylline samples (Processing conditions for samples 1-9 were described in Table 4.2)*

147
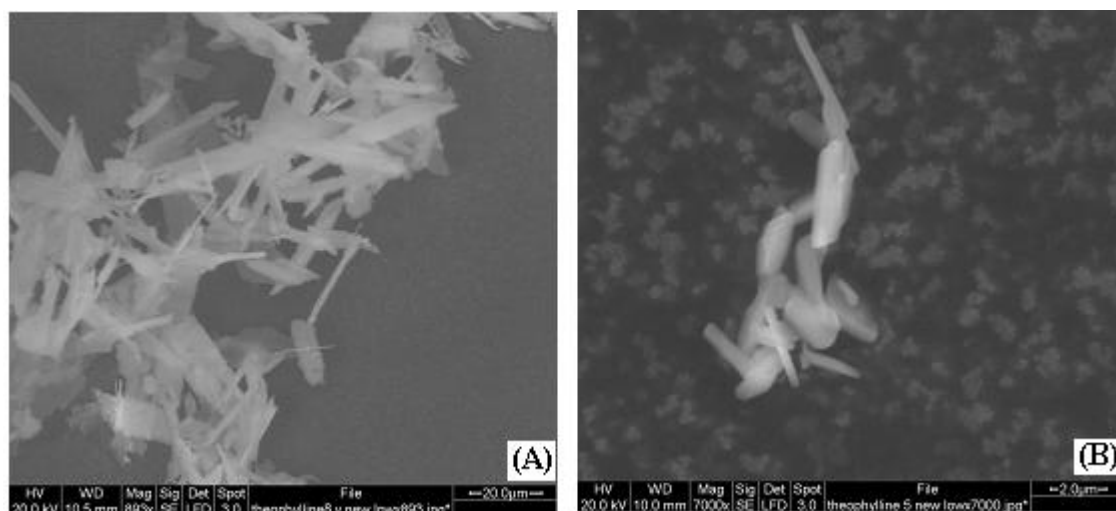
Figure 4. 5. *SEM images the theophylline SEDS sample 8 (A), at T= 40 °C and SEDS sample 5 (B), at T= 60 °C.*

4.3.2.2. Effect of pressure

An increase in the particle size was observed upon increasing the pressure at constant temperature (Figure 4.6). Subra and co workers [12] suggested that an increase in the pressure might increase the particle aggregation leading to the formation of larger particles. It was also reported [258] that an increase in the pressure decreases the diffusivity, which in turn reduces the mass transfer resulting in lower mixing efficiency of the SCF and solute solution. This will suppress the supersaturation and nucleation rate leading to larger particles. Contradictory results concerning trends of particle size as a function of pressure were reported in other literatures [259]. Figure 4.7 shows the SEM images of SEDS samples 4 and 6 at the lowest and highest pressures studied.
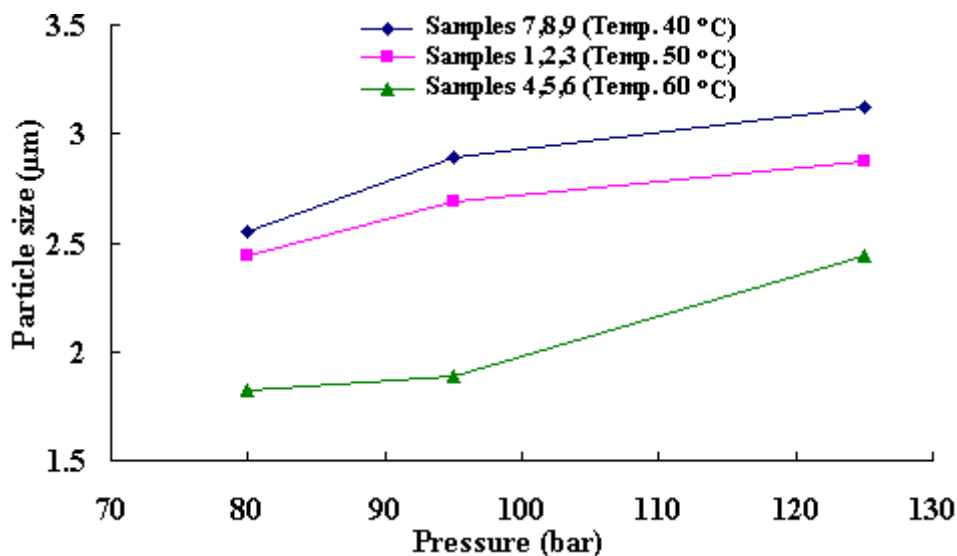
Figure 4. 6. *The effect of pressure on the particle size of the processed theophylline samples (Processing conditions for samples 1-9 were described in Table 4.2)*
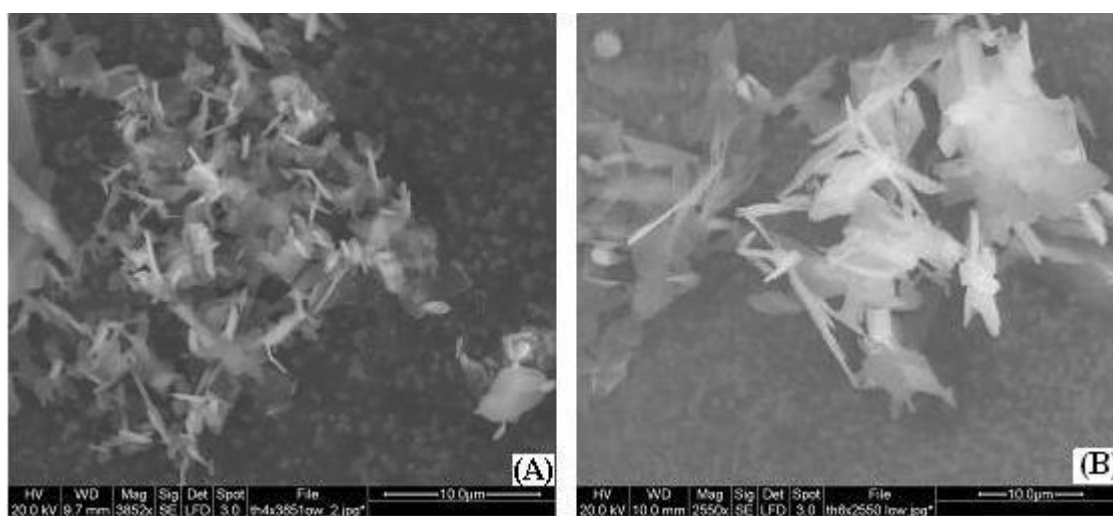
Figure 4. 7. *SEM images the theophylline SEDS sample 4 (A), at P= 80 bar and SEDS sample 6 (B), at P= 125 bar*

4.3.2.3. Effect of drug solution flow rate

As seen in the data presented in Table 4.2 there is an increase in the particle size of the processed samples upon increasing the solution flow rate (Figure 4.8.). This is primarily attributed to a high theophylline solution flow rate, at a constant CO_2 flow rate, leading

149

to a decrease in mass transfer which in turn causes a decrease in the supersaturation

level, and thereby the rate of nucleation resulting in larger particles. On comparing the

experimental condition for SEDS 13 (low solution flow rate) with experimental

condition for SEDS 15 (high solution flow rate), it can be observed that the particle size

obtained for both samples were 1.81, and 3.04 μm respectively. Figure 4.9 illustrates the

SEM images of samples 13 and 15 showing the difference between their particle sizes.
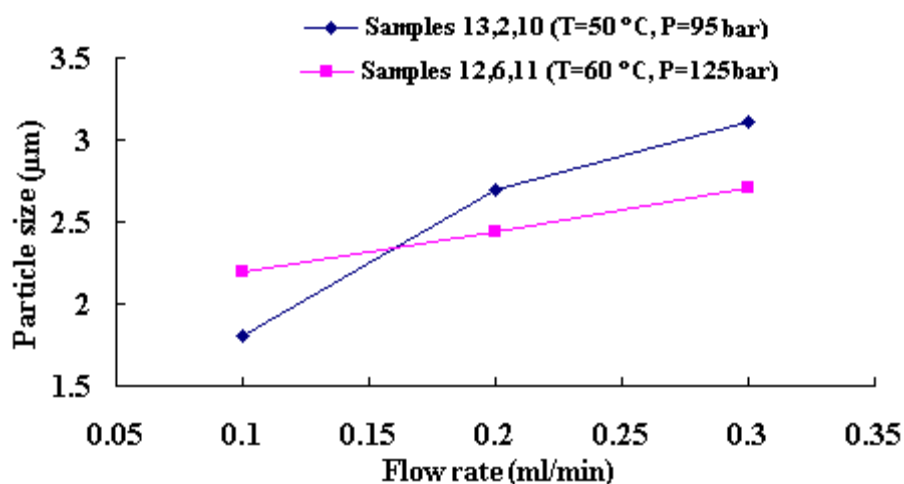
Figure 4. 8. *The effect of solution flow rate on the particle size of the processed theophylline samples (Processing conditions for samples 1-9were described in Table 4.2)*
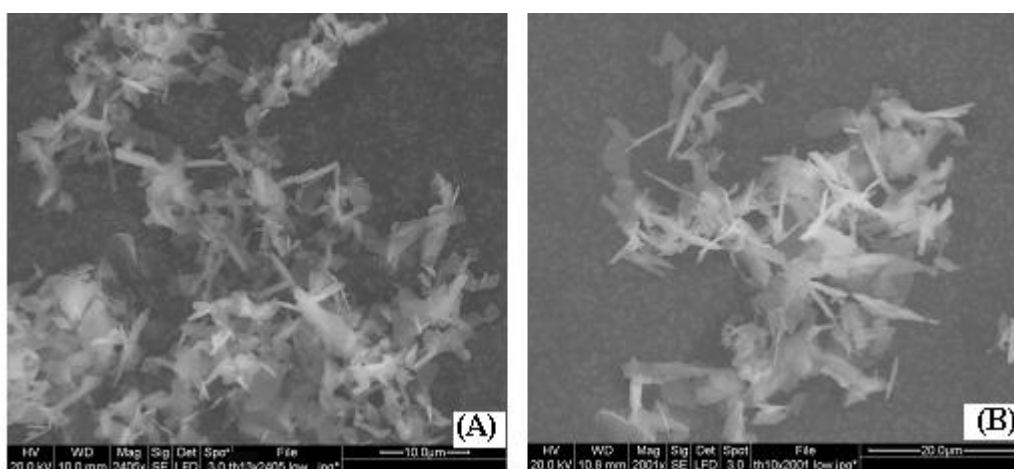
Figure 4. 9. SEM images the theophylline SEDS sample 13 (A), at drug solution flow rate= 0.1ml min^{-1} bar and SEDS sample 10 (B), at drug solution flow rate = 0.3 ml min^{-1}

4.3.3. Analysis of the precipitated theophylline particles

4.3.3.1. Morphology

The processed samples were generally recovered as free flowing powders composed of agglomerated particles with a morphology of needles or flakes (Figure 4.10.). The unprocessed particles exhibited a different morphology compared with the processed samples, rod-like morphology with scaly characteristics (Figure 4.10.a). This variation may result from the different effect of the processing parameters on the mass transfer during theophylline precipitation as explained by Franceshi and co-workers [13].
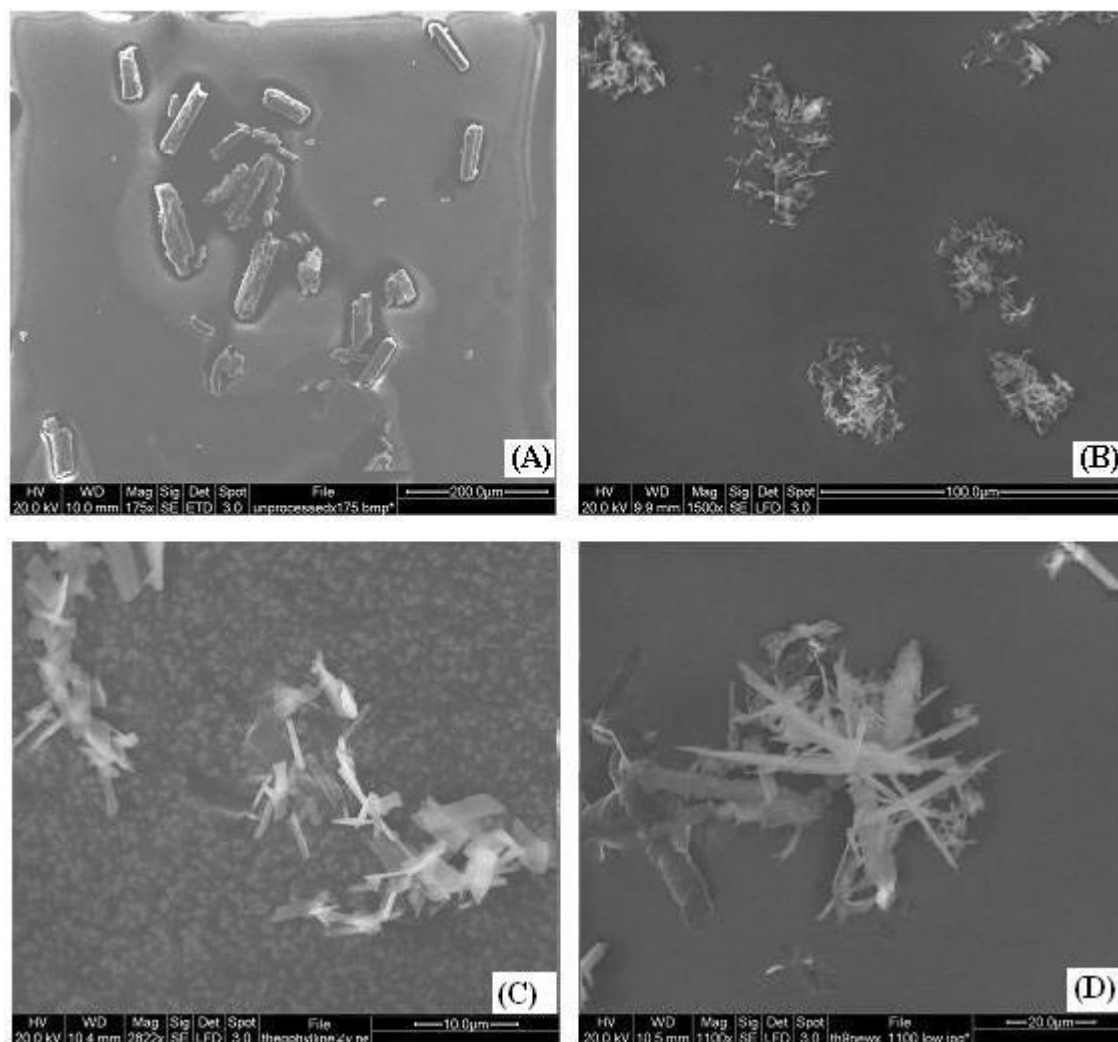
Figure 4. 10. *SEM images of unprocessed theophylline (A) compared with different SEDS samples; sample 1(B), sample 2 (C), and sample 9 (D). (Processing conditions for samples 1, 2, 9 were described in Table 4.2)*

4.3.3.2. Thermal analysis

All the results of the thermal analyses (transition temperature, melting point, and latent heat of fusion ΔH_f) of the unprocessed and processed theophylline samples are reported in Table 4.4.

Table 4. 4. *Thermal properties of unprocessed and SEDS theophylline samples*

Sample	TGA	DSC	
	Transition temp. (°C)	Melting point (°C)	ΔH_f (J/g)
Unprocessed	281.03	272.36	154.40
1	235.07	271.82	156.80
2	238.02	271.92	158.60
3	238.43	271.78	156.90
4	232.92	271.68	156.60
5	234.08	271.58	156.80
6	235.91	272.26	156.50
7	236.53	271.73	158.40
8	240.45	271.57	159.60
9	242.11	271.49	159.60
10	242.30	271.79	159.80
11	237.12	272.04	158.60
12	233.97	271.71	152.80
13	232.15	271.95	157.40
14	239.23	271.60	155.50
15	239.89	272.05	160.70

(1) Thermal gravimetric analysis (TGA)

TGA analyses were carried out on the unprocessed theophylline and all the SEDS samples to determine any change in the weight of each sample in relation to the change in the temperature. From the TGA curves, the point at which weight loss is most apparent (transition temperature) was determined for all the samples (Table 4.4.). From these results it can be observed that the transition temperature for unprocessed

theophylline was 281.03°C, higher than that of all the processed samples. This may be attributed to the facts that the particle size has a predictable effect on the TGA curve the smaller the particle sizes, the lower the temperature required for mass loss by melting or decomposition. This is because, smaller particles have larger surface areas and so more escape of the product gas is allowed [128]. While for larger particles, the mass loss is more hindered and so higher temperatures are required. This proves that there is a pronounced reduction in the particle size of the processed samples compared with the unprocessed theophylline. Although these observations are consistent with other reported results [12- 14], as yet this change in the transition temperature is not fully understood and is worthing of further investigation. Figure 4.11 represents the thermal gravimetric analysis curve of the unprocessed theophylline and SEDS 5 as representative example. From this curve it can be observed that the transition temperature of SEDS sample 5 is about 46°C below that of the unprocessed theophylline.
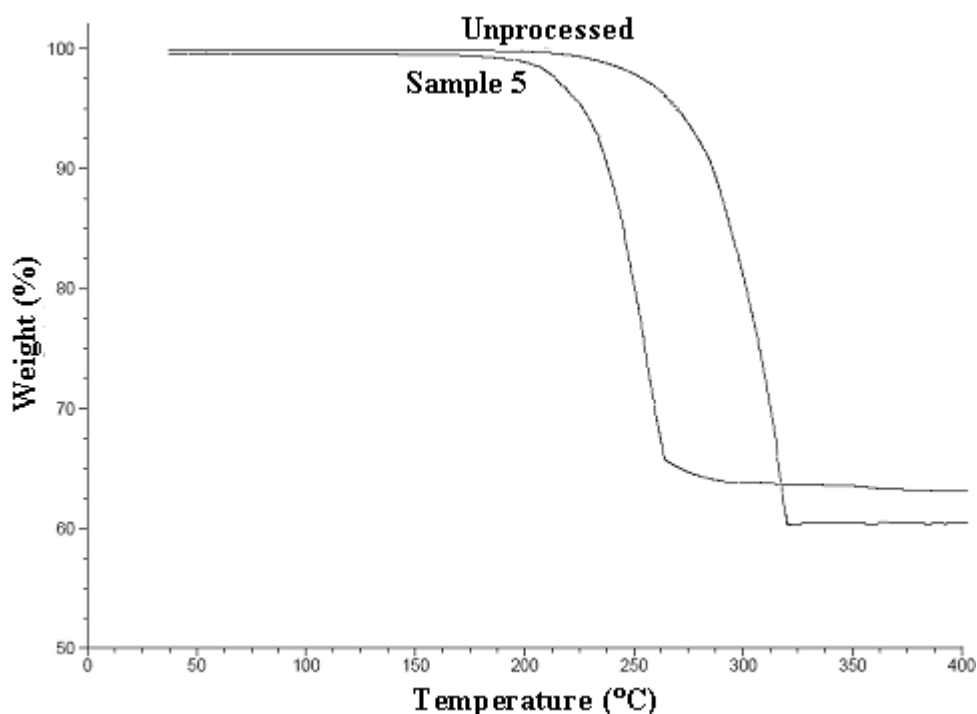
Figure 4. 11. *TGA curves of unprocessed theophylline compared with SEDS sample 5 (Processing conditions for sample 5 was described in Table 4.2)*

(2) Differential scanning calorimetry (DSC)

DSC was used to determine the melting point and the latent heat of fusion ΔH_f (the change in the enthalpy associated with the thermal event i.e. melting) for the unprocessed theophylline and SEDS samples. From the results presented in Table 4.4 it can be noted that the melting point of the unprocessed theophylline and of all the processed samples are almost equivalent. The melting point of the unprocessed sample 272.36°C is in agreement with those reported in literatures, 271.15-275.15°C [14, 237] while, the melting points of the processed samples ranged from 271.49- 272.26°C. Figure 4.12 illustrates the DSC profile of SEDS sample 5 as a representative example. The enthalpy change was calculated by integration of the area under the endothermic peaks (melting peaks) in the DSC curves of the unprocessed and SEDS samples (Table 4.4.). The latent heat of melting for the unprocessed sample was 154.40 J/g and the mean of the enthalpies change for all the processed samples was 157.57 J/g. All the results obtained from the DSC analyses confirm that the processed samples have high degrees of crystallinity for all the studied processing parameters.
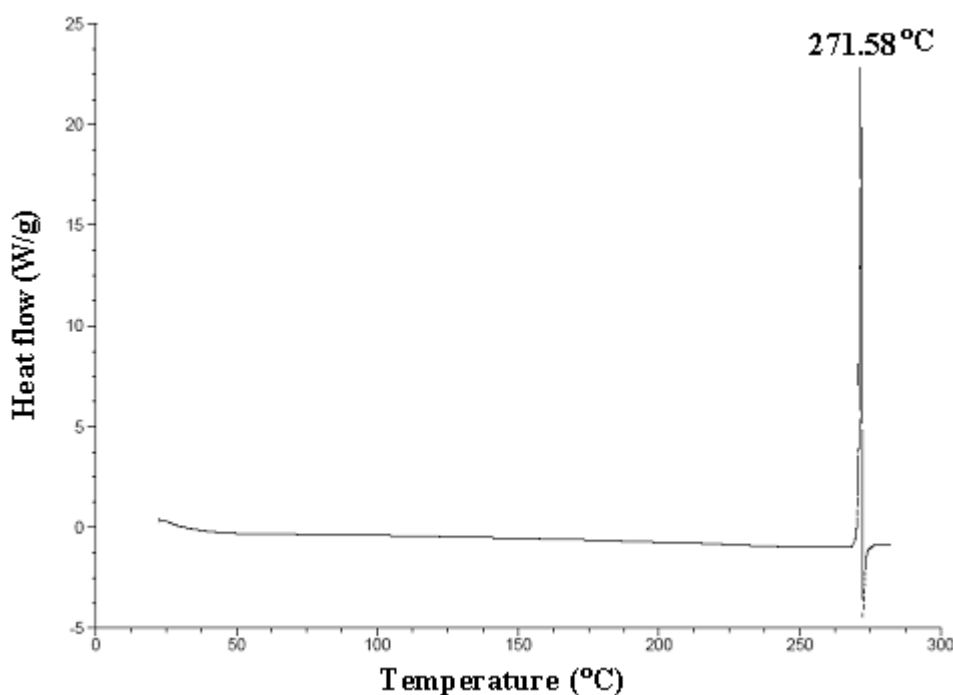
Figure 4. 12. *DSC profile of SEDS sample 5 (Processing conditions for sample 5 was described in Table 4.2)*

4.3.3.3. Crystallinity

X-ray powder diffraction (XRPD) analyses were carried out for the unprocessed and SEDS theophylline samples. Figure 4.13 shows XRPD patterns of samples 2, 4, 6, and 8 compared with the unprocessed samples as representative examples.
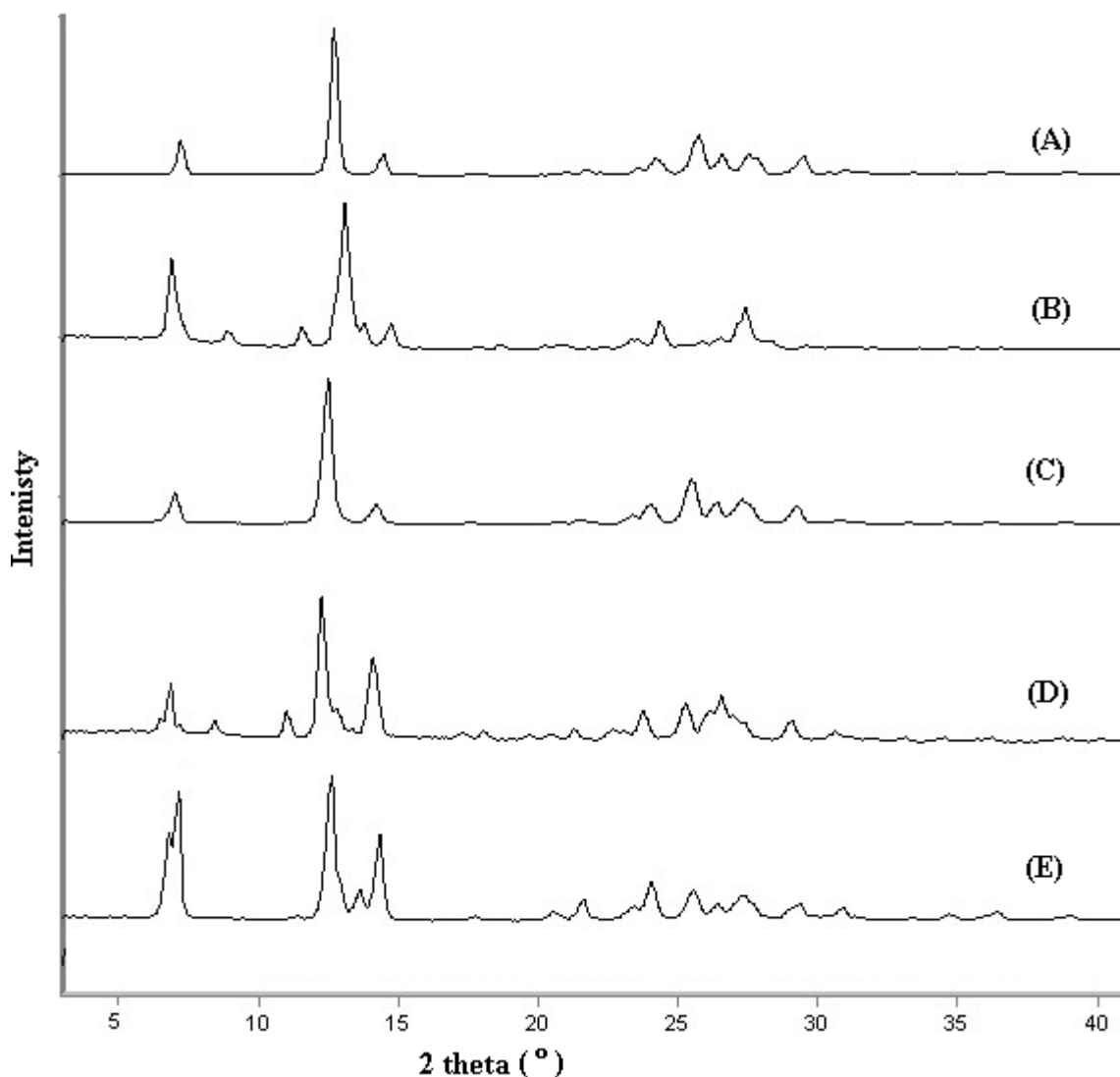
Figure 4. 13. *XRPD patterns of unprocessed theophylline (A) compared with SEDS sample 2 (B), sample 4 (c), sample 6 (D), and sample 8 (E). (Processing conditions for SEDS samples were described in Table 4.2)*

The characteristic diffraction peaks of unprocessed anhydrous theophylline (Figure 4.13 a) occur approximately at 7°, 12.6°, and 14.5°, which is matched with its pattern reported in literatures [12, 13, 260]. From Figure 4.13 it can be noted that the diffraction patterns of the processed samples exhibit the same characteristic peaks of the unprocessed theophylline but with different intensities or minor peaks displacement in some samples. In addition, some of the processed samples also show new peaks at approximately 6.8°, 11.6°, and 13.9°. These minor variations may be due to some changes in the growing pattern of the particles during precipitation process that promotes changes of both the diffraction peaks intensities [13]. However the DSC, TGA, FT-IR, and FT-Raman data for these samples compared with all other processed materials, show that theses minor changes in some of the XRPD profiles may be associated with instruments error.

4.3.3.4. Vibrational spectroscopic techniques

These techniques provide excellent methods for probing solid state bonding interactions between molecules.

(1) Fourier Transform Infra-Red (FT-IR)

IR analyses for the unprocessed and SEDS theophylline samples were done. All the obtained spectra were compared with that of the unprocessed sample as well as reference IR spectra (Figure 4.14.) of theophylline obtained from the British pharmacopoeia [252] and different literatures [237, 253, 261]. It was observed that there was no difference between the spectra of the processed samples and that of the unprocessed theophylline or the standard reference spectra. Figure 4.15 shows the spectra of three SEDS samples compared with the spectrum of the unprocessed sample as representative examples.
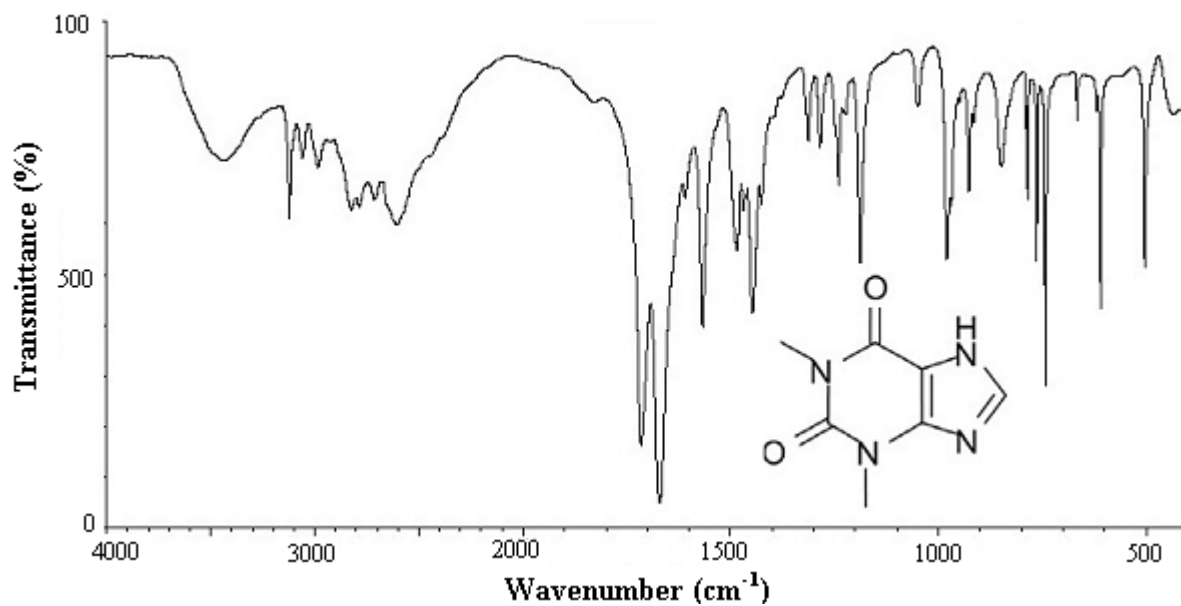
Figure 4. 14. R*eference FT-IR spectrum of theophylline*
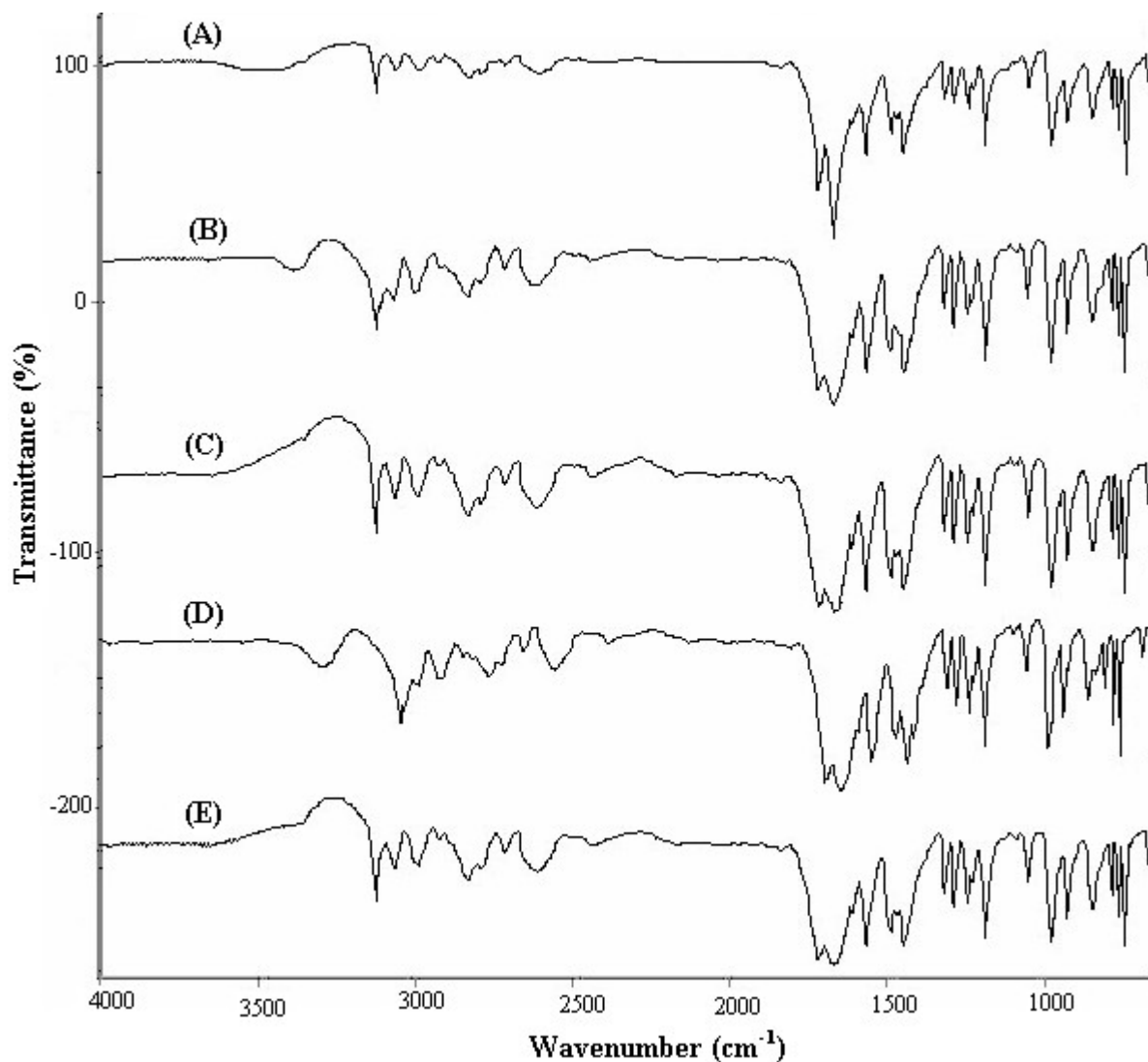
Figure 4. 15. *FT-IR spectra of unprocessed theophylline (A) compared with SEDS sample 2 (B), sample 4 (c), sample 6 (D), and sample 8 (E) (Processing conditions for SEDS samples were described in Table 4.2)*

The IR spectrum of theophylline shows a number of bands related to its structure. The band present at 3448 cm^{-1} is assigned for N-H stretch of the amine and the band at 2998 cm^{-1} is assigned to the C-H stretching. Two bands at 1718, 1668 cm^{-1} are assigned to C=O stretching, while bands present at 1610 cm^{-1}, and 1566 cm^{-1} are assigned to C=C and C=N stretching, respectively. Bands at 1314, 1286,1240 cm^{-1} are assigned to C-N stretching and that at 927 cm^{-1} to N-CH3 stretching [253, 261]. The IR spectra for the processed samples illustrate all these bands, which demonstrate that there is no modification in the bonding interaction between molecules and hence the structure of theophylline during the SEDS process over all the processing conditions studied.

(2) Fourier Transform Raman spectroscopy (FT-Raman)

As a complementary study to the FTIR, FT-Raman analyses were performed on the unprocessed and all of the processed samples. From the comparison between the obtained spectra, it was observed that the spectra of the SEDS samples were closely resembled each other and to that of the unprocessed theophylline. Figure 4.16 shows the FT-Raman spectra of the unprocessed and processed samples 2, 4, 6, and 8 as representative examples.

The Raman spectrum of theophylline illustrates various bands, which are related to chemical features such as; band at 3120 cm^{-1} being assigned to N-H group. The band presents at 2966 cm^{-1} is assigned for C-H group, while bands at 1706, and 1664 cm^{-1} are assigned to the C=O group. Bands present at 1611 and 1569 cm^{-1} are assigned to C=C, and C=N groups respectively. Bands at 1314, 1285, 1248 cm^{-1} are assigned to the C-N group with that at 949 cm^{-1} is assigned for N-CH3 group [261]. These peaks are illustrated in all the spectra of the processed samples and this finding confirms the results obtained by IR analysis, that the precipitation by SEDS technique has no effect on the theophylline structure under different conditions.
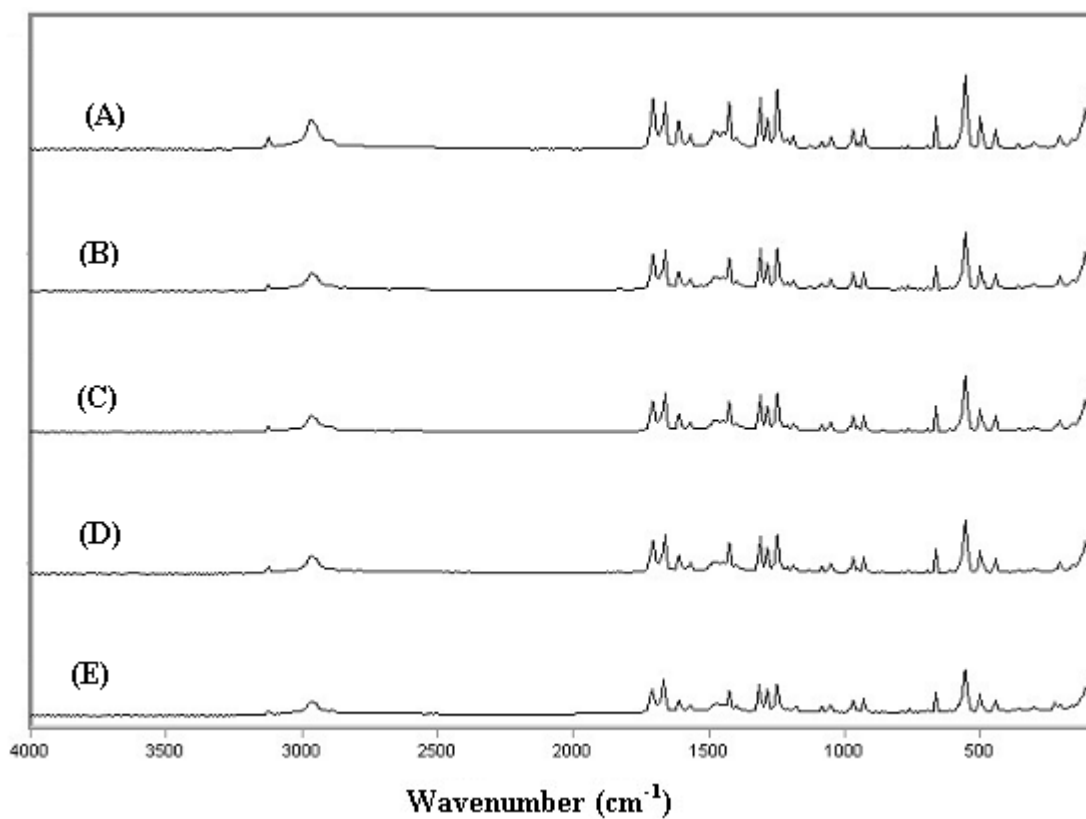
Figure 4. 16. *FT-Raman spectra of unprocessed theophylline (A) compared with SEDS sample 2 (B), sample 4 (C), sample 6 (D), and sample 8 (E) (Processing conditions for SEDS samples were described in Table 4.2)*

4.3.4. Theophylline monohydrate

Hydrates of pharmaceuticals frequently exhibit differences in physicochemical properties such as bioavailability, stability, solubility and dissolution rate. Therefore knowledge of transformation of anhydrous to hydrate form is essential for the development of stable formulations. Incorporation of water molecule (s) in the crystal lattice of anhydrous form changes the dimensions, shape, symmetry and capacity of the unit cell. As a result the hydrate form exhibit different physical properties. As a rule in solubility behaviour the anhydrous form of a substance is always more soluble in water than the corresponding hydrates [262].

It was reported that the aqueous solubility of anhydrous theophylline is consistently higher than that of theophylline monohydrate, below 60°C [263]. There is a significant difference in the initial dissolution rate of monohydrate compare to anhydrous theophylline [264]. It was reported that at the same transport rate, the dissolution rate of the anhydrous form is greater than that of the corresponding hydrate [262]. The differences in the solubility and the dissolution rates of the hydrate and anhydrous forms may alter the bioavailability of the drug. The bioavailability of anhydrous theophylline is higher than that of monohydrate. This may be attributed to the difference in aqueous solubility and dissolution rate between them. On the other hand the crystallographic changes between two phases may be an important factor controlling the bioavailability of the formulation [262, 265].

Trials have been carried out to assess the amount of water required to prepare theophylline monohydrate using the SEDS technique and this was traced by XRPD, TGA and DSC techniques. As the gram molecular weight (M.wt) of theophylline monohydrate is 198.20 where the water ratio is 10 % (180.2 g of anhydrous theophylline and 18.0 g of water), solutions of theophylline anhydrous (1g % w/v) containing different amounts of water (0.1 − 0.5 ml) were prepared. The processed

samples were prepared at T= 40 °C and P= 125 bar using 20 ml min^{-1} and 0.2 ml min^{-1} as the flow rate of CO_2 and drug solution, respectively.

Figure 4.17 illustrates the XRPD patterns of the theophylline anhydrous (unprocessed and processed), and all other processed samples precipitated from drug solution containing different quantities of water (0.1-0.5 ml). The XRPD pattern of theophylline monohydrate is in agreement with the reported patterns [266]. This figure shows the differences in the XRPD pattern of the anhydrous theophylline (characteristics peaks at 7°, 12.6°, and 14.5°) and the monohydrate form (characteristics peaks at 8.8°, 11.6°, and 14.8°).
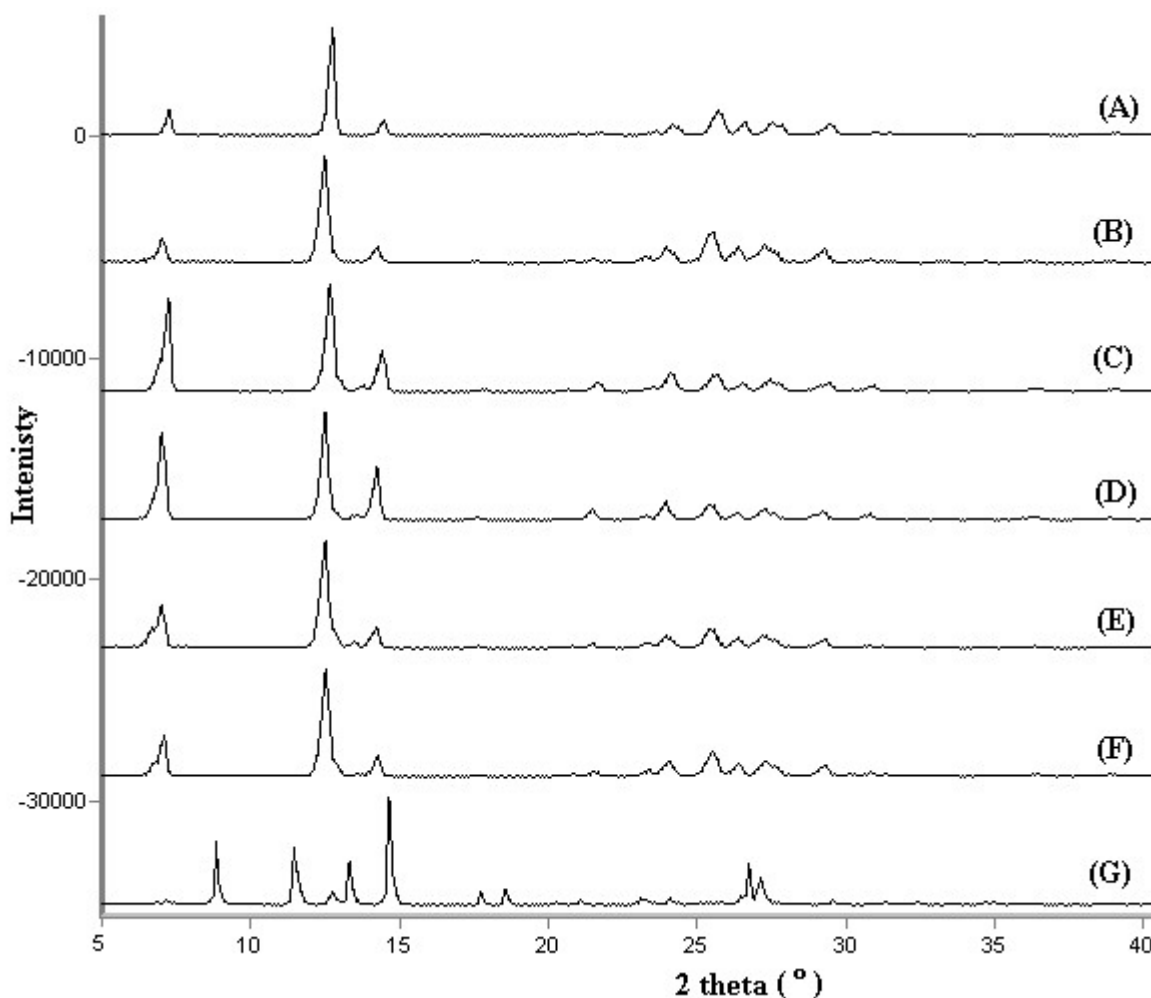
Figure 4. 17. *XRPD patterns of different theophylline samples; anhydrous unprocessed (A), anhydrous SEDS sample (B), sample with 0.1 ml water (C), sample with 0.2 ml water (D), sample with 0.3ml water (E), sample with 0.4 mlwater (F), sample with 0.5 ml water (monohydrate) (G)*

Figures 4.18, and 4.19 illustrate the DSC and TGA traces for processed theophylline samples from solutions containing different ratios of water, respectively.
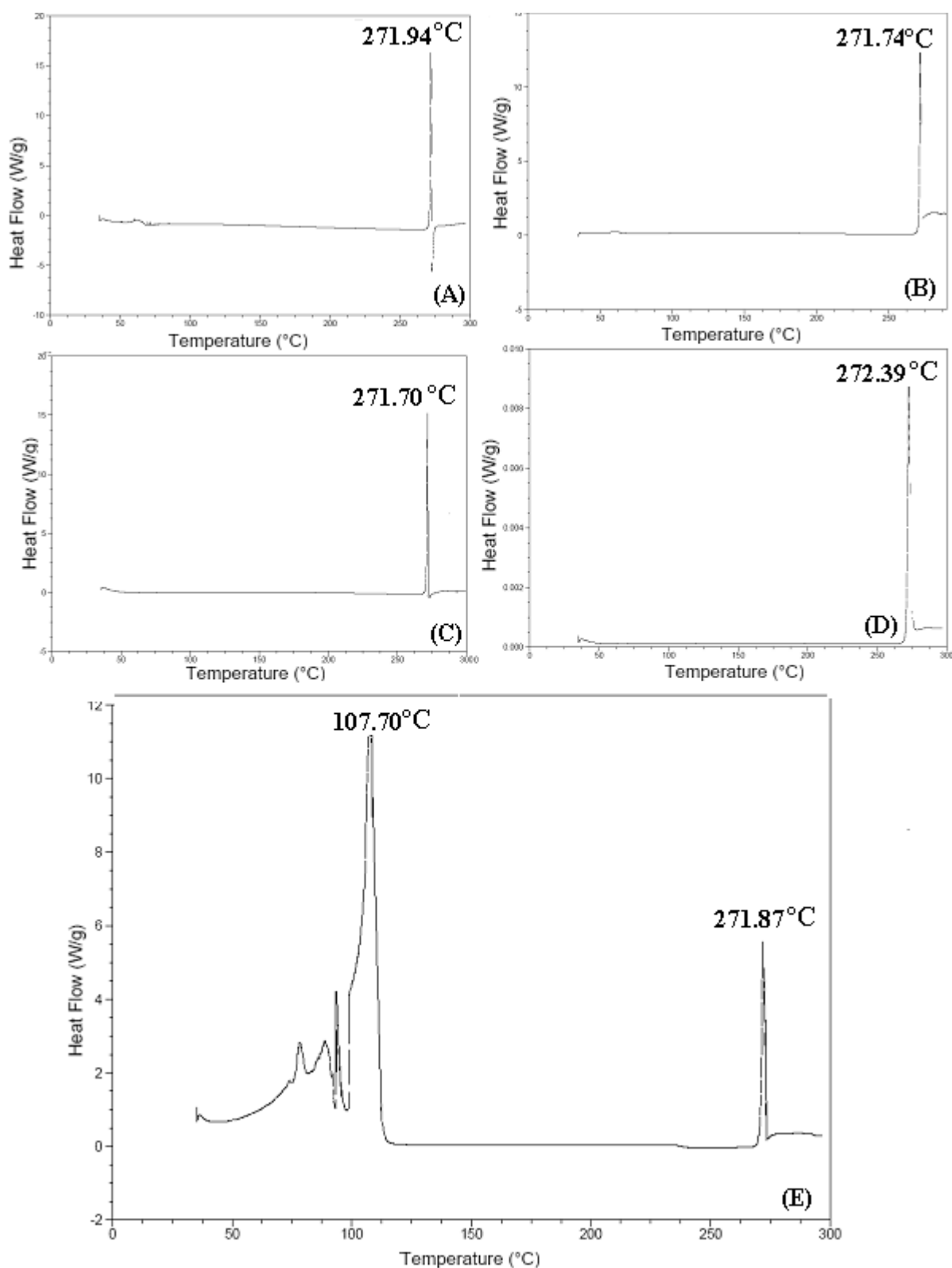
Figure 4. 18. *DSC traces of SEDS samples processed with different amounts of water; 0.1 ml (A), 0.2 ml (B), 0.3ml (C), 0.4 ml (D), and 0.5 ml (E).*
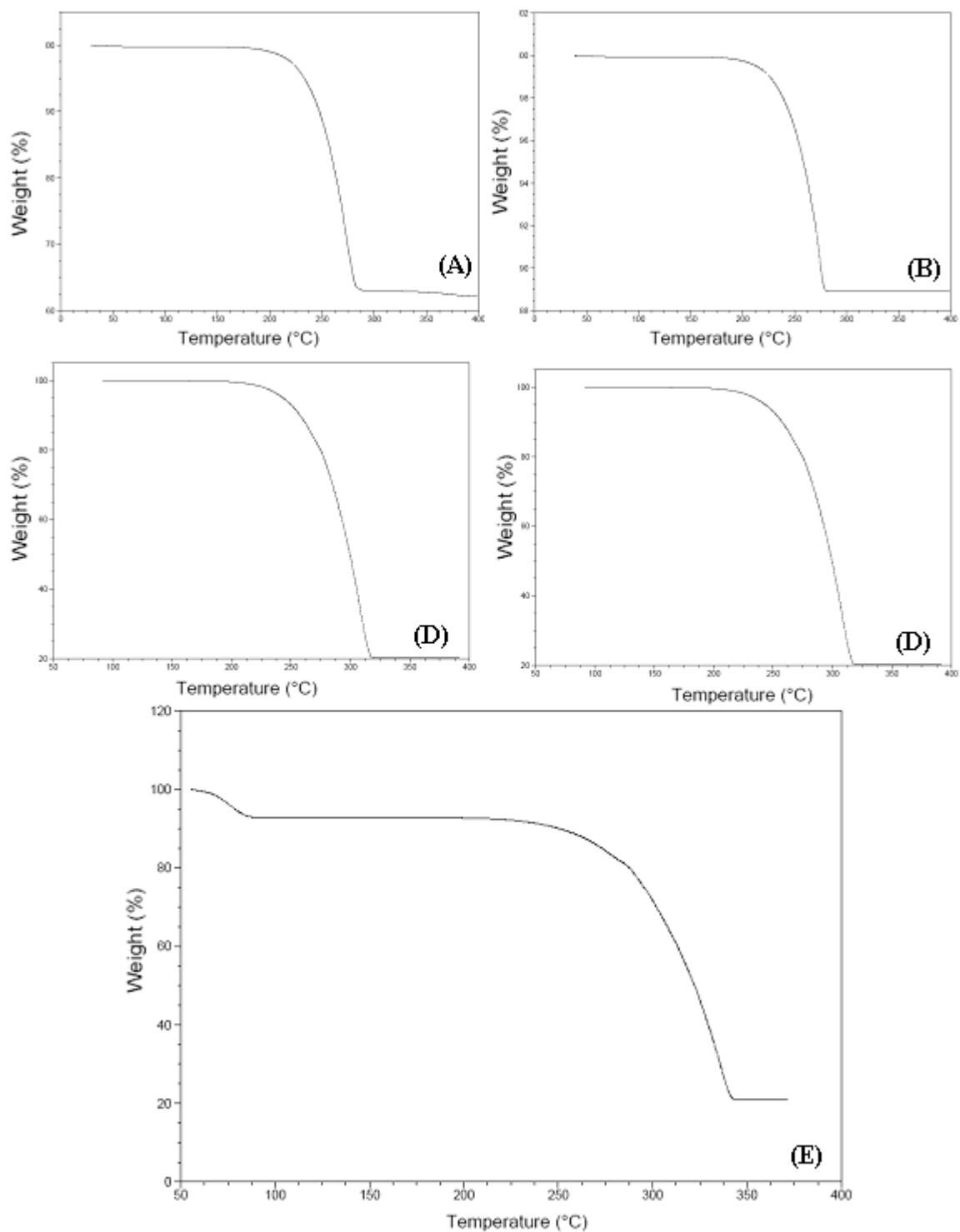
Figure 4. 19. *TGA traces of SEDS samples processed with different amounts of water; of water; 0.1 ml (A), 0.2 ml (B), 0.3ml (C), 0.4 ml (D), and 0.5 ml (E).*

From the DSC traces it was observed that the melting point of the products obtained from drug solutions containing from 0.1-0.4 ml of water ranged from 271.70-272.39°C, which is similar to the melting point of the precipitated theophylline anhydrous. There are no additional endothermic peaks over the melting peak were observed in these traces. On the other hand the DSC trace of the product obtained from theophylline solution containing 0.5 ml of water illustrates one extra endothermic peak over the melting peak (271.87°C) at 107.70°C, which represents the water loss from the hydrated theophylline before complete melting of the product. This confirms that the theophylline product accepts a molecule of water during its precipitation.

While one transition temperature (one step) is observed at each TGA trace of the first four products. It was also observed that the transition temperature of these products increases by increasing the amount of water from 0.1 ml to 0.4 ml. These temperatures were 245.18, 250.48, 274.36, and 274.44 °C respectively. For the product obtained from the theophylline solution containing 0.5 ml of water, two transition temperatures (two-steps) at 96.28, and 298.91°C were observed. The first temperature represents the temperature at which the product losses the accepted water molecule from the precipitation process. This demonstrates the potential of preparation of theophylline monohydrate using SEDS technique by the addition of appropriate amounts of water to the starting drug solution.

Finally, it can be concluded that anhydrous theophylline was successfully re-crystallised by the SEDS process. This technique can produce smaller particles 2-5 μm compared to the unprocessed sample (30-100 μm). The structure and the crystallinity of theophylline products were not affected by different processing parameters. In further study, the next objective is to investigate the efficiency of the produced theophylline particles for efficient respiratory delivery as inhalable formulations.

Chapter 5

In-vitro evaluation of the aerodynamic behaviour of SEDS theophylline samples as inhaled dry powder formulation

5.1 introduction

The in-vitro characterisation of an aerosol is a useful pre-clinic tool to predict the emitted dose and its aerodynamic behaviour with respect to particle size, and the fine particle dose (FPD) available upon inhalation. This provides indications about the *in-vivo* therapeutic efficiency of the drug [267]. All the methods that are recommended by regulatory bodies for the determination of the *in-vitro* efficiency of inhaled drug are based on inertial impaction techniques. These techniques are able to predict the amount of the drug that will be deposited in the lungs by using models that mimic the dimensions of the human airways. In this study, the dose sampling unit and the Andresen Cascade Impactor were used to determine the *in-vitro* emitted dose and the deposition profiles, respectively of SEDS formulations at inhalation flows 28.3, and 60 L min^{-1} with 4 L inhalation volume. Two types of DPIs were investigated in this study; Easyhaler$^{®}$ (multidose reservoir device) and Spinhaler$^{®}$ (single dose device).

In this study three samples having different particle sizes (SEDS 1, 5 and 9) were selected out of the prepared powders by SEDS technique to be tested. The mean particle size of the three samples is 2.44, 1.89, and 3.12 μm, respectively. These samples as presented in Chapter 4 were prepared under different conditions covering all the studied range of temperatures (40-60°) and pressures (80-125 bar). They were selected as representative examples for all the studied operating parameters. The aim of the work is to study the *in-vitro* aerodynamic performance of the selected SEDS samples either pure or blended with lactose using commercially available DPIs.

5.2. Materials and methods

5.2.1. Instruments

5.2.1.1. Apparatus used for *in-vitro* assessment of dry powder inhalers (DPIs)

(1) For the determination of the emitted dose from the DPIs

- Empty Easyhaler® dry powder inhaler device (Orion Pharma, Orionintie, Finland)

- Empty Spinhaler® dry powder inhaler device (Fisons, Loughborough, UK), It has been used with empty gelatine capsules (Parke, Davis Co., London, UK)

- GAST 1023 Pump, 0-100 L/ min (GAST, Brook Hampton, Doncaster, UK)

- PR 4000 flow-meter (MKS Instruments, Andover, MA, USA)

- Dry Powder controller Model TPK (Copely Scientific Ltd, Nottingham, UK)

- Dose sampling unit for DPIs (Copely Scientific Ltd, Nottingham, UK)

- Glass micro-fibre filters 47mm (Whatman International Ltd, Maidstone, UK)

(2) For the determination of the aerodynamic behaviour of theophylline formulations

- Andersen cascade impactor (Copely Scientific, Nottingham, UK)

- Glass micro-fibre filters 81 mm (Whatman International Ltd, Maidstone, UK)

- Copely inhaler testing data analysis software (CITDAS) version 2.00 (Copely Scientific Ltd, Nottingham, UK)

5.2.1.2. General Laboratory Instruments

- Utrasonic bath (Decon Laboratories, Hove, UK)

- Nylaflo® nylon membrane filter, 47 mm, 0.45 μm pore size (Pall Gelman Sciences, Michigan, USA).

- Spiromixer S, roller mixer (Denley Instruments Ltd, Sussex, UK)

- Tumbler mixer (Willy A., Bachofen AG Maschinenfabrik, Basel, Swizerland)

5.2.2. Materials

5.2.2.1. Pharmaceutical excipients

α-Lactose monohydrate; Respitose® SV003, sieved inhalation grade lactose with narrow particle size distribution (DMV-Fonterra, Veghel, Netherlands)

5.2.2.2. Theophylline formulations

• Pure SEDS 1 (prepared as shown in Chapter 4)

• SEDS 1 (25 %) / Lactose (75 %) blend

• SEDS 1 (50 %) / Lactose (50 %) blend

• Pure SEDS 5 (prepared as shown in Chapter 4)

• SEDS 5 (25 %) / Lactose (75 %) blend

• SEDS 5 (50 %) / Lactose (50 %) blend

• Pure SEDS 9 (prepared as shown in Chapter 4)

• SEDS 9 (25 %) / Lactose (75 %) blend

• SEDS 9 (50 %) / Lactose (50 %) blend

5.2.3. Methods

5.2.3.1. Preparation of theophylline blends

Two blends from the selected SEDS samples were prepared by mixing of theophylline and lactose for 20 min. using Spiromixer, and Tumbler mixer (10 min each). The uniformity of the mixture was assessed by taking three aliquots from each blend after mixing and then quantitatively analysed by HPLC (Chapter 3).

5.2.3.2. *In-vitro* evaluation of the performance of theophylline SEDS samples

Empty DPIs; Easyhaler® and Spinhaler® were filled with either pure SEDS samples or their blends with lactose. For Easyhaler® its reservoir was filled with 40 mg of each sample or blend. While for Spinhaler®, each capsule was filled with 10 mg of each sample or blend. For the *in-vitr*o evaluation of the performance of all these formulations, the dose sampling unit and Andersen Cascade Impactor were used.

(1) Dose sampling unit and its operating procedure

The total emitted dose of theophylline from either Easyhaler® or Spinhaler® was determined by sampling apparatus for dry powder inhalers (DPIs) with a critical flow controller model TPK. The basic methodology is described in BP [252], EP [173] and the USP [174]. The standard compendial methodology used an inhalation volume 4L and pressure drop of 4 Kpa. In this study two different inhalation flows 28.3, and 60 L min^{-1} were examined at an inhalation volume 4 L to study the effect of flow rate on the total emitted dose. The sampling unit for DPIs has a larger diameter compared to the one used for metered dose inhalers, to enable the collection of the dose at flows up to 100 L min^{-1}. Figure 5.1 represents a schematic diagram of the dose sampling unit used in the study.
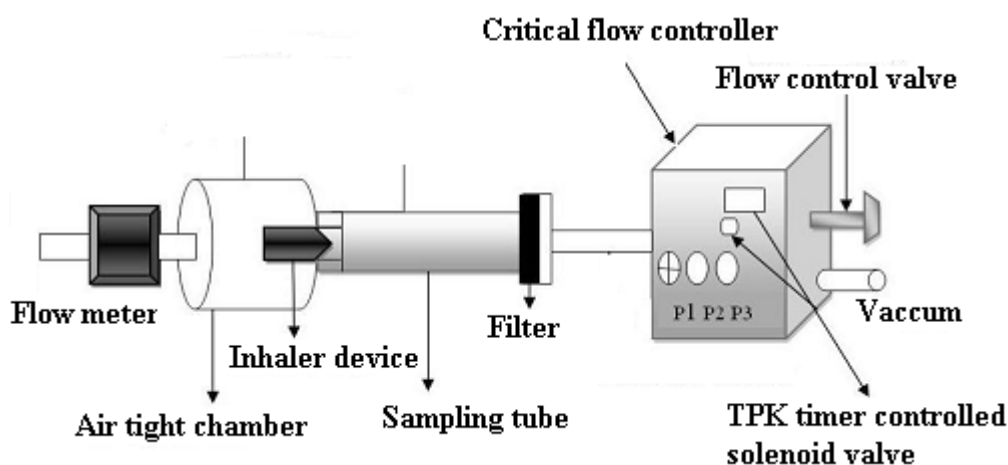
Figure 5. 1. *Schematic diagram of the dose sampling unit for DPI*

The unloaded inhaler device was inserted inside the chamber using a rubber mouthpiece adapter, which prevents the powder loss between the collection tube and the inhaler mouthpiece. A vacuum pump with sufficient capacity was used to achieve the desired inhalation flows. It was switched on for 20 minutes prior to each determination to attain a stable flow.

A time controlled two-way solenoid valve (P2 and P3), connected between the vacuum pump and the flow controller valve was opened and the desired flow rate adjusted using the flow controller valve. The two-way solenoid valve allows measurements of individual values of absolute pressure on either side of the flow controller valve. The flows stability is ensured (sonic flow) when the absolute pressure ratio $P3/P2 \leq 0.5$ [174]. Once the flow was set using an electronic flow digital meter (MKS Instruments, USA), the two-way solenoid was closed. The inhaler device was then loaded with the theophylline dose according to the instructions in the patient information leaflet and re-inserted in the mouthpiece adapter. The dosing time was set using the following equation described in the USP (2005) [174]

$$T = (60 \ sec. \times X)/ \ Q$$

Where; T   The time required for withdrawal of 4 L of air from the inhaler

     Q   Airflow rate

     X   2or 4 L to be withdrawn

Depending on the above equation the flow duration required for inhalation flows 28.3, and 60 L min^{-1} were; 8.5, and 4 seconds, respectively to allow an inhalation volume 4L. After complete delivery of the emitted dose into the sampling unit, the amount of the drug on the collection filter (Glass micro-fibre filters 47mm) and the sampling tube were carefully rinsed with 20 ml of methanol: water (30:70 % v/v) mixture containing 30 µg ml^{-1} of the 8-chlorotheophylline as internal standard. The obtained solution was placed in an ultrasonic bath for 15 min. to ensure complete solubilization of

theophylline and then filtered through nylon membrane filter. The emitted dose of

theophylline was quantitatively analysed using the developed HPLC method (Chapter 3)

and the mean, SD and RSD were calculated. Similarly ten separate single doses (n=10)

were determined for each formulation at each flow rate (28.3 and 60 L min^{-1}) using 4 L

as the inhalation volume.

(2) Determination of the aerodynamic behaviour of formulation using Andresen
cascade impactor (ACI)

The ACI stages, preseparator and the induction port were washed with methanol and left

to dry at room temperature. The impactor collection plates were sprayed with silicon (in

hexane) to prevent the particle bouncing and then allowed to dry for 1 hour at room

temperature prior to analysis. The ACI was assembled with the throat (induction port),

preseparator (PS), stages and the filter in the final stage. To entrain large particles

(usually > 10 µm) which may be contained in the DPI, preseparator filled with 10 ml of

methanol: water mixture (30:70 % v/v) was used [174] (Figure 5.2).
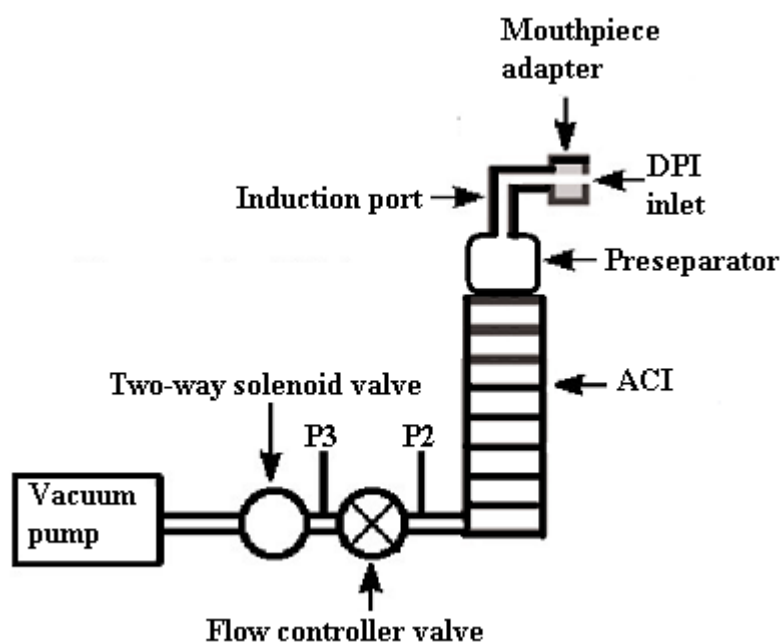
Figure 5. 2. *Schematic diagram of the Andersen Cascade Impactor parts including the preseparator*

The tested DPIs (Easyhaler[®], or Spinhaler[®]) were fitted onto the induction port by the rubber mouthpiece adapter. The flow control valve was adjusted until the required steady flow measured with the calibrated flow meter is achieved through the system. Sonic flow is achieved by ensuring an absolute pressure ratio P3/P2 ≤ 0.5.

Although, the EP [173] and USP [174] recommend the evaluation of the aerodynamic performance of the emitted dose using a flow rate that creates a pressure drop of 4 Kpa at a constant flow volume of 4 L across the inhaler. In this case different inhalation rates have been used to study the effect of inhalation flows on the deposition profile of the SEDS theophylline. The determinations of each formulation were performed at flow rates of 28.3, and 60 L min^{-1} (n = 3) with discharge times of 8.5, and 4 seconds, respectively to ensure an inhalation volume of 4 L.

For the determinations at 60 L min^{-1} the stages number 0 and 7 (used at flow rate 28.3 L min^{-1}) were replaced by stages –1 and –0. As the ACI is designated for operation at flow rate 28.3 L min^{-1}, so upon using the higher flow rate the effective cut off diameter (ECD) of the stages should be recalculated using Van Oort equation [179].

Two separate single doses were used from each formulation for each determination, except for the Spinhaler[®] where only one single dose was used for each test due to the high emitted dose.

After the complete sampling, the pump was turned off and the ACI was disassembled. The impactor components were then rinsed separately with different volumes of methanol: water (30:70 v/v) mixture containing 30 μg ml^{-1} of the 8-chlorotheophylline as internal standard. Table 5.1 represents the washing volumes of methanol: water mixtures used for rinsing the ACI stages at different flow rates.

Table 5.1. The effective cut-off diameters and the washing volume of ACI stages

Stage	Flow rate L min^{-1}			
	28.3		60	
	ECD * (μm)	Washing volume (ml)	ECD* (μm)	Washing volume (ml)
Induction port	-----	20	-----	20
Preseparator	-----	20	-----	20
-1	-----	-----	9.0	10
-0	-----	-----	5.8	10
0	9.0	10	-----	-----
1	5.8	10	4.7	10
2	4.7	10	3.3	5
3	3.3	5	2.1	5
4	2.1	5	1.1	5
5	1.1	5	0.7	5
6	0.7	5	0.4	5
7	0.4	5	-----	-----
Filter	0	5	0	5

* Effective cut off Diameter Adapted from Copley Scientific 2007.

5.2.3.3. Sample analysis using HPLC method

The resulting solutions recovered from cascade impactor were analysed using the developed HPLC method (Chapter 3) for quantitative determination of the amount of the drug deposited on each stage in the impactor.

5.2.3.4. Data analysis

The Copley Inhaler testing data analysis software (CITDAS version 2.0) was used to calculate all the aerodynamic parameters for the studied SEDS theophylline formulations including;

Total emitted dose (TED); was determined as the total amount of the drug deposited on the stages and the filter of the cascade impactor (excluding the inhaler deposition)

Fine particle dose (FPD) as specified by CITDAS was the amount of the drug with aerodynamic diameter less than 5 μm.

Fine particle fraction (FPF) was calculated as FPD/emitted dose * 100%

The Mass median aerodynamic diameter (MMAD) was calculated from the logarithm of the ECD corresponding to 50% undersize particles (on probability scale).

The Geometric standard deviation (GSD) was calculated from the following equation;

$GSD = (d_{84.13\%} / d_{15.87\%})^{\wedge 0.5}$ [174].

Where $d_{84.13\%}$, and $d_{15.87\%}$ are the aerodynamic particle size at 15.87% and at 84.13% less than the stated size, respectively for the cumulative size distribution.

The mean and SD of the TED, FPD, FPF, MMAD, and GSD were determined for each formulation at two inhalation flows of 28.3, and 60 L min^{-1}.

5.2.3.5. Statistical analysis

Statistical analysis of FPD, FPF, MMAD, and GSD was carried out using the SPSS (version 15.0) computer programme for the studied formulations at two flows 28.3 and 60 L min^{-1}. A two-way analysis of variance (ANOVA) with the application of general linear model univariate, was used to determine any significant differences between the aerodynamic behaviour of the same formulation under different flows and between different formulations under the same flows. The mean difference (95% confidence interval) was also calculated.

5.3. Results and discussion

The *in-vitro* testing of DPIs is an important stage in the development of a new inhalable formulation. The results provided gave an idea about the aerodynamic behaviour of theophylline prepared by SEDS technique. Furthermore, these results determine any differences in the emitted dose, deposition profiles, between different theophylline samples with different particle size. The effect of blending theophylline with inhalable lactose as a carrier on its deposition profile was also investigated.

5.3.1. Determination of the emitted dose of SEDS theophylline formulations recovered from Easyhaler® at different inhalation flows

Tables 5.2, 5.3, and 5.4 show the mean (n =10), SD, and RSD of the total emitted dose of theophylline recovered from the Easyhaler® using two different inhalation flows (28.3, and 60 L min^{-1}) for pure SEDS samples and their blends with lactose. Two blends were prepared in this study 50 % and 25 % blends, the first blend consists of 50 % of SEDS theophylline and 50 % of inhalable lactose. While, the second blend consists of 25 % of SEDS theophylline and 75 % of lactose.

A summary of these data is shown in Table 5.5 and Figure 5.3. The statistical comparisons for the dose emission results of each formulation at different inhalation flows and the dose emitted from different formulations under the same inhalation flow were represented in Tables 5.6. and 5.7, respectively.

Table 5. 2. *The emitted dose of pure theophylline SEDS samples recovered from the Easyhaler® at different inhalation flows*

Dose No.	Emitted dose (µg)					
	SEDS 1		SEDS 5		SEDS 9	
	28.3 L min^{-1}	60 L min^{-1}	28.3 L min^{-1}	60 L min^{-1}	28.3 L min^{-1}	60 L min^{-1}
1	184.32	213.24	186.37	215.32	173.71	211.17
2	175.56	212.60	174.23	211.25	182.35	224.32
3	183.01	197.35	187.01	212.37	181.21	212.30
4	179.37	210.21	184.07	216.99	183.59	205.59
5	178.42	216.97	180.85	220.25	192.96	211.35
6	197.49	212.34	188.63	215.32	185.55	211.26
7	187.24	220.78	185.42	200.21	183.32	205.55
8	185.42	213.65	192.55	215.29	169.05	213.63
9	181.32	212.24	184.30	182.36	180.32	215.21
10	182.12	212.15	184.85	205.32	187.33	206.91
Mean	**183.43**	**212.16**	**184.83**	**212.36**	**181.94**	**211.73**
SD	**6.02**	**5.99**	**4.84**	**5.86**	**6.71**	**5.52**
RSD	**3.28**	**2.83**	**2.62**	**2.76**	**3.69**	**2.61**

Table 5. 3. *The emitted dose of 50% blend of SEDS theophylline samples recovered from the Easyhaler® at different inhalation flows*

Dose No.	Emitted dose (µg)					
	SEDS 1		SEDS 5		SEDS 9	
	28.3 L min^{-1}	60 L min^{-1}	28.3 L min^{-1}	60 L min^{-1}	28.3 L min^{-1}	60 L min^{-1}
1	154.24	183.34	149.99	185.63	150.35	186.24
2	149.24	172.21	154.50	181.96	139.85	184.53
3	146.37	187.63	157.33	182.86	151.97	192.35
4	149.55	180.55	154.19	176.17	150.64	187.66
5	148.65	186.01	150.69	180.06	152.41	180.21
6	149.66	182.97	138.36	185.82	148.99	181.72
7	157.22	175.75	155.67	188.34	155.10	177.91
8	155.65	183.32	152.76	185.46	155.30	173.35
9	151.65	182.67	154.35	172.69	141.82	185.85
10	152.49	182.59	154.22	186.22	157.94	186.36
Mean	**151.47**	**181.70**	**152.21**	**182.52**	**150.44**	**183.68**
SD	**3.42**	**4.58**	**5.33**	**4.94**	**5.74**	**5.47**
RSD	**2.26**	**2.52**	**3.50**	**2.71**	**3.81**	**3.13**

Table 5. 4. *The emitted dose of 25% blend of SEDS theophylline samples recovered from the Easyhaler® at different inhalation flows*

Dose No.	Emitted dose (µg)					
	SEDS 1		SEDS 5		SEDS 9	
	28.3 L min^{-1}	60 L min^{-1}	28.3 L min^{-1}	60 L min^{-1}	28.3 L min^{-1}	60 L min^{-1}
1	140.43	150.75	136.52	155.32	136.25	156.39
2	135.34	158.24	140.26	152.25	136.69	154.26
3	136.64	154.76	137.89	152.37	127.26	150.64
4	132.16	150.39	150.26	154.99	140.68	151.46
5	138.43	156.63	140.37	150.25	141.91	158.23
6	142.49	140.47	138.25	165.32	139.03	159.37
7	149.99	153.68	139.69	150.21	138.65	153.32
8	135.37	153.53	139.48	155.29	141.59	153.21
9	137.24	162.56	140.37	152.36	139.69	155.09
10	140.89	151.75	136.64	156.32	137.65	156.36
Mean	**138.90**	**153.28**	**139.97**	**154.47**	**137.94**	**154.83**
SD	**4.95**	**5.83**	**3.90**	**4.38**	**4.22**	**2.81**
RSD	**3.57**	**3.80**	**2.79**	**2.84**	**3.06**	**1.82**

Table 5. 5. *Summary of the mean emitted dose of SEDS samples recovered from the Easyhaler® at different inhalation flows*

| Formulations | Dose emitted in (µg) | | | | | |
| | SEDS 1 | | SEDS 5 | | SEDS 9 | |
	28.3 L min⁻¹	60 L min⁻¹	28.3 L min⁻¹	60 L min⁻¹	28.3 L min⁻¹	60 L min⁻¹
Pure samples						
Mean	183.43	212.16	184.83	212.36	181.94	211.73
SD	6.02	5.99	4.84	5.86	6.71	5.52
RSD	3.28	2.83	2.62	2.76	3.69	2.61
50 % blend						
Mean	151.47	181.70	152.21	182.52	150.44	183.68
SD	3.42	4.58	5.33	4.94	5.74	5.47
RSD	2.26	2.52	3.50	2.71	3.81	3.13
25% blend						
Mean	138.90	153.28	137.97	154.47	137.94	154.83
SD	4.95	5.83	3.90	4.38	4.22	2.81
RSD	3.57	3.80	2.79	2.84	3.06	1.82
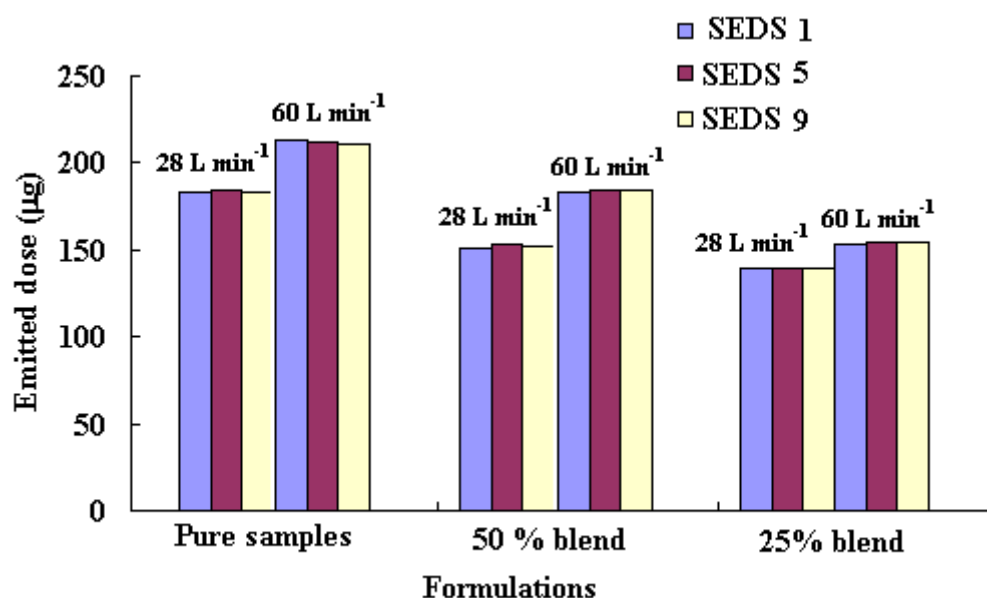
Figure 5. 3. *Total emitted dose from the Easyhaler® at inhalation flows 28.3 and 60 L min⁻¹ for all the studied SEDS formulations (Processing conditions for samples 1,5, 9 were described in Table 4.2.)*

Table 5. 6. *Statistical comparison for the emitted dose of SEDS samples in pure form and lactose blends recovered from the Easyhaler$^®$ at inhalation flows 60 L min^{-1}and 28.3 L min^{-1}*

Formulations	Mean difference (95% confidence Interval)		
	Emitted dose from Easyhaler (µg)		
	SEDS 1	SEDS 5	SEDS 9
Pure samples	28.73 (22.89, 34.56)***	27.54 (22.49, 32.88) ***	28.19 (23.43, 32.95)***
25% blend	14.38 (8.24,3.20.51) ***	15.50 (11.76, 19.23) ***	16.89(14.06, 19.72) ***
50% blend	30.23 (25.58, 34.88)***	30.31 (24.57, 36.06) ***	33.24 (26.90, 39.58) ***

Table 5. 7. *Statistical comparison for the emitted dose of SEDS samples in pure form and in lactose blends recovered from the Easyhaler$^®$ at the same inhalation flow.*

Formulations	Mean difference (95% confidence Interval)		
	Emitted dose from Easyhaler (µg)		
	SEDS 1	SEDS 5	SEDS 9
At 28.3 L min^{-1}			
Pure samples vs. 25% blend	31.95 (28.44, 35.46) ***	32.62 (27.97, 37.27) ***	31.50 (26.32, 36.68) ***
Pure samples vs. 50% blend	44.53 (41.62, 48.04) ***	44.86 (40.20, 49.51) ***	43.99 (38.82, 49.78) ***
25 % blend vs. 50 % blend	12.58 (9.07, 16.09) ***	12.23 (7.59, 16.88) ***	12.50 (7.31, 17.68) ***
At 60 L min^{-1}			
Pure samples vs. 25% blend	30.44 (24.82, 36.07) ***	29.84 (25.03, 34.66) ***	28.05 (23.46, 32.65) ***
Pure samples vs. 50% blend	58.88 (53.25, 64.50) ***	57.90 (53.08, 62.71) ***	56.90 (52.30, 61.49) ***
25 % blend vs. 50 % blend	28.43 (22.80, 34.06) ***	28.05 (23.24, 32.86) ***	28.84 (24.25, 33.43) ***

***P < 0.001

For the determination of the total emitted dose, the pharmacopoeias recommended an inhalation volume of 4 L through the inhaler with inhalation flow corresponding to a pressure drop 4 Kpa across the inhaler. The inhalation flows equivalent to pressure drop of 4 Kpa across the Easyhaler[®] is equivalent to 40.2 L min^{-1} [268]. This method is a quality control test when there is intra-patients or intra-device variability [269]. The determination of the total emitted dose at different inhalation flows provides an appreciation of the results obtained during normal practice. Also the main object in this study is to examine the effect of different inhalation flows on the total emitted doses of SEDS theophylline formulations. Therefore, two inhalation flows were used low (28.3 L min^{-1}) and high (60 L min^{-1}).

Data obtained from the dose emission test shows that the three samples in all the studied formulations provided good dose emission. The total emitted dose ranged from 138.94-184.83 μg, and from 152.68- 212.65 μg upon using inhalation flows of 28.3 and 60 L min^{-1} respectively for all the tested samples. The results indicate good reproducibility of the delivered theophylline doses, as the RSDs for all samples were lower than 5 %. Thus sufficient homogeneity and flowability of the SEDS powder were achieved.

As shown in Tables 5.2-5.4, generally small variations were found in the emitted dose between the samples within the same formulations at the same inhalation flow. But significant differences were observed when working with different inhalation flows. There was an increase in the emitted dose upon increasing the inhalation flow from 28.3 to 60 L min^{-1} for all the studied samples. This significant difference ($p < 0.001$) was confirmed by the statistical comparison between obtained data at different inhalation flows for all the tested samples (Table 5.6.). Although the emitted dose seemed to be flow rate dependant (Figure 5.3), no sharp differences observed at different inhalation flows. This is consistent with the reported results [218] which show that Easyhaler[®] is less affected by changes in inhalation rates than other DPIs such as the Turbuhaler[®].

Furthermore, the doses emitted at 28.3 L min^{-1} was found to be approximately 85% of that created at 60 L min^{-1} for all the tested formulations. Therefore, reasonably good theophylline dose can be achieved with patients who may have difficulties in generating high levels of inhalation flow such as children and the elderly, and this agrees with the reported results in different literatures [215, 270].

On the other hand there was a significant difference (p< 0.001) between the emitted doses of the three samples in different formulations under the same inhalation flow (Table 5.7).

The scope of this work was further extended to study the *in-vitro* aerodynamic behaviour and the lung deposition pattern of the inhaled SEDS formulations using the ACI.

5.3.2. *In-vitro* aerodynamic particle size distribution of SEDS theophylline formulations delivered from the Easyhaler® at different inhalation flows

5.3.2.1. Pure SEDS theophylline formulation

Tables 5.8 and 5.9 show the particle size distribution for the pure SEDS formulation recovered from the Easyhaler® at two different inhalation flows, after actuation of two puffs into the ACI for each sample. They also show the total emitted dose (TED), TED per shot, fine particle dose (FPD), fine particle fraction (FPF), Mass median aerodynamic diameter (MMAD), and Geometric standard deviation (GSD) for each sample.

Figures 5.4 and 5.5 represent the mean amount of theophylline deposited on each stage of the ACI at two inhalation flows; 28.3 and 60 L min^{-1}.

Table 5. 8. *Particle size distribution of pure SEDS theophylline samples recovered from the Easyhaler® at 28.3 L min⁻¹*

Stages	Stage ECD (µm)	Amount in (µg) ± SD (n =3)		
		SEDS1	SEDS 5	SEDS 9
Throat		152.12 (1.22)	139.15 (1.01)	124.98 (3.83)
Preseparator		183.39 (1.57)	184.74 (2.07)	218.89 (1.52)
Stage 0	9	7.27 (0.22)	7.99 (0.20)	5.50 (0.16)
Stage 1	5.8	4.23 (0.15)	7.33 (0.07)	2.5 (0.30)
Stage 2	4.7	3.65 (0.51)	6.20 (0.55)	2.26 (0.10)
Stage 3	3.3	3.28 (0.21)	8.72 (0.23)	1.99 (0.20)
Stage 4	2.1	4.72 (0.10)	5.53 (0.25)	2.46 (0.05)
Stage 5	1.1	2.92 (0.09)	5.11 (1.09)	1.85 (0.02)
Stage 6	0.7	1.63 (0.11)	2.32 (0.23)	1.29 (0.21)
Stage 7	0.43	1.53 (0.12)	1.27 (0.36)	0.73 (0.17)
Filter	0	0.37 (0.12)	0.52 (0.25)	0.14 (0.001)
TED (µg)		365.11 (1.59)	369.07 (3.94)	362.62 (2.41)
Number of Doses		2	2	2
TED per shot (µg)		182.56 (0.79)	184.70 (1.93)	181.31 (1.20)
FPD (µg)		7.79 (0.17)	13.00 (0.20)	4.55 (0.05)
FPF (%)		4.27 (0.09)	7.04 (0.04)	2.51 (0.03)
MMAD (µm)		4.80 (0.01)	4.47 (0.07)	5.12 (0.14)
GSD		3.30 (0.07)	2.71 (0.04)	3.43 (0.14)
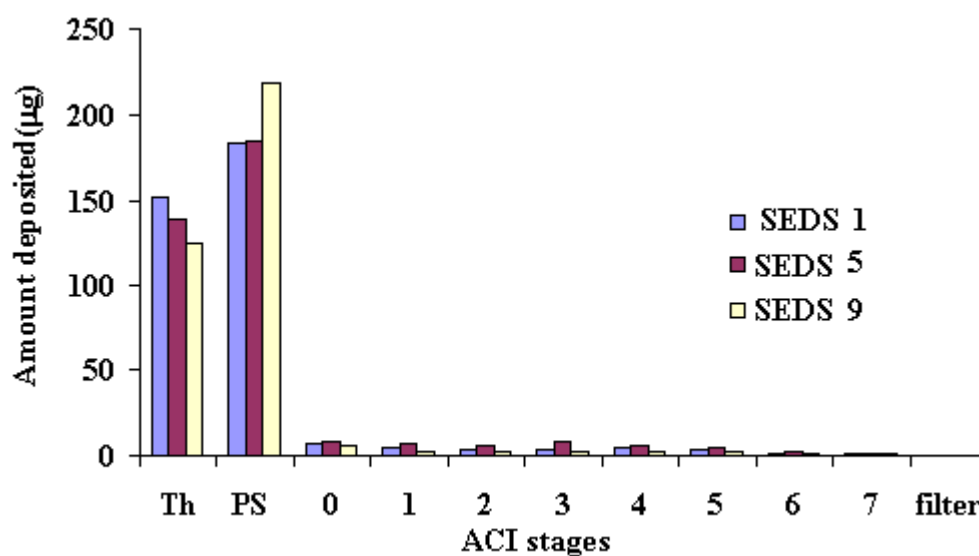
Figure 5. 4. *Mean amounts (µg) of pure SEDS theophylline deposited in ACI stages at 28.3 L min⁻¹ from the Easyhaler® (Processing parameters of samples 1, 5, 9 were described in Table 4.2.)*

Table 5. 9. *Particle size distribution of pure SEDS theophylline samples recovered from the Easyhaler® at 60 L min⁻¹*

Stages	Stage ECD (µm)	Amount in (µg) ± SD (n =3)		
		SEDS1	SEDS 5	SEDS 9
Throat		127.19 (3.36)	124.39 (0.32)	112.79 (3.97)
Preseparator		261.15 (1.37)	245.40 (2.82)	287.81 (4.88)
Stage -0	9	5.73 (0.11)	9.34 (0.25)	5.643 (0.05)
Stage -1	5.8	7.17 (0.06)	8.50 (0.40)	2.88 (0.07)
Stage 1	4.7	4.97 (0.04)	6.54 (0.31)	3.54 (0.13)
Stage 2	3.3	4.82 (0.05)	8.41 (0.33)	3.11 (0.06)
Stage 3	2.1	5.42 (0.08)	9.49 (0.22)	3.11 (0.02)
Stage 4	1.1	3.90 (0.08)	6.78 (0.04)	1.22 (0.03)
Stage 5	0.7	2.16 (0.09)	2.27(0.057)	1.57 (0.05)
Stage 6	0.43	1.54 (0.02)	1.88 (0.01)	1.03 (0.03)
Filter	0	0.37 (0.10)	1.20 (0.08)	0.32 (0.002)
TED (µg)		424.36 (4.65)	424.194 (2.45)	423.03 (0.99)
Number of Doses		2	2	2
TED per shot (µg)		212.18 (2.32)	212.10 (1.23)	211.52 (0.48)
FPD (µg)		9.88 (0.02)	16.12 (0.31)	5.70 (0.05)
FPF (%)		4.70 (0.06)	7.60 (0.16)	2.70 (0.02)
MMAD (µm)		4.62 (0.01)	4.17 (0.05)	4.95 (0.02)
GSD		3.13 (0.03)	2.67 (0.02)	3.29 (0.05)
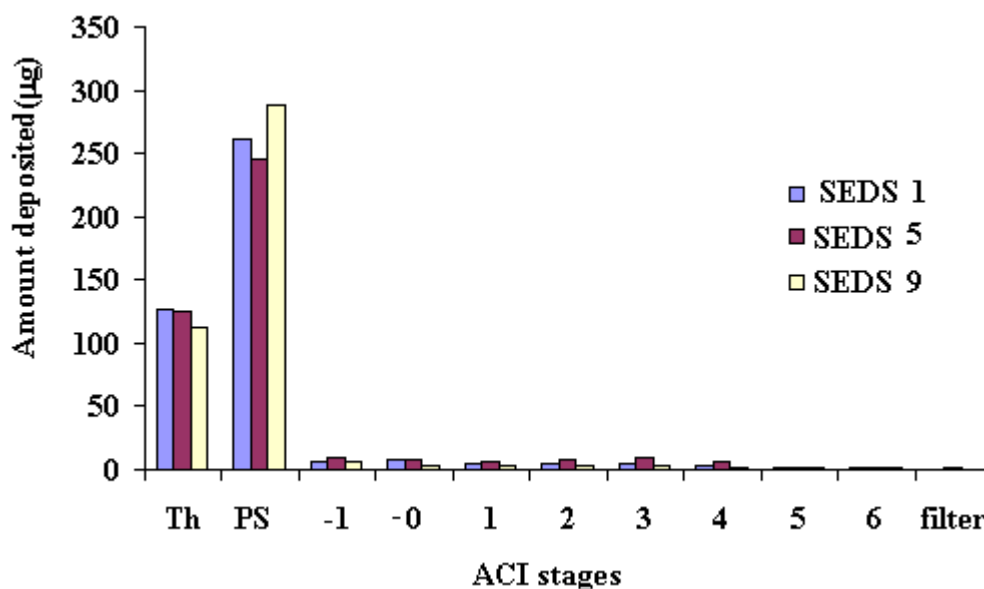
Figure 5. 5. *Mean amounts (µg) of pure SEDS theophylline deposited in ACI stages at 60 L min⁻¹ from the Easyhaler®. (Processing parameters of samples 1, 5, 9 were described in Table 4.2.)*

Data obtained from the ACI show that for a pure SEDS sample, the largest deposits were in the throat and the preseparator and only small amounts were recovered from the ACI stages and the filter. This may be attributed to the fact that pure powder particles without any carrier are stuck together and needed high inhalation flow to be de-aggregated into fine particles. Therefore, these adhered particles are too large to be carried by the air stream to the lower stages of the ACI. The TED was quite similar for the three samples but there was a significant difference between them in other aerodynamic characteristics under the same inhalation flows (Table 5.10).

Table 5. 10. *Statistical comparison for the ACI results of different pure SEDS theophylline samples recovered from the Easyhaler® at the same inhalation flows.*

	Mean difference (95% confidence Interval)		
	SEDS 1 vs SEDS 5	SEDS 1 vs SEDS 9	SEDS 5 vs SEDS 9
At 28.3 L min^{-1}			
FPD (µg)	-5.21 (-5.61, -4.86)***	3.24 (2.84, 3.64)***	8.45 (8.05, 8.85)***
FPF (%)	-2.77 (-2.92, -2.62)***	1.76 (1.61, 1.91)***	4.53 (1.61, 1.91)***
MMAD (µm)	0.33 (0.17, 0.49)**	-0.32 (-0.48, -0.16)*	-0.29 (-0.45, -0.15)*
GSD	0.54 (0.45, 0.64)***	-0.24 (-0.34, -0.14)**	-0.78 (-0.88, -0.69)***
At 60 L min^{-1}			
FPD (µg)	-6.21 (-6.66, -5.83)***	4.14 (3.76, 4.59)***	10.42 (10.0, 10.83)***
FPF (%)	-2.96 (-3.15,-2.76)***	1.95 (1.75,2.14)***	4.90 (4.71, 5.09)***
MMAD (µm)	0.46 (0.25, 0.67)**	-0.48 (-0.69, -.27)**	-0.95 (-1.16, -0.74)***
GSD	0.46 (0.31, 0.61)**	-0.29 (-0.45, -0.15)*	-0.76 (-0.91, -0.61)***

*$P < 0.01$ **$P < 0.005$ ***$P < 0.001$

The highest FPD and FPF were obtained from the SEDS 5; 13.00 µg, 7.04 %, respectively. The lowest FPD and FPF were obtained from SEDS 9; 4.55 µg, 2.51 %, respectively. On the other hand SEDS 5 shows the lowest MMAD and GSD, 4.47 µm, 2.71, respectively. This is in agreement with SEM images and particle size analysis results discussed in Chapter 4. The particle size of SEDS samples 1, 5, 9 was 2.44, 1.89, and 3.12 µm, respectively. Therefore SEDS 5 with the lowest particle size (small rod-shape) shows better aerodynamic characteristics than sample 1 and 9 (long needles). The results also indicate an increase in the FPD and FPF as the flow increases from 28.3 to 60 L min^{-1}. It was also observed that the MMAD and GSD decrease as the flow increases. There was a statistically significant difference in FPD, FPF, MMAD and GSD for all the studied samples at different inhalation flows (Table 5.11). To enhance the FPD and FPF for pure formulation, theophylline was blended with different proportions of inhalable lactose (DMV-Fonterra) and the aerodynamic behaviour of these new formulations was tested. Lactose is the commonly used as a carrier as it can accomplish many of the ideal requirements. It is readily available in an acceptable pharmaceutical grade, chemically and physically stable and inert to the drug substances. Furthermore, it is readily cleared from the airway without any harmful effect on the respiratory tract [227, 230]. Lactose is available in two basic isomeric forms namely α- and β-lactose or as an amorphous form. α-lactose exists as monohydrate and anhydrous forms. α-lactose monohydrate is thermodynamically stable form and is commonly used as a carrier in DPIs. The physical properties of lactose such as particle size, shape and surface texture have been shown to affect the dispersion and deaggregation of adhered drugs [225-227].

Table 5. 11. *Statistical comparison for the ACI results of different pure SEDS theophylline samples recovered from the Easyhaler® at inhalation flows 60 L min^{-1} and 28.3 L min^{-1}.*

	Mean difference (95% confidence Interval)		
	SEDS 1	SEDS 5	SEDS 9
FPD (μg)	2.13 (1.84, 2.43)***	3.01 (2.44,3.57)**	1.17 (1.04, 1.29)***
FPF (%)	0.42 (0.24, 0.59)**	0.53 (0.21, 0.86)**	0.19 (0.11, 0.26)**
MMAD (μm)	-0.16 (-0.18, -0.15)**	-0.31 (-0.46, -0.16)*	-0.21 (-0.41, -0.01)*
GSD	-0.21 (-0.37, -0.05)*	-0.07 (-0.12, -0.01)*	-0.21 (-0.32, -0.09)*

*P< 0.01   **P< 0.005   ***P < 0.001

5.3.2.2. SEDS theophylline and lactose blends

Tables 5.12-5.15 show the particle size distribution of theophylline blends (25 % and 50 % blends) delivered from Easyhaler® at two different inhalation flows (28.3 and 60 L min^{-1}), after actuation of two puffs into the ACI. They also illustrate TED, TED per shot, FPD, FPF, MMAD, and GSD for each sample. Figures 5.6 - 5.9 represent the mean amount of theophylline deposited on each stage of the ACI at two inhalation flows. A summary of the ACI data for all SEDS theophylline formulations recovered from Easyhaler® is shown in Table 5.16.

Table 5. 12. *Particle size distribution of 50% blend of SEDS theophylline from the Easyhaler® at 28.3 L min⁻¹*

| Stages	Stage ECD (μm)	Amount in (μg) ± SD (n =3)		
		SEDS 1	SEDS 5	SEDS 9
Throat		81.56 (2.43)	71.57 (2.43)	98.72 (1.50)
Preseparator		110.77 (0.18)	90.12 (1.27)	151.91 (2.98)
Stage 0	9	19.77 (1.30)	22.43 (0.20)	13.50 (0.39)
Stage 1	5.8	15.61 (0.12)	17.61 (0.12)	7.30 (0.04)
Stage 2	4.7	17.52 (0.27)	18.25 (0.20)	6.41 (0.51)
Stage 3	3.3	19.15 (0.16)	27.14 (0.15)	7.56 (0.37)
Stage 4	2.1	19.65 (0.30)	27.65 (0.30)	7.15 (0.12)
Stage 5	1.1	10.08 (0.06)	16.08 (0.06)	4.24 (0.07)
Stage 6	0.7	5.82 (0.66)	7.72 (0.21)	2.59 (0.06)
Stage 7	0.43	3.24 (0.25)	3.57 (0.33)	2.14 (0.16)
Filter	0	1.26 (0.06)	1.26 (0.06)	0.66 (0.15)
TED (μg)		304.42 (3.11)	303.39 (3.40)	302.17 (1.85)
Number of Doses		2	2	2
TED per shot (μg)		152.22 (1.56)	151.70 (1.70)	151.08 (0.93)
FPD (μg)		32.43 (0.59)	44.84 (0.14)	13.31 (0.17)
FPF (%)		21.31 (0.31)	29.56 (0.30)	8.68 (0.07)
MMAD (μm)		4.43 (0.03)	3.99 (0.02)	4.93 (0.06)
GSD		2.62 (0.04)	2.36 (0.02)	2.91 (0.02)
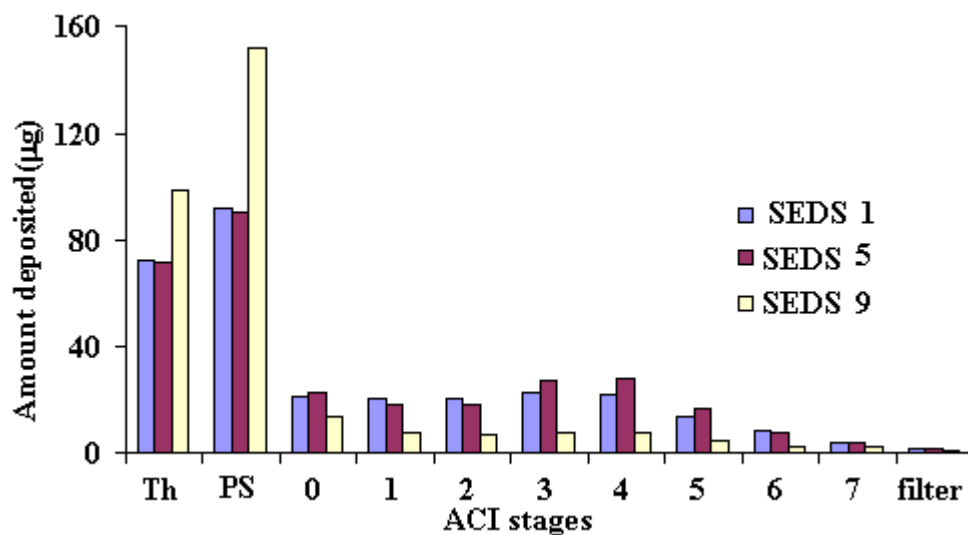
Figure 5. 6. *Mean amounts (μg) of 50% blend of SEDS theophylline deposited in ACI stages at 28.3 L min⁻¹ from the Easyhaler®.(Processing parameters of samples 1, 5, 9 were described in Table 4.2.)*

Table 5. 13. *Particle size distribution of 50% blend of SEDS theophylline recovered from the Easyhaler® at 60 L min⁻¹*

Stages	Stage ECD (μm)	Amount in (μg) ± SD (n =3)		
		SEDS1	SEDS 5	SEDS 9
Throat		91.62 (2.24)	71.63 (2.24)	109.63 (1.19)
Preseparator		123.60 (3.79)	118.60 (0.89)	170.73 (0.51)
Stage -0	9	24.63 (1.23)	26.13 (0.20)	21.01 (0.77)
Stage -1	5.8	23.98 (0.35)	20.65 (0.26)	12.31 (0.09)
Stage 1	4.7	20.63 (0.07)	23.63 (0.07)	10.62 (0.33)
Stage 2	3.3	24.06 (0.67)	29.39 (0.19)	12.43 (0.26)
Stage 3	2.1	25.22 (0.23)	29.22 (0.23)	12.48 (0.43)
Stage 4	1.1	18.30 (0.81)	27.63 (0.25)	7.24 (0.09)
Stage 5	0.7	7.45 (0.29)	10.45 (0.29)	5.24 (0.01)
Stage 6	0.43	3.50 (0.19)	3.50 (0.189)	2.43 (0.21)
Filter	0	1.38 (0.32)	2.38 (0.32)	0.36 (0.14)
TED (μg)		364.35 (1.58)	363.18 (2.48)	364.47 (1.53)
Number of Doses		2	2	2
TED per shot (μg)		182.18 (0.79)	181.59 (1.24)	182.24 (0.76)
FPD (μg)		43.34 (0.96)	55.29 (0.42)	21.69 (0.26)
FPF (%)		23.79 (0.60)	30.45 (0.22)	11.90 (0.09)
MMAD (μm)		4.34 (0.32)	3.87 (0.02)	4.88 (0.04)
GSD		2.55 (0.03)	2.29 (0.01)	2.75 (0.08)
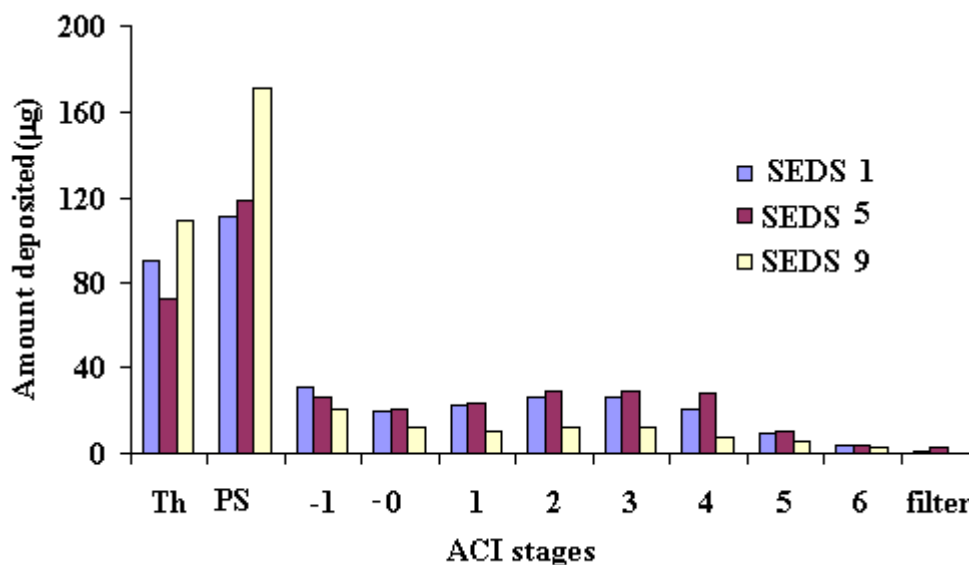
**Figure 5. 7.** *Mean amounts (μg) of 50% blend of SEDS theophylline deposited in ACI stages at 60 L min⁻¹ from the Easyhaler®. (Processing parameters of samples 1, 5, 9 were described in Table 4.2.)*

Table 5. 14. *Particle size distribution of 25% blend of SEDS theophylline recovered from the Easyhaler® at 28.3 L min⁻¹*

Stages	Stage ECD (μm)	Amount in (μg) ± SD (n =3)		
		SEDS 1	SEDS 5	SEDS 9
Throat		61.21 (0.94)	51.04 (1.13)	81.64 (4.16)
Preseparator		53.91 (1.03)	41.72 (0.80)	103.54 (2.89)
Stage 0	9	26.26 (0.06)	27.91 (0.07)	20.25 (0.18)
Stage 1	5.8	22.48 (0.44)	23.28 (0.08)	15.55 (0.36)
Stage 2	4.7	28.14 (0.08)	27.28 (0.16)	12.66 (0.30)
Stage 3	3.3	27.47 (0.58)	28.30 (0.23)	12.86 (0.31)
Stage 4	2.1	27.79 (0.73)	28.36 (0.29)	13.44 (0.30)
Stage 5	1.1	18.28 (0.07)	26.48 (0.43)	12.56 (0.25)
Stage 6	0.7	10.19 (0.06)	15.18 (0.07)	2.76 (0.05)
Stage 7	0.43	3.28 (0.08)	6.73 (0.103)	1.86 (0.02)
Filter	0	1.23 (0.084)	2.53 (0.042)	0.84 (0.04)
TED (μg)		280.25 (0.38)	278.80 (2.85)	277.97 (2.68)
Number of Doses		2	2	2
TED per shot (μg)		140.13 (0.44)	139.40 (1.42)	139.02 (1.37)
FPD (μg)		48.65 (0.56)	58.37 (0.50)	24.12 (0.24)
FPF (%)		34.72 (0.35)	41.87 (0.10)	17.34 (0.33)
MMAD (μm)		4.36 (0.03)	3.92 (0.02)	4.86 (0.05)
GSD		2.57 (0.03)	2.25 (0.002)	2.66 (0.01)
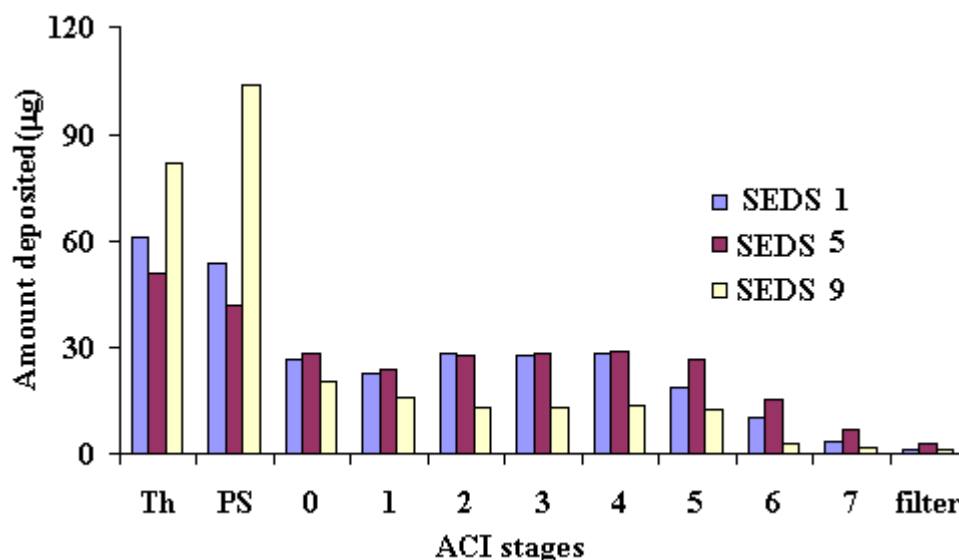
Figure 5. 8. *Mean amounts (μg) of 25% blend of SEDS theophylline deposited in ACI stages at 28.3 L min⁻¹ from the Easyhaler®(Processing parameters of samples 1, 5, 9 were described in Table 4.2.)*

Table 5. 15. *Particle size distribution of 25% blend of SEDS theophylline recovered from the Easyhaler® at 60 L min⁻¹*

Stages	Stage ECD (µm)	Amount in (µg) ± SD (n =3)		
		SEDS1	SEDS 5	SEDS 9
Throat		31.72 (1.29)	27.32 (1.81)	80.76 (4.32)
Preseparator		80.96 (0.80)	79.28 (2.23)	114.66 (4.16)
Stage -0	9	30.36 (0.23)	22.61 (0.36)	20.36 (0.30)
Stage -1	5.8	27.58 (0.41)	25.52 (0.23)	17.61 (0.39)
Stage 1	4.7	29.09 (0.68)	27.38 (0.27)	16.63 (0.19)
Stage 2	3.3	31.83 (1.06)	30.52 (0.14)	14.24 (0.35)
Stage 3	2.1	31.52 (0.15)	33.82 (0.16)	15.75 (0.26)
Stage 4	1.1	28.35 (0.03)	28.44 (0.21)	15.70 (0.11)
Stage 5	0.7	9.555 (0.03)	15.45 (0.15)	3.85 (0.04)
Stage 6	0.43	3.25 (0.13)	8.37 (0.31)	0.75 (0.08)
Filter	0	1.66 (0.34)	4.55 (0.53)	0.18 (1.15)
TED (µg)		305.88 (2.13)	303.26 (1.18)	300.49 (0.32)
Number of Doses		2	2	2
TED per shot (µg)		152.94 (1.07)	150.544 (0.59)	151.03 (0.26)
FPD (µg)		57.88 (0.64)	65.20 (0.24)	27.76 (0.25)
FPF (%)		37.84 (0.33)	42.99 (0.22)	18.48 (0.18)
MMAD (µm)		4.22 (0.03)	3.61 (0.03)	4.83 (0.03)
GSD		2.51 (0.01)	2.11 (0.01)	2.59 (0.02)
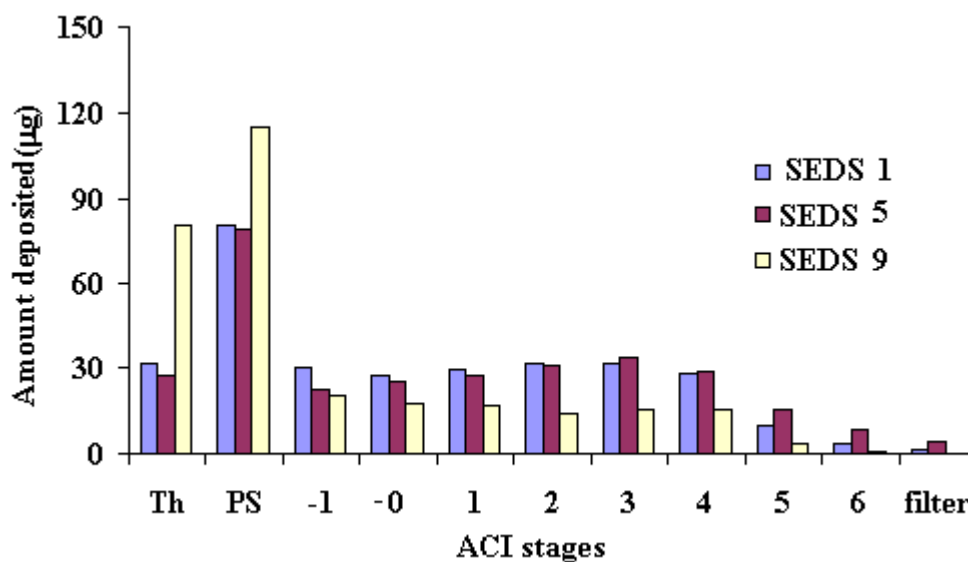
Figure 5. 9. *Mean amounts (µg) of 25% blend of SEDS theophylline deposited in ACI stages at 60 L min⁻¹from the Easyhaler®(Processing parameters of samples 1, 5, 9 were described in Table 4.2.)*

Table 5. 16. *Summary of ACI results for all SEDS formulations recovered from Easyhaler® at inhalation flows of 28.3 and 60 L min^{-1}*

	Formulations								
	Pure samples			50 % blend			25 % blend		
	SEDS 1	SEDS 5	SEDS 9	SEDS 1	SEDS 5	SEDS 9	SEDS 1	SEDS 5	SEDS 9
At 28.3 L min^{-1}									
FPD (µg)	7.79 (0.17)	13.00 (0.20)	4.55 (0.05)	32.43 (0.59)	44.84 (0.14)	13.31 (0.17)	48.65 (0.56)	58.37 (0.50)	24.12 (0.24)
FPF (%)	4.27 (0.09)	7.04 (0.04)	2.51 (0.03)	21.31 (0.31)	29.56 (0.30)	8.86 (0.07)	34.72 (0.35)	41.87 (0.10)	17.34 (0.33)
MMAD (µm)	4.80 (0.01)	4.47 (0.07)	5.12 (0.14)	4.43 (0.03)	3.99 (0.02)	4.93 (0.06)	4.36 (0.03)	3.92 (0.02)	4.86 (0.05)
GSD	3.30 (0.07)	2.71 (0.04)	3.43 (0.14)	2.62 (0.04)	2.36 (0.02)	2.91 (0.02)	2.57 (0.03)	2.25 (0.002)	2.66 (0.01)
At 60 L min^{-1}									
FPD (µg)	9.88 (0.02)	16.12 (0.31)	5.70 (0.05)	43.34 (0.96)	55.29 (0.42)	21.69 (0.26)	57.88 (0.64)	65.20 (0.24)	27.76 (0.25)
FPF (%)	4.74 (0.06)	7.60 (0.16)	2.70 (0.02)	23.97 (0.60)	30.45 (0.22)	11.90 (0.09)	37.84 (0.64)	42.99 (0.22)	18.48 (0.18)
MMAD (µm)	4.62 (0.01)	4.17 (0.05)	4.95 (0.02)	4.34 (0.32)	3.87 (0.02)	4.88 (0.04)	4.22 (0.03)	3.61 (0.03)	4.83 (0.03)
GSD	3.13 (0.03)	2.67 (0.02)	3.29 (0.05)	2.55 (0.03)	2.29 (0.01)	2.75 (0.08)	2.51 (0.01)	2.11 (0.01)	2.59 (0.02)

The particle size of the inhaled drug is responsible for fine particle dispersion. Usami *et al* [113] reported that the particle size influences the extent, distribution and site of the inhaled drug deposition within the airways. The ACI results for theophylline blends demonstrate the importance of the particle size on the aerodynamic behaviour and deposition profile of its inhaled particles. As SEDS 5, which has the smallest particle size (1.89 μm), provides higher FPD, FPF and lower MMAD and GSD compared with SEDS 9 with larger particle size (3.12 μm). Therefore this study proves that the smaller the particles the greater the total lung deposition for all the tested formulations (Figures 5.10, 5.11). These significance differences in FPD, FPF, MMAD and GSD between the three samples in each blend were presented in Table 5.17.
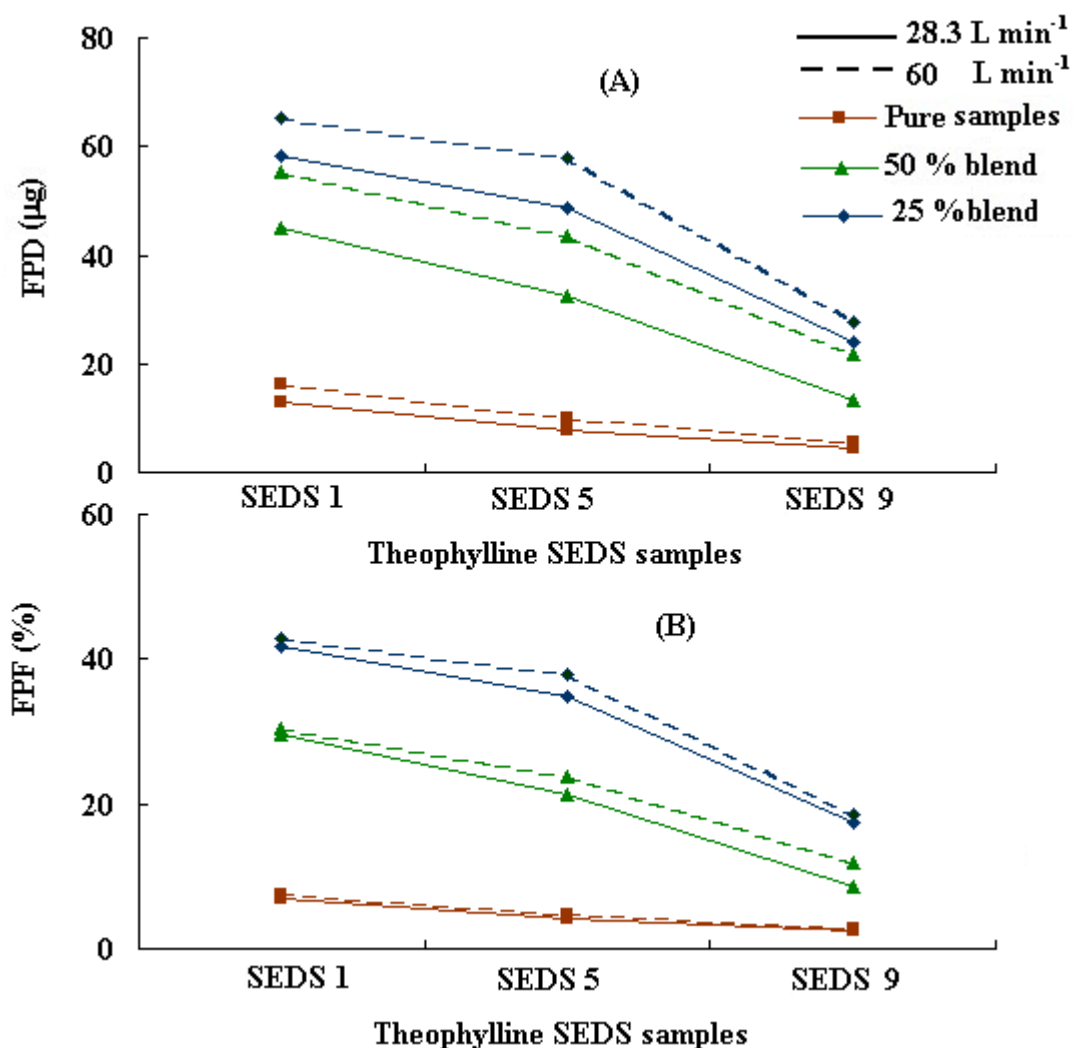
Figure 5. 10. *Fine particle dose (A), and fine particle fraction (B) of SEDS theophylline samples recovered from the Easyhaler® at inhalation flows of 28.3, and 60 L min⁻¹.*
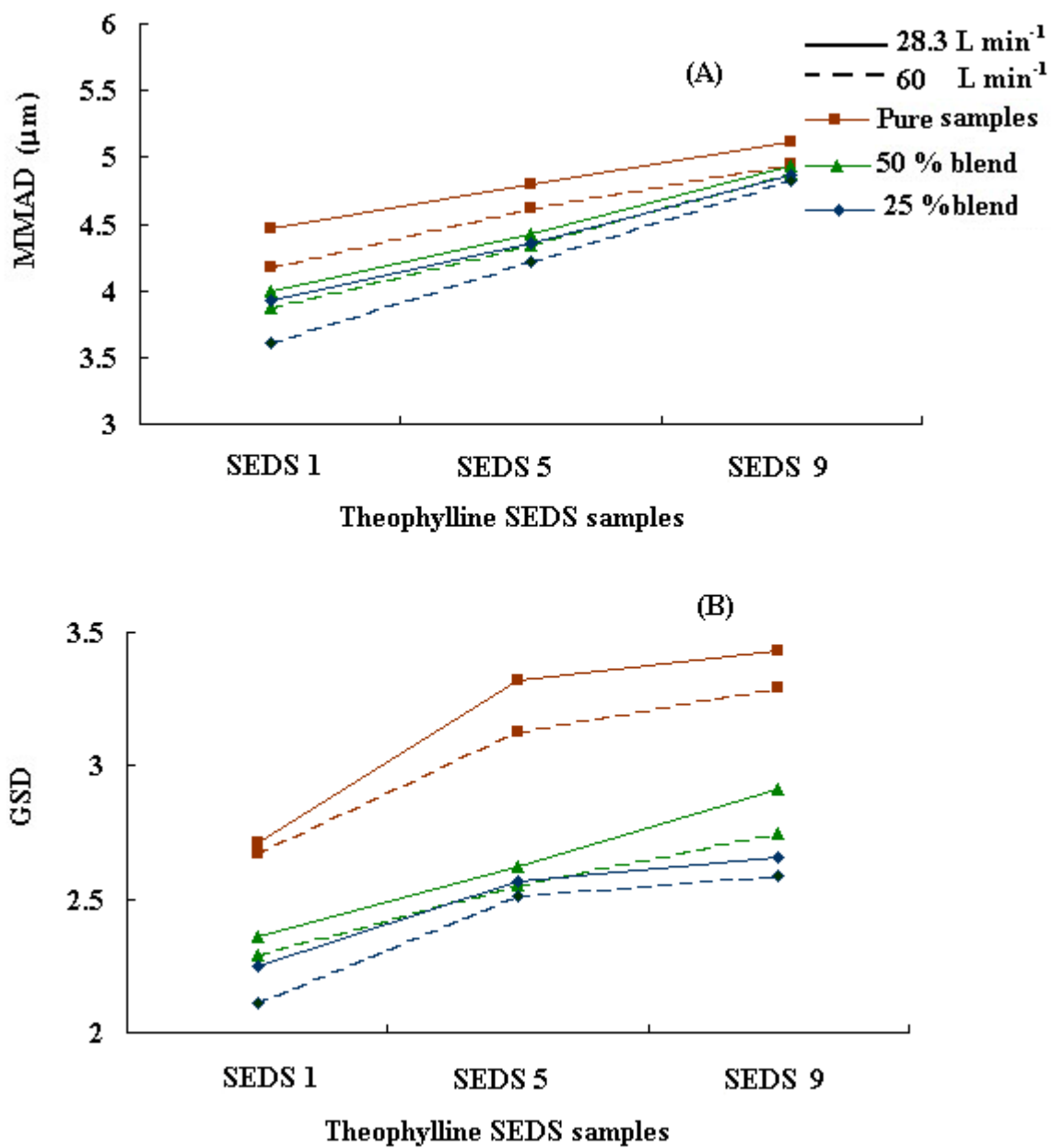
Figure 5. 11. *MMAD (A), and GSD (B) of SEDS theophylline samples recovered from the Easyhaler® at inhalation flows of 28.3, and 60 L min⁻¹.*

Table 5. 17. *Statistical comparison for ACI results of different SEDS theophylline blends recovered from Easyhaler® at the same inhalation flow*

Formulations	Mean difference (95% confidence Interval)			
	FPD (μg)	FPF (%)	MMAD (μm)	GSD
At 28.3 L min⁻¹	**50 % blend (50 % theophylline + 50 % lactose)**			
SEDS 1 vs. SEDS 5	-6.64 (-7.10, -6.18)***	-3.74 (-4.19, -3.29)***	0.41 (0.30, 0.52)***	0.264 (0.18, 0.35)**
SEDS 1 vs. SEDS 9	25.05 (24.59, 25.51)***	17.14 (16.69, 17.59)***	-0.53 (-0.63, -0.42)***	-0.29 (-0.37, -0.21)**
SEDS 5 vs. SEDS 9	31.69 (31.23, 32.15)***	20.88 (20.43, 21.33)***	-0.94 (-1.04, -0.83)***	-0.55 (-0.63, -0.47)***
At 60 L min⁻¹				
SEDS 1 vs. SEDS 5	-7.71 (-8.48, -6.94)***	-4.24 (-4.69, -3.79)***	0.39 (0.34, 0.45)***	0.35 (0.32, 0.38)***
SEDS 1 vs. SEDS 9	25.88 (25.12, 26.65)***	14.31 (13.86, 14.75)***	-0.61 (-0.67, -0.56)***	-0.16 (-0.19, -0.13)***
SEDS 5 vs. SEDS 9	33.59 (32.83, 34.37)***	18.55 (18.09, 18.99)***	-1.01 (-1.06, -0.95)***	-0.51 (-0.54, -0.48)***
At 28.3 L min⁻¹	**25 % blend (25 % theophylline + 75% lactose)**			
SEDS 1 vs. SEDS 5	-9.72 (-10.57, -8.87)***	-7.15 (-7.89, -6.413)***	0.45 (0.39, 0.50)***	0.32 (0.29, 0.35)***
SEDS 1 vs. SEDS 9	24.54 (23.69, 25.39)***	17.38 (16.64, 18.12)***	-0.50 (-0.56, -0.44)***	-0.09 (-0.12, -0.55)**
SEDS 5 vs. SEDS 9	34.26 (33.41, 35.11)***	24.53 (23.79, 25.27)***	-0.95 (-1.01, -0.89)***	-0.40 (-0.43, -0.37)***
At 60 L min⁻¹				
SEDS 1 vs. SEDS 5	-7.65 (-8.54,-6.76)***	-5.16 (-5.54, -4.77)***	0.55 (0.38, 0.72)**	0.41 (0.38, 0.45)***
SEDS 1 vs. SEDS 9	30.12 (29.23, 31.015)***	19.37 (18.99, 19.75)***	-0.67 (0.83, 0.49)***	-0.07 (-0.10, -0.04)**
SEDS 5 vs. SEDS 9	37.77 (36.88, 38.67)***	24.52 (24.14, 24.91)***	1.22 (-1.38, -1.05)***	-0.42 (-0.51, -0.45)***

*P< 0.01   **P< 0.005   ***P <0.001

The inhalation flows had an effect on the FPD, and FPF, as the respirable amount increased by increasing the flow rate. This might be due to increase in the breakdown of small particles into fine particles as the flow increase. The results of MMAD and GSD showed that they are decreased as the flow was increased. This may be due to the increase in the release of their carrier particles at higher flow rates [271]. For a patient achieving high inhalation flows it would be expected that lung deposition would be increased and theoretically more dose would be concentrated in the central zone of the lung and hence the FPD increases. However, the effect of inhalation flow is less pronounced on either the emitted dose or the respirable fraction recovered from Easyhaler® than on other DPIs as the Turbuhaler®. It was reported by Koskela et al [270] that even a reasonably low peak inspiratory flow rate through the Easyhaler produces an improvement in lung function. This is considered as an advantage of the Easyhaler® especially for asthmatic patients, children, and elderly patients have problems achieving high inhalation flows as 60 L min^{-1}. The significance differences between FPD, FPF, MMAD, and GSD under different inhalation flows for all the studied samples for each blend rate were reported in Table 5.18.

Table 5. 18. *Statistical comparison for the ACI results of SEDS theophylline blends recovered from the Easyhaler$^{®}$ at inhalation flows of 60 L min^{-1} and 28.3 L min^{-1}*

Formulations	Mean difference (95% confidence Interval)			
	FPD (μg)	FPF (%)	MMAD (μm)	GSD
50% blend				
SEDS 1	9.40 (8.92, 9.89)***	0.75 (0.29, 1.22)*	-0.14 (-0.21, 0.06)*	-0.05 (-0.07, -0.03)***
SEDS 5	10.43 (9.47, 11.40)***	0.89 (0.05, 1.74)*	-0.11 (-0.18, -0.05)*	-0.19 (-0.31, -0.07)**
SEDS 9	8.57 (7.65, 9.49)**	3.13 (2.85, 3.59)**	-0.11 (-0.22, -0.003)*	-0.22 (-0.36, -0.07)*
25% blend				
SEDS 1	9.08 (7.38,10.77)***	3.08 (2.03, 4.13)**	-0.29 (-0.52, -0.08)*	-0.06 (-0.12, -0.001)*
SEDS 5	6.91 (5.761, 8.06)***	1.12 (0.573, 1.66)**	-0.32 (-0.36, -0.27)***	-0.14 (-0.16, -0.13)***
SEDS 9	3.66 (2.88, 4.45)**	1.16 (0.33, 1.99)*	-0.11(-0.19, -0.03)*	-0.07 (-0.12, -0.02)*

* $P < 0.05$ **$P < 0.01$ ***$P < 0.001$

From the obtained results it was noticed that, most of the pure theophylline formulation dose was retained in the throat and preseparator. Inhalable formulation showing significantly less clinical effects when the amount of the drug retained in the throat and preseparator increased [113]. Blending of theophylline with lactose as a carrier in different proportions decreases its deposition in the throat and preseparator and so increases the amounts of theophylline held by air stream down to the ACI stages (Figure 5.12).
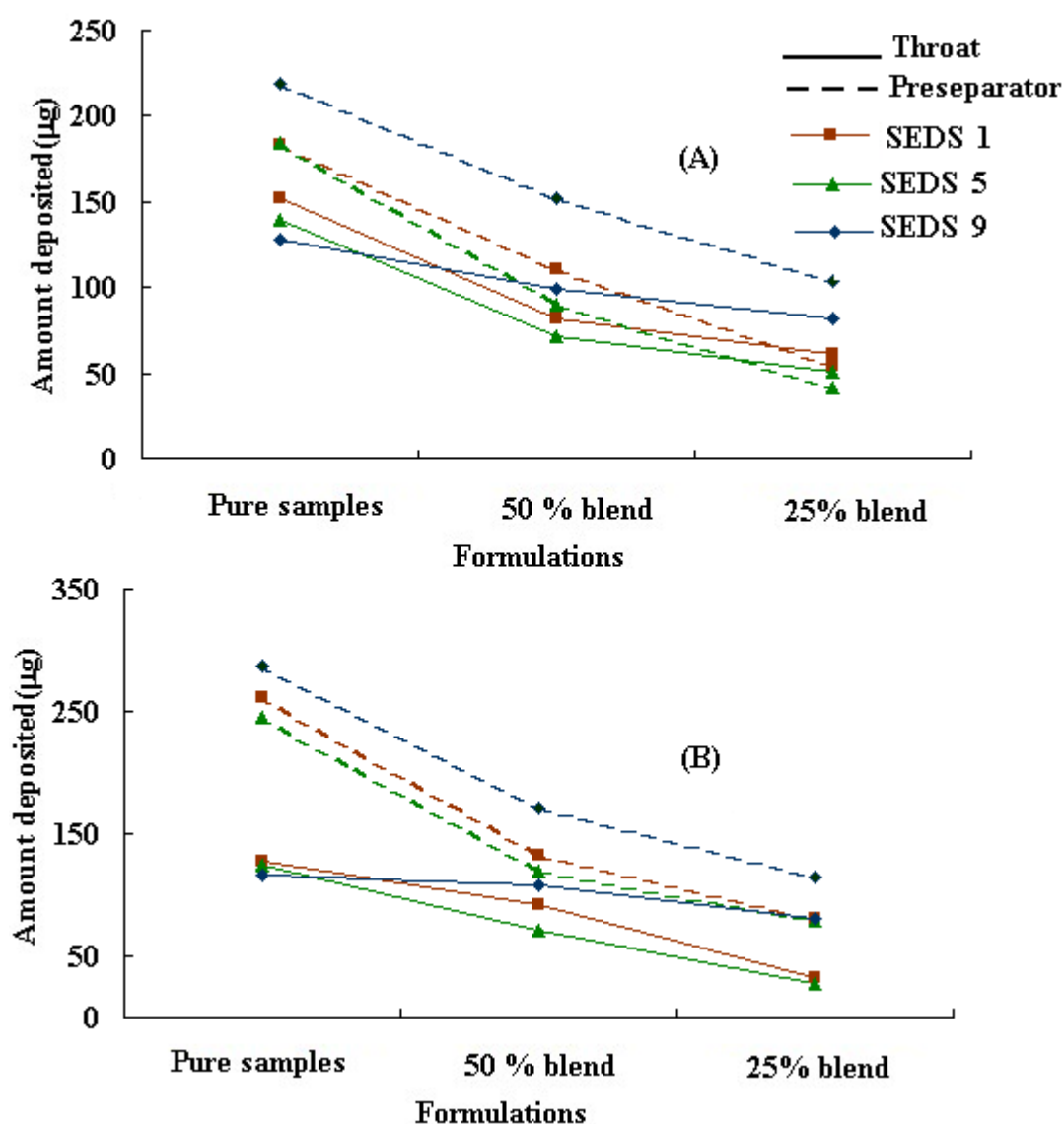
Figure 5.12. *Mean amount of different SEDS theophylline formulations deposited in throat and preseparator at inhalation flows of 28.3L min^{-1}(A) and 60 L min^{-1}(B)*

The carrier aids the flow and dispersion properties of pure SEDS theophylline powder, which is somewhat cohesive due to its small particle size. Therefore, this can potentially improve the deaggregation of the particles into fine particles and so the respirable fraction [272]. The particle size of the carrier has an important effect on the drug delivery from the DPI. Studies using different grades of lactose for inhalation have shown that the fine lactose particles added to inhalation formulations produced a more efficient delivery of the drug than the other grades of lactose [230]. Therefore fine inhalable lactose (Raspitose® SV003) was used in this study. Consequentially, FPD and FPF for the 25 % blend are higher than the 50 % blend, which in turn shows better aerodynamic performance than the pure formulation. The FPD and FPF of theophylline blends are about 3 times higher than those of pure formulations (Figures 5.13). When statically tested, there was significant difference (p< 0.001) in the FPD and FPF between the tested formulations (Tables 5.19, 5.20). It was also observed that the MMAD and GSD for theophylline blends were smaller than those of pure formulations (Figure 5.14). When the mean difference (95% confidence interval) between pairs of formulations was compared, significant differences in MMAD and GSD were noticed (Tables 5.19, 5.20). The 25 % blend showed not only the lowest MMAD (3.61-4.86) μm but also a more uniform particle size distribution with the smallest GSD (2.11-2.66) compared with 50 % blend or pure formulation.
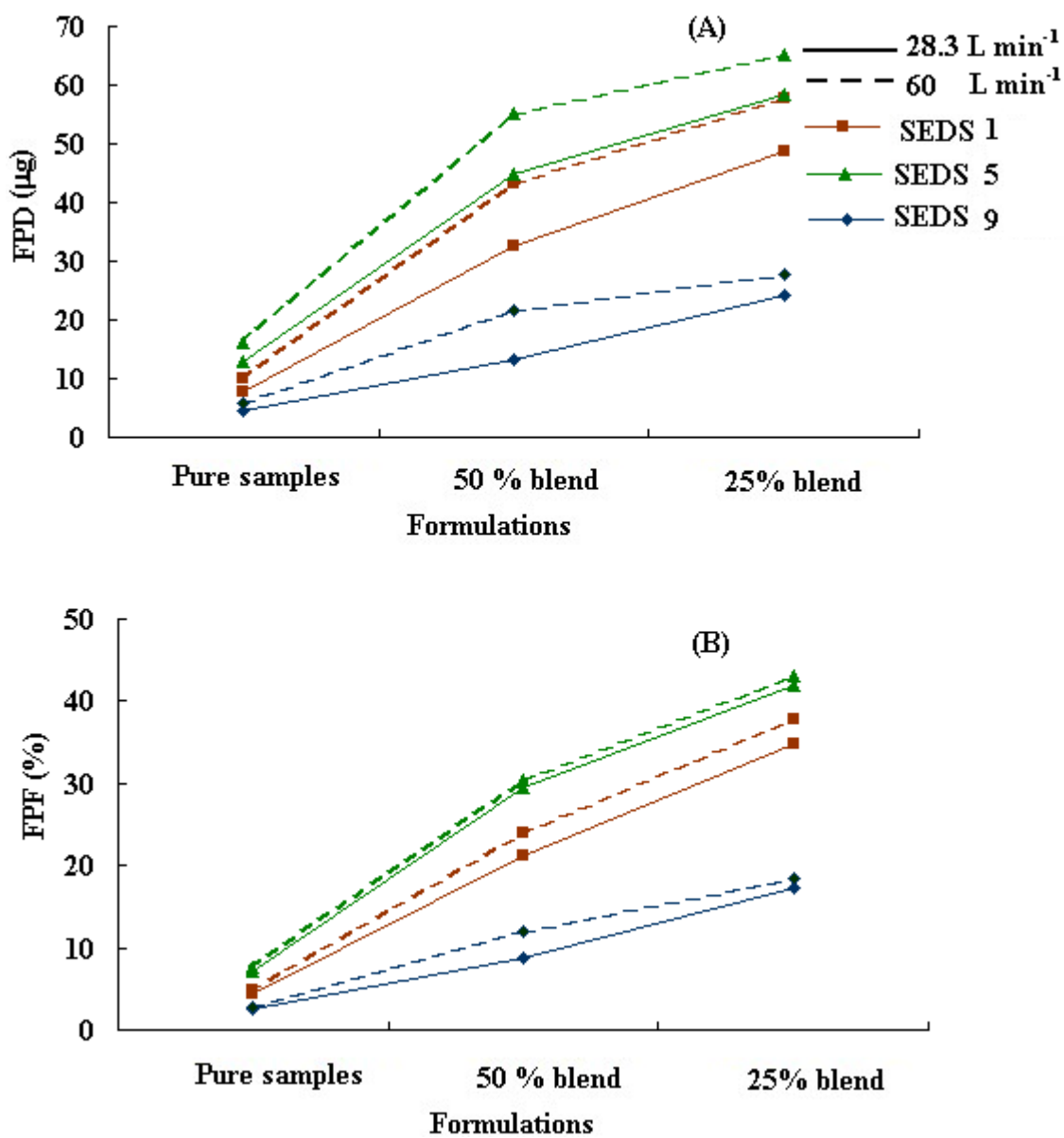
Figure 5.13. *Fine particle dose (A) and f*ine particle fraction (B) *of different SEDS theophylline formulations recovered from the Easyhaler® at inhalation flows of 28.3 and 60 L min^{-1}.*
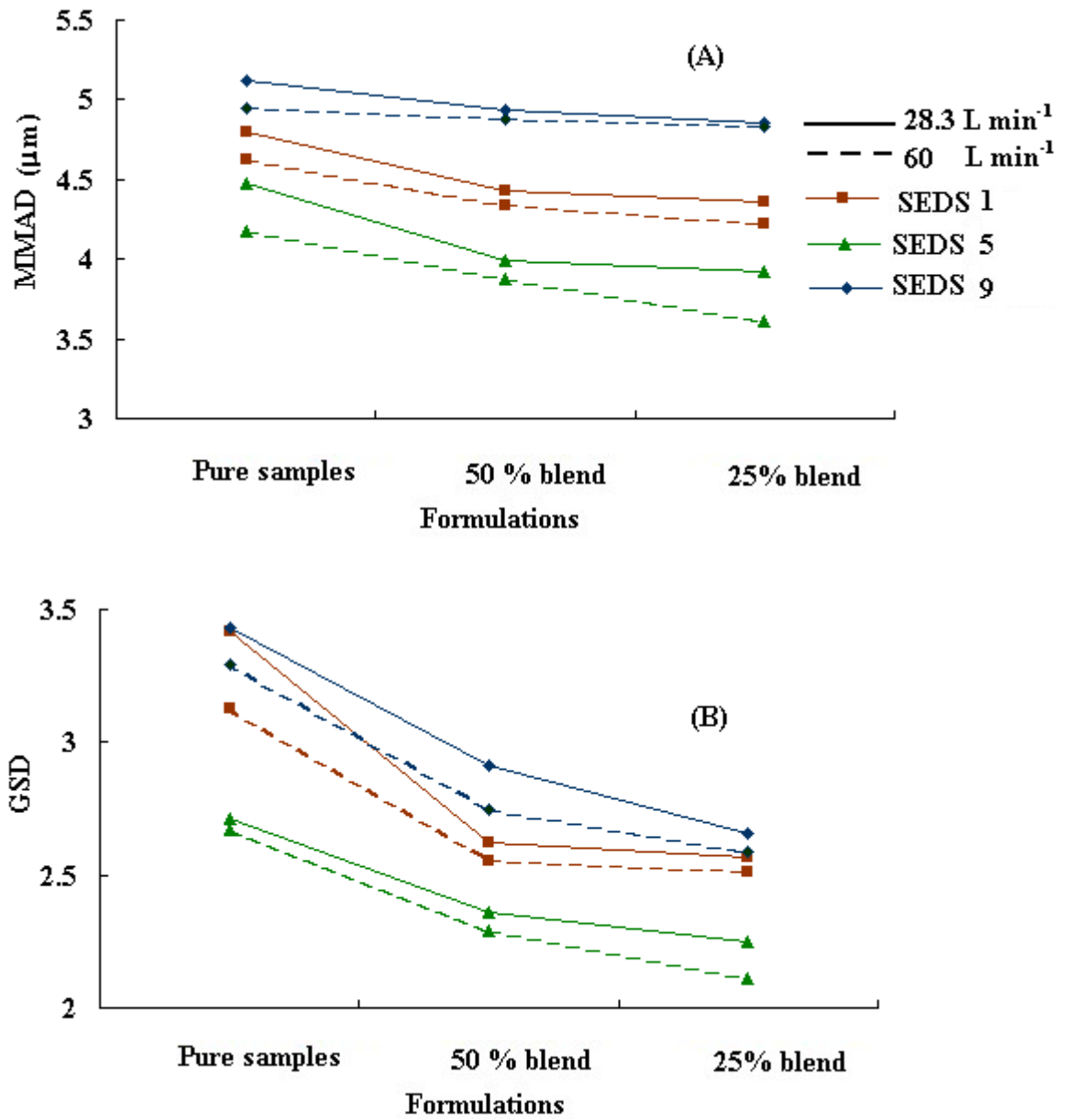
Figure 5.14. *MMAD (A) and GSD (B) of different SEDS theophylline formulations recovered from the Easyhaler[®] at inhalation flows of 28.3 and 60 L min^{-1}*

Table 5. 19. *Statistical comparison for the ACI results of different SEDS theophylline formulations recovered from the Easyhaler® at inhalation flow of 28.3 L min^{-1}*

Formulations	Mean difference (95% confidence Interval)			
	FPD (µg)	**FPF (%)**	**MMAD (µm)**	**GSD**
SEDS 1				
pure vs. 25% blend	-40.87 (-41.44, -40.29)***	-30.45 (-30.99, -29.91)***	0.45 (0.38, 0.53)***	0.75 (0.65, 0.85)***
pure vs. 50% blend	-30.38 (-30.95,-29.81)***	-21.33 (-21.88, -20.79)***	0.37 (-0.29, -0.44)***	0.65 (-0.55, -0.75)***
25% blend vs. 50% blend	10.48 (9.91, 11.05)***	9.123 (8.578, 9.67)***	-0.09 (-0.16, -0.01)*	-0.10 (-0.20, -0.001)*
SEDS 5				
pure vs. 25% blend	-45.37 (-4621, -44.52)***	-34.83 (-35.25, -34.41)***	0.61 (0.50, 0.73)***	0.44 (0.35, 0.54)***
pure vs. 50% blend	-31.81 (-32.66, -30.97)***	-22.52 (-22.94, -22.10)***	0.47 (0.35, 0.58)***	0.33 (0.24, 0.426)**
25% blend vs. 50% blend	13.55 (12.71, 14.39)***	12.31 (11.89, 12.73)***	-0.15(-0.26, -0.04)*	-0.11 (-0.20, -0.014)*
SEDS 9				
pure vs. 25% blend	-19.56 (-19.92, -19.19)***	-14.83 (-15.28, -14.38)***	0.17 (0.032, 0.31)*	0.78 (0.61, 0.94)***
pure vs. 50% blend	-8.57 (-8.93, -8.21)***	-6.17 (-6.62, -5.73)***	0.31 (0.172, 0.45)**	0.52 (0.35, 0.68)**
25% blend vs. 50% blend	10.99 (10.63, 11.35)***	8.66 (8.21, 9.11)***	-0.14 (-0.28, -0.003)*	-0.26 (-0.42, -0.09)*

*P< 0.01   **P< 0.005   ***P < 0.001

Table 5. 20. *Statistical comparison for the ACI results of different SEDS theophylline formulations recovered from the Easyhaler® at inhalation flow of 60 L min⁻¹*

Formulations	Mean difference (95% confidence Interval)			
	FPD (µg)	FPF (%)	MMAD (µm)	GSD
SEDS 1				
pure vs. 25% blend	-48.00 (-48.84, -47.16)***	-33.19 (-33.76, -32.62)***	0.54 (0.41, 0.67)***	0.61 (0.55, 0.67)***
pure vs. 50% blend	-37.69 (-38.53, -36.86)***	-21.55 (-22.12, -20.98)***	0.37 (-0.24, -0.49)**	0.40 (0.44, 0.55)***
25% blend vs. 50% blend	10.31 (9.47, 11.15)***	11.64 (11.07, 12.21)***	-0.17 (-0.29, -0.05)*	-0.12 (-0.18, -0.06)**
SEDS 5				
pure vs. 25% blend	-49.08 (-49.95,-48.21)***	-35.39 (-35.88, -34.92)***	0.56 (0.49, 0.82)***	0.56 (0.54, 0.59)***
pure vs. 50% blend	-39.17 (-40.04, -38.30)***	-22.85 (-23.33, -22.36)***	0.29 (0.23, 0.36)***	0.38 (0.36, 0.40)***
25% blend vs. 50% blend	9.910 (9.044, 10.78)***	12.55 (12.07, 13.03)***	-0.26 (-0.32, -0.20)***	-0.18 (-0.20, -0.16)***
SEDS 9				
pure vs. 25% blend	-22.05 (-22.62, -21.98)***	-15.78 (-16.09, -15.46)***	0.14 (0.0.08, 0.19)**	0.71 (0.56, 0.85)***
pure vs. 50% blend	-15.98 (-16.56, -15.41)***	-9.20 (-9.52, -8.89)***	0.07 (0.01, 0.12)**	0.54 (0.39, 0.69)***
25% blend vs. 50% blend	6.07 (5.49, 6.64)***	6.57 (6.26, 6.89)***	-0.73 (-0.13, -0.02)*	-0.17 (-0.31, -0.02)*

*P< 0.01   **P< 0.005   ***P < 0.001

Finally it can be concluded that the 25 % blends for all the studied samples were the best formulation regarding the FPD, FPF as well as the MMAD and GSD. Therefore the next step was to investigate the aerodynamic behaviour of 25% blend upon using single dose DPI as Spinhaler® at two different inhalation flows 28.3, and 60 L min^{-1}.

5.3.3. Spinhaler®

5.3.3.1. Determination of the emitted dose of SEDS theophylline formulations from Spinhaler® at different inhalation flows

Table 5.21 shows the mean (n =10), SD, and RSD of the emitted dose of 25 % blend of SEDS theophylline recovered from Spinhaler® using two different inhalation flows; 28.3, and 60 L min^{-1}.

Table 5. 21. *The emitted dose of 25% blend of SEDS theophylline recovered from the Spinhaler® at different inhalation flows*

Dose No.	Emitted dose (mg)					
	SEDS 1		SEDS 5		SEDS 9	
	28.3 L min^{-1}	60 L min^{-1}	28.3 L min^{-1}	60 L min^{-1}	28.3 L min^{-1}	60 L min^{-1}
1	0.99	1.48	0.94	1.36	0.99	1.37
2	0.97	1.27	0.98	1.45	0.97	1.44
3	0.96	1.34	0.99	1.40	1.09	1.26
4	1.10	1.30	1.04	1.40	1.12	1.35
5	0.97	1.29	1.06	1.34	0.94	1.39
6	0.94	1.29	1.11	1.32	1.00	1.32
7	1.05	1.33	0.99	1.29	0.99	1.44
8	1.10	1.35	0.98	1.34	0.96	1.43
9	0.96	1.32	1.00	1.23	0.98	1.35
10	1.00	1.43	0.99	1.39	0.91	1.39
Mean	1.00	1.34	1.01	1.35	1.00	1.37
SD	0.06	0.07	0.05	0.06	0.06	0.06
RSD	5.98	5.22	4.75	4.67	6.43	4.38

Results presented in Table 5.21 showed that the emitted dose from the three samples were quite similar. The total emitted dose increased by increasing the inhalation flow from 28.3 to 60 L min^{-1} (Figure 5.15).
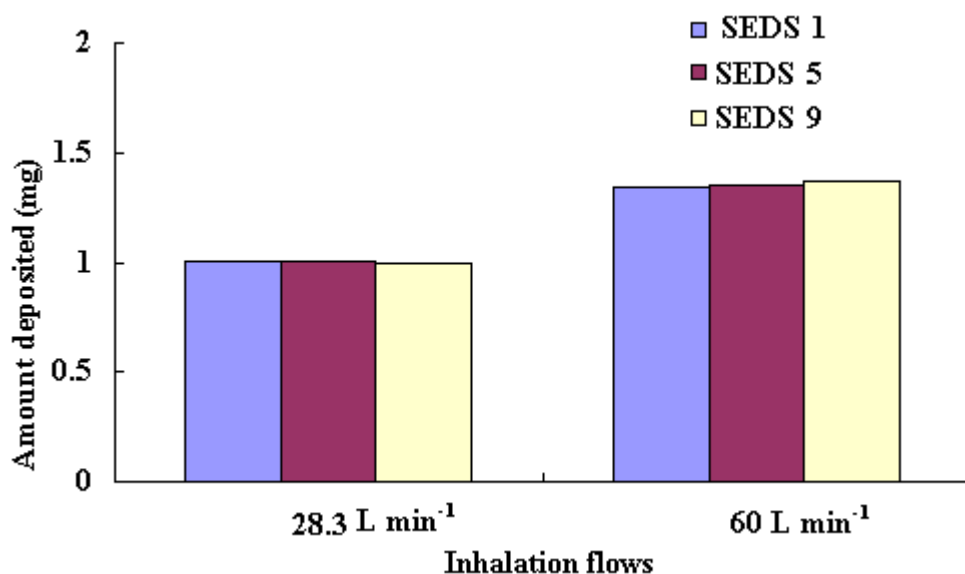
Figure 5. 15. *Total emitted dose of 25% blend of SEDS theophylline recovered from Spinhaler® at inhalation flows of 28.3 and 60 L min^{-1} (Processing parameters of samples 1, 5, 9 were described in Table 4.2.)*

Boer et al [273] reported that the capsule discharge rate depends on the flow properties of the drug and the rotation speed of the capsule. Therefore, the emitted dose from Spinhaler® depends on the inspiratory flow rate. Although the total emitted dose is flow dependant, the Spinhaler® as a low resistance device the inspiratory flows > 60 L min^{-1} are typically achieved by more than 90 % of asthmatic patients [274]. The difference in the total emitted dose at different inhalation flows was statistically significant ($p < 0.001$) (Table 5.22).

Table 5. 22. *Statistical comparison for the emitted dose of 25% blend of SEDS samples recovered from Spinhaler® at inhalation flows of 60 L min^{-1} and 28.3 L min^{-1}*

Samples	Mean difference (95% confidence Interval) Emitted dose from Spinhaler® (mg)
SEDS1	0.34 (0.28, 0.40)***
SEDS 5	0.34 (0.28, 0.41) ***
SEDS 9	0.38 (0.30, 0.46)***

***$P < 0.001$

5.3.3.2. In-vitro aerodynamic particle size distribution of 25% blend of SEDS theophylline delivered from Spinhaler® at different inhalation flows

Tables 5.23, 5.24 and Figures 5.16, 5.17 show the particle size distribution 25% blend of SEDS theophylline from Spinhaler® at two different inhalation flows, after actuation of one puff into the ACI for each sample.

Table 5. 23. *Particle size distribution of 25% blend of SEDS theophylline recovered from Spinhaler® at 28.3 L min⁻¹*

Stages	Stage ECD (µm)	Amount in (mg) $\pm$ SD $\times$ 10^{-1} (n =3)		
		SEDS1	SEDS 5	SEDS 9
Throat		0.40 (0.61)	0.29 (0.15)	0.64 (0.21)
Preseparator		0.39 (0.21)	0.43 (0.22)	0.21 (0.25)
Stage 0	9	0.04 (0.03)	0.03 (0.02)	0.04 (0.03)
Stage 1	5.8	0.03 (0.62)	0.05 (0.11)	0.02 (0.01)
Stage 2	4.7	0.02 (0.24)	0.04 (0.01)	0.01 (0.33)
Stage 3	3.3	0.04 (0.71)	0.05 (0.02)	0.02 (0.01)
Stage 4	2.1	0.04 (0.22)	0.05 (0.03)	0.03 (0.24)
Stage 5	1.1	0.02 (0.22)	0.06 (0.11)	0.02 (0.03)
Stage 6	0.7	0.01 (0.01)	0.03 (0.01)	0.004 (0.15)
Stage 7	0.43	0.002 (0.02)	0.04 (0.01)	0.001 (0.45)
Filter	0	0.001 (0.11)	0.002 (0.12)	0.0002 (0.11)
TED (mg)		0.992 (0.21)	1.03 (0.21)	1.00 (0.24)
FPD (mg)		0.11 (0.42)	0.20 (0.42)	0.08 (0.01)
FPF (%)		11.43 (3.12)	19.69 (6.60)	5.36 (2.71)
MMAD (µm)		4.22 (0.41)	3.74 (0.93)	4.73 (0.27)
GSD		2.28 (0.41)	2.02 (0.42)	2.38 (0.45)
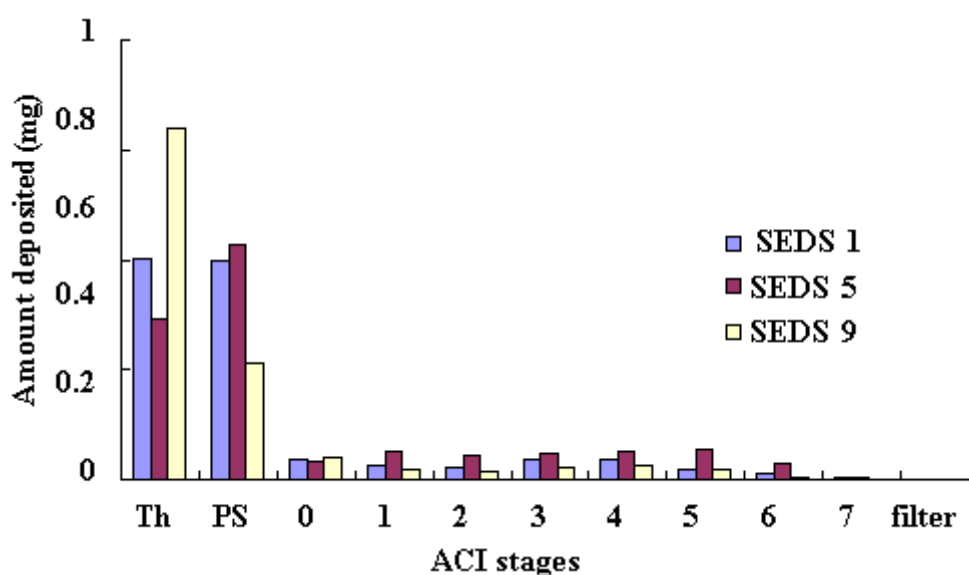
Figure 5. 16. *Mean amounts (mg) of 25% blend of SEDS theophylline deposited in ACI stages at 28.3 L min⁻¹ from the Spinhaler®(Processing parameters of samples 1, 5, 9 were described in Table 4.2.)*

Table 5. 24. *Particle size distribution of 25% blend of SEDS theophylline recovered from the Spinhaler® at 60 L min^{-1}*

Stages	Stage ECD (µm)	Amount in (mg) ± SD × 10^{-1} (n =3)		
		SEDS1	SEDS 5	SEDS 9
Throat		0.46 (0.22)	0.39 (0.22)	0.72 (0.14)
Preseparator		0.51 (0.13)	0.53 (0.53)	0.34 (0.32)
Stage -0	9	0.06 (0.20)	0.02 (0.02)	0.06 (0.15)
Stage -1	5.8	0.05 (0.03)	0.03 (0.11)	0.03 (0.15)
Stage 1	4.7	0.06 (0.71)	0.06 (0.21)	0.03 (0.01)
Stage 2	3.3	0.06 (0.55)	0.10 (0.13)	0.04 (0.23)
Stage 3	2.1	0.07 (0.34)	0.11 (0.14)	0.05 (0.11)
Stage 4	1.1	0.06 (0.11)	0.07 (0.25)	0.04 (0.12)
Stage 5	0.7	0.02 (0.16)	0.01 (0.02)	0.01 (0.23)
Stage 6	0.43	0.01 (0.03)	0.01 (0.03)	0.001 (0.01)
Filter	0	0.001 (0.31)	0.004 (0.24)	0.0001 (0.22)
TED (mg)		1.37 (0.11)	1.33 (0.43)	1.32 (0.11)
FPD (mg)		0.24 (0.12)	0.32 (0.14)	0.15 (0.11)
FPF (%)		17.68 (4.91)	23.67 (1.11)	11.45 (4.63)
MMAD (µm)		4.14 (0.33)	3.51 (0.62)	4.38 (0.83)
GSD		2.11 (0.55)	1.67 (0.81)	2.30 (0.1)1
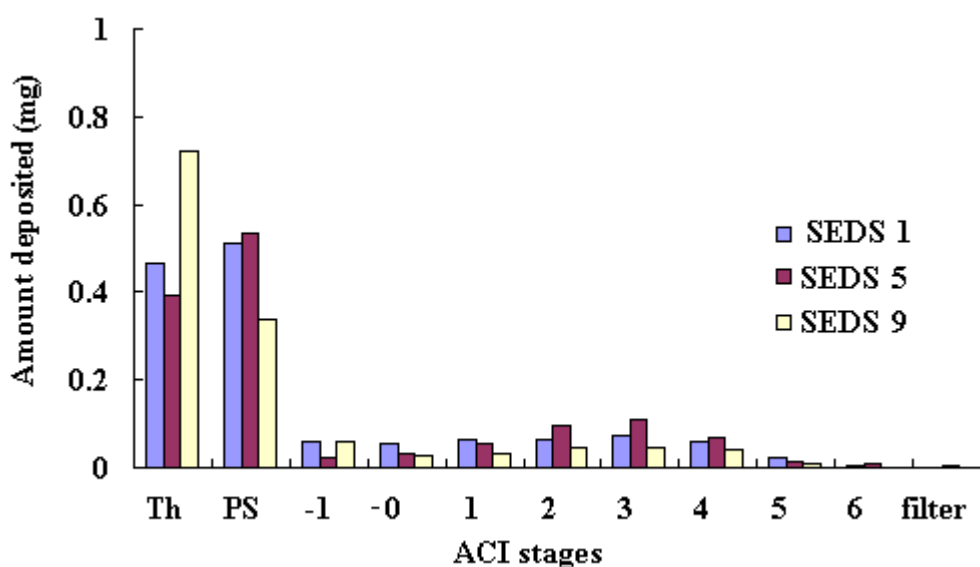
Figure 5. 17. *Mean amounts (mg) of 25% blend of SEDS theophylline deposited in ACI stages at 60 L min^{-1}from the Spinhaler®(Processing parameters of samples 1, 5, 9 were described in Table 4.2.)*

In agreement with Easyhaler®, the ACI results recovered from Spinhaler® showed that SEDS 5 produced the highest FPD and FPF at each flow rate compared with SEDS 1 and 9. SEDS 5 also exhibited the smallest and uniform particle size powder with MMAD and GSD of 3.62 μm and 1.85, respectively. Significant differences in FPD, FPF, MMAD, and GSD were found between pairs of samples when tested statistically (Table 5.25).

Table 5. 25. *Statistical comparison for the ACI results of 25% blend of different SEDS theophylline samples recovered from the Spinhaler® at the same inhalation flow.*

	Mean difference (95% confidence Interval)		
	SEDS 1 vs SEDS 5	SEDS 1 vs SEDS 9	SEDS 5 vs SEDS 9
At 28.3 L min^{-1}			
FPD (mg)	-0.09	0.04	0.13
	(-0.09, -0.08)***	(0.03, 0.05)***	(0.12, 0.14)***
FPF (%)	-8.26	3.76	12.02
	(-8.90, -7.62)***	(3.12, 4.40)***	(11.38, 12.60)***
MMAD (μm)	0.47	-0.51	-0.99
	(0.36, 0.59)***	(-0.63, -0.40)***	(-1.11, -0.87)***
GSD	0.26	-0.09	-0.36
	(0.19, 0.34)**	(-0.17, -0.02)*	(0.43, 0.28)***
At 60 L min^{-1}			
FPD (mg)	-0.73	0.09	0.16
	(-0.94, -0.53)**	(0.07, 0.11)***	(0.14, 0.19)***
FPF (%)	-5.99	6.23	12.22
	(-7.06, -4.92)***	(5.16, 7.30)***	(11.15, 13.29)***
MMAD (μm)	0.79	-0.24	-1.02
	(0.63, 0.94)***	(-0.40, -0.08)*	(-1.18, -0.87)***
GSD	0.44	-0.19	-0.63
	(0.33, 0.55)***	(-0.30, -0.09)**	(-0.74, -0.53)***

*P< 0.05   **P< 0.01   ***P < 0.001

It was also noticed that the FPF and FPD increased by increasing the flow rate from 28.3 to 60 L min^{-1} this might be attributed to the increase the break down of the particles into more fine ones. But the fraction of fine particles delivered to the lower respiratory tract may not increase to the same extent as the amount released from the inhaler [274]. At higher flows the oropharyngeal deposition increased (Figure 5.18) resulting in a decrease in the amount of particles deposited in the regions of the lung appropriate to the inhaled drug effects. It was also observed that there are differences in MMAD and GSD obtained when using the different inhalation flows. MMAD decreased by about 0.1-0.3 μm upon increasing the inhalation flow to 60 L min^{-1}. These results are consistent with data obtained by Nichols *et al* [275] who found that using different inhalation flows produced different particle size distribution due to the use of different particle size cut-off at different inhalation flows. On the other hand, a decrease in GSD was determined at higher inhalation flows indicating the increase in the particle size uniformity. The differences in all these aerodynamic parameters were statistically analysed and presented in Table 5.26.
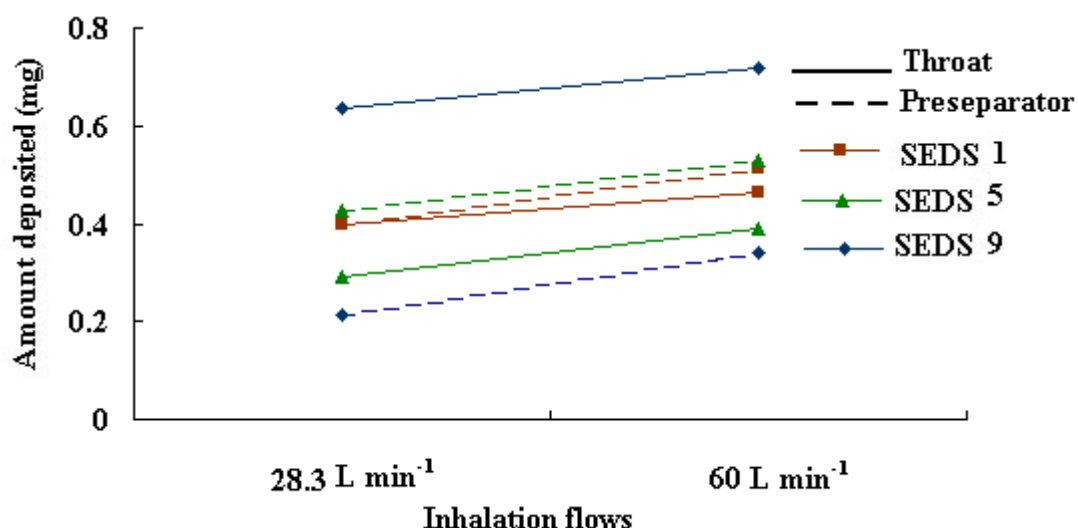
Figure 5. 18. *Mean amount (mg) deposited of SEDS theophylline in throat and preseparator from the Spinhaler$^{®}$ at different inhalation flows.*

Table 5. 26. *Statistical comparison for the ACI results of 25% blend of SEDS theophylline samples recovered from the Spinhaler® at inhalation flows of 60 L min⁻¹ and 28.3 L min⁻¹.*

	Mean difference (95% confidence Interval)		
	SEDS 1	SEDS 5	SEDS 9
FPD (mg)	0.13	0.11	0.08
	(0.11, 0.15)**	(0.09, 0.13)**	(0.06, 0.09)**
FPF (%)	6.25	3.98	3.76
	(4.35, 8.15)**	(2.68, 5.28)**	(2.59, 4.94)**
MMAD (μm)	-0.11	-0.39	-0.35
	(-0.20, -0.02)*	(-0.77, -0.01)*	(-0.59, -0.12)*
GSD	-0.22	-0.33	-0.08
	(-0.43, -0.01)*	(-0.54, -0.12)*	(-0.12, -0.04)*

*P< 0.05   **P< 0.01

It was also noticed that the single-dose capsule inhaler exhibited a higher total emitted dose compared with the Easyhaler® (1.01 mg, 0.14 mg, respectively) at 28.3 L min⁻¹ and (1.34 mg, 0.15 mg, respectively) at 60 L min⁻¹. However, Spinhaler® delivered a lower average FPF (percentage of the emitted dose) compared with Easyhaler® at different inhalation flows 12.14 %, 32.21 %, respectively. MMAD and GSD recovered from Spinhaler® were lower than those recovered by Easyhaler® for 25 % blend of theophylline. The differences in *in-vitro* deposition from different DPIs at the same inspiratory flows are primarily the result of different inhaler designs [273] as well as the drug formulation. As the same formulation (25 % blend) was used, the differences in the aerodynamic behaviour of theophylline recovered from Spinhaler® and Easyhaler® may be attributed to the design differences such as the internal resistance. Spinhaler® has much lower internal resistance than that of Easyhaler®; 0.05, 0.16 cm $H_2O^{0.5}$/L/min, respectively [274]. In addition to the powder flowability in a single unit containing 10 mg of the formulation might be higher than that of large amounts (40 mg) of the powder

placed in a reservoir. Table 5.27 illustrates the significant differences between FPD, FPF, MMAD and GSD recovered from Spinhaler® compared with Easyhaler®. The main disadvantage of the Spinhaler® is poor consistency of the emitted dose compared with Easyhaler®. Also it must be loaded before use, which is considered a difficulty especially for patients with an asthmatic attack or elderly patients.

Table 5. 27. *Statistical comparison for the ACI results of 25% blend of different SEDS theophylline samples recovered from Spinhaler® and Easyhaler® at the same inhalation flow*

Samples	Mean difference (95% confidence Interval)			
	FPD (mg)	**FPF (%)**	**MMAD (μm)**	**GSD**
SEDS 1				
At 60 L min^{-1}	0.19	-20.17	-0.09	-0.35
	(0.17, 0.20)***	(-21.38, -18.95)***	(-0.12,-0.05)**	(-0.67,-0.02)*
At 28.3 L min^{-1}	0.07	-23.29	-0.15	-0.29
	(0.06, 0.07)**	(-23.86,-22.73)***	(-0.18,-0.12)**	(-0.40,-0.18)**
SEDS 5				
At 60 L min^{-1}	0.25	-19.33	-0.34	-0.44
	(0.22, 0.28)**	(-20.15, -18.51)***	(-0.49,-0.20)**	(-0.66,-0.22)*
At 28.3 L min^{-1}	0.15	-22.18	-0.21	-0.23
	(0.13, 0.16)***	(-23.90, -20.47)***	(-0.27,-0.16)**	(-0.33,-0.14)**
SEDS 9				
At 60 L min^{-1}	0.12	-7.01	-0.45	-0.29
	(0.11, 0.14)**	(-8.44,-5.58)**	(0.30, 0.59)**	(-0.34,-0.24)**
At 28.3 L min^{-1}	0.05	-9.67	-0.13	-0.28
	(0.05, 0.06)***	(-10.60,-8.74)***	(0.02, 0.25)*	(-0.30,-0.26)***

    * $P< 0.05$ **$P< 0.01$ ***$P < 0.001$

As a general conclusion, this chapter demonstrated the *in-vitro* aerodynamic behaviour of SEDS theophylline as inhaled drug using multidose reservoir and single dose DPIs. The results show the effect of the particle size on the drug deposition profile within the airways, where samples with small particle size show the highest fine particle dose. The results also highlighted the enhancement of *in-vitro* performance of inhaled theophylline by using inhalation grade lactose as a carrier. From the data obtained it can be predicted that at higher flow rate, the fine particle fraction is high and so lung deposition is increased. The effect of different inhalation flows on the emitted dose and fine particle fraction delivered from Easyhaler[®] is lower than on those delivered from Spinhaler[®]. The theophylline deposition in throat and preseparator is decreased upon increasing the inhalation flows with Easyhaler [®], while reverse trend happened with Spinhaler[®].

Chapter 6
General Conclusion

This thesis is considered the first study on the suitability of using theophylline as inhalable dry powder formulation. The need for developing such a formulation originated from senior medics in hospitals who are still prescribing theophylline as a low cost therapeutic option for treatment of chronic asthma. However, the serious side effects associated with the available dosage forms hinder its use as first line for treatment of asthma.

The new inhalation products of theophylline allow much reduction in its therapeutic dose compare to the oral dosage forms (as shown in the dose emission study in Chapter 5) and therefore decrease the undesirable side effects associated with available dosage and enhance the patient's compliance. These new formulations show promising *in-vitro* aerodynamic behaviour, which considered as a starting point in the improvement of the commercial use of theophylline by asthmatic patients. The *in-vitro* efficiency of inhalable theophylline formulations was tested using the standard compendial methodology for testing at different inspiration flows to provide an appreciation to the results obtained during normal practice. As the particle size and shape have an important effect on the deposition profile of the inhaled drug, these formulations were prepared by SCF technology (Solution Enhanced Dispersions by Supercritical fluid (SEDS) which considered as one of the most efficient techniques for the production of discrete particles. SEDS technique by the aid of its coaxial nozzle allows more proficient control to the particle size and other physicochemical properties of produced particles comparing with other reported methods [12-14]. The output from all the *in-vitro* testing was analyzed by a developed fast and sensitive HPLC method using monolith C_{18} column that is considered as a new approach for reduction of the analysis time without loss of the resolution power. The analysis time is considered as an important concern in the *in-vitro* evaluation of the inhalation products due to the large numbers of samples have to be analyzed. Although there is a number of HPLC methods,

which report the simultaneous determination of methylxanthines and their metabolites in one run, these methods could not achieve both a reasonably short run time with a satisfied resolution as the HPLC method developed in this study.

The following points summarize the objectives and the main key findings of the thesis.

1- *To develop a fast HPLC method for separation and quantitation of theophylline and its related compounds in aqueous and urine samples.*

Key findings:

1.1. A novel, fast and efficient HPLC assay can be readily used in any laboratory for a quantitative determination of theophylline and its related compounds in urine samples in less than 15 min was developed and validated.

1.2. The developed method provides a mean for the assessing of theophylline concentration in urine samples for asthmatic patients consuming methylxanthines-containing food without confliction between metabolites peaks.

1.3. A simple solid phase extraction (SPE) technique using Baker octadecyl (C_{18}) disposable cartridge was optimised to isolate theophylline and its related compounds from urine followed by HPLC analysis. The urinary analysis was performed in accordance with ICH guidelines for validation of bioanalytical samples. The studied mixture was separated on monolithic column RP-18e (100×4.6 mm) at room temperature using UV detection at 274 nm. The optimised mobile phase consisted of methanol: 10 mM KH_2PO_4 (pH 4) (12.5: 87.5 % v/v). The mean extraction recoveries achieved for all the methylxanthines and their metabolites from the urine matrix ranged from 82.28 to 98.73 % w/w.

1.4. The recoveries of these compounds were found to be consistent, precise and reproducible as their RSDs were < 2.5 %.

1.5. The values of the correlation coefficients (R^2) of the calibration curves for the extracted compounds from the spiked urine were > 0.9991 (n = 6), which proves that the response of the detector showed a good linearity over the studied concentration range. LODs and LOQs were ranged from 0.004 - 0.014 μg ml^{-1}, and 0.014 - 0.041 μg ml^{-1}, respectively, indicating the good sensitivity of the developed analytical method.

1.6. The inter- and intra-day precision of the developed method show RSDs < 2.6 %, while the accuracy percentages of all compounds were ranged from 82.60 to 98.08 %w/w. On the other hand, good precision and reproducibility were observed upon working on different batches of monolith column.

1.7. The developed method was also validated to analyze theophylline in aqueous solution to evaluate the dose emission properties and the aerodynamic behaviour of its inhaled particles. The standard calibration curve for theophylline in aqueous samples was linear (y = 0.19x + 0.06, R^2 = 0.9993) over the studied concentration range 20-200 μg ml^{-1}. LOD and LOQ of theophylline were 0.08 and 0.23 μg ml^{-1}, respectively.

1.8. The developed HPLC procedure was applied for the analysis of the commercially available dosage forms of theophylline. Good extraction recovery of theophylline from the studied formulations was obtained (95.24-98.62 % w/w) with RSDs < 2 % confirms the absence of interference due to common excipients.

1.9. The performance the monolithic column was compared with traditional and newly introduced (Platinum^{TM}) C_{18} columns initially for separation of acidic and basic test mixtures and finally for the methylxanthines and methyluric acids mixture.

1.10. The obtained results show that the separation efficiency of the monolith for the methylxanthines and methyluric acid mixture was less than the symmetry,

Hypersil or platinum columns even after extensive trials in the optimization step. However, for all the tested columns at least 28 min (except platinum 16.72 min) was required for complete separation of the compounds of interest, while only 14.06 min was required with the monolithic column.

1.11. Furthermore, lower backpressure (60 bar) was obtained upon working with the monolith which was far less than the other particulate packed columns (150-180 bar).

1.12. As a general conclusion the monolithic column is a useful tool of achieving efficient separation under lower backpressure and shorter analysis time.

1.13. The monolith also provides rapid washing and equilibrium times while some of the tested packed columns take more time (about 30 min.). These advantages should aid in the reduction of the total time to develop a method using monolith compared with packed columns.

1.14. The high permeability and total porosity in the monolithic column allows the use of high flow rate without a significant increase in backpressure or substantial loss in the resolution power. This provides time saving analysis with minimal resolution loss.

1.15. Packed columns which are filled with 3-5 μm particles can be easily blocked, especially with biological samples thereby reducing the column lifetime. On the other hand, with monolithic columns, there is reduced need for tedious sample preparation, as they are very resistant to blocking (even with biological samples).

2- *To produce different batches of anhydrous theophylline particles using Solution Enhanced dispersion by Supercritical Fluids (SEDS) process under different crystallization parameters.*

Key finding

2.1. SEDS process has been successfully applied to crystallize anhydrous theophylline.

2.2. Fifteen theophylline samples were prepared under different crystallisation parameters. The SEDS process has enabled the production of small crystalline particles 2-5 μm (needles or flakes) compared to the unprocessed sample 30-100 μm (rod-like).

3- *To determine the effect of different practical parameters on the physicochemical properties of the produced SEDS theophylline samples mainly the particle size.*

<u>Key findings</u>

3.1. The particle size of SEDS theophylline is significantly influenced by different crystallisation parameters including; temperature, pressure and solution flow rate.

3.2. Increasing the temperature during the precipitation process led to a decrease in the particle size of the processed samples. An increase in the particle size was observed upon increasing the pressure as well as the solution flow rate.

3.3. The process has also demonstrated good reproducibility for the produced particle size on repeated crystallisation.

4- *To study the solid-state chemistry of the prepared SEDS theophylline samples using different analytical techniques.*

<u>Key finding</u>

4.1. Different analytical tools were used in this study for the determination of the solid-state chemistry the SEDS theophylline samples and for assessing any changes at different crystallisation parameters; including scanning electron microscope, Differential scanning calorimetry (DSC), thermal gravimetric analysis (TGA), x-ray powder diffraction (XRPD), Fourier Transform Infra-Red (FT-IR), and Fourier Transform Raman spectroscopy (FT-Raman).

4.2. The TGA results show that the transition temperature for the unprocessed theophylline was 281.03°C, higher than that of all the processed samples. This may be attributed to that the SEDS samples exhibiting smaller size thus lower temperatures are required for mass loss by melting or decomposition.

4.3. Results obtained from the DSC analyses confirm that the processed samples have high degrees of crystallinity under all the studied processing parameters.

4.4. Minor variations were observed between the XRPD patterns of the processed and unprocessed samples.

4.5. The IR spectra for the processed samples illustrate all the characteristic peaks of the unprocessed theophylline indicating that there is no modification in the bonding interaction between molecules and hence the structure of theophylline during the SEDS process over all the processing conditions. This finding was confirmed by the results obtained from FT-Raman analyses.

4.6. Therefore, it could be concluded that, the structure and the crystallinity of SEDS theophylline products compared with unprocessed samples were not affected by the crystallisation process under different practical parameters.

4.7. This study also demonstrates the potential of preparation of theophylline monohydrate using SEDS technique by the addition of appropriate amounts of water (0.5 ml) to the starting drug solution and this was traced by XRPD, TGA and DSC techniques.

5- *To evaluate the in-vitro efficiency of the different particle-sized batches of SEDS samples as inhaled dry powder formulation using Easyhaler® and Spinhaler® by dose sampling unit and Andersen Cascade Impactor.*

Key finding

5.1. The *in-vitro* efficiency of the SEDS theophylline samples as inhaled dry powder

formulation was investigated using two inhalation flows of 28.3, and 60 L min^{-1}.

5.2. The dose sampling unit and the Andresen Cascade Impactor (ACI) were used for the determination of the *in-vitro* emitted dose and the deposition profiles, respectively of SEDS formulations.

5.3. The total emitted dose for the three tested samples within the same formulation and the same inhalation flow were quite similar. However it varied significantly (p< 0.001) in different formulations and different flows; 182.86, 151.67, 138.52 µg at 28.3 L min^{-1} and 211.93, 182.00, 151.50, at 60 L min^{-1} for the pure formulation, 50 %, and 25 % blends, respectively.

5.4. The dose emission results indicate good reproducibility of the delivered theophylline doses, as the RSDs for all samples were lower than 5 %.

5.5. The doses emitted at 28.3 L min^{-1} were found to be approximately 85 % of that provided at 60 L min^{-1} for all the tested formulations. Therefore, reasonably good theophylline dose can be achieved with patients who may have difficulties in generating high levels of inhalation flow such as children and the elderly.

5.6. The ACI results recovered from Easyhaler® prove the importance of the particle size on the aerodynamic behaviour and deposition profile of inhaled theophylline particles. The sample with the smallest particle size (SEDS 5) provides better respirable fraction and lower mass median aerodynamic diameter (MMAD) than samples with lager particle size (SEDS 9).

5.7. The fine particle dose (FPD), fine particle fraction (FPF) and the mass median aerodynamic diameter (MMAD) were found to be affected by the change in the inhalation flows.

5.8. The results also highlight the enhancement of *in-vitro* performance of inhaled theophylline by using inhalation grade lactose as a carrier. The results indicted that statistically (p<0.001) the theophylline blends produce better respirable

fractions (about 3 times higher) than pure formulations.

5.9. The 25 % blend (25 % theophylline and 75 % inhalable lactose) showed not only the highest FPD (24.12-65.20 μg), and FPF (17.34-42.99 %) but also the smallest MMAD (3.61-4.86 μm) compared with 50 % blend or pure formulation.

5.10. The performance of the 25 % blend was also tested using the Spinhaler® as another type of dry powder inhalers (single dose device).

5.11. The total emitted dose recovered from the Spinhaler® for the three samples were quite similar 1.01, 1.34 mg at 28.3 and 60 L min^{-1} and it seemed to be flow dependant.

5.12. In agreement with the results recovered from the Easyhaler®, SEDS 5 (with the smallest particle size) produced the highest FPD and FPF at each flow rate compared with other tested samples. SEDS 5 also exhibited the smallest and the most uniform particle size powder with MMAD and GSD of 3.62 μm and 1.85, respectively.

5.13. The total emitted dose and the respirable fraction recovered from the Spinhaler® is more affected by changes in the inhalation flows than the Easyhaler®.

5.14. It was also noticed that the Spinhaler® exhibited a higher total emitted dose compared with the Easyhaler® (1.01 mg, 0.14 mg, respectively) at 28.3 L min^{-1} and (1.34 mg, 0.15 mg, respectively) at 60 L min^{-1}. However it delivered a lower average FPF; 12.14 %, 32.21 %, respectively (percentage of the emitted dose), compared with the Easyhaler® at the same inhalation flows. Furthermore, the Spinhaler provides lower MMAD and GSD than those recovered by the Easyhaler®.

5.15. The theophylline deposition in throat and preseparator is decreased upon increasing the inhalation flows with the Easyhaler®, while reverse trend happened with the Spinhaler®.

5.16. These differences in the *in-vitro* deposition of the 25 % blend in different DPIs at the same inspiratory flows using the same formulation are primarily the result of different inhaler designs.

5.17. Generally, this study gave an overview for the *in-vitro* behaviour of theophylline prepared by SEDS process as a newly developed inhaled dry powder formulation by the aid of different pharmaceutical analytical tools.

6.1. Future work

This study has shown the *in-vitro* dose emission and lung deposition of SEDS theophylline at different inhalation flows using two types of dry powder inhaler; multidose reservoir and single dose devices. The obtained results show good aerodynamic performance of the new inhaled formulations. Therefore it will be useful to extend this work to determine the *in-vivo* performance of inhaled SEDS theophylline using the urinary excretion to determine the relative amounts of the drug delivered to the lungs following an inhalation. The collected urine samples could be analyzed using the developed fast HPLC method for separation and quantitation of theophylline and its related compounds. The *in-vitro* studies were performed on small scale however the *in-vivo* studies needs the preparation of larger amounts of theophylline under GMP conditions to assure the reproducibility.

Chapter 7

References

[1] P. J. Barnes and S. Godfrey; A*sthma*; London; Dunitz Ltd; 1995.

[2] British Thoracic Society/Scottish Intercollegiate Guidelines Net work; British Guidelines on the Management of Asthma; *Thorax*; 2008; **63** (suppl. 4); iv33- iv45.

[3] B. J. Lipworth; *Br. Med. J.*; 1999; **318**; 380-384.

[4] A. Murphy; *Asthma in Focus*; London, Pharmaceutical Press; 2007.

[5] K. Fan Chung and I. Adcock; *Asthma: Mechanisms and Protocols;* USA, Humana Press; 2000.

[6] O. Cole; Introduction to asthma; *Hospital Pharmacist*; 2001; **8**; 238-240.

[7] A. J. Hickey; *Pharmaceutical inhalation aerosol technology*; In: *Drugs and the pharmaceutical science*; **vol. 54**; Eds. J. Swarbrick; New York; Marcel Dekker Inc.; 1992.

[8] G. Charbit, E. Badens, and O. Boutin; *Methods of particle production*; In: *Supercritical fluid technology for drug product development,* **vol. 138**; Eds. P. York, U. B. Kompella, and B.Y. Shekunov; New York; Marcel Dekker, Inc.; 2004; 152-200.

[9] P. York; *Pharm. Sci, Technol. Today*; 1999; **2**; 430-440

[10] M. H. Hanna and P. York; *patent WO 95/01221*; 1994.

[11] M. H. Hanna and P. York, *patent WO 95/00 610*; 1996.

[12] P. Subra, C. Laudani, A. Vega-Gonzalez, and E. Reverchon; *J. Supercrit. Fluids;* 2005; **35**; 95-105.

[13] E. Franceschi, M. Kunita, M. V. Tres, A. F. Rubira, E. C. Muniz, M. L. Corazza, C. Dariva, S. R. Ferreira, and V. Oliveira; *J. Supercrit. Fluids;* 2008; **44**; 8-20.

[14] C. Roy, A. Vega-Gonzalez, and P. Subra-Paternault; *Int. J. Pharm.;* 2007; **343**; 79-89.

[15] K. Cabrera; *J. Sep. Sci.* ; **27**, 2004; 843- 852.

[16] S. El Deeb, L. Preu, and H. Watzig; *J. Sep. Sci.;* 2007; **30**; 1993- 2001.

[17] J. Moxham and J. F. Costello; *Respiratory diseases*; In: *Textbook of medicine*s, **vol. 13**; Ed. R. L. Souhami and J. Moxham; Edinburgh; Churchill Livingstone; 1994; 605-722.

[18] R. J. Davie; *Respiratory disease*; In *Clinical medicine*, Eds. P. Kumar and M. Clark; London; W.B. Saunders Co.; 1998; 774-780.

[19] M. Zydron, J. Baranowski, and I. Baranowska; *J. Sep. Sci.;* 2004; **27**; 116-1172.

[20] C. G. Persson; *Thorax*; 1985; **40**; 1183-1187.

[21] P. J. Barnes, I. W. Rodger, and N. C. Thomson; A*sthma: Basic Mechanisms and Clinical Management,* California; Academic Press, 1998.

[22] D. I. Macht and G. Ting *J. Pharmacol. Exper. Ther.;* 1921; **18**; 373-398.

[23] J. C. Kips, J. Tavernier, and R. A. Pauwels; *Am. Rev. Respir. Dis.;* 1992; **145**; 332-336.

[24] P. H. Howarth, K. S. Babu, H. S. Arshad, L. Lau, M. Buckley, W. McConnell, P. Beckett, M. Al Ali, A. Chauhan, S. J. Wilson, A. Reynolds, D. E Davies, and S. T Holgate; *Thorax*; 2005; **60**; 1012-1018.

[25] H. Ulbrich, E. E. Eriksson, and L. Lindbom; *Pharmacol. Sci.*; 2003; **24**; 640-647.

[26] M. Weinberger; *J. Allergy Clin. Immunol.*; 1984; **73**; 525-540.

[27] C. G. Persson; *J. Allergy Clin. Immunol.*; 1986; **78**; 817-824.

[28] K. F. Rabe, H. Magnussen, and G. Dent; *Eur. Respir. J.*; 1999; **8**; 637-642.

[29] R. A. Pauwel and G. F. Joos; *Arch. Int. Pharmacodyn. Ther.*; 1995; **329**; 151-156.

[30] M. J. Cushley, A. E. Tattersfield, and S. T. Holgate; *Am. Rev. Respir. Dis.*; 1984; **129**; 380-384.

[31] M. D. Higbee, M. Kumar, and S. P. Galant; *J. Allergy Clin. Immunol.*; 1982; **70**; 377-382.

[32] J. J. Mascali, P. Cvietusa, J. Negri, and L. Borish; *Ann. Allergy Asthma Immunol.*; 1996; **77**; 34-38.

[33] M. Souhrada and J. F. Souhrada; *Respir. Physiol.*; 1985; **60**; 157-168.

[34] M. Weinberger and L. Hendeles; *N. Engl. J. Med.*; 1996; **334**; 1380-1388.

[35] K.Y. Tserng, K.C. King, and F.N. Takieddine; *Clin. Pharmacol. Ther.* ; 1981; **29**; 594-600.

[36] M. Richer and Y. Lam; *Clin. Pharmacokin.*; 1993; **25**; 283-299.

[37] K.A. George, V. F. Samanidou, and I. N. Papadoyannis; *J. Chromatogr. B*; 2001; **759**; 20-2018.

[38] G. F. Johnson, W. A. Dechtiaruk, and H. M. Solomon; *Clin. Chem.*; 1975; **21**; 144-147.

[39] L. M. Tsanaclis and J. F. Wilson; *Ther. Drug Monit.* ; 1997; **19**; 420-426.

[40] K. A. Regal, W. N. Howald, R. M. Peter, C. A. Gartner, K. L. Kunze, and S. D. Nelson; *J. Chromatogr. B*; 2001; **758**; 235–248.

[41] M. Sheehan and P. Haythorn; *J. Chromatogr.* ; 1976; **117**; 392-398.

[42] M. Elefant, L. Chafetz, and J. M. Talmage; *J. Pharm. Sci.*; 1967; **56**; $1181 - 1183$.

[43] A. Takeda, H. Tanaka, T. Shinohara, and I. Ohtake; *J. Chromatogr B*; 2001; **758**; 235–248.

[44] B. Vinet and L. Zizian; *Clin. Chem.*; 1979; **25**; 156-158

[45] V. P. Devarajan, P. N. Sule, and D. V. Parmar; *J. Chromatogr B*; 1999; **736**; 289-293.

[46] A. Mirfazaelian, M. Goudarzi, M. Tabatabaiefar, and M. Mahmoudian; *J. Pharm. Pharm. Sci*; 2002; **5**;131-134.

[47] M. Fenske; *Chromatographia*; 2007; **65**; 233-238.

[48] W. Thormann, A. Minger, S. Molteni, J. Caslavska, and P. Gebauer; *J. Chromatogr. A.*; 1992; **593**; 275-288.

[49] I. M. Johansson, M. B. Gron-Rydberg, and B. Schmekel; *J. Chromatogr. A*; 1993; **652**; 487-493.

[50] N. Rodopoulos and A. Norman; Scand. *J. Clin. Lab. Invest.*; 1994; **54**; 305 – 315.

[51] Z. Y. Zhang, M. J. Fasco, and L. S. Kaminsky; *J. Chromatogr. B*; 1995; **665**; 201-208.

[52] W. S. Huang, S. J. Lin, H. L. Wu, and S. H. Chen; *J. Chromatogr. B*; 2003; **795**; 329-335.

[53] C. H. Feng, H. L. Wu, S. J. Lin, and S. H. Chen; *J. Liq. Chromatogr. Relat. Tech.*; 2003; **26**; 1913-1925.

[54] U. L. Peri-Okonny, S. X. Wang, R. J. Stubbs, and N. A. Guzman; *Electrophoresis*; 2005; **26**; 2652–2663.

[55] A. F. Fell, G. W. Haddow, and J. M. Neil; *J. Pharm. Pharmacol. (suppl. Brit Pharm. Conf.)* 1978; **3030**; 65.

[56] K. T. Muir, M. Kunitani, and S. Riegelman; *J. Chromatogr. A*; 1982; **231**; 73- 82.

[57] A. Wahllander, E. Renner, and G. Karlagains; *J. Chromatogr. A*; 1985; **338**; 369-375.

[58] J. Chakraborty and V. Marks; *J. Chromatogr. A*; 1986; **375**; 321-329.

[59] R. Chiou, R. J. Stubbs, and W. F. Bayne; *J. Chromatogr.* ; 1987; **422**; 281-287.

[60] S. A. Hotchkiss and J. Caldwell; *J. Chromatogr.*; 1987; **423**; 179-188.

[61] L. Richard, B. Leducq, C. Baty, and J. Jambou; *Annales de biologie clinique*; 1989; **47**; 79-84.

[62] M. E. B. Leakey; *J. Chromatogr.*; 1990; **507**; 199-220.

[63] J. Blanchard, C. W. Weberm, and L. Shearer; *J. Chromatogr. Sci.*; 1990; 28; 640-642.

[64] J. Moncrieff; *J. Chromatogr.*; 1991; **568**; 177-185.

[65] P. Parra and A. Limon; *J. Chromatogr.*; 1991; **570**; 185-190.

[66] E. Tanaka; *J. Chromatogr.*; 1992; **575**; 311-314.

[67]   O. H. Drummer, A. Kotsos, and I. M. Mclntyre; *J. Anal. Toxicol.*; 1993; **17**; 225-229.

[68] A. H. Chalmers; *Clin. Chem.* ; 1993; **39**; 1348-1349.

[69] H. Tajerzadeh and S. Dadashzadeh; *J. Pharm. Biomed. Anal.* ; 1995; **13**; 507-1512.

[70] M. R. Souping Zhai, X. W. Korrapati, S. Muppalla, and R. E. Vestal; *J. Chromatogr. B*; 1995; **669**; 372-376.

[71] B. B. Rasmussen and K. Brosen; *J. Chromatogr. B*; 1996; **676**; 169-174.

[72] E. S. Deturmeny and B. Bruguerolle; *J. Chromatogr. B*; 1996; **677**; 305-312.

[73] C. Krul and G. Hageman; *J. Chromatogr. B*; 1998; **709**; 27-34.

[74] L. Dinna, J. Ambrose, and S. Fritz; *J. Chromatogr B*; 1998; **709**; 89-96.

[75] O. Umemura, R. Kitaguchi, K. Inagaki, and H. Haraguchi; *Analyst*; 1998; **123**; 1767-1770.

[76] E. Schrader, G. Klaunick, U. Jorritsma, H. Neurath, K. I. Hirsch-Ernsta, G. F. Kahla, and H. Fothb; *J. Chromatogr. B*; 1999; **726**; 195-201.

[77] J. Contreras, E. Ontivero, R. Gonzalez, M. Lopenz, and D. Marrero; *J. High Res. Chromatogr.*; 1999; **22**; 131-132.

[78] J. Kizu, S. Watanabe, N. Yasuno, Y. Arakawa, S. Uzu, S. Kanda, T. I. F. Komoda, H. Hayakawa, T. Hayakawa, and K. Imai; *Biomed. Chromatogr.*; 1999; **13**; 15-23.

[79] K. A. George, V. F. Samanidou, and I. N. Papadoyannis; *J. Chromatogr. B*; 2001; **759**; 209-218.

[80] M. Caubet, W. Elbast, M. Dubuc, and J. Brazier;; *J. Pharm. Biomed. Anal.*; 2002; **27**; 261-270.

[81] H. Schneider, L. Ma, and H. Glatt; *J. Chromatogr. B*; 2003; **789**; 227-237.

[82] Y. Chen, H. Junga, X. Jiang, and W. Naidong; *J. Sep. Sci.*; 2003; **26**; 1509-1519.

[83] C. G. Zambonin, A. Aresta, and F. Palmisano; *J. Pharm. Biomed. Anal.*; 2004; **34**; 621-624.

[84] S. E. Emara; *Biomed. Chromatogr.*; 2004; **18**; 479-485.

[85] J. Song, K. Un Park, H. D. Park, Y. Yoon, and J. Q. Kim; *Clin. Chem.*; 2004; **50**; 2176-2179.

[86] E. Marchi, M. pellegrini, R. Pacific, I. Palmi, and S. Pichini; *J. Pharm. Biomed. Anal.*; 2005; **37**; 499-507.

[87] A. Weimann, M. Sbroe, and H. E. Poulsen; *J. Mass Spec.* ; 2005; **40**; 307-316.

[88] A. Martinavarro-Dominguez, D. Boseb, A. Durgbanshib, M. Gil-Agustic, M. Capella-Peiroc, S. Carda Brochc, and J. Esteve-Romeroc; *J. Chromatogr. A*; 2005; **1073**; 309-315.

[89] H. Sun, F. Qiao, and G. Liu; *J. Chromatogr. A*; 2006; **1134**; 194-200.

[90] R. V. S. Nirogi, V. N. Handikere, M. Shukla, K. Mudigonda, and D. R. Ajjala; *J. Chromatogr. B*; 2007; **848**; 271-276.

[91] M. R. Brunettoa, L. Gutierreza, Y. Delgadoa, M. Gallignania, A. Zambranob, A. Gomezb, G. Ramosb, and C. Romerob; *Food Chem.*; 2007; **100**; 459-467.

[92] S. Zuhre, E. Nevin, O. Sibe, and C.S. A. Cemal; *J. Pharm. Biomed. Anal.* ; 2002; **29**; 291-298.

[93] N. Erk; *J. Pharm. Biomed. Anal.* ; 2000; **23**; 255-261.

[94] D. K. Singh and S. Archana; *Anal. Biochem.*; 2006; **2**; 176-180.

[95] S. R. El-Shabouri, S. A. Hussein, and S. E. Emara; *Talanta*; 1989; **36**; 1288-1290.

[96] A. Ozlem, B. Abdurrezzak, and K. Gonul; *Int. J. Chem.*; 2003; **13**; 45-48.

[97] M. A. Abuirjeie, M. S. El-Din, and I. I. Mahmoud; *J. Liq. Chromatogr.*; 1992; **15**; 101- 125.

[98] Z. Shihong and L. Tong; *Guangdong Yixue*; 1998; **19**; 39-740.

[99] S. D. Xuebao; *Ziran Kexueban*; 1996; **19**; 51-55.

[100] M. A. Elsayed , H. Abdine, and Y. M. Elsayed; *J. Pharm. Sci.*; 1979; **68**; 9-11.

[101] Y. S. Chae and W. H. Shelver; *J. Pharm Sci.*; 1976; **65**; 1178-1181.

[102] P. Jatlow ; *Clin. Chem.*; 1975; **21**; 1518- 1520.

[103] N. Abo El-Maali; *Bioelectrochemistry*, 2004; **64**; 99-107.

[104] C. J. McNeil, J. M. Cooper, and J. A. Spoors; *Biosens. Bioelectron.*; 1992; **7**; 375-380.

[105] C. L. Eugene and C. J. Dennis; *Clin. Chem.*; 1978; **24**; 1711-1719.

[106] M. El Sayed and S. I. Islam; *J. Clin. Pharm. Ther.*; 1989; **14**; 127-134.

[107] L. M. Tsanaclis and J.F. Wilson; *Ther. Drug. Monit.*; 1997; **19**; 420-426.

[108] H. Yuan, W.M. Mullet, and J. Pawliszyn; *Analyst*; 2001; **126**; 1456-1461.

[109] L. Locascio-Brown, A. L. Plant, V. Horvath, and R. A. Durst; *Anal. Chem.*; 1990; **62**; 2587-2593.

[110] R. M. Garcinuno, P. Fernandez, C. Perez-Conde, A. M. Gutierre, and C. Camara; *Talanta*; 2000; **52**; 825-832.

[111] N. J. Pritchard; *J. Aerosol Med.*; 2001; **14**; S19- S26.

[112] G. Rudolf, J. Gebhart, J. Heyder, C. F. Schiller, and W. Stahlhofen; *J. Aerosol Sci.*; 1986; **17**; 350-355.

[113] O. S. Usami, M. F. Biddiscombe, and P.J. Barnes; *Respir. Crit. Care Med.*; 2005; **172**; 1497-1504.

[114] S. Yeo, G. Lim, P. G. Debenedetti, and H. Bernstein; *Biotechnol Bioeng.*; 1993; **41**; 343- 346.

[115] M. A. McHugh and V. J. Krukonis; *Supercritical Fluid Extraction: Principles and Practice*; Michigan; Butterworth-Heinemann, 1994.

[116] J. B. Hanny and J. Hogarth; *Proc. R. Soc. London;* 1879; **29**; 324-326.

[117] P. Subra and P. Jestin; *Ind. Eng. Chem. Res.*; 2000; **39**; 4178-4184.

[118] E. Reverchon and G. Della Porta; *Pure Appl. Chem.*; 2001; **73**; 1293–1297.

[119] H. Krober and U. Teipel; *J. Supercrit. Fluids*; 2002; **22**; 229-235.

[120] E. Reverchon; *J. Supercrit. Fluids*; 1999; **15**; 1-12.

[121] J. Fages, H. Lochard, J. Letourneau, M. Sauceau, and E. Rodier; *Powder Technol.*; 2004; **141**; 219– 226.

[122] J. Jung and M. Perrut; *J. Supercrit. Fluids*; 2001; **20**; 179–219.

[123] P. M. Gallagher, M. P. Coffey, V. J. Krukonis, and N. Klasutis; *SCF science and Technology, ACS Symposium;* **406**; Eds. J. M. L Penniger; Washington, DC; American Chemical Society; 1989.

[124] M. H. Hanna and P. York, 1998, European patent WO 98/36825

[125] P. M. Gallagher, V. J. Krukonis, and M. P. Coffey, 1992, USA patent 5389263

[126] P. Chattopadhyay and R. B. Gupta; *Int. J. Pharm.*; 2001; **228**; 19-31.

[127] S. Palakodaty and P. York; *Pharm. Res.*; 1999; **16**; 976-985.

[128] S. R. Byrn; *Solid-State Chemistry of Drugs*; London; Academic press; 1982; 3-58.

[129] B. Stuart, *Modern Infrared Spectroscopy*; Eds D. J. Ando; New York; John Wiely & Sons Ltd; 1998.

[130] C. N. Banwell and E. M. McCash; *Fundamentals Of Molecular Spectroscopy*; New York; McGraw-Hill;1994; 100-126.

[131] Y. Kazakevich and R. Lobrutto; HPLC For Pharmaceutical Science; USA; John Wiley and Sons Inc; 2007.

[132] J. E. O'Gara, D. P. Walsh, C. H. Phoebe, B. A. Alden, I. S. P. Bouvier, P. C. Iraneta, M. Capparella, and T. H. Walter; *LC-GC North America*; 2001; **19**; 632-642.

[133] S. Ahuja and M. Dong; *Handbook of Pharmaceutical Analysis by HPLC: Separation Science and Technology*; USA; Elsevier Academic Press; 2005.

[134] L. Kaminski, S. El Deeb, and H. Watzig; *J. Sep. Sci.*; 2008; **31**; 1745- 1749.

[135] M. Al -Bokari, D. Cherrak, and G. Guiochon; *J. Chromatogr. A*; 2002; **975**; 275- 284.

[136]   H. Kobayashi, W. Kajiwara, Y. Inui, K.H. T. Hara, T. Ikegami, and N. Tanaka; *Chromatographia*; 2004; **60**; S19- S23.

[137]   H. Y. Aboul-Enien and M. M. Hefnawy; *J. Liq. Chromatogr. Rel. Technol.*; 2003; **26**; 2897- 2903.

[138]   J. H. Smith and H. M. McNair; *J. Chromatogr. Sci.*; 2003; **41**; 209- 214.

[139]   M. Kubin, P. Spacek, and R. Chromecek; *Collection Czech. Chem. Commun.*; 1967; **32**; 3881- 3887.

[140]   W. D. Ross and R. T. Jefferso; *J. Chromatogr. Sci.*; 1970; **8**; 386- 389.

[141]   S. Hjerten, J. L. Liao, and R. Zhang; *J. Chromatogr.*; 1989; **473**; 273- 275.

[142]   F. Svec and J. M. J. Frechet; *Anal. Chem.*; 1992; **64**; 820- 822.

[143]   K. Cabrera, G. Wieland, D. Lubda, K. Nakanishi, and N. Soga; *Trac-Trends In Anal. Chem.*; 1998; **17**; 50- 53.

[144]   N. Ishizuka, H. Minakuchi, K. Nakanishi, N. Soga, and N. Tanaka; *J. Chromatogr. A;* 1998; 797; 133-137.

[145]   H. Minakuchi, K. Nakanishi, V. Soga, N. Ishizuka, and N. Tanaka; *J. Chromatogr. A*; 1997; **762**; 135- 146.

[146]   K. Nakanishi, H. Minakuchi, N. Soga, and N. Tanaka; *J. Sol-Gel Sci. Technol.*; 1998; **13**; 163- 179.

[147]   Y. Wang, M. Harrison, and B. J. Clark; *J. Chromatogr. A*; 2006; **1105**, 199- 207.

[148]   T. P. Hen, R. I. Boysen, M. I. Huber, K. K. Unger, and M. T. W. Hearn; *J. Chromatogr. A*; 2003; **1009**; 15- 28.

[149]   A. R. Ivanov, C. Horvath, and B. L. Karger; *Electrophoresis*; 2003; **24**; 3663- 3673.

[150]   C. Legido-Quigley, N. D. Marlin, V. Melin, A. Manz, and N. W. Smith; *Electrophoresis*; 2003; **24**; 917- 944.

[151] N. Tanaka, H. Kobayashi, K. Nakanishi, H. Minakuchi, and N. Ishizuka; *Anal. Chem.* ; 2001; **73**; 420A-429A.

[152] M. Bedair and Z. El Rassi; *Electrophoresis*; 2004; **25**; 4110- 4119.

[153] A. Jungbauer and R. Hahn; *J. Sep. Sci.* ; 2004; **27**; 767- 778.

[154] F. Svec; *J. Sep. Sci.*; 2004; **27**; 1419-1430.

[155] A. Vegvari; *J. Chromatogr. A*; 2005; **1079**; 50- 58.

[156] F. Svec; *J. Chromatogr. B*; 2006; **841**; 52-64

[157] B. Bidlingmaier, K. K. Unger, and N. Von Doehren; *J. Chromatogr. A*; 1999; **832**; 11- 16.

[158] A. M. van Nederkassel, A. Aerts, A. Dierick, D. L. Massart, and Y. Vander Heyden; *J. Pharm. Biomed. Anal.*; 2003; **32**; 233- 249.

[159] N. J. Wu, J. Dempsey, P. M. Yehl, A. Dovletoglou, D. Ellison, and J. Wyvratt; *Anal. Chem. Acta*; 2004; **523**; 149- 157.

[160] I. Sperlingova, L. Dabrowska, V. Stransky, and M. Tichy; *Anal. Bioanal. Chem.*; 2004; **378**; 536- 543.

[161] N. R. Herbert, I. Chappell, J. Wang, S. Anderson, M. Jacyno, and W. Luo; *Grace Davison Discovery Sciences*, www.discoverysciences.com.

[162] L. R. Snyder, J. W. Dolan, and P.W. Carr; *Anal. Chem.*; 2007; **79**; 3252-3262.

[163] M. T. Vidgren, K. P. Karkkainen, T. P. Parrorien, and J. Nuutinen; *Int. J. Pharm.*; 1988; **42**; 211- 216.

[164] A. J. Hickey; *Inhalation aerosols*; physical and biological basis for therapy; New York; Marcel Dekker Inc., 1996; 85-151.

[165] E. R. Weibel; *Morphometry of the human lung*; Berlin; Springer Verlag; 1963.

[166] M. F. Biddiscmbe, O. S. Usmani, and P. J. Barnes; *Int. J. Pharm.*; 2003; **254**; 243- 253.

[167] J. D. Brian and P. A. Valberg; *Am. Rev. of Respir. Dis.*; 1979; **120**; 1325- 1373.

[168] S. P. Newman, G. R. Pitcairn, P. H. Hirst, and L. Rankin; *Adv. Drug Deliv. Rev.*; 2003; **55**; 851-867.

[169] S. P. Newman and S. W. Clarke; *Thorax*; 1983; **38**; 881- 886.

[170] J. D. Brain and J. D. Blanchard; *Mechanisms of particle deposition and clearance. In: Aerosols in medicine: principles, diagnosis, and therapy*; Eds. F. Moren, M. B. Dolovich, M. T. Newhouse, and S. P. Newman; Amsterdam; Elsevier, 1993; 24–135.

[171] T. R. Gerrity, P. S. Lee, F. J. Hass, A. Marinelli, P. Werner, and R.V. Lourenco; *J. Appl. Physiol. Respir.;* 1979; **47**; 867- 873.

[172] K. R. May; *J. Aerosol Sci.*; 1982; **13**; 37- 47.

[173] *European Pharmacopoeia* 6th Edition; **vol. 1**;Council of Europe; Strasbourg; European Pharmacopoeia Convention; 2007, 287- 300.

[174] *The United States pharmacopoeia* (USP 32-NF 27), **vol. 1**, Rockville, MD, US Pharmacopoeial Convection, 2009; 204- 224.

[175] P. C. Reist; *Introduction to Aerosol Science*; New York; Macmillan; 1984.

[176] V. A. Marple, B. A. Olson, and N. C. Miller; *J. Aerosol Med.*; 1998; **11** (suppl. 1); S139- S153.

[177] J. P. Mitchell and M. W. Nagel; *J. Aerosol Med.*; 2003; **16**; 341- 376.

[178] Copley Scientific; Quality Solutions for Inhaler Testing; 2007.

[179] M. Van Oort, B. Downey, and W. Robert; *Pharm. Forum*; 1996; **22**; 2211- 2215.

[180] M. J. Le Belle, S. J. Graham, E. D. Ormsby, R. M. Duhaime, R. C. Lawrance, and P. K. Ake; *Int. J. Pharm.*; 1997; **151**; 209- 221.

[181] M. Weda, P. Zanan, A. H. De Boer, D. Gjaltema, A. Ajaoud, D. M. Barends, and H. W. Frijlink; *Int. J. Pharm.*; 2002; **249**; 247- 255.

[182] S. W. Stein and B. A. Olson; *Pharm. Res.*; 1997; **14**; 1718- 1725.

[183] K. R. May; *J. Aerosol Sci.*; 1975; **6**; 413- 419.

[184] M. M. Naser, D. L. Ross, and N. C. Miller; *Pharm. Res.*; 1997; **14**; 1437- 1443.

[185] M. J. Telko and A. J. Hickey; *Respir. Care;* 2005; **50**; 1209- 1227.

[186] C. Mobleya and G. Hochhaus; *Drug Discovery Today*; 2001; **6**; 367-375

[187] N. Esmailpour, P. Hogger, K. F. Rabe, U. Heitmann, M. Nakashima, and P. Rohdewald; *Eur. Respir. J.*; 1997; **10**; 1496-1499.

[188] H. Chrystyn; *Respir. Med.*; 1997; **91**(Suppl A); 17-19.

[189] H. Chrystyn; *Br. J. Clin. Pharmacol.*; 2001; **51**; 289- 299.

[190] L. Thorsson, S. Edsbacker, and T. B.Conradson; *Eur. Respir. J.*; 1994; **7**; 1839–1844.

[191] L. Borgstroem and M. Nilsson; *Pharm. Res.*; 1990; **7**; 1068-1070.

[192] M. Hindle, D. A. G. Newton, and H. Chrystyn; *Thorax*; 1993; **48**; 433–434.

[193] B. J. Lipworth and D. J. Clark; *Eur. J. Clin. Pharmacol. *; 1997; **53**; 47–49.

[194] N. J. Snell and D. Ganderton; *Respir. Med. *; 1999; **93**; 123–133.

[195] S. P. Newman, D. Pavia, F. Morean, N. F. Sheahun, and S. W. Clarke; *Thorax*; 1981; **36**; 52-55.

[196] D. Kohler, W. Fleischer, and H. Mathys; *Respiration*; 1988; **53**; 65-73.

[197] P. R. Phipps, I. Gonda, S. D. Anderson, D. Bailey, and G. Bautovich; *Eur. Respir. J.*; 1994; **7**; 1474-1482.

[198] M. S. Berridge, Z. Lee, and D. L. Heald; *J. Nucl. Med.*; 2000 ; **41**; 1603-1611.

[199] J. S. Fleming, P. Halson, J. Conway, E. Moore, M. A. Nassim, A. H. Hashish, A. G. Bailey, S. T. Holgate, and T. B. Martonen; *J. Nucl. Med.*; 1996; **37**; 873–877.

[200] M. S. Berridge, Z. Lee, G. P. Leisure, F. Moraldi, and D. L. Heald; *J. Pharm. Sci.*; 1998; **1,** (Suppl 4); S208-S209.

[201] J. Grossman; *J. Asthma*; 1994; **31**; 55-64.

[202] P. P. H. Le Brun, A. H. De Boer, H. G. M. Heijerman, and H. W. Frijlink; *Pharm. World Sci.*; 2000; **22**; 75-81.

[203] C. Terzano; *Pulm. Pharm. Ther.*; 2001; **14**; 351- 366.

[204] G. R. Crompton; *Eur. J. Respir. Dis.*; 1982; **63** (suppl 19); 57-65.

[205] R. Niveen; *Adv. Drug Deliv. Rev.*; 1997; **26**; 1-2.

[206] A. R. Clark; *Aerosol Sci. Technol.*; 1995; **22**; 374- 391.

[207] I. Ashurst, A. Malton, D. Prime, and B. Sumby; *Pharm. Sci. Technol. Today*; 2000; **3**; 246–256.

[208] I. J. Smith and M. Parry-Billings; *Pulm. Pharm.Ther.* ; 2003; **16**; 79–95.

[209] J. H. Bell, P. S. Hartley, and J. S. G. Cox; *J. Pharm. Sci.* ; 1971; **60**; 1559–1564.

[210] G. W. Hallworth; *Br. J. Clin. Pharmacol.* ; 1977; **4**; 689–690.

[211] N-I. M. Kjellman and B. Wirenstrand; *Allergy;* 1981; **36**; 437- 438.

[212] D. Prime, P. J. Atkins, A. Slater, and B. Sumby; *Adv. Drug Deliv. Rev.*; 1997; **26**; 51- 58.

[213] K. Wetterlin; *Pharm. Res.*; 1988; **5**; 506–508.

[214] S. Pedersen; *J. Aerosol Med.*; 1994; **7**; S67- S71.

[215] H. Chrystyn; *Clin. Drug Invest.* ; 2006; **26**; 175-183.

[216] W. M. Nsour, A. Alldred A, O. J. Corrado, and H. Chrystyn; *Respir. Med.*; 2001; **95**; 965-968.

[217] W. Tarsin, K. H. Assi, and H. Chrystyn; *J. Aerosol Med.*; 2004; **17**; 25-32.

[218] A. Palander, T. Mattila, M. Karhu, and E. Muttonen; *Clin Drug Invest;* 2000; **20**; 25-33.

[219] K. Malmstrom, R. Sorva, and M. Silvasti; Pediatr. *Allergy Immunol.;* 1999; 10; 66-70.

[220] T. Vanto, K. M. Hamalainen, M. Vahteristo, S. Wille, F. Nja, and N. Hyldebrandt; *J. Aerosol Med.*; 2004; **17**; 15-24.

[221] M. Vidgren, M. Silvasti, P. Vidgren, H. Sormunen, K. Laurikainen, and P. Korhonen; *Aerosol Sci. Technol.*; 1995; **22**; 335-345.

[222] A. Lahelma, M. Kirjavainen, M. Kela, J. Herttuainen, M.Vahteristo, M.Silvasti, and M.Ranki-Pesonen; *Br. J. Clin. Pharmacol.*; 2005; **59**; 167-173.

[223] L. Maggi, R. Bruni, and U. Conte; *Int. J. Pharm.*; 1999; **177**; 83-91

[224] H. Steckel and B. W. Muller; *Int. J. Pharm.*; 1997; **154**; 31–37.

[225] J. A. Hersey; *Powder Technol.*; 1975; **11**; 41–44.

[226] M. P. Timsina, G. P. Martin, C. Marriott, D. Ganderton, and M. Yianneskis; *Int. J. Pharm.*; 1994; **101**; 1–13.

[227] X. M. Zeng, G. P. Martin, C. Marriott, and J. Pritchard; *Int. J. Pharm.*; 2000; **200**; 93–106.

[228] V. Berard, E. Lesniewska, C. Andr`es, D. Pertuy, C. Laroche, and Y. Pourcelot; *Int. J. Pharm.*; 2002; **232**; 213–224.

[229] G. Saint-Lorant, P. Leterme, A. Gayot, and M. P. Flament; *Int. J. Pharm.*; 2007 **334**; 85–91.

[230] H. Larharib, X. M. Zeng, G. P. Martin, C. Marriott, and J. Pritchard; *Int. J. Pharm.*; 1999; **191**; 1-14.

[231] R. Vevtura, C. Jimenez, N. Closas, J. Segura, and R. De la Torre; *J. Chromatogr. B* ; 2003; **795**; 167-177.

[232] K. Cabrera, D. Lubda, H. M. Eggenweiler, H. Minakuchi, and K. Nakanishi; *J. High Res. Chromatogr.*; 2000; **23**; 93- 99

[233] Y. Wang, M. Harrison, and B. J. Clark; *J. Chromatogr. A*; 2006; **1105**; 77-86.

[234] Good Manufacturing Practice Guide For active pharmaceutical ingredients; ICH Harmonised Tripartite Guideline (Validation Analytical Procedures); 2000.

[235] M. Cledear-Castro, A. Santos-Montes, and R. Izquierdo-Hornillos; *J. Chromatogr. A.*; 2005; **1087**; 57-63.

[236] S. El Deeb, L. Preu, and H. Watzig; *J. Pharm. Biomed. Anal.*; 2007; **44**; 85-95.

[237] J. L. Cohen; *Theophylline; In Analytical profiles of drug substances Series*, Eds. K. Florey; London; Academic press; 1975; 467- 493.

[238] H. F. Walton, G. A. Eiceman, and J. L. Otto; *J. Chromatogr.*; 1979; **180**; 145-156.

[239] M. J. Del Nozal, J. L. Bernal, A. Pamphega, M. I. L. P. Marinero, and R. Coco; *J. Chromatogr. A.*; 1996; **727**; 231-238.

[240] R. V. Nirogi, V. N. Handikere, M. Shukla, K. Mudigonda, and D. M. Ajjala; *J. Chromatogr. A.*; 2006; **1134**; 194-200.

[241] Supelco Guide to Solid Phase Extraction Sigma-Aldrich Co.; USA; 1998.

[242] Merck Application Guide; ChromCircle 2.0 Merck Hitachi, Darmstadt, Germany; 2000.

[243] Baker Application Notes; Mallinckrodt Baker Inc., Philipsburg, USA; 2000.

[244] R. L. Davis, H. W. Kelly, R. W. Quenzer, J. Standefer, B. Steinberg, and J. Gallegos; *Antimicrob. Agents Chemother.*; 1989; **33**; 212- 214.

[245] M. Kele and G. Guiochon; *J. Chromatogr. A.*; 2002; **960**; 19-49.

[246] L. Novakovaa, L. Matysovaa, D. Solichovab, M. A. Koupparisc, and P. Solich; *J. Chromatogr. B.*; 2004; **813**; 191-197.

[247] S. El Deeb, U. Schepers, and H. Watzig; *Pharmazie*; 2006; **61**; 751-756.

[248] F. Gerber, M. Krummen, H. Potgeter, and A. Roth; *J. Chromatogr. A.*; 2004; **1036**; 127-133.

[249]   M. H. Hanna, P. York, and B. Y. Shkunov, *Control of the polymeric forms of a drug substance by SEDS in 5th meeting of SCFs*. Nice, France, 1998.

[250] P. York, M. H. Hanna, S. Palakodaty, and G.O. Humphreys. *Controlled Particle Formation Using The Solution Enhanced Dispersin By Super critical Fluids*. *In Process. 16th Pharmaceutical Technology Conference;* Athens; 1997.

[251] Malvern Instruments Zetamaster- Hardware reference manual; 1993; pp.1.2, 3.1.

[252] *British Pharmacopoeia*; **vol. IV**; The stationary office; London; 2008; S120, A306- A319.

[253] Spectral Database for Organic Compounds (SDBS)

[254]   K. B. Sloan, H. D. Beall, H. E. Taylor, J. J. Getz, R. Villaneuva, R. Nipper, and K. Smith; *Int. J. Pharm.*; 1998; **171**; 185-193.

[255] L. Diantree, *Personnal communication;* 2008; University of Bradford.

[256] S. M. Cooper; *Glaxosmithkline report*, WPD/96/008; 1996.

[257] B. Yu. Shekunov and P. York; *J. Cryst. Growth*; 2000; **211**; 122-136.

[258] J. O. Werling and P. G. Debeneditti; *J. Supercrit. Fluids*; 2000; **18**; 11-24.

[259] S. Bristow, T. Shekunov, and P. York; *J. Supercrit. Fluids*; 2001; **21**; 257-271.

[260] S. Airaksinen, M. Karjalainen, E. Rasanen, J. Rantanen, and J. Yliruusi; *Int. J. Pharm.*; 2004; **276**; 129-141.

[261] S. Gunasekaran, G. Sankari, and S. *Ponnusamy, Spec. Acta part A*; 2005; **61**; 117-127.

[262] R. K. Khankari and D. J. W. Grant; *Thermochimica Acta*; 1995; **248**; 61-79.

[263] N. Rodriguez-Hornedo, D. Lechuga-Ballesteros, and H. J. Wu; *Int. J. Pharm.*; 1992; **85**; 149-162.

[264] K. R. Morris and N. Rodriguez-Hornedo; Encyclopedia of Pharmaceutical Technology; 1993; **7**; 393-440; New York; Marcel Dekker;

[265] J. Herman, N. Visavarungroj, and J. P. Remon; *Int. J. Pharm.*; 1989; **55**; 143-146.

[266] S. Airaksinen, P. Luukkonen, A. Jqrgensen, M. Jakarjalainen, J. Rantanen, and J. Yliruusi; *J. Pharm. Sci.*; 2003; **92**; 516-528.

[267] M. Weda, P. Zanen, A. H. Boer, D. M. Barends, and H. W. Frijlink; *Int. J. Pharm.*; 2004; **287**; 79-87.

[268] K. H. Assi and H. Chrystyn; *Respir. Crit. Care Med.*; 2001; **163** (supplement); A443.

[269]   W. Tarsin, O. J. Corrado, K. Brownlee, P. Kanthapillai, S. Pearson, P. Chetcuti, and H. Chrystyn; *Eur Respir. J.*; 2001; **18** (suppl. 33); P 900; 133S.

[270] T. Koskela, K. Malmstrom, U. Sairanen, S. Peltola, J. Keski-karhu, and M. Silvasti; *Respir. Med.*; 2000; **94**; 1229-1233.

[271] A. R. Clark and A. M. Hollingsworth; *J. Aerosol. Med.* ; 1993; **6**; 99–110.

 [272] X. M. Zeng, G. P. Martin, C. Marriott, and J. Pritchard; *J. Pharm. Sci.*; 2001; **90**; 1424-1434.

[273] A. H. de Boer, D. Gjaltema, and P. Hagedoorn; *Int. J. Pharm.*; 1996; **138**; 45-56.

[274]C. P. Criee, T. Meyer, W. Petro, K. Sommerer, and P. Zeising; *J. Aerosol. Med.*; 2006; **19**; 466-472.

[275] S. C. Nichols, D. R. Brown, and M. Smurthwaite; *Copely Scientific*; 2000; 2-8.